Fourth Japan-China-Korea Joint Conference on Meteorology

8-10 November 2009, Tsukuba, Japan

Abstract collection

気象
气象
기상

Organized by

Meteorological Society of Japan
Chinese Meteorological Society
Korean Meteorological Society

Hosted by

Local Organizing Committee (LOC) of Japan-China-Korea Joint Conference,
Meteorological Society of Japan
Supported by Tsukuba City
Conference URL:http://wwwsoc.nii.ac.jp/msj/jckjc09/

Table of contents

Oral Sessions

S-1 Numerical Weather Prediction

Session Conveners: Kazuo SAITO, Xueshun SHEN, and Hyeong-Bin CHEONG

8 Nov. 13:00-14:45 Chair: Xueshun SHEN (Location: Conference Room 406)

Climate, global model and scheme

Break

8 Nov. 15:15-17:00 Chair: Hyeong-Bin CHEONG

Typhoon, regional model and heavy rainfall

9 Nov. 8:30-9:30 Chair: Kazuo SAITO (Location: Conference Room 202B)

Data assimilation

S-2 Monsoon

Session Conveners: Jun MATSUMOTO, Jianping LI, and Kyung-Ja HA

8 Nov. 13:00-15:15 Chair: Riyu LU (Location: Conference Room 102)

Monsoon seasonal change

Land-atmosphere interactions

Break

8 Nov. 15:30-17:15 Chair: Dong-Hyun CHA

Monsoon modeling

9 Nov. 8:30-9:45 Chair: Jun MATSUMOTO (Location: Conference Room 202A)

Tibetan Plateau

East Asian summer monsoon

Break

9 Nov. 10:15-11:45 Chair: WonMoo KIM

9 Nov. 14:00-15:30 Chair: Jiangyu MAO

Break

9 Nov. 16:00-17:30 Chair: Kenichi UENO

East Asian winter monsoon

S-3 Atmospheric Aerosol, Gases, and Radiation

Session Conveners: Masao MIKAMI, Zifa WANG, and Maeng-Ki KIM

8 Nov. 13:00-15:00 Chair: Masao MIKAMI (Location: Convention Hall 200)

Break

8 Nov. 15:30-17:15 Chair: Maeng-Ki KIM

9 Nov. 8:30-10:00 Chair: Zifa WANG (Location: Convention Hall 200)

Break

9 Nov. 10:30-11:45 Chair: TBD

9 Nov. 14:00-15:45 Chair: Rokjin PARK

Break

9 Nov. 16:15-17:45 Chair: Hajime FUKUSHIMA

S-4 Future Climate Projection and Impact

Session Conveners: Akio KITOH, Xiuqun YANG, and Won-Tae KWON

8 Nov. 13:00-15:00 Chair: Akio KITOH (Location: Conference Room 101)

Break

8 Nov. 15:30-17:30 Chair: Shoji KUSUNOKI

S-5 Typhoon and Meso-scale Phenomenon

Session Conveners: Tetsuo NAKAZAWA, Xiaotu LEI, and Jong-Jin BAI

8 Nov. 13:00-14:50 Chair: Takuya KOMORI (Location: Conference Room 405)

Break

8 Nov. 15:20-16:50 Chair: Tetsuo NAKAZAWA

9 Nov. 8:30-10:00 Chair: Jong-Jin BAIK (Location: Conference Room 201B)

Break

9 Nov. 10:30-11:45 Chair: Il Ju MOON

9 Nov. 14:00-15:30 Chair: Taro SHINODA

Break

9 Nov. 16:00-17:00 Chair: Naoko KITABATAKE

S-6 Satellite Remote Sensing

Session Conveners: Riko OKI, Peng ZHANG, and Myoung-Seok SUH

9 Nov. 10:00-12:00 Chair: Masato SHIOTANI (Location: Conference Room 202B)

9 Nov. 14:00-15:45 Chair: TBD

Break

9 Nov. 16:00-18:15 Chair: Myoung-Seok SUH

S-7 Boundary Layer Meteorology

Session Conveners: Hiroaki KONDO, Shuhua LIU, and Yign NOH

9 Nov. 14:00-16:00 Chair: Hiroaki KONDO (Location: Conference Room 201A)

S-8 General Session and Other Topics

Session Conveners: Hiroshi L. TANAKA, Chunyi WANG, Jhoon KIM

9 Nov. 8:30-10:15 Chair: Jhoon KIM (Location: Conference Room 201A)

Break

9 Nov. 10:30-12:15 Chair: Wang CHUNYI

Poster Session

S-1 Numerical Weather Prediction

S-2 Monsoon

S-3 Atmospheric Aerosol, Gases, and Radiation

S-4 Future Climate Projection and Impact

S-5 Typhoon and Meso-scale Phenomenon

S-6 Satellite Remote Sensing

S-7 Boundary Layer Meteorology

S-8 General Session and Other Topics

Author index

SEASONAL FORECAST USING A STATISTICAL DOWNSCALING METHOD: ITS VERIFICATION AND APPLICATION

Daisuke NOHARA[1], Yoshikatsu YOSHIDA[1], Howeng KANG[2], and Ashok KARUMURI[2]
1: Central Research Institute of Electric Power Industry, Abiko, Japan
2: APEC Climate Center, Busan, Korea
nohara@criepi.denken.or.jp

Abstract

In this study, a statistical downscaling method developed by APEC Climate Center is applied to three-month seasonal forecast of monthly temperature and precipitation over Japan in order to improve skill of the forecast. The downscaling method predicts future weather using highly correlated pattern between observation at station and hindcast simulated by the numerical models. In addition, multi-model ensemble is applied to reduce model biases. The downscaled forecast during summer in 2008 is verified compared with original multi-model ensemble mean. Temperature and precipitation anomaly by the downscaled forecast indicates realistic distribution over Japan compared with the original forecast. Additionally, quantitative forecast skill is verified based on the hindcast in cross-validation framework from 1984 to 2003. Anomaly correlation coefficient (ACC) of the downscaled forecast exceeds 0.6 at most of stations, although ACC of the original forecast is almost 0.2. The improved seasonal forecast by the downscaling method is helpful in its indastrial application such as electricity demand prediction.

Keywords: seasonal forecast statistical downscaling method, multi-model ensemble, electricity demand

Development of New Global Forecast System in CMA

Xueshun SHEN
Wei Han, Jishan Xue, Jian Sun, Zhaorong Zhuang, Xingliang Li and Zhiyan Jin
Center for Numerical Prediction and Research
Chinese Academy of Meteorological Sciences
China Meteorological Administration

Since 2007, a new global NWP system-GRAPES_GFS (GRAPES Global Forecast System) has been being developed in China Meteorological Administration (CMA). The GRAPES_GFS is based upon the GRAPES global model and global 3-DVAR system. To develop the GRAPES_GFS, the GRAPES global model has been carefully tuned to better represent the global energy balance, precipitation distribution and mean circulations. As for the global 3-DVAR system, much more efforts have been made in satellite radiance data assimilation. At present, 3-year re-forecast experiments have been conducted, showing rather encouraging results. And, this system has been put into pre-operational test from March of 2009.

Renovation of JMA-GSM

Kengo MIYAMOTO
AESTO/JMA, Tokyo, Japan
miyamoto@naps.kishou.go.jp

Abstract

JMA-GSM is the global atmospheric model for official weather forecasting in Japan. The model is also used for research on climate. The model was renovated at 5 August, 2008. Although the principles were not changed from the conventional model, the implementation was renovated: reduced spectral transformation was introduced; the calculation domain was two-dimensionally decomposed; the procedures of inter-node communication were refined; OpenMP was adopted for shared memory parallelization; some defectives were corrected; the source program was reorganized.

In this presentation, we will introduce the details of the renovation and show how the renovation makes the model faster and improves the accuracy.

Keywords: Numerical Weather Prediction, Global Spectral Atmospheric Model

NUMERICAL SIMULATION OF ARCTIC AND TROPICAL CYCLONES USING NICAM INSTALLED AT CCS, UNIVERISTY OF TSUKUBA

H. L. Tanaka and Shinji Takahashi

Center for Computational Science, University of Tsukuba,
Tsukuba Japan (First Author)
tanaka@ccs.tsukuba.ac.jp

Abstract

A series of numerical experiments are conducted using NICAM with various horizontal resolutions from 224 km (Glevel=5) to 7 km (Glevel=10). An atmospheric blocking is simulated with an initial condition of 27 November 2007 interpolated from the Grid Point Value (GPV) analysis data provided by the Japan Meteorological Agency (JMA) with Glevels from 5 to 9. It is found that the blocking is predicted from the initial condition one week before, but the intensity of the blocking appears to be weak for all resolutions. A pronounced tropical cyclone is simulated over the Gulf Stream with the numerical simulation starting from an initial condition of 21 June 2008 in the model, which is absent in the real atmosphere. The detail of the fine structures of vorticity, vertical motion, and specific humidity is analyzed for this event. Another interesting feature of the Arctic cyclone is analyzed for the numerical experiment starting from the same initial condition. The surface Arctic cyclone stays over the Arctic more than three weeks within the same Arctic air mass. Therefore, the cold and warm front is absent around the cyclone. The vorticity extends up to the lower stratosphere with quasi-barotropic structure. The Arctic cyclone looks similar to the tropical cyclone to some extent, but the warm core is seen at the lower stratosphere associated with the descending motion from the higher altitude in the stratosphere, which is the notable distinction from the tropical cyclone. The detailed structure of the vorticity, vertical motion, and specific humidity is compared with those of tropical cyclones and extra-tropical cyclones.

Keywords: Arctic cyclone, Tropical Cyclone, Blocking, NICAM

SEMI-LAGRANGIAN COMPUTATION OF GRAVITY WAVES ON SPHERE

Xindong PENG[1], Yan CHANG[2], Feng XIAO[3], Keiko TAKAHASHI[4]

[1] State key laboratory of severe weather,
Chinese Academy of Meteorological Sciences, Beijing, China.
[2] College of Atmospheric Sciences, Lanzhou University, Lanzhou, China
[3] Institute of Mechanics, Chinese Academy of Sciences, Beijing, China
[4] Earth Simulator Center, JAMSTEC, Yokohama, Japan
pengxd@cams.cma.gov.cn

Abstract

Rapid gravity waves must be carefully arranged for high computational efficiency and economical simulation in numerical weather prediction, because of its strict restriction to the time step for stable numerical integration. For explicit computation, forward-backward scheme is used many places. Semi-implicit algorithm is also popularly used to deal with the gravitational term when semi-Lagrangian scheme is usually applied to the advection term in numerical models, so that to enlarge time step for stable integration. In a semi-implicit scheme, however, matrix inversion is necessary in the solution steps. With the model resolution grows higher and higher, matrix inversion in a semi-implicit procedure becomes much more expensive. Computational time increases rapidly with the grid point numbers. And in the high-resolution case, dynamical and physical processes tolerate large time steps in the sense of computational accuracy. In this paper, we try a so-called Characteristic CIP method to compute the gravity wave directly on sphere with semi-Lagrangian advection scheme instead of the semi-implicit computation for a shallow water model, to avoid expensive matrix inversion. The primary idea is to treat wave terms the same as the current. Using of the semi-Lagrangian scheme makes the numerical model always stable for any Courant number, and which serves to save CPU time, especially in high-resolution cases. To illustrate the efficiency of the Characteristic method, some numerical results are shown for idealized test cases on sphere in the Yin-Yang grid system besides some simple tests on Cartesian coordinate.

Keywords: Characteristic method, gravity wave, sphere, semi-Lagrange, Yin-Yang grid

The program structure designing and optimizing tests of GRAPES physics

Xu Guoqiang Xue Jishan Sun Jiang Shen Xuexun Chen Dehui Shen Yuanfang Huang Liping Wu Xiangjun Wang Shiyu
Chinese Academy of Meteorological Sciences.
Beijing, 100081

ABSTRACT

According to the modularization and standardization of program structure in Global / Regional Assimilation and Prediction System (GRAPES), the plug-compatible and transplantable regional meso-scale and global middle-range physics software package is established. The package's component integrality is comparative with the other advanced models physics. A three-level structure of connecting GRAPES physics and dynamic frame has been constructed. The friendly interface is designed for users to plug in their own physics packages. Phenomenon of grid-point storm rainfall in numerical prediction is analyzed with the numerical tests. The scheme of air vertical velocity calculation is improved. Optimizing tests of physics schemes are performed with the correlative parameters adjusting. The results show that the false grid-point storm rainfall is removed by precipitation scheme improving. Then the score of precipitation forecast is enhanced.

Key words: Physics, program structure, grid-point storm rainfall, optimizing numerical tests

Using Kernel Neighbor Nonparametric Estimation Technique to Predict Wind

M.X.Shao[1], M.Q.Xiong[1], H.Z.Liu[1], H.Xu[2]
1.National Meteorological Center, CMA, Beijing 100081, China
2.China Meteorological Administration, Beijing 100081, China
Shaomx123@sina.com

Abstract

In the experimentation wind was predicted by kernel neighbor nonparametric estimation technique from December 1, 2007 to November 30, 2008. More than 2200 stations of China were tested with daily predicting 7 days 56 times wind direction and speed of each point. A control test was made to use DMO (Direct Model otputs) for the same period. The forecast area was divided into 5 areas in Northeast, Northwest, Southwest Southeast and North China. A detailed grade of test was given, from different areas, different times and different seasons. The grades of More than 2200 stations as a whole, in the winter, summer and fall the test predictions were better than control test for wind direction forecast, while the control test predictions were better than that of test in the spring. For wind speed prediction of less than 3.3m/s, the mean TS grade of test is 0.768, while that of control test is 0.752. For wind of more than 3.4m/s, the test is 0.233, while control test 0.154. For wind of more than 8.0m/s, the test is 0.139, while control test 0.047. The new method is proved to be a useful tool to wind prediction.

Key Word: Nonparametric estimation technique, Kernel neighbor forecast, DMO forecast, Wind prediction

TYPHOON TRACK AND INTENSITY PREDICTION WITH THE TROPICAL CYCLONE INITIALIZATION SCHEME AND WRF MODEL

In-Hyuk KWON, Hyeong-Bin CHEONG, Hyun-Jun HAN, and Hyun-Gyu KANG

Pukyong National University, Busan, Korea

Email: doogy@pknu.ac.kr and hbcheong@pknu.ac.kr

A Tropical Cyclone (TC) initialization method with idealized three-dimensional bogus vortex is presented for the tropical cyclone track and intensity prediction. The method shares some basic ideas with the GFDL method, such as the separation of the disturbance from the analysis, determination of the TC domain, and generation of symmetric bogus vortex. Detailed procedures in each step, however, are significantly different from to each other. On separating the disturbance field, an efficient spherical harmonics filter is used whose cutoff scale can be varied depending on the scale of the TC of interest. The TC domain is determined from the streamfunction field instead of the tangential velocities. The axisymmetric vortex to replace the poorly resolved TC in the analysis is designed with a careful treatment of the upper layer flows as well as the vertical circulations. The geopotential field of the bogus vortex is determined as the empirical 2-Dimensional (vertical-radial) function based on the RSMC typhoon information. The inflow and outflow in the TC are given to resemble closely the observed or model simulated structures. The bogus vortex is merged with the disturbance field without any discontinuity near the boundary of the TC domain. The initialization method was applied to the track and intensity prediction of the TCs observed in the western Pacific region in 2007 using the WRF model. Compared to the results without the TC initialization, the present method presented much improvement in both the track and intensity forecasts. The average track and intensity errors were found to be better than the results of the some operational forecasts.

Acknowledgement: This work was funded by the Korea Meteorological Administration Research and Development Program under Grant CATER 2007-2206

Keywords: tropical cyclone initialization, spherical harmonics filter, WRF model simulation, idealized bogus vortex

The operational meso-scale NWP system in CMA: GRAPES_Meso

Jian SUN Xueshun SHEN Dehui CHEN Jishan XUE

Chinese Academy of Meteorological Sciences, Beijing 100081, China

GRAPES is a short form of Global /Regional Assimilation and Pr*E*diction System. In 2001, a state-key Research&Development project was launched in China to develop a unified numerical weather prediction (NWP) system. One of the major objectives of the project is to develop new NWP systems for both operational and research uses. GRAPES is the achievement of this 5-years project and it is almost totally developed with the efforts of Chinese scientists.

GRAPES is designed as a multi-scale unified model. In this presentation, we will focus on the meso-scale version which is names as GRAPES_Meso. The main features of GRAPES_Meso includes: (1) full compressible dynamical core with hydrostatic or non-hydrostatic approximation in options; (2) a semi-implicit and semi-Lagrangian scheme; (3) height terrain following vertical coordinate; (4) full physical package; (5) 3DVAR/4DVAR for data assimilation; (6) modularized and parallelized code architecture; (7) latitude-longitude grid

In July 2006, GRAPES_Meso run as the operational NWP systems twice a day at Chinese National Meteorological Center (NMC/CMA) with a horizontal resolution of 30km and 31 vertical levels. And in October 2007, an updated version, with 15km horizontal resolution, replaced the 30km version.

The important difference between the15km and 30km versions include: 1) tuned analysis scale of vapor in the 3DVar system; 2) a smoothed or a filtered topography; and 3) more reasonable physics packages. A whole-year but not-real-time forecast experiment had been finished to evaluate the 15km version, including the rainfall threat score, the RMSE of the HGT/Temp. And analyses of some high impact weather cases were also given.

RADIATION PROCESS OF THE JMA NONHYDROSTATIC MODEL

Ryoji NAGASAWA
Numerical Prediction Division, Japan Meteorological Agency
1-3-4 Otemachi, Chiyoda-ku, Tokyo 100-8122, Japan
r-nagasawa@met.kishou.go.jp

Abstract

Under the framework of the "Projection of the change in future weather extremes using super-high-resolution atmospheric models" supported by the KAKUSHIN Program of the Ministry of Education, Culture, Sports, Science, and Technology (MEXT), the improvement of the cloud resolving regional atmospheric model based on the JMA nonhydrostatic model (JMA-NHM) and the projection of the change in future weather extremes by grobal warming are executed.

A radiation process is important for accurate forecasts of the vertical profile of the temperature and the surface air temperature. Especially long term integration requires more detailed radiation scheme. Accordingly, refinement of the radiation process has been executed as a part of the improvement of the cloud resolving regional atmospheric model.

In this talk, improvement of the cloud-radiation process in March 2006, improvements of the clear-sky-radiation process and the cloud diagnostics method used in the cloud-radiation process in May 2007, results of the recent developments and the future subjects on the radiation process are presented.

Keywords: nwp, nonhydrostatic model, radiation

EXPERIENCES OF MRI/JMA AT THE WWRP BEIJING OLYMPIC 2008 RESEARCH AND DEVELOPMENT PROJECT (B08RDP)

Kazuo SAITO, Masaru KUNII, Masahiro HARA, Hiromu SEKO
Meteorological Research Institute, Tsukuba, Japan
ksaito@mri-jma.go.jp

Abstract

The WWRP Beijing Olympic 2008 Research and Development Project (B08RDP) is an international research project on the mesoscale ensemble prediction. Aims of the project are to improve understanding of the high-resolution probabilistic prediction processes through numerical experimentation and to share experiences in the development of the real-time MEP system. The Meteorological Research Institute (MRI) has developed a mesoscale ensemble prediction system based on the JMA nonhydrostatic model collaborating with the Numerical Prediction Division of JMA. As for initial perturbation methods, following five methods, i) Downscale of JMA one-week EPS (WEP), ii) Targeted global Singular vector (GSV), iii) Mesoscale Singular Vector (MSV), iv) Mesoscale BGM (MBD), v) Local ensemble transform (LET), were compared with a same condition prior to the B08RDP experiment.

Following interesting findings have been obtained;

1) Singular vector methods showed large growth rates compared with MBD and LET. Ensemble spreads of MSV increase most rapidly in the early forecast stage up to FT=6 while spreads by GSV were largest after FT=18. For area of ROC, GSV was best for weak rain less than 3mm, while MBD and MSV were better than GSV for moderate or intense rains. The reason is likely that GSV tends to perturb synoptic scale disturbances while MBD and MSV perturb mesoscale disturbances (especially low level moisture field) which are relate to local intense rains.

2) In the comparison of MBD and LET, magnitude of initial ensemble spread in LET reflects the distribution of observation density, however, the growth of ensemble spread in LET is slow and the merit of the masking of initial perturbation according to the analysis error was unclear in the statistical scores such as the RMSE of ensemble mean and area of ROC. Localization, sampling error and ensemble transform may affect the synoptic structures of initial perturbations in LET.

3) Lateral boundary perturbations are indispensable to increase the ensemble spread in the later half of the forecast period (after FT=18). In BGM and LET, lateral boundary perturbations are important not only in the forecast period of EPS but throughout the breeding/DA cycles in BGM/LET to make better initial perturbations.

Keywords: WWRP, ensemble prediction, perturbation method (**within 5 words**)

MESOSCALE ENSEMBLE FORECAST EXPERIMENT AND SENSITIVITY ANALYSIS OVER JAPAN AREA

Masaru KUNII, Masahiro HARA, Kazuo SAITO and Hiromu SEKO
Meterological Research Institute, Tsukuba, Japan
mkunii@mri-jma.go.jp

Abstract

From the end of August to September 2008, a mesoscale ensemble forecast experiment and a sensitivity analysis experiment using the singular vector was performed by MRI/JMA to support T-PARC (THORPEX Pacific Asian Regional Campaign) and to validate their usefulness.

In the former experiment, the JMA nonhydrostatic model (NHM) has been employed as the forecast model. Horizontal resolution is 15km and vertical resolution changes linearly from 40m at the bottom and 1180m at the top. For initial perturbations, the global singular vector method (GSV, T63L40) whose final norm is targeted on Japan area (25.0-40.0N, 125.0-145.0N) is used. In addition, the mesoscale singular vector method (MSV) was employed for initial perturbations for conspicuous cases. The number of ensemble member is 11, including no-perturbed control run and the forecasts were performed once a day, 12 UTC initial.

Fig.1 shows the ROC area skill score of 3-hour accumulated precipitation for GSV and MSV ensemble forecasts and control run, for 3 days from 27 to 29 August when a torrential rainfall occurred at Chubu district. GSV has an advantage over weak and moderate rainfall, while MSV is superior to others for intense precipitation. This is because MSVs reflect the small scale structures which affect mesoscale disturbances rather than synoptic events that GSVs focus on.

In the latter experiment, for the case of TY0813 (SINLAKU), which caused a torrential rainfall at Kyushu district, a data denial experiment over sensitivity area was conducted to examine the validity of the sensitivity analysis based on MSV. In the near-real time operation, the 24-hour forecast of the JMA Global model (GSM; TL959L60) is used for initial condition to calculate MSVs, so that leadtime of about 14 hours is kept prior to the observation time of T-PARC.

The data denial experiment shows that the exclusion of observations over the sensitivity region has impact on forecast fields, however deterioration of forecast accuracy was not clear because the differences of analyzed moisture fields with and without the data was small in this case. To further assess the propriety of the MSV-based sensitivity region, OSSE on water vapor fields around typhoon center is necessary.

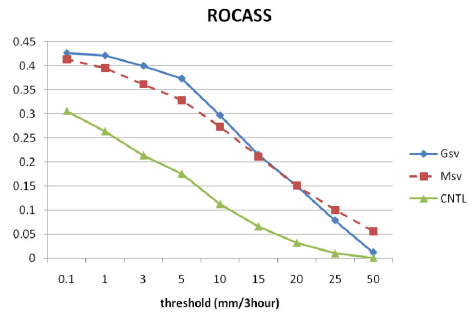

Fig. 1 ROC area skill score for ensemble forecasts perturbed the global singular vector (GSV) and the mesoscale singular vector (MSV) and no-perturbed run (CNTL). The scores were averaged all the forecast time (ft=03 - 36) from 27 to 29 August.

Keywords: ensemble prediction, sensitivity analysis, singular vector

MESOSCALE ENSEMBLE EXPERIMENTS OF HEAVY RAINFALLS IN JAPAN AREA BY USING NHM-LETKF

HIROMU SEKO[1], KAZUO SAITO[1], MASARU KUNII[1],
and TAKEMASA. MIYOSHI[2]
[1]Meterological Research Institute, Tsukuba, Japan
[2]Maryland Univaersity, Maryland, USA
Email: hseko@mri-jma.go.jp

Abstract

In ensemble Kalman filter (EnKF), assimilation is performed sophisticatedly considering the error structure that fluctuates from day to day, and the perturbations of ensemble forecasts are produced by reflecting properly the analysis error. Because assimilation using EnKF is easier than that of the variational method, EnKF is expected to be one of useful techniques for numerical weather prediction.

In this study, mesoscale ensemble experiments on heavy rainfall events occurred in Japan were performed with a Local Ensemble Transform Kalman Filter (NHM-LETKF) (Miyoshi and Aranami, 2006). Non-hydrostatic model of the Japan Meteorological Agency (NHM) with a grid interval of 20 km was used as the forecast model. Operational observations, such as surface and upper sounding data and GPS derived precipitable water vapor (PWV), were assimilated. Number of the ensemble member was 20. Downscale forecasts from the analyzed fields were further performed by NHM with grid intervals of 5 km and 1.6 km.

One of heavy events is the intense rainfall band occurred at Kobe on 28 July 2008, in which 5 people were claimed by the rapid rising the Toga river (Fig. 1a). This intense rainfall band was not reproduced by the operational forecast of JMA. When the GPS-derived PWV etc. were assimilated, a few members in the downscale forecasts reproduced the rainfall band (Fig.1b). This result indicates that misses of severe events can be reduced by ensemble forecast. Because the environment (vertical profile of temperature etc.) around the rainfall band affects the rainfall amount, the relation between rainfall amount and environments were plotted (Fig.1c). This scattergram shows that the temperature and equivalent potential temperature at the height of 500 hPa significantly influenced the rainfall amount. This result also indicates that ensemble forecasts provide the information of factors that cause heavy rainfall.

Keywords:LETKF, heavy rainfall

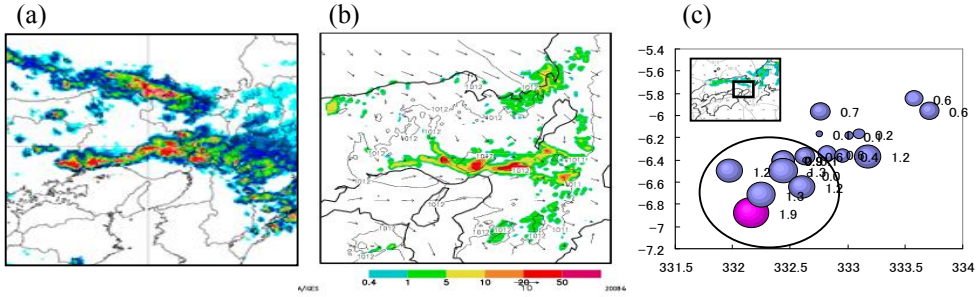

Fig.1 (a) Rainfall distribution observed by operational radar. (b) Rainfall distribution of downscale prediction of ensemble member of #001. (c) Relation between rainfall amount (circle), temperature (vertical axis) and equivalent potential temperature (horizontal axis) of the height of 500 hPa.

RADAR AND SURFACE DATA ASSIMILATION FOR THE SIMULATION OF HEAVY RAINFALL

Ji-Hyun Ha, Suk-Jin Choi and Dong-Kyou Lee
Atmospheric Science Program, Shool of Earth and Environmental Science,
Seoul National University, Seoul, Korea
dearhaji@nwp2.snu.ac.kr

Abstract

The effects of radar and surface data assimilation to the simulation of a rapidly developing heavy rainfall that occurred over Goyang in the central Korean Peninsula on 12 July 2006 are investigated. The heavy rainfall evolved from an intensive MCS embedded in the quasi-stationary Changma front system. The accumulated rainfall amount exceeded more than 250 mm during 6 hours. The 3DVAR Incremental Analysis Updates (IAU) technique of the WRF (Weather Research and Forecast) model is used for providing better initial data of the model. In the nested experiments with 6 km horizontal resolution, observed radar and surface (including AWS) data are assimilated using the simulated outputs of 18 km horizontal resolution with/without the GTS data assimilation.

The experiment with the GTS data assimilation simulates substantially improved synoptic features, especially intensified low-level southwesterly flows, which are in good agreement with observation. The improved simulation of the 18 km resolution model provides the nested model with proper initial/boundary conditions which also help improve low-level circulations and related rainfall distribution in the 6 km resolution simulation. The radar and surface data assimilation by IAU for the nested model simulations further improves the development of an organized MCS and the intensity of maximum heavy rainfall. In particular, the assimilation of surface data is essential in the development of a surface cold pool which significantly intensifies the MCS in this case.

Keywords: MCS, Data assimilation, Incremental analysis updates

RECENT IMPROVEMENT OF THE GLOBAL GRAPES-3DVAR ANALYSIS SYSTEM

Zhaorong ZHUANG, Jishan XUE, Wei HAN, Yan LIU,
Huijuan LU, Xueshun SHEN
State Key Laboratory of Severe Weather,
Center for Numerical Prediction and Research,
Chinese Academy of Meteorological Sciences, Beijing, China
zhuangzr@cams.cma.gov.cn

Abstract

The development and recent improvements of the global GRAPES 3DVar system are described in this paper. The global 3D-Var system with flexible horizontal Arakawa A grid and vertical pressure levels, based on an unified framework for GRAPES model developed in the Center for Numerical Prediction and Research (CNPR), Chinese Meteorological Administration (CMA), has made a great progress through lots of experiments. The reasonable analysis can be obtained by using horizontal correlation function of SOAR instead of the Gaussian function and new bias correction of ATOVS satellite. The quality control of TEMP geopotential is stricter in the area of India and Siberia than other area, and the TEMP observations are scanned through for blacklisting to remove the bad observation stations. The parallelization of global 3DVar greatly reduces the computational cost. Furthermore, the recent digital filter and increment interpolation are applied in the annual every 6h cycle, and 10d forecasting has been started from each day at 12UTC. Through comparing the analysis and the prediction in the cycle with the observation, it is proved that the 3D-Var analysis quality has been more improved than previous serial experiments.

Keywords: Assimilation, 3 dimensional variational, global

DEVELOPMENT OF GRAPES 4DVAR

XUE Jishan, ZHANG Lin
State Key Laboratory of Severe Weather,
Chinese Academy of Meteorological Sciences, Beijing, China
jsxue@cams.cma.gov.cn

Abstract

This paper reviews the development of 4DVar in the Chinese new generation NWP system GRAPES. GRAPES-4DVar inherits all the observational operators and optimization algorithms of GRAPES-3DVar and introduces the time integration of tangent linear and adjoint models in the computation of innovation and gradient of the cost function. The tangent linear and the adjoint models are adiabatic taking the large scale condensation, convection and PBL into account. After a series of idealized experiments to ensure the correctness of the coding, real data case experiments are conducted and the results are compared with the analyses derived by 3DVar. It is shown that generally the 3D analyses are closer to the observations than the results of 4DVar for single observation time, but the forecasts error initiated by the former increase more rapidly than the error of forecast initiated by the latter implying the improvement of the consistency of the analysis and the model in the 4DVar and forecast cycles. The ATOVS data assimilation with 4DVar also results in better forecasts in the selected cases. Further studies indicate that in terms of satellite data assimilation, the superiority of 4DVar may come from the less time gap between the observations and model states and the propagation of the influences of satellite observation on the analyses in accordance with the flow pattern. Limited by the computer resources, the number of the experiments and the size of model domain may not be large enough to assess the performance of the new 4DVar system, more experiments with more reasonable model configuration are undertaken.

Keywords: Assimilation, 4 dimensional, variational

NEW OPERATIONAL MESOSCALE 4D-VAR USING JMA NONHYDROSTAIC MODEL

Yuki HONDA and Ken SAWADA
Numerical Prediction Division, Japan Meteorological Agency
Tokyo, JAPAN
Email: honda.yuuki@met.kishou.go.jp

Abstract

For disaster prevention and aviation forecasting, the Japan Meteorological Agency (JMA) operates a mesoscale numerical weather prediction system known as Mesoscale Model (MSM). In April 2009, its operational mesoscale analysis system was upgraded from a four-dimensional variational data assimilation system (4D-Var) based on a hydrostatic spectral model (Meso 4D-Var) to a new 4D-Var system based on the JMA non-hydrostatic model (JNoVA). By this upgrade, MSM has become a consistent analysis-forecast cycle system in the sense both are based on the non-hydrostatic dynamics.

Main differences of two 4D-Var systems are as follows. First, time integration operators are different: JNoVA adopts the JMA nonhydrostatic model which is a current operational forecast model although Meso 4D-Var adopts the hydrostatic spectral model which is a previous operational forecast model. These models are also used as the outer model in each system. Second, the model resolution is increased. The horizontal resolution of the inner model and outer model are raised from 20km to 15km and from 10km to 5km, respectively. Third, the detailed configurations of data assimilation system are modified. Especially, data windows is shortened from 6 hours to 3 hours. Additionally, several other aspects (ex. control variables, penalty term and error charactersitcs) are also different.

To compare the performance of JNoVA with that of Meso 4D-Var, twin experiments were conducted under almost the same conditions as the operational system in summer (2006/7/16 – 8/31) and in winter (2007/12/23 – 2008/1/23). The quantitative precipitation forecast (QPF) of JNoVA is better than that of Meso 4D-Var for all thresholds according to the equitable threat score of three-hourly accumulated precipitation forecasts. Upper-air verification reveals that the analysis of JNoVA is better than that of Meso 4D-Var, although the impact on the forecast is quite limited. From surface verification, it is found that the root mean square errors of the surface temperature in summer and the surface wind in winter are reduced, and that the scores of other surface variables are neutral. Among individual forecasts, a remarkable improvements of typhoon track forecast and thus QPF are seen in the case of typhoon Wukong in 2006. In general, JNoVA outperforms Meso 4D-Var.

Keywords: 4D-Var, nonhydrostatic model, mesoscale, analysis, JNoVA

IMPACTS OF GPS RADIO OCCULTATION DATA OF CHAMP AND COSMIC ON THE PREDICTIONS OF HEAVY RAINFALL AND TYPHOON FORMATION

[1]HIROMU SEKO, [1]MASARU KUNII, [1]YOSHINORI SHOJI
and [2]TOSHITAKA TSUDA
[1]Meterological Research Institute, Tsukuba, Japan
[2]Research Institute for Sustainable Humanosphere, Uji, Japan
hseko@mri-jma.go.jp

Abstract

Impacts of the GPS radio occultation data observed by CHAMP and COSMIC were investigated using the mesoscale 4-dimensional variational data assimilation system of the JMA. We adopted the method of Chen et al. (2005) to consider the vertical correlation of the observation error. This method was extended so that it can assimilate the average of the refractivity over the path from GPS satellite to LEO satellite. We applied this method to predict the intense rainfall by Baiu front and the typhoon in the formation stage.

On 16 July 2004, the rainfall system was developed at the northern Japan (Fig. 1a) and the rainfall amount of 133 mm/day was observed at Oyu in Niigata prefecture . The rainfall system was not reproduced when the operational data (e.g. upper sounding data, etc.) were assimilated (Fig. 1b). When this system was in the developing stage, the path from GPS satellite to CHAMP passed at the southern side of the rainfall system. Because the observed refractivity was larger than the model first guess at the lowest layer, water vapor at the lower layer was increased when refractivity data was assimilated. The predicted rainfall system using this analyzed field was succeeded to predict the observed one (Fig. 1c). In addition to the occultation data, the ground-based GPS can improve water vapor fields. When both GPS-derived PWV and occultation data were assimilated, the contrast of water vapor across the Baiu front became larger, and then the rainfall prediction was further improved.

In the typhoon case, the occultation data observed by COSMIC were assimilated. COSMIC is composed of 6 LEO satellites and observes over 1500 atmospheric profiles per day. Because occultation events occurr uniformly over the ocean, this data is expected to have great impact for the typhoon prediction. When the initial fields that were directly produced from the global and mesoscale analysis data were used, the predicted typhoon central pressure was not deepened sufficiently. However, when COSMIC data were assimilated, the contrast of water vapor near the low-pressure area became larger, and the typhoon was formed successfully. These results indicate that the occultation data has the potential for improving the mesoscale numerical forecast.

Keywords:GPS occultation, data assimilation

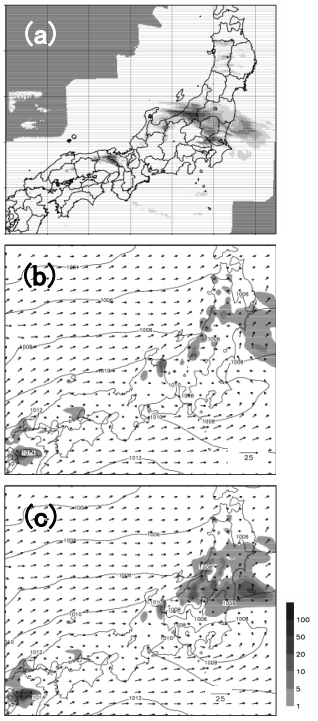

Fig.1 (a) Rainfall distribution observed operational radar. (b) Rainfall distribution predicted from the analyzed fields that was produced by assimilation of only conventional data. (c) Same as (b) except for by assimilation of conventional data and CHAMP data.

TIME EVOLUTION OF THE EAST ASIAN SUMMER MONSOON ANALYSED IN HIGHLY-RESOLUTED GRIDDED PRECIPITATION DATA BASED ON OBSERVED RAIN GAUGES

Natsuko YASUTOMI
Research Institute of Humanity and Nature, Kyoto, Japan
yasutomi@chikyu.ac.jp

Abstract

A highly-resoluted gridded precipitation dataset based on rain gauge observation data network is analyzed and published by the project named Asian Precipitation - Highly-Resoluted Observational Data Integration Towards Evaluation of the Water Resources (APHRODITE's Water Resources). The dataset covers most of Eurasian continent: Monsoon Asia, Russia and Middle East within the grid of 0.05x0.05 degree, 0.25x025 degree and 0.5x0.5 degree. The dataset begins in January 1961 and ends in December 2004 in daily. The 0.25 degree and 0.5 degree versions of the dataset are published on the web (http://www.chikyu.ac.jp/precip).

In this study, seasonal march (averaged over 1961-2000) of the East Asian summer monsoon (Meiyu/Baiu/Changma) is analysed to validate the dataset. Furthermore, changes between averages of 1961-1980 and 1981-2000 are derived to evaluate the effect of the global warming. The climatological mean and change are derived by using 0.05 degree grid.

The structure of the rain band is identified though precipitation of the dataset does not exist over the sea (since observation over the sea surface scarcely exist). Meiyu starts in the middle of May in southern China, and the frontal zone migrates northward. Then Baiu starts in Japan in the middle of June, Changma starts in late June. Distrubution and amount of the precipitation is comparable to the CMAP rainfall.

In the southern China, precipitation amount in the first half of June decreases in the late 20th century. Development and northward migration of the Meiyu front is earlier in 1981-2000 than 1961-1980. The precipitation over the southwestern part of Japan increases in the late 20th century. That is correspondent with the results of global warming simulation (Kusuniki and Mizuta, 2008; Yoshizaki et al., 2005). Baiu starts earlier and ends later in 1981-2000 than 1961-1980, while several breaks are found in the longer rainy season.

Decadal changes in the seasonal march of the East Asian summer monsoon are derived by analysing the long-term, daily high-resolution dataset, APHRODITE's Water Resources. However, number of gauges used in the analysis varies in time. So the trend needs carefully tested.

This work is supported by the Global Environment Reserch Found (GERF-B062).

Keywords: climate system, Asian summer monsoon

DECADAL CHANGE OF THE SOUTH CHINA SEA SUMMER MONSOON ONSET

Yoshiyuki KAJIKAWA and Bin WANG
International Pacific Research Center, University of Hawaii at Manoa, Honolulu, Hawaii, USA.
Email: ykaji@hawaii.edu

Abstract

A significant decadal change in the timing of the South China Sea summer monsoon (SCSSM) onset is detected around 1993/1994: the climatological mean onset day is shifted from beginning of June to middle May after 1993 (Figure 1). The relatively late onsets during the period of 1979-1993 are primarily associated with northward seasonal march of the Intertropical convergence zone (ITCZ), whereas the advanced onsets during 1994-2008 is affected by enhanced northwestward moving tropical disturbance from the equatorial western Pacific. During 1994-2008, enhanced intraseasonal variability (ISV) over the western Pacific is observed in April and May. The number of tropical cyclones (TC) which passed through the South China Sea and Philippine Sea in April and May during 1994-2008 is about doubled compared with those occurring during 1979-1993. Since there is no significant difference of surface pre-condition over the South China Sea and Philippines, the enhancements of the ISV activity and TC genesis after 1994 are major triggers for the advanced SCSSM onset. The SST over the western Pacific has significantly increased between 1980s and 2000s. It is suggested that it makes more favorable background condition for the TC genesis and the ISV activity.

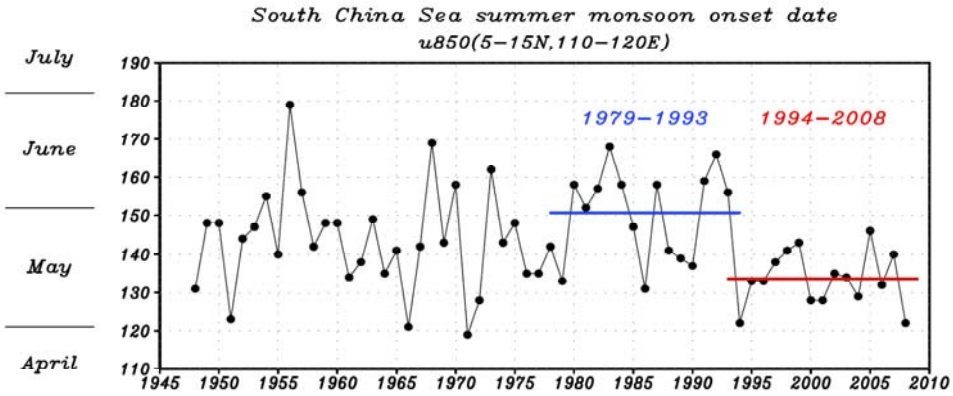

Figure 1
Time series of the SCSSM onset date by using daily mean NCEP/NCAR reanalysis. The definition of the SCSSM onset date is followed as *Wang et al.* [2004].

Keywords: monsoon, onset, decadal change

The Characteristic of Sea Surface Temperature Anomalies in Tropical Ocean and its Influences on the Onset of South China Sea Summer Monsoon

Zhiping Wen and Jieyi Liang
Center for Monsoon and Environment Research /Department of Atmospheric Sciences, Sun Yat-sen University, Guangzhou, P.R. China, 510275
eeswzp@mail.sysu.edu.cn

Abstract

The characteristic of sea surface temperature anomalies (SSTA) in Tropical Ocean and its influences on the onset of South China Sea Summer Monsoon (SCSSM) have been studied by use of 1979~2004 NOAA monthly-mean SST data and 1979~2004 NCAR/NCEP-2 monthly-mean re-analysis data. The results are as follows:

1. Results from EOF analysis show that ENSO is the most significant signal in Tropical Ocean. And it is found that there are two significant oscillations with periods about 5 yr and 10 yr in the variation of temporal coefficient of the EOF of Tropical Ocean SST. The inter-annual variability (5 yr) may be more outstanding than the inter-decadal variability (10 yr).

2. There exists obviously seasonal variation of the correlation pattern between SSTA in the warm pool (WP) area and its adjacent region. Both simultaneous correlation and inter-seasonal correlation between WP SSTA and Equatorial central-eastern Pacific SSTA are significant. The periodic analysis of them during four seasons show that the main period of the oscillation of SSTA in two regions is 4~6 yr. Wavelet coherence (WTC) analysis is conducted for the SSTA in these two sea areas. The results show that the periods with the most significant correlation between WP SSTA and Equatorial central-eastern Pacific SSTA are one-half yr and 2~6 yr .

3. The anomaly of SST in tropical exerts a persistence impact on atmospheric circulation, their correlation is significant in simultaneous and when atmospheric lag 1~3 months.

4. There are close relationship between SCSSM onset and SSTA in Tropical Ocean because of ENSO events. SVD analysis results indicate that positive (negative) phase of ENSO, which means positive (negative) SSTA in central-eastern Pacific Ocean and negative (positive) SSTA in WP, will firstly do favor to a weaker (stronger) Subtropical High over Tropical Western Pacific Ocean and weaker (stronger) convection over “maritime continent”, then lead to the late (early) onset of SCSSM.

5. In La Nĩna pattern, the convection over WP will occur earlier and be stronger than normal, which is in favor of the convergence at lower layer over WP, as well as the strengthen of upwelling branch of Walker circulation, and leads to earlier burst of westerly in the southern SCS. What's more, the convection in Sumatra also appears earlier than normal and has a good advantage to the westerly evolution in eastern Indian Ocean, which will finally result in the splitting of the subtropical high belt and the early onset of SCSSM. However, when the El nĩn o pattern appears, the atmospheric circulation anomaly is reverse.

Key Words: Sea surface temperature anomaly; tropical Ocean; South China sea summer monsoon; ENSO; Cross Wavelet

INFLUENCES OF THE TYPHOON CHANCHU ON THE 2006 SOUTH CHINA SEA SUMMER MONSOON ONSET

Jiangyu MAO and Guoxiong WU

LASG, Institute of Atmospheric Physics, Chinese Academy of Sciences, Beijing, China

mjy@lasg.iap.ac.cn

Abstract

This study reveals some unique features associated with the impact of Typhoon Chanchu on the South China Sea (SCS) summer monsoon (SCSSM) onset in 2006. With Typhoon Chanchu entering the SCS in mid-May, southwesterlies were induced over the SCS and its upstream region due to a thermally forced Rossby wave response, leading to a reversal of low-level winds and a positive meridional temperature gradient (MTG) in the upper troposphere over the SCS. Thus Typhoon Chanchu acted as an immediate trigger for the 2006 SCSSM onset, and the onset date was suggested to occur in the third pentad of May. Such a triggering process was different from the normal SCSSM onset. In the normal onset case, significant southwesterlies are usually present over the northern Indian Ocean before the onset, thus the onset is completed by stronger heating over the land surface north of the SCS. But in the case of 2006, the full development of the significant southwesterlies concurred with the typhoon intrusion. After the typhoon landed in the coast of southern China, it still contributed to the establishment of the SCSSM due to warming the air column over the northern SCS, resulting in a persistent positive MTG with the ridge surface tilting northward. Also found was the generation of the typhoon to be linked with the triggering of the Madden-Julian oscillation (MJO).

Keywords: Summer monsoon onset, Typhoon Chanchu, trigger, and meridional temperature gradient.

DYNAMICS OF A WAVE-LIKE TELECONNECTION PATTERN ALONG THE SUMMERTIME ASIAN JET

Yu KOSAKA[1], Hisashi NAKAMURA[1,2], Masahiro WATANABE[3] and Masahide KIMOTO[3]
[1]Department of Earth ad Planetary Science, University of Tokyo, Tokyo, Japan
[2]Frontier Research Center for Global Change, JAMSTEC, Yokohama, Japan
[3]Center for Climate System Research, University of Tokyo, Tokyo. Japan
ykosaka@eps.s.u-tokyo.ac.jp

Abstract

The Silk Road pattern, a wave-like anomaly pattern observed along the summertime Asian jet, is one of the major teleconnection patterns that can influence East Asian summertime climate. Our analysis based on a reanalysis dataset confirms the conventional notion that the pattern has a characteristic of a free stationary Rossby wavetrain, with its horizontal wavenumber close to the stationary Rossby wavenumber determined by the mean intensity of the jet. However, our analysis reveals its more essential characteristic as a dynamical mode whose extraction of available potential energy from the baroclinic Asian jet is efficient enough for its self-maintenance against dissipative processes. The barotropic energy conversion for the pattern around the western core of the jet over the Aral Sea is efficient enough to compensate the energy loss in other longitudinal sectors, and the conversion is found sensitive to subtle longitudinal structure of the Asian jet. The locally efficient barotropic energy conversion thus acts to anchor the strongest vorticity anomaly around the western jet core and thereby determine the preferred longitudinal phase alignment of the wavetrains as observed. In fact, we can identify a perturbation pattern similar to the observed pattern as the second least-damped mode in a global baroclinic model linearized about the observed mean state for boreal summer whose energetics is similar to that of the observed pattern.

Keywords: dynamical mode, energy conversion, Rossby wave, Silk Road pattern

GENERATION PROCESS OF STABLE LAYERS IN THE LOWER TROPOSPHERE OVER THE INLAND OF INDOCHINA PENINSULA

Masato I. NODZU[1] , Shin-Ya OGINO[2, 3] and Manabu D. YAMANAKA[2, 3]
1: Research Institute for Humanity and Nature, Kyoto, Japan
2: Institute of Observational Research for Global Change, Japan Agency for Marine-Earth Science and Technology, Yokosuka, Japan
3: Graduate School of Science, Kobe University, Kobe, Japan
Corresponding author e-mail address: nodzu@chikyu.ac.jp

Abstract

Thermal budgets are investigated in order to comprehend the seasonal-vertical variation of stable layers in the lower-troposphere over the Indochina Peninsula with the Japanese 25-year Reanalysis (JRA-25).

Stability is defined as increasing rate of potential temperature between the lower and higher levels. Temporal change of potential temperature is separated into three elements: horizontal advection, vertical advection, and apparent heat source (hereafter Q_1). Therefore, a stable layer forms from difference of the three elements between the higher and lower levels. We define a main thermal element as a formation factor for each stable layer comparing the differences.

Composite features in the stable layer formation are characterized along the seasonal march for three stages, Stage-A: Strong and weak cooling by horizontal advection correspond to formation and dissipation of stable layers, respectively, in the boreal midwinter below the 700 hPa; Stage-B: Stable layers form above Q_1 cooling at the 700 hPa level in the latter half of the winter (shown in Figure); Stage-C: Stable layers form below Q_1 heating above the 500 hPa level and coincide with the convective activity in the end of the winter.

The seasonal change of stable layer height can be explained as the variety of characteristic formation factor of stable layers. Stage-A is characterized by intrusions of winter monsoonal cold surge. It is implied that higher stable layers occurrence of Stage-B reflects development of mixing boundary layers due to increasing solar radiation heating. The cooling caused by melting of precipitation at 0℃ level is another possible mechanism for Stage-C.

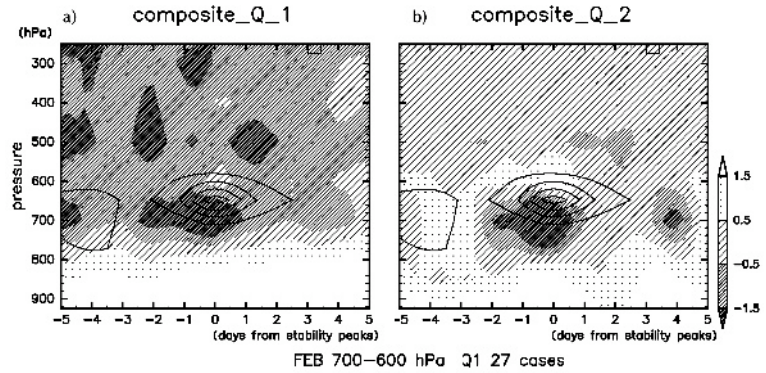

Figure: Time-height sections of composite a) Q_1 , b) Q_2 (K/day) in February over the inland of Thailand (15° N, 105° E). Contours are drawn in the region where stability (vertical gradient of potential temperature: $\Delta\theta/\Delta z$) anomaly is over 0.2 K/km with the interval of 0.4 K/km.

Keywords: stability, seasonal change, monsoon, cold surge

WHY DO DUST STORMS DECREASE IN NORTHERN CHINA CONCURENTLY WITH THE RECENT GLOBAL WARMING?

Congwen ZHU[1], Bin WANG[2] , Weihong QIAN[3]
[1] Chinese Academy of Meteorological Sciences, Beijing 100081, China
Email: tomzhu@cams.cma.gov.cn
[2]Department of Meteorology and International Pacific Research Center, School of Ocean and Earth Science and Technology, University of Hawaii, Honolulu, Hawaii 96822,USA
Email: wangbin@hawaii.edu
[3] Monsoon and Environment Research Group, School of Physics, Peking University, Beijing 100871, China
Email: qianwh@pku.edu.cn

Abstract

Recent studies have shown that the spring dust storm frequency (DSF) in Northern China exhibits an obvious downward trend over the past 50 years concurrently with the recent global warming. We found that the decline of DSF is significantly correlated with the increase of the surface air temperature (SAT) in the region of 70°E-130°E, 45°N-65°N around Lake Baikal, where anthropogenic forcing induces prominent warming in the recent decades. Corresponding to the SAT rise in this region, an anomalous dipole circulation pattern is found in the troposphere that consists of a warm anti-cyclone centered at 55°N and a cold cyclone centered around 30°N. The DSF is positively correlated to the activity of Mongolian cyclones. The warming trend around Lake Baikal possibly induces a weakening of the westerly jet stream and the atmospheric baroclinicity in northern China and Mongolian regions, which suppress the frequency of occurrence and the intensity of the Mongolian cyclones and result in the decreasing DSF in North China. This mechanism will likely further reduce the spring DSF in the future global warming scenario.

Keywords: Global warming, climate change, dust storm, Northern China

Vegetation fraction effect on early summer large rain band in East Asia

T. Yoshikane[1], M. Hara[1,], H. Kawase[2], F. Kimura[1, 3]
[1]*JAMSTEC, Yokohama, Japan;* [2]*NIES, Tsukuba, Japan;* [3]*Tsukuba Univ., Tsukuba, Japan*

Your Abstract: Vegetation fraction effect on early summer large rain band is investigated using a regional climate model. We use the WRF Ver.2.2 in this study. The calculation domain is almost global scale except for the polar circle. The spacing grid is 50km. In the STANDARD run, the initial and boundary conditions are estimated from ten-day averaged global zonal mean of ERA40 data in middle June of 1998. The simulation is time-integrated during 90 days without the seasonal change of the radiation and the vegetation fraction distribution. The first ten-day period is defined as a spin-up duration and the last 80 days period is evaluated as the simulation result. The radiation and vegetation fraction distribution are fixed in 15 June during the time integration. The large-scale features of rain band, which is indicated by previous studies, are well simulated in STANDARD run. The amount of rainfall is very small in northern China, while the amount is very large in southern China. In DEFOREST run, which is same as STANDARD run except for 0% vegetation fraction in whole of the domain, the precipitation is remarkably decreased even in southern China. In FOREST run, which is same as STANDARD run except for 99% vegetation fraction only in artificially land use area, the precipitation is drastically changed in northern China and the rain band move to north. It is speculated that the formation of the large rain band is greatly influenced by the vegetation fraction distribution in China.
.

Impacts of land use changes between 1700 and 1850 on monsoon seasonal changes

Jun Matsumoto[1], Ryoji Yamashima[1] and Kumiko Takata[2]

[1]Department of Geography, Tokyo Metropolitan University (Jun@center.tmu.ac.jp)

[2]JAMSTEC/FRCGC

Key words: monsoon, seasonal changes, land use change impact

In the present study, as did in Takata et al. (2009), impacts of historical land uses changes (HLUC) between 1700 and 1850 on Asian summer monsoon are investigated by conducting AGCM experiments. Research focus has set on the Asian monsoon seasonal changes, in particular, difference between India and China. We conducted two numerical experiments, 1700VEG and 1850VEG, by using a MIROC3.2 coupled a MATSIRO.

As a result, we found that the land use changes from natural forest to man-induced cultivation delay the beginning in summer rainy season over the Indian subcontinent, while they bring about early end of summer rainy season. On the other hand, they bring about both early beginning and end of rainy season in South China. We also found that they also have impacts on broad-scale Asian summer monsoon later onset and earlier withdrawal.

SIMULATED EAST ASIAN SUMMER MONSOON IN FGOALS-S1.1

Qing BAO[1], Guoxiong WU[1], Yimin LIU[1], Jing YANG[2], Zaizhi WANG[3] and Tianjun ZHOU[1]

[1]State Key Laboratory of Numerical Modeling for Atmospheric Sciences and Geophysical Fluid Dynamics (LASG), Institute of Atmospheric Physics, Chinese Academy of Sciences, Beijing, China
[2]State Key Laboratory of Earth Surface Processes and Resource Ecology Beijing Normal University Beijing, Beijing, China
[3] Beijing Climate Center, China Meteorological Administration, Beijing, China

baoqing@mail.iap.ac.cn

Abstract

The spectral version 1.1 of Flexible Global Ocean-Atmosphere-Land System (FGOALS-s1.1) is developed in State Key laboratory of Numerical Modeling for Atmospheric Sciences and Geophysical Fluid Dynamics in Institute of Atmospheric and physics (LASG/IAP). This paper firstly reports the major modifications of physical parameterization package in its atmospheric component, including radiation scheme, convection scheme and cloud scheme. Afterwards, the simulation of East Asian Summer Monsoon (EASM) in FGOALS-s1.1 is particularly examined in mean state and interannual variability.

The simulated results indicate that FGOALS-s1.1 exhibits significant improvements in the simulation of the balance of energy at the top of the atmosphere; the net radiative energy fluxes at the top are about 0.003W/m2 in 40 years fully coupled integration. The distributions of sea surface temperature in the model are quite reasonable, no obvious climate drift is found. FGOALS-s1.1 also show a strong ability to simulate East Asian Summer Monsoon (EASM) climatologically, and the simulations of main rainfall centers, seasonal match of precipitation and lower level monsoon flow are highly consistent with the observations in EASM regions. Nevertheless, the model underestimates the upper level jet flow in East Asia and western Pacific subtropical high.

On the other hand, the simulation of the EASM leading patterns and its relationship with sea surface temperature are also examined. The results show that FGOALS-s1.1 can fairly reproduce the leading pattern of EASM and its close relationship with the decay phase of ENSO, but the model have no significant skill to reproduce both the second major mode of EASM and its relationship with the developing phase of ENSO.

Keywords: Simulation, EASM, FGOALS-s

DIURNAL VARIATION OF THE SIMULATED PRECIPITATION OVER EAST ASIA

Myung-Seo KOO and Song-You HONG
Department of Atmospheric Science, Yonsei University, Seoul, Korea
mskoo@yonsei.ac.kr

Abstract

Simulation of precipitation has been recognized as one of the most difficult problems in modeling weather and climate system. In atmospheric models, it can be produced by not only the grid-resolvable forcing explicitly but also sub-grid processes using cumulus parameterization so that many uncertainties still remain in correctly reproducing observed precipitation. Particularly its diurnal cycle is actual phenomena, which may be changed with the season as a changing circulation pattern may lead to changes in the dominating physical process giving rainfall in a region or different with geographical features, but very challenging task in atmospheric models.

The purpose of this study is to compare the performances of two different regional climate models (RCMs) focusing on the diurnal variation of precipitation over East Asia. The studies on the diurnal variation of precipitation in model experiments can serve the validation of various physical parameterizations, and enhance our understanding of the importanat mechanisms embedded within atmospheric phenomena. The used RCMs are the Weather Research and Forecasting (WRF) model and National Centers for Environmental Prediction (NCEP) Regional Spectral Model (RSM), which are compared with the Tropical Rainfall Measuring Mission (TRMM) Multi-satellite Precipitation Analysis (TMPA) for observation data. Note that the previous modeling studies using the TRMM satellite-derived data are limited to the precipitation over the tropical regions, especially uncommon over East Asia, and that the selected RCMs are rarely compared each other with a focus of the diurnal cycle of precipitation.

The preliminary results showed that the RCMs well reproduces the diurnal variation of observed precipitation, which is dominated by 1st harmonic (diurnal cycle). However, it was found that the simulations tend to lag its phase about one or two hours, and to overestimate (underestimate) the amplitude over land (oceans). Moreover, different chracteristics between the simulations was also apparent with region (Land/Oceans or Korea/Japan/China) or in amplitude and phase. Further details will be discussed in the conference.

Keywords: diurnal cycle, precipitation, East Asia, RCM, TMPA

Towards local air–sea interaction in ITCZ simulations

Anmin Duan[1], Chung-Hsiung Sui[2], and Guoxiong Wu[1]

1. State Key Laboratory of Numerical Modelling for Atmospheric Sciences and Geophysical Fluid Dynamics (LASG), Institute of Atmospheric Physics (IAP), Chinese Academy of Sciences (CAS), Beijing, China

2. Graduate Institute of Hydrological and Oceanic Sciences, National Central University, Jhongli, 320, Taiwan (R.O.C)

Abstract

We investigate the cause of a double Inter-Tropical Convergence Zone (ITCZ) problem produced by the SAMIL2.08 atmospheric general circulation model (AGCM). In the AGCM control run with the observed sea surface temperature (SST) forcing field, there occur related problems of excessive precipitation over much of the Tropics and insufficient precipitation over the equatorial Indian Ocean and the Pacific. The equatorial drought belt arises from the compensatory descending motion associated with exaggerated deep convection over the Tropics in both hemispheres. The double ITCZ disappears in a coupled experiment with the same AGCM coupled to an interactive ocean mixed layer within the great warm pool. Similar results are obtained in another sensitivity experiment with the AGCM driven by the SST field derived from the coupled run. The two experiments demonstrate the fundamental role of air–sea interaction in maintaining the climate mean state through the following reactions. Local air–sea flux exchanges in tropical convective regions such as the ITCZ tend to cool SST via negative SST–precipitation feedbacks. Such changes further modify the tropical atmospheric circulation structure such that the equatorial compensatory descent in the AGCM control run is replaced by the equatorial convergence zone, as seen in nature. Therefore, in addition to improvements in physical parameterization schemes, a reasonable depiction of the air–sea coupling process is necessary to completely overcome the double-ITCZ problem, as the atmosphere is closely coupled with the ocean over the Tropics.

REGIONAL-SCALE INTERACTIONS AMONG LAND, OCEAN AND ATMOSPHERE IN REGIONAL CLIMATE SIMULATIONS OF EAST ASIAN SUMMER MONSOON

Dong-Hyun CHA and Dong-Kyou LEE
School of Earth and Environmental Sciences, Seoul National University, Seoul, Korea
atmos77@nwp2.snu.ac.kr

In the East Asian summer monsoon (EASM), regional-scale interactions among land, ocean and atmosphere were investigated through sensitivity experiments to local SST and soil moisture using a regional climate model. In both strong and weak EASM years, local SST anomaly which resulted from anomalous large-scale features played a role to decrease the anomalies of local Hadley circulation, low-level westerly between the Indian Ocean and the South China Sea, and the western North Pacific subtropical high. Consequently, the decreased anomalies resulted in the decrease of precipitation anomaly. The negative feedback process between soil moisture and precipitation was relatively dominant over East Asia as compared with the positive feedback process between them. The impact of soil moisture on the EASM was considerably weak, because not only the soil moisture anomaly was small but also the negative and positive feedback processes canceled out each other. Therefore, in EASM of the extreme years, precipitation anomaly was substantially attributed to the effect of local SST anomaly rather than that of soil moisture anomaly.

Keywords: East Asian summer monsoon, Regional climate model, Regional-scale interactions among land, ocean and atmosphere.

Can the uncertainties on the MJO-related equatorial zonal wind forcing cause a significant spring predictability barrier for El Nino events?

Wansuo DUAN and Mu MU
LASG, Institute of Atmospheric Physics, Chinese Academy of Sciences, Beijing, China
Email: duanws@lasg.iap.ac.cn

Abstract

Within a theoretical ENSO model, the effect of the external MJO-related equatorial zonal wind forcing on ENSO predictability is explored by the approach of condition nonlinear optimal perturbation (CNOP). We reduce the MJO-related wind forcing into a simple sine function with amplitude, period, and phase, and consider the uncertainties in the MJO-related wind forcing originating from those in the parameters of amplitude, period, and phase of sine function representing external wind forcing. By investigating the optimal parameter perturbation standing for the parameter error that has the largest negative effect on the prediction results, we find that this kind of uncertainties in the MJO-related wind forcing do not behave a significant season-dependent evolution in the adopted model, failing to yield a spring predictability barrier (SPB) phenomenon for ENSO events. However, when the optimal initial errors are superimposed on the ENSO events, there occurs a significant season-dependent evolution with the largest error growth rate occurring in spring and cause the SPB phenomenon for ENSO events. When we consider both the initial error and the parameter error in the adopted model, the error growth rate during spring becomes smaller and smaller with the increasing parameter errors. It is therefore inferred that the errors in the external MJO-related equatorial zonal wind forcing could not be responsible for the SPB for ENSO events, while the initial error would be the dominant contribution to the uncertainties of ENSO prediction related to the SPB.

Keywords: predictability, ENSO events, optimal perturbation, parameter

AN AGCM STUDY ON THE TELECONNECTION OF IOD TO THE TIBETAN PLATEAU IN EARLY WINTER

Chaoxia YUAN, Tomoki TOZUKA and Toshio YAMAGATA
Department of Earth and Planetary Science, Graduate School of Science,
The University of Tokyo, Tokyo, Japan
yuan@eps.s.u-tokyo.ac.jp

Abstract

The excessive snow accumulation in winter over the Tibetan Plateau (TP) can lower the ground temperature till the subsequent spring and early summer through albedo and hydrological processes. Thus the decreased ground temperature reduces the land-sea thermal contrasts and impacts the Asian summer monsoon. Therefore, understanding of the interannual variation in winter snow over TP contributes to the monsoon prediction. Using observation data, Yuan et al. (2009) found a significant positive partial correlation between Indian Ocean Dipole (IOD) and the Tibetan snow cover in early winter. In the pure positive IOD years with no co-occurrence of El Niño, the negative geopotential height anomalies are present north of India and associated with warm and moist southwesterlies that enter TP from the northern Indian Ocean after rounding cyclonically and supply more moisture. This leads to more precipitation and more snow cover over the plateau.

To understand origins of the circulation anomalies, an AGCM called FrAM is used to perform sensitivity experiments with various SSTA forcings. Results show that with SSTA forcing in all basins, FrAM is capable of reproducing the circulation anomalies over the Eurasian continent in the early winter of positive IOD years. The anomalous moisture transport from the northern Indian Ocean to TP due to the negative geopotential height anomalies north of India is also well simulated. With the SSTA forcing only within the tropical Indian Ocean, the circulation anomaly pattern is also reproduced with the amplitude about half of that with the SSTA forcing in all basins.

Keywords: IOD, Teleconnection, Rossby Wave, Tibetan Plateau, Snow Cover

The impact of Atlantic Ocean on the multidecadal fluctuation of ENSO–south Asian monsoon relationship in a coupled GCM

Wei Chen[1], Riyu Lu[1], and Buwen Dong[2]

[1] Center for Monsoon System Research, Institute of Atmospheric Physics, Chinese Academy of Sciences, Beijing 100029, China
[2] Walker Institute for Climate System Research, University of Reading, and National Centre for Atmospheric Science-Climate, Reading, UK
Email：chenwei@mail.iap.ac.cn

Abstract

The multidecadal variability of El Niño-Southern Oscillation (ENSO)–South Asian monsoon relationship is elucidated in a 1000-year control simulation of a coupled general circulation model (GCM). The results indicate that the Atlantic Multidecadal Oscillation (AMO), resulting from the fluctuation of Atlantic Thermohaline Circulation (THC), plays an important role in modulating the multidecadal variation of ENSO–monsoon relationship. The sea surface temperature (SST) anomalies associated with the AMO induce not only significant climate impact in the Atlantic, but also the coupled feedbacks in the tropical and North Pacific regions. The remote response to a positive phase of AMO in the Pacific ocean is characterized by a warming in North Pacific, a relaxation of tropical easterly trades in the central and east tropical Pacific and a deeper thermocline in the tropical east Pacific. These changes in mean states lead to a reduction of ENSO variability, and therefore a weakening of the ENSO–monsoon relationship. This study suggests a non-local mechanism for the low frequency fluctuation of ENSO–monsoon relationship.

Keywords: ENSO–south Asian monsoon relationship, multidecadal fluctuation, Atlantic Multidecadal Oscillation (AMO)

RECENT PROGRESS ON THE STUDY OF LAND-ATMOSPHERIC INTERACTION OVER THE TIBETAN PLATEAU AREA

Yaoming MA
Laboratory of Tibetan Environment Changes and Land Surface Processes, Institute of Tibetan Plateau Research, the Chinese Academy of Sciences, Beijing , China,
E-mail: ymma@itpcas.ac.cn

Abstract

As a unique geological and geographical unit, the Tibetan Plateau dramatically impacts the world's environment and especially controls climatic and environmental changes in China, Asia and even in the Northern Hemisphere. Tibetan Plateau, therefore, provides a field laboratory for studying global change. With support from various agencies in the People's Republic of China, a Tibetan Observation and Research Platform (TORP) is now implementing. Firstly the background of the establishment of the TORP, the establishing and monitoring plan of long-term scale (5-10 years) of the TORP has been introduced. Then the preliminary observational analysis results, such as the characteristics of land surface heat fluxes and CO_2 flux partitioning, the characteristics of atmospheric and soil variables, the structure of the Atmospheric Boundary Layer (ABL) and the turbulent characteristics have also been shown.

The study on the regional distribution of land surface heat fluxes of paramount importance over heterogeneous landscape of the Tibetan Plateau. Therefore, here the parameterization methods based on satellite data (NOAA/AVHRR, Landsat-7 ETM, ASTER and MODIS) and ABL observations have been proposed and tested for deriving surface reflectance, surface temperature, NDVI, MSAVI, vegetation coverage, LAI, net radiation flux, soil heat flux, sensible heat flux and latent heat flux over heterogeneous landscape. As cases study, the methods were applied to the experimental area of the CAMP/Tibet (CEOP (Coordinated Enhanced Observing Period) Asia-Australia Monsoon Project (CAMP) on the Tibetan Plateau), which located at the central Tibetan Plateau and the whole Tibetan Plateau area. Five scenes of Landsat-7 ETM data, four scenes of NOAA/AVHRR data, three scenes of ASTER data and four MODIS data were used in this study. To validate the proposed methods, the ground-measured values are compared to satellite derived values. The results show that the derived surface variables and land surface heat fluxes over the study area are in good accordance with the land surface status. These parameters show a wide range due to the strong contrast of surface features. And the estimated land surface variables and land surface heat fluxes are in good agreement with ground measurements, and all their absolute percent difference is less than 10% in the validation sites. It is therefore concluded that the proposed methods are successful for the retrieval of land surface variables and land surface heat fluxes over heterogeneous landscape of the Tibetan Plateau area. Further improvement of the methods and its applying field were also discussed.

Key Words: recent progress; land-atmospheric interaction; Tibetan Plateau

THE INCREASE IN ATMOSPHERIC TEMPERATURE OVER THE TIBETAN PLATEAU IN EARLY SPRING AND PRE-MONSOON SEASON

Kenji TANIGUCHI[1], Toru TAMURA[2], Toshio KOIKE[2], Ken'ichi UENO[3] and Xiangde XU[4]
1: Faculty of Environmental Design, Kanazawa University, Kanazawa, Japan
2: Department of Civil Engineering, The University of Tokyo, Tokyo, Japan
3: Graduate School of Life and Environmental Sciences, University of Tsukuba, Tsukuba, Japan
4: Chinese Academy of Meteorological Sciences, Beijing, China
taniguti@t.kanazawa-u.ac.jp

Abstract

Seasonal differences in atmospheric temperature increases were investigated using radiosonde observation data in two regions of the Tibetan Plateau (Naqu and Gaize) for 2008. Intensive radiosonde observations in the two observation sites revealed the characteristics of the atmospheric structure and an increase in atmospheric temperature at the early spring and in the pre-monsoon season in 2008. The 6-hourly increase in potential temperature (PT) had a clear diurnal cycle. This indicated that the atmosphere warmed with the development of a mixing layer during the daytime in both observation periods. The total increase in PT during each observation period is quite different between the early spring and the pre-monsoon season. The total increase in PT showed a significant temperature rise in the pre-monsoon season in the upper troposphere but not in the early spring. Such a seasonal difference is observed for both Gaize and Naqu. In daytime, significant increase in PT was observed from the surface to above the mixing layer in both regions during the two observation periods. Seasonal variation of cumulus activity was investigated using MTSAT observation data from February to July around the both observation sites. The results indicated that latent heat was released in the upper troposphere by cumulus cloud at early spring in both Gaize and Naqu. On the other hand, cumulus activity hardly occurs in pre-monsoon season. The mixing layer is shallower in IOP2 than in IOP1, but there is a large increase in PT in the upper layer. The results from the radiosonde observations and MTSAT data suggest the significant increase in PT during IOP2 is not because of either dry thermal convection or a latent heat release in the upper layer by cumulus activity. The resutls of synoptic scale analyses using JMA Climate Data Analysis System (JCDAS) data indicated that the variation in PT in the upper layer is affected by horizontal advection ralated to mid-latitude atmospheric conditions during the pre-monsoon season. At the same time, convective activities around the South Asia was also indicated to affect the atmospheric conditions around the plateau.

Keywords: Tibetan Plateau, atmospheric temperature, seasonal variation

IMPACTS OF LAND-SURFACE CONDITION ON FORMATION OF LOW-LEVEL CONVERGENCE AND DEVELOPMENT OF MESOSCALE CONVECTIVE SYSTEMS OVER THE TIBETAN PLATEAU

Shiori Sugimoto and Kenichi Ueno
University of Tsukuba, Tsukuba, Japan
Email: shioris@geoenv.tsukuba.ac.jp

Abstract

Over the Tibetan Plateau, mesoscale convective systems (MCSs) occur during monsoon season, although absolute amount of atmospheric moisture is small because of low pressure and low temerature conditions. Generally, vertical wind shear, convective instability, and large-scale low-level convergence play important roles in formation of MCSs. It is revealed in previous studies that convective instability associated with thermal forcing is one of factor in MCSs formation. However, impact of large-scale low-level convergence on MCSs development has not been discussed yet. In this study, formation mechanisms of low-level convergence and the MCSs were revealed using a numerical model, focusing on land surface condition. According to numerical simulation, plateau-scale low was formed by heating from land surface. Cyclonic circulation associated with this low was maintained in the nighttime and moved eastward especially from night to next morning. Low-level convergence developed at southeastern edge of the plateau-scale low, and the MCSs was generated over the this convergence area. We will present about 1) detail mechanisms of maintenance/movement of cyclonic circulation during the nighttime and 2) effect of plateau-scale distribution of sensible/lantent heat flux on formation of low-level convergence and the MCSs.

Keywords: Mesoscale convective systems, Tibetan Plateau, Land-surface condition

USE OF A DENSE RAIN-GAUGE NETWORK OVER MONSOON ASIA FOR IMPROVING BLENDED TRMM PRODUCTS AND DOWNSCALED WEATHER MODELS

Akiyo YATAGAI[1]*, T. N. KRISHNAMURTI[2], A.K. MISHRA[2], and Anu SIMON[2]
[1]Research Institute for Humanity and Nature, Kyoto, Japan
[2]Dept. of Meteorology, Florida State University,Tallahassee, FL, USA
*akiyo@chikyu.ac.jp

Abstract

This study makes use of a network of nearly 2100 rain gauges over India in order to statistically modify the Tropical Rainfall Measuring Mission (TRMM) algorithm 3B42. The validation and usefulness of the modified product is determined against rain gauge datasets and from the training and forecast phase of the Florida State University (FSU) multimodel superensemble. We use downscaled member model forecasts to construct superensemble forecasts. The member model forecasts are scaled down using the modified high-resolution TRMM rains during the training phase of the multimodel superensemble. We demonstrate that a mesoscale superensemble thus constructed carries higher forecast skills compared to all of the member models as well as compared to the ensemble mean (ENSM) and bias-corrected ensemble mean (BcorENSM). The forecast procedure includes a high-resolution downscaling of the model forecast rain and the construction of a multimodel superensemble. This procedure clearly provides a much-improved forecast of rain using skill metrics such as equitable threat scores (ETSs), anomaly correlations, root mean square (RMS) errors, and their bias scores. We also demonstrate that the performance of this modified TRMM algorithm provides results very clearly comparable to those obtained from the direct use of rain gauges throughout India. Similar studies are underway for the East Asia by using a rain-gauge based daily precipitation product developped by Asian Precipiation –Highly-Resolved Observational Data Integration Towards Evaluation of the Water Resources (APHRODITE's water resources) project.

Keywords: precipitation, rain-gauge, super-ensemble, TIGGE, TRMM

THE INTERDECADAL CHANGE OF RELATIONSHIP BETWEEN ENSO AND EAST CHINA SUMMER RAINFALL

YE Hong, LU Riyu
Institute of Atmospheric Physics, Chinese Academy of Sciences, Beijing, China
yehong@mail.iap.ac.cn

Abstract

After the late 1970s the relationship between El Niño-Southern Oscillation (ENSO) and the eastern China summer-mean rainfall is weakened significantly. However, the cause is still not clear. In this study we examined the interdecadal change in the sub-seasonal evolution of relationship between ENSO and the eastern China rainfall with monthly and ten-day rainfall data in summer. The results show that before the late 1970s, the spatial distribution of the ENSO-related eastern China rainfall in June, July and August are similar. However, after the late 1970s the signs of ENSO-related eastern China rainfall anomalies, especially in south China and Huai River-Yellow River valley, in June are opposite to that in August. Hence, the ENSO's effect on the summer-mean eastern China rainfall decreases remarkably after the late 1970s. The change in sub-seasonal evolution of ENSO-related eastern China rainfall may be attributed to the enhancement and westward extension of the western North Pacific subtropical high and the southward displacement of the East Asian upper-tropospheric jet stream in the decaying phase of El Niño after the late 1970s. This study, thus, provide a new perspective of the decadal change in the ENSO's effect on eastern China rainfall.

Keywords: ENSO, eastern China, summer rainfall, decadal change, subseasonal scale

CONTRIBUTION OF THE INDIAN OCEAN SSTA TO THE IMPACTS OF EL NINO ON THE ATMOSPHERIC CIRCULATION OVER EAST ASIA

SUN-Xuguang[1, 2] YANG-Xiuqun[1] ZHAO-Shanshan[3] ZHU-Yimin[4] LIN-Yihua[2]

[1]School of Atmospheric Sciences, Nanjing University, Nanjing, China

phone: +86-025-83597203, E-mail: xgsun@nju.edu.cn

2LASG, Institute of Atmospheric Physics, Chinese Academy of Sciences, Beijing, China

3 National Climate Center, China Meteorological Adminstration, Beijing, China

4Institute of Meteorology, PLA University of Science and Technology, Nanjing, China

Abstract

Based on the time-varying composite sea surface temperature anomaly (SSTA) in the tropical Pacific-Indian Ocean by 8 significant El Nino events (1957/58, 1965/66, 1972/73, 1976/77, 1982/83, 1986/87, 1991/92, 1997/98) during the period from 1949 to 1998, contribution of the Indian Ocean SSTA to the impacts of El Nino during its different stages on the interannual climate variability over East Asia is studied. Three experiments are carried out, i.e., TPOGA, TPIOGA and CTRL, with time-varying composite SSTA and climatological SST prescribed in the tropical Pacific, the tropical Pacific-Indian Ocean, and the whole ocean, separately. To reduce the internal variability, each experiment contains 10 realizations with different initial conditions. Ensemble results show that, during the El Nino developing summer (during both the El Nino maturing winter and decaying summer), SSTA in the tropical Indian Ocean manifests as a "West Positive and East Negative" dipole pattern (Basin Warming mode), and it can enhance (reduce) the effects of SSTA in the tropical Pacific which causes obvious divergence and convergence at higher troposphere over both the tropical Pacific-Indian Ocean and East Asia, therefore, the atmospheric responses are accordingly strong (weak). And at the same time, due to the presence of the SSTA in the tropical Indian Ocean, the simulation of the impacts of El Nino on the climate variability over East Asia is much more comparable with the analyses results of NCEP reanalysis data. On the other hand, during the El Nino developing and decaying summers, the atmospheric response over the Indian Ocean in the TPIOGA is almost reverse to that in the TPOGA, indicating that the SSTA in the tropical Indian Ocean mainly determines the local atmosphere variability and reduces the impacts of that in the tropical Pacific during these time periods. However, during the El Nino maturing winter, the atmospheric responses in the TPOGA and the TPIOGA closely resemble each other over the Indian Ocean, indicating the comparable impacts of the SSTA in both the tropical Indian Ocean and the tropical Pacific, and during this time, the SSTA in the tropical Indian Ocean acts as an intensifier.

Keywords: El Nino, SSTA, tropical Pacific Ocean, tropical Indian Ocean

Role of Subtropical Precipitation Anomalies in Maintaining the Summertime Meridional Teleconnection over the Western North Pacific and East Asia

Riyu Lu and Zhongda Lin

Institute of Atmospheric Physics, Chinese Academy of Sciences, Beijing, China

Abstract

The meridional teleconnection patterns over the western North Pacific and East Asia (WNP−EA) during summer have a predominant role in affecting East Asian climate on the interannual time scale. A well-known seesaw pattern of tropical-subtropical precipitation is associated with the meridional teleconnection, and the subtropical precipitation anomaly has been previously viewed as a result of anomalous circulations associated with the teleconnection.

In this study, however, the authors suggest that subtropical precipitation anomalies, in turn, can significantly affect large-scale circulations and may be crucial for maintenance of the meridional teleconnection. Diagnosis by using observational and reanalysis data indicates that the meridional teleconnection patterns are clearer in summers when the subtropical rainfall anomalies are greater. The simulated results by a linear baroclinic model indicate that a subtropical heat source, which is equivalent to the diagnosed positive subtropical precipitation anomaly, induces zonally-elongated zonal wind anomalies that resemble the diagnosed ones in both the upper and lower troposphere over the extratropical WNP-EA. The simulated results also indicate that the horizontal and vertical structures of circulation responses are insensitive to the locations and shapes of imposed subtropical heat anomalies, which implies the important role of basic flow in circulation responses. This study suggests that for confidential dynamical seasonal forecasting in East Asia, general circulation models should be required to capture the features of interannual subtropical rainfall variability and basic-state flows in WNP-EA.

Some results on the seasonal variation of the meridional teleconnections will be also given in the presentation.

Abrupt Northward Jump of the East Asian Upper-tropospheric Jet Stream in Mid-summer

Zhongda Lin and Riyu Lu

Center for Monsoon System Research, Institute of Atmospheric Physics, Chinese Academy of Sciences, Beijing, China
E-mail: zdlin@mail.iap.ac.cn

Abstract

In this study we document the abrupt seasonal migration of the East Asian upper-tropospheric jet stream (EAJS) in boreal mid-summer over the East Asian coast, based on the NCEP/NCAR reanalysis data from 1958 to 2002. In climatology, an abrupt northward jump of the EAJS is identified in late July. By examining each of the total 45 years there are 27 years in which the EAJS exhibits an abrupt northward jump in mid-summer, and about half of the jump cases occur in late July, suggesting the characteristic of phase locking with the calendar year. A cluster analysis on the meridional variation of the upper-tropospheric zonal wind anomalies along the eastern Asian coast associated with the northward jump of the EAJS reveals that the northward jump of the EAJS is dominated by two categories, in which the intensity of the EAJS is enhanced and weakened, respectively. For both categories, there is a pair of westerly and easterly anomalies which are located to the north and south of the EAJS's axis. However, these westerly and easterly anomalies exhibit distinct temporal variations between the two categories: The pair of westerly and easterly anomalies shifts southward from the high latitudes to the EAJS region for the first category, but appears as a quasi-stationary meridional dipole pattern for the second category.

Key words: East Asian upper-tropospheric jet stream (EAJS), abrupt northward jump, cluster analysis

CHANGE IN SUMMER PRECIPITATION STRUCTURE IN KOREAN PENINSULA DURING MID-1990S

WonMoo KIM[1)], Jong-Ghap JHUN[1)] and Bin WANG[2)]
[1)]School of Earth and Environmental Sciences, Seoul National University, Seoul, Korea
[2)]International Pacific Research Center, University of Hawaii, Honolulu, USA
kwmski7@snu.ac.kr

Abstract

It is reported that there had been a significant change in east Asian summer monsoon ciculation during mid-1990s, and previous studies have revealed that the temporal distribution of summer precipitation in Korea has altered during the similar period.

In early part of summer (May-June), northward migration of the rainband, so called Meiyu (China), Baiu (Japan), or Changma (Korea), is the main feature over the east Asian monsoon region. Such rainband seems to migrate faster in recent decade, resulting a draught in late spring and increased rainfall in early July.

After the prolonged rainy period, or Changma, there had been (1979-1993) a clear monsoon break from late July to mid-August, which is then followed by secondary rainfall period. In recent decade, such a break in monsoon is lost and rainfall amount in late July to early August had increased significantly. There seems to have some shift in Typhoon track approaching to the peninsula although the number doesn't change. Such a change is related to the shift in position of westward flank of North Pacific high in the break period, which, in tern, affects the moisture flux to the monsoon trough. These changes dominate as a trail of positive and negative anomalies along the eastern edge of continent.

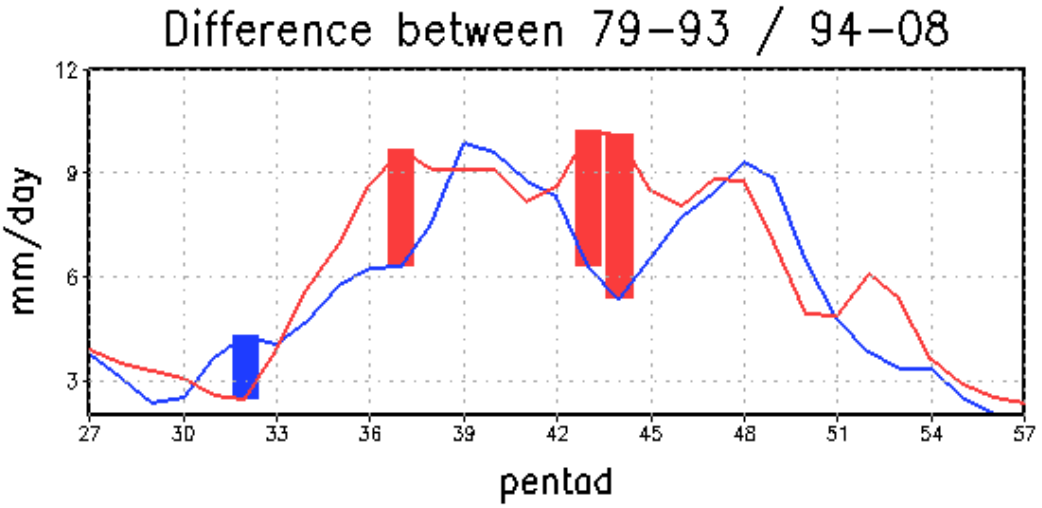

Keywords: monsoon, decadal change, summer precipitation

ON THE PRECIPITATION PEAK AROUND THE NORTHWESTERN KYUSHU IN JAPAN AS THE SEASONAL TRANSITION FROM MIDSUMMER TO AUTUMN RAINFALL (AKISAME) SEASON IN EAST ASIA

Yoshinori MORI and Kuranoshin KATO*
Graduate School of Education, Okayama University, Okayama, Japan
Email: kuranos@cc.okayama-u.ac.jp (Corresponding Author, KATO)

Abstract

In East Asia, the two significant rainy seasons called the Baiu and the Akisame (Autumn Rainfall) appear before and after midsummer,respectively. As for the Baiu (which is called the Meiyu in China and the Changma in Korea), many studies have been made so far. On the other hand, characteristics of large-scale fileds in the Akisame season have also examined by some previous studies comparing with those in the Meiyu/Changma/Baiu season. However, transition from midsummer to Akisame season has not been understood yet, and the present study will pay attention to that transition based on the analyses of operational observation data from 1971 to 2000.

In the western part of Kyushu District in Japan, precipitation attains the maximum from late August to early September as the climatological seasonal transition, before so-called the Akisame season in most part of the Japan Islands. According to the EOF analysis based on the 11-day running mean daily precipitation at the 141 stations (whole Japan Islands area), the score of the second EOF indicating such pattern presented the maximum from late August to early September. It is noted that the precipitation peak at that period was limited to the northwestern part of Kyushu. Furthermore, the precipitation there in that period was greatly contributed to by the relatively heavy rainfall events such as more than 50 mm/day.

It is well known that the typhoons also tend to affect the large precipitation over the Japan Islands in the Akisame season. From late August to early September, although appearance frequency of typhoons or tropical depression in East Asia is no so low, the precipitation directly related to the typhoons (including to the interaction to the Autumn rainfall front) contributed only to about 30% of the total precipitation around the northwestern Kyushu at that period.

Although the eastward pressure gradient in the subtropical area to the south of Japan is not so large and the time mean low-level southerly wind toward the Japan Islands is not so strong in the Akisame season, the wide spread low pressure area in South Asia associated with the monsoon still remained at the beginning of September. This would result in the relatively strong southerly wind toward the frontal zone just to the north of Kyushu. Such "large-scale" situation, in addition to intrusion of the relatively cool air from the continent, would result in the "regional" climatological precipitation peak around the northwestern Kyushu (warm sector of the front) at that period.

Keywords: Autumn rainfall, Seasonal transition, Climate System in East Asia

Long-Term Variability of Hadley and Walker Circulation Intensities Shown in Water Vapor Transport Field

Byung-Ju Sohn and Seong-Chan Park

School of Earth and Environmental Sciences
Seoul National University, NS80, Seoul, 151-747, Korea
Tel: +82-2-880-7783 Fax: +82-2-874-3289
Email: sohn@snu.ac.kr

Abstract

The interannual variations of the atmospheric circulation over the tropical oceans were investigated by using the divergent component of water vapor transport field ($\mathbf{Q}_D$) derived from the Special Sensor for Microwave Imager (SSM/I) and the global reanalysis data such as the National Centers for Environmental Prediction (NCEP) and the European Centre for Medium-Range Weather Forecasts (ECMWF) 40-year Reanalysis (ERA40). Introducing an effective wind ($\mathbf{V}_E$) to remove the effect of trend in the total precipitable water (W), the divergent component of effective wind ($\mathbf{V}_E$) can be obtained from $\mathbf{V}_E=\mathbf{Q}_D/W$, and its associated divergence $(\nabla \bullet \mathbf{V}_E)$ and effective velocity potential (Φ_E) are readily calculated from the obtained $\mathbf{V}_E$ and a relationship of $(\nabla \bullet \mathbf{V}_E = -\nabla^2 \Phi_E)$, respectively. Since the total precipitable water resides mainly in the lower tropospheric layer, the effective wind may largely represent a divergent wind of a lower tropospheric boundary layer. The obtained effective winds ($\mathbf{V}_E$) and the convergence of effective wind $(-\nabla \bullet \mathbf{V}_E)$ are then used for calculating the Hadley and Walker circulation index.

The Hadley circulation index obtained from both ERA40 and NCEP reanalysis indicates the intensifying trend during the boreal winter whereas no clear trend is found during the boreal summer, although there is an increasing trend after 1979. On the other hand, the Walker circulation index shows a weakening trend for last fifty years, consistent with recent fluctuations of El Niño signal. Despite larger fluctuation signals found during El Niño years, an opposite trend after 1979. The recent trend of Walker circulation noted in water vapor transport field may suggest that the tropics have experienced more extreme climate over the last three decades.

LARGE-SCALE DYNAMICS OF THE MEIYU-BAIU FORMATION: ROLE OF THE WESTERLY JET

Takeaki SAMPE, and Shang-Ping XIE
International Pacific Research Center, University of Hawaii, Honolulu, HI 96822, USA
takeaki@hawaii.edu

Abstract

Large-scale characteristics and environmental forcing of Meiyu-Baiu are investigated based on a reanalysis dataset. In climatology, the Meiyu-Baiu rain band is formed over central China and Japan from June to mid-July and accompanied by a trough of sea-level pressure, horizontal shears and sharp moisture gradients near the surface, a westerly jet tilted northward with height, and large northeastward moisture transport from the south.

Our analysis illuminates the significance of the westerly jet for the formation of the Meiyu-Baiu rain band. Along the rain band, mean ascending motion corresponds well with a band of warm horizontal temperature advection in the mid-troposphere, which is a large-scale forcing of upward motion. This induction of upward motion originates from the advection of warm air by the westerlies from the south of the Tibetan Plateau along the southern flank of the jet stream. The induced ascending motion favors convection and is enhanced by the resultant condensational heating, forming a band of large rainfall and ascent. In addition, diabatic heating around the Meiyu-Baiu region tends to force warm advection and ascending motion downstream along the jet, further supporting the association between the jet and the rain band. To the east of Japan, the low-level atmosphere is more stable than over China and Japan due to lower SST, so convection is suppressed and the ascent weakens eastward over the North Pacific.

The westerly jet anchors the Meiyu-Baiu rain band also by steering transient eddies, which creates periods conducive to convection through convective instability and adiabatic updrafts. Indeed in Meiyu-Baiu region the probability distribution of convective instability shows large spreads with a sharp cutoff on the unstable side, indicating effective removal of the instability by convection. Thus weather disturbances in the westerly waveguide increase a trigger for active convection to contribute to the formation of the rain band. In addition to the westerly jet, low-level southerly winds between the heat low over the Asian continent and the subtropical high pressure belt over the Pacific are another important environmental forcing for Meiyu-Baiu by supplying moisture to sustain convective instability.

Keywords: Asian monsoon, Baiu,

THE INFLUENCE OF AIR-SEA FLUX ON TROPICAL CYCLONE OVER WESTERN NORTH PACIFIC: THE ROLE OF MONSOON TROUGH

LIANG WU [1], ZHIPING WEN [1], RONGHUI HUANG [2]
1.Center for Monsoon and Environment Research / Department of Atmospheric Sciences, Sun Yat-sen University, Guangzhou, China
2.Institute of Atmospheric Physics, Chinese Academy of Sciences, Beijing, China
Email: 580848@163.com, eeswzp@mail.sysu.edu.cn

Abstract

This study investigates the influence of the large-scale Air-Sea Flux on the interannual variability of July-November tropical cyclone (TC) activity in the western North Pacific basin. The track and intensity function (TIF), constructed from the best-track dataset for the region for the period 1984-2002, and Air-Sea Flux variable are analyzed using the maximum covariance analysis (MCA). The results show a teleconnection between the central and eastern Pacific Air-Sea Flux anomalies and western North Pacific (WNP) TC activity during the TC season (July-November). The key system that bridges the warm (cold) events in the eastern Pacific and the strong (weak) WNP TC activity is an anomalous monsoon trough located in WNP. During the warm years, the monsoon trough enhances and extends eastward and TC tended to form mainly within the eastern part of monsoon trough regions and TC activity is above normal over most parts of the WNP east of ~125°E and slightly fewer TC tend to occur near Philippines and the South China Sea. This was accompanied by enhanced barotropic energy conversions and wave accumulation as compared to the cold years. On the contrary, during the cold years, those sign reverses.

With the monsoon trough background flow, the barotropic energy conversions process could be conductive to erosion of the synoptic-scale tropical wave structure and acceleration of the wave transition. These equatorially trapped TD and MRG waves undergo a prominent transition in the structure and eventually evolve into small-scale tropical disturbances when they moved to north of the eastern part of the monsoon trough. The development can be maintained with the tropical disturbances perturbation grow and play an important role in the formation of initial disturbances, which may be an important mechanism for TC genesis and developing.

Keywords: tropical cyclone, Air-Sea Flux, monsoon trough, wave transition

INTERACTIONS BETWEEN THE SUMMER MEAN MONSOON AND THE INTRASEASONAL OSCILLATION IN THE INDIAN MONSOON REGION

Yanjun QI[1], Renhe ZHANG[1], Tim LI[2], Min WEN[1]

[1] Chinese Academy of Meteorological Sciences, Beijing, China

[2] International Pacific Research Center and Dept. of Meteorology, University of Hawaii, HI, USA

Email: qiyj@cams.cma.gov.cn

Abstract

The relationship between interannual variations of the seasonal mean monsoon and intraseasonal oscillation (ISO) during boreal summer over the Indian monsoon region is investigated. The result shows a negative correlation between all-India summer monsoon rainfall and the ISO intensity. It is argued that the negative correlation is primarily attributed to the impact of the mean state of Indian summer monsoon on ISO. A strong Indian monsoon leads to the weakening of convection over the equatorial eastern Indian Ocean. The latter may further suppress the eastward and northward propagating ISO variances over the Indian Ocean and lead to a weakened intraseasonal activity over the Indian monsoon region. The ISO may feed back to the Indian summer mean monsoon through nonlinear eddy momentum transport. In addition, the ISO intensity over India increases (decreases) during the ENSO developing (decaying) summers.

Keywords: seasonal mean, Indian summer monsoon, ISO intensity, interactions

DIURNAL PHASE OF LATE-NIGHT AGAINST LATE-AFTERNOON OF STRATIFORM AND CONVECTIVE PRECIPITATION IN SUMMER SOUTHERN CONTIGUOUS CHINA

YU Rucong[1,2], YUAN Weihua[1,*], LI Jian[2], and FU Yunfei[1,3]

1. LASG, Institute of Atmospheric Physics, Chinese Academy of Sciences, Beijing, China，100029

2. LaSW, Chinese Academy of Meteorological Sciences, China Meteorological Administration, Beijing, China, 100081

3. Laboratory of Satellite Remote Sensing and Climate Environment, University of Science and Technology of China, Hefei, Anhui, China, 230026

*Email: yuanweihua@mail.iap.ac.cn;Weihua.Yuan116@gmail.com

Abstract

Using the Tropical Rainfall Measuring Mission (TRMM) Precipitation Radar (PR) observations during 1998-2006, the robust diurnal features of stratiform and convective precipitation in the summer southern contiguous China are revealed by exploring the diurnal variations of rain rate and precipitation profile. The precipitation over most of the southern contiguous China exhibits two distinguishing diurnal phases: late-night (midnight to early morning) and late-afternoon (afternoon to evening), dependent on the location, precipitation type and duration time. However, there are two distinctive sub-regions. Over the eastern periphery of the Tibetan Plateau and the southeastern coastal regions, the diurnal phases of precipitation are very weakly dependent on precipitation type and duration time.

Keywords: Diurnal cycle, stratiform precipitation, convective precipitation, rainfall duration

DROUGHT CLIMATOLOGY FOR KOREA

Do-Woo KIM, Su-Bin OH, Sang-Min Lee, Ji-Sun LEE, Ki-Seon CHOI, and Hi-Ryong BYUN
Pukyong National University, Busan, Korea
dow1112@nate.com

Abstract

This study presents drought climatology for Korea using daily values of the Effective Drought Index from 60 stations for the period 1954-2008. We divided Korea into 4 drought sub-regions using a hierarchical clustering method, and constructed the spatiotemporal map of historical droughts.

Total 20 national severe droughts and 16 regional severe droughts were described in terms of drought onset, peak, and termination date, drought duration, central regions, drought seasonality, and drought return period. Based on these drought statistics, features of each drought event are described, and droughts are categorized as having similar spatial and temporal characteristics.

Severe drought developed extensively for 1967-68 with severity having the longest return period of 69.5 years, for 1977-78 with the most intensive drought peak, and for 1994-96 with longest drought duration of 635 days. In addition, severe drought occurred widely for 1982-83 as well.

Keywords: Drought map, Historical droughts, Drought return period, Drought seasonality, Effective Drought Index

MAPPING AFTER REGIONALIZATION ON DROUGHT CLIMATOLOGY FOR JAPAN

Sang-Min LEE[1)], Do-Woo KIM[1)], Su-Bin OH[1)], Hi-Ryong BYUN[1)]
and Hiroshi L. TANAKA[2)]
[1)] Pukyong National University, Busan, South Korea
[2)] University of Tsukuba, Tsukuba, Japan
lsmin9@nate.com

Abstract

Using daily values of the Effective Drought Index (EDI) on 49 stations for the period of 1902~2004, this study presented the drought climatology of Japan

By the hierarchical clustering method Japan islands are regionalized into four divisions. Also, we made the drought map of Japan that was available to understand at a glance the dates of onset, peak and termination, and the duration, seasonality, severity, return period of all droughts occurred in Japan for 103 years.

In Hokkaido region, droughts with various durations were detected. But in other regions be affected by summer monsoon the droughts of short duration (30-90days) had shown higher frequencies. It has also known that there were two severe droughts (1939-41, 1984-85) nationwide and the second period of the two was drier than the first one. Using these two and the thirty four regional severe droughts as well we presented detailed statistics of Japanese droughts.

Keywords: Drought climatology, Japanese drought map, Effective Drought Index, regionalization on drought.

Interannual Variations of East Asian Trough Axis at 500hPa and Its Association with the East Asian Winter Monsoon Pathway

Lin WANG, Wen CHEN, Wen ZHOU, and Ronghui HUANG

Center for Monsoon System Research, Institute of Atmospheric Physics, Chinese Academy of Sciences, P.O. Box 2718, Beijing 100190, China

Email: wanglin@mail.iap.ac.cn

Abstract Interannual variations of the East Asian trough (EAT) axis at 500hPa are studied with the ERA-40 reanalysis data. The associated circulation pattern and pathway of the East Asian winter monsoon (EAWM) with the EAT axis tilt are specially investigated with a trough axis index, which is closely related to the midlatitude baroclinic process and mainly represents the intensity of the eddy-driven jet over the East Asia-North Pacific sector. When the tilt of EAT is smaller-than-normal, the EAWM prefers to take the southern pathway and less cold air moves to the central North Pacific. However, the EAWM prefers the eastern pathway and brings more cold air to the North Pacific when the tilt of EAT is larger-than-normal. These differences induce pronounced changes in both the precipitation and the surface air temperature over East and Southeast Asia. Furthermore, the tilt status of the EAT has a significant modulation effect on the regional climate anomalies related to the intensity of the EAWM. Our findings suggest an increase in the temperature anomaly associated with the EAWM intensity and a clear northward/southward shift in its pattern in anomalous tilt phase of the EAT. And the modulation tends to be confined mainly to East Asia and expanded to larger area during the weak and the strong EAWM winters, respectively. The possible reasons for interannual variations of the EAT tilt are discussed with the reanalysis data and simulations of the MAECHAM5. It is speculated that the mid-latitude air-sea interaction in the North Pacific plays a dominant role. This study on the EAT tilt may enrich our knowledge of the East Asian winter monsoon beyond the conventional intensity index and may be helpful to improve the regional climate prediction in East Asia.

Key words: East Asian winter monsoon, East Asian trough, eddy-driven jet

Another Look at Interannual to Interdecadal Variations of the East Asian Winter Monsoon: The Northern and Southern Temperature Modes

Bin Wang[1], Zhiwei Wu[2,1], Chih-Pei Chang[3,4], Jian Liu[5],
Jianping Li[2], Tianjun Zhou[2]

1. Department of Meteorology and IPRC, University of Hawaii, Honolulu, Hawaii
2. LASG, Institute of Atmospheric Physics, Chinese Academy of Sciences, Beijing, 100029, China.
3. Department of Meteorology, Naval Postgraduate School, Monterey, CA.
4. Department of Atmospheric Sciences, National Taiwan University, Taipei, Taiwan
5. State Key Laboratory of Lake Science and Environment, Nanjing Institute of Geography and Limnology, Chinese Academy of Sciences, Nanjing, China.

Key words: East Asia, Winter monsoon, Interannual variation, interdecadal variation

Abstract

This study elucidates the causes of interannual-to-interdecadal variability of the East Asian (EA) winter monsoon (EAWM) over a 50-year (1958–2007) period by focusing on the surface air temperature and the north-south differences between extratropics and tropics. Two empirical modes accounting for 74% of the total temperature variance dominate the variability in the northern and southern domains, respectively. The northern mode, characterized by a westward shift of the EA major trough and intensification of the Central Siberian High, represents a cold winter in the northern EA due to cold air intrusion from northeastern Siberia. The southern mode features a deepening EA trough and strengthening Mongolian High and represents a cold winter and enhanced monsoon circulation south of 40°N due to cold air intrusion from Mongolia. The northern mode is attributed to excessive autumn snow covers over the southern Siberia, whereas the southern mode is preceded by development of La Niña episodes and reduced autumn snow

covers over the northeast Siberia. While the interannual variations of the two modes exhibit remarkably different spatial-temporal structures and origins, on the interdecadal time scale their structures are somewhat similar with an abrupt regime transition in the mid-1980s and are preceded by comparable autumn sea surface temperature anomalies over the North Atlantic and tropical Indian Ocean. The ways by which the lower boundary forcing affects the dominant modes and related issues are discussed. The two modes found for the EA region also represent the winter temperature variability over the entire Asian continent and study of the predictability of the two modes may shed light on understanding the predictable dynamics of the Asian winter monsoon.

Mechanism for the extreme weather of South China in January 2008

Cholaw Bueh
DCRP & LASG, Institute of Atmospheric Physics, Chinese Academy of Sciences, Beijing, China

Abstract: The South China weather during January 2008 was record-breaking in its persistent low temperature and frequent severe snowstorms. The persistent collocation of a pair of warm and cold anticyclonic anomalies at the upper and lower troposphere over East Asia is vital for the extreme weather-climate event. The underlying mechanisms for the associated circulation anomalies are analyzed in terms of the transient eddy feedback forcing and Rossby wave propagation, based on the daily data of the NCEP/NCAR reanalysis for the period 1979-2008. The anticyclonic anomaly aloft was maintained by the upstream Rossby waves on sub-monthly time scale, while its lower troposphere counterpart was formed and sustained with the southeastward extension of the North Eurasian anticyclonic anomaly along the eastern side of the Tibetan Plateau. It is hypothesized that the preceding warm NWP SST anomalies, together with those of the accompanying La Nina event, possibly constituted an optimal SST configuration for facilitating the northwestward expansion of the East Asian Jet (EAJ) and the associated anticyclonic anomaly aloft in January 2008.

Key words: Extreme weather, Rossby wave, transient eddy feedback forcing

Synoptic-Scale controls of Persistent Low Temperature and Icy Weather over Southern China in January 2008

Wen Zhou[1], Johnny C. L. Chan[1*], Wen Chen[2], Jian Ling[2], Joaquim G. Pinto[3], Yaping Shao[3]

[1]{Guy Carpenter Asia-Pacific Climate Impact Centre, City University of Hong Kong, Hong Kong, China}

[2]{Institute of Atmospheric Physics, Chinese Academy of Sciences, Beijing, China}

[3] {Institute for Geophysics and Meteorology, University of Cologne, Cologne, Germany}

Abstract

In January 2008, southern China experienced persistent low temperatures, icy rain and snow. A succession of four intense snow storms swept over southern China within three weeks, leading to extensive damage, travel disruption and power shortages affecting millions of people. An analyse the average temperature for the region mostly affected by the event (Hunan and Jiangxi provinces) during the period 21-30 January shows return periods exceeding 20 years, in some cases even exceeding 50 years. As the temperature did not rise significantly during this period, no snow melted and hence snow continued to accumulate leading to an extensive snow cover over southern China by the end of January.

The large-scale conditions associated with the occurrence and development of these snowstorms are examined in order to indentify the key synoptic controls leading to this event. Three main factors are indentified: (1), the persistent blocking High over Siberia, which remained quasi stationary around 65°E for three weeks, led to advection of dry and cold Siberian air down to southern China, (2), the strong western Pacific subtropical High led to enhanced moisture advection from the Bay of Bengal into southern China, and (3), the deep inversion layer in the lower troposphere associated with the extended snow cover over Eurasia in the second half of January 2008, when it covered most of southern China. The combination of these three factors is likely responsible for the unusual severity of the event, and hence long return period.

The Roles of Tropical Synoptic-scale Disturbances and Asian Winter Monsoon in the Widespread Heavy Rainfall over Hainan Island during 11 to 14 October 2008

Peiming Wu[1], Yoshiki Fukutomi[1] and Jun Matsumoto [1, 2]
[1]Research Institute for Global Chang, Japan Agency for Marine-Earth Science and Technology, Natsushima 2-15, Yokosuka, Kanagawa, 237-0061 Japan
[2]Department of Geography, Tokyo Metropolitan University, Hachioji, Japan
Email: pmwu@jamstec.go.jp

Abstract

This study investigates the roles of tropical synoptic-scale disturbances and Asian winter monsoon in the persistent torrential rains over Hainan Island in China in October 2008. The four consecutive days of widespread heavy rains that occurred during 11 to 14 October resulted in the worst flooding event in the island in 42 years. The results from analysis of the JCDAS/JRA-25 reanalysis data show that the tropical synoptic-scale disturbances that originated from the western North Pacific propagate northwestward passing through over the island in this early winter season. Meanwhile, a strong northeasterly monsoonal flow occurs along the southern China coast, which is caused by the slowly southeastward movement of a mid-latitude anticyclone from the area near the Altay Mountains toward the southeast coasts of China. The northeasterly monsoonal flow interacts with the southerly winds that resulted from the tropical synoptic-scale disturbances, creating a low-level wind convergence and a strong vertical shear of wind over the island. Moreover, the increase in strength and westward extension of the North Pacific subtropical high causes a distinct dry layer at the mid-levels over the island, which lead to an increase of convective instability. These atmospheric conditions are maintained with little variation through the period, with the consequence that severe convection occurred over the island for the four consecutive days. In conclusion, the primary cause of the heavy rains is the cooperative effect of the tropical synoptic-scale disturbances and the strong northeasterly Asian winter monsoon. The tropical synoptic-scale disturbances originating from the western North Pacific play a substantial role in the persistent widespread heavy rainfall over Hainan Island in the early winter season.

Keywords: heavy rainfall, Hainan Island, Asian winter monsoon, tropical synoptic-scale disturbances.

Issues in understanding the aerosol-cloud-radiation interaction processes

Teruyuki Nakajima
Center for Climate System Research, The University of Tokyo
5-1-5 Kashiwanoha, Kashiwa, Chiba 277-8568, Japan
Tel. +81-(0)4-7136-4370; Fax. +81-(0)4-7136-4375; teruyuki@ccsr.u-tokyo.ac.jp

Abstract

Recent data analyses and model studies have revealed that the earth-atmosphere system is seamlessly connected and can produce complex interaction among various parts of the system. This observation is especially true in the response of the system to the radiative forcing caused by anthropogenic aerosols and related cloud field change, as reproduced by recent various climate models. However, we should recognize that our level of understanding is still unsatisfactory to attain accurate estimates of the magnitude of the interaction, e.g. amount of precipitation change due to direct and indirect aerosol forcing. This is because there are many pathways to link between aerosols and change in the atmospheric structure. Also the response of the cloud system is so different between western and eastern parts of the Pacific, for example.

I like to discuss several estimates of the radiative forcings using passive and active remote sensing and modeling, and study how these forcings can produce various change in cloudiness and precipitation field. Use of CALIPSO and CLOUDSAT data will be one of important keys to the solution of the problems.

CHEJU ABC PLUME-ASIAN MONSOON EXPERIMENT (CAPMEX) 2008: UNMANNED-AIRCRAFT MEASUREMENT OF AEROSOLS AND CLOUDS PROPERTIES IN JEJU, KOREA

Soon-Chang Yoon[1], Sang-Woo Kim[1], Sang-Cheon park[1], Man-Hae Kim[1],
V. Ramanathan[2] and M. V. Ramana[2]
[1]School of Earth and Environmental Sciences, Seoul National University, Seoul, Korea
[2]Scripps Institution of Oceanography, Univ. of California at San Diego, La Jolla, USA.
Email: yoon@snu.ac.kr

Cheju ABC Plume-Monsoon Experiment (CAPMEX), a series of data-gathering flights by specially equipped unmanned aircraft known as autonomous unmanned aerial vehicles (AUAVs), have been conducted at the South Korean island of Cheju (Jeju) during August – September 2008 to improve our understanding of how atmospheric brown clouds (ABCs) influences the reduction of solar radiation reaching at the surface and on clouds. Miniaturized instruments on the aircraft measure a range of properties such as the quantity of soot (aethalometer), size of the aerosols (optical particle counter, condensation particle counter), cloud droplets (cloud droplet spectrometer) and meteorological variables such temperature and humidity during and after the so-called "great shutdown" in China for Summer Beijing Olympic Games 2008.

The preliminary results from CAPMEX will be presented focusing on: (1) the vertical distribution of aerosol number density and black carbon concentration, (2) direct measurement of aerosol solar heating, and comparison with those calculated from the ground-based micropulse lidar and AERONET sun/sky radiometer synergy, (3) cloud microphysics and radiative forcing, and (4) aerosol-cloud interactions in conjunction with measurements by satellites and ABC Gosan ground observatory.

Keywords: ABC, CAPMEX, UAV, Aerosol, Cloud

TRANSPORT OF BLACK CARBON FROM THE ASIAN CONTINENT

Y. KONDO, N. OSHIMA, N. MOTEKI, N. TAKEGAWA, M. KAJINO

Research Center for Advanced Science and Technology, University of Tokyo, Tokyo, Japan.

M. KOIKE

Department of Earth and Planetary Science, Graduate School of Science, University of Tokyo, Tokyo, Japan

K. KITA

Department of Environmental Science, Graduate School of Science, Ibaraki University, Japan

Email: y.kondo@atmos.rcast.u-tokyo.ac.jp

Black carbon (BC) aerosol is emitted from fossil fuel combustion and biomass burning. It efficiently absorbs visible sunlight and heats the atmosphere. The photo-absorption of BC depends on its size distribution and mixing state. In addition, the efficiency of wet removal of BC is sensitive to its mixing state. Therefore, it is critically important to understand the evolution of the mixing state of BC for improved estimates of the impacts of BC on climate.

Aircraft measurements of BC particles and CO were made over the East China Sea and Yellow Sea in March-April 2009. The size distributions and mixing state of BC were measured using an SP2 instrument, based on laser-induced incandescence. The measurements were made as a part of the A-FORCE (Aerosol-Radiative Forcing) campaign. On March 30, high concentrations of BC and CO were observed at 3-6 km, due to upward transport of air from the boundary layer. Correlated increases in BC and CO indicate efficient transport of BC from the boundary layer. The updraft was caused by a cyclone developed over north eastern China. Meteorological analysis and WRF-CMAQ model calculations indicate insignificant wet removal of BC due to little precipitation. On April 23, in the air masses transported from middle part of China, high concentrations of CO were observed at 5-6 km over the East China Sea. However, no significant enhancement of BC was observed, indicating significant wet removal of BC, consistent with the meteorological analysis and model calculations. WRF-CMAQ model calculations, which reproduces the observed BC distributions, predicts that BC is transported to the free troposphere over China more efficiently north of 35°N than south of 35°N due to the smaller rates of precipitation associated with convective activities.

Keywords: aerosol, black carbon, transport, wet removal, and East Asia

WATER-SOLUBLE ORGANIC CARBON AND DIACIDS IN AEROSOLS IN NEW DELHI, INDIA IN WINTER: CHARACTERISTICS AND FORMATION PROCESSES

Yuzo MIYAZAKI,[1] Shankar G. AGGARWAL,[1] Khem SINGH,[2]
Prabhat K. GUPTA,[2] and Kimitaka KAWAMURA[1]
[1] Institute of Low Temperature Science, Hokkaido University, Sapporo, Japan
[2] National Physical Laboratory (NPL), New Delhi, India
yuzom@lowtem.hokudai.ac.jp

Abstract

Day- and night-time aerosol samples were collected at an urban site in New Delhi, India, in winter 2006-2007. They were investigated for low molecular weight dicarboxylic acids and related compounds as well as total water-soluble organic carbon (TWSOC). A macroporous nonionic (DAX-8) resin was used to quantify more- and less-WSOC, which are defined as the fractions of WSOC that passed through and retained on the DAX-8 column, respectively. High concentrations of diacids (up to 6 μg m^{-3}), TWSOC, and OC were obtained, which are substantially higher than those previously observed at other urban sites in Asia. Daytime WSOC/OC ratio (37%) was on average higher than that in nighttime (25%). In particular, more water-soluble OC (M-WSOC) to TWSOC ratio in daytime (50%) was twice higher than in nighttime (27%), suggesting that aerosols in New Delhi are photochemically more processed in daytime to result in more water-soluble organic compounds. Oxalic acid (C_2) was found as the most abundant dicarboxylic acid, followed by succinic (C_4) and malonic (C_3) acids. Contributions of C_2 to M-WSOC were greater (av. 8%) in nighttime than daytime (av. 3%). Positive correlations of C_2 with malic acid (hC_4) and glyoxylic acid (ωC_2) suggest that secondary production of C_2 probably in aqueous phase is important in nighttime via the oxidation of both longer-chain diacids and ωC_2. C_2 also showed a positive correlation with potassium (K^+). This suggests that the enhanced C_2 concentrations in nighttime are associated with biomass/biofuel burning. More tight, positive correlation between less water-soluble OC (L-WSOC) and K^+ was found in both day- and night-time, suggesting that L-WSOC, characterized by longer chain and/or higher molecular weight compounds, is significantly affected by primary emissions from biomass/biofuel burning.

Keywords: WSOC, diacids, urban aerosols

CARBONACEOUS AEROSOLS AND THEIR OPTICAL PROPERTIES IN ULAANBAATAR, MONGOLIA

Tsatsral BATMUNKH[1], Jin Sang JUNG[1], Young J. KIM[1*], Bulgan TUMENDEMBEREL[2]

[1]*Advanced Environmental Monitoring Research Center (ADEMRC), Department of Environmental Science and Engineering, Gwangju Institute of Science and Technology (GIST), Gwangju 500-712, Korea*

[2] *Central Laboratory of Environment and Meteorology, Ulaanbaatar-36, Mongolia*

*corresponding author: Young J. Kim, yjkim@gist.ac.kr

Keywords: $PM_{2.5}$ particles, carbonaceous aerosol, extinction coefficient, single scattering albedo.

In order to understand the chemical characteristics of atmospheric aerosol, $PM_{2.5}$ fine particulate matter samples were collected at an urban site in the centre of Ulaanbaatar, Mongolia during a winter season, 15 December 2007 ~ 15 February 2008. Although carbonaceous aerosol is an abundant component of atmospheric particulate matter in Ulaanbaatar, there has been lack of measurements of it. This paper reports the levels of carbonaceous aerosol pollution, organic carbon (OC) and elemental carbon (EC) in Ulaanbaatar and their optical properties. OC and EC were analyzed by the thermal–optical transmittance (TOT) method. Very high OC and EC levels were observed compared to other major cities in Asia. Daily average OC concentration varied in the range of 2.5 ~ 33.8 μg m^{-3}, with a mean of 17.5±7.1 μg m^{-3}, while daily average EC concentration ranged from 0.9 ~ 6.8 μg m^{-3}, with a mean of 4.5±1.4 μg m^{-3}. The average OC/EC ratio varied between 2.13 and 5.53 with a mean of 3.84±0.91. The OC and EC were moderately correlated during the entire sampling period, which suggested that they were emitted from different sources. The ratios of OC/EC at day time and night time were found to be 4.2 and 3.0, respectively. On average, carbonaceous species accounted for 32.2% of the $PM_{2.5}$ in Ulaanbaatar. Positive artifacts of the organic carbon for the entire sampling period were estimated to be 10 ~30% by measuring organic carbon concentrations on the backup quartz filter behind a front Teflon filter. Single scattering albedo (SSA) of dry fine particles was estimated based on the extinction coefficient (b_{ext}) calculated by the IMPROVE method. On average SSA of dry $PM_{2.5}$ particles was determined to be 0.83±0.03. It was found that SSA decreased to lower values to 0.77 when $PM_{2.5}$ concentration was < 50 μg m^{-3} while it increased up to 0.88 during polluted condition periods due to increased contributions by nonabsorbing components such as sulfate and OC.

A contribution of brown carbon aerosol to the aerosol absorption and its radiative forcing in East Asia

Rokjin J. Park, Minjoong J. Kim, Jaein I. Jeong, Daeok Youn, Sangwoo Kim
[1]*School of Earth and Environmental Sciences, Seoul National University, Seoul, Korea*

rjpark@snu.ac.kr

Abstract

Brown carbon aerosols were recently found to be ubiquitous and effectively absorb solar radiation. We use the GEOS-Chem and aircraft observations from the TRACE-P and the ACE-Asia campaigns to examine their contribution to aerosol absorption and radiative forcing over East Asia in spring 2001. We estimated brown carbon aerosol concentrations using the observed mass ratio of brown carbon to black carbon (BC) aerosols in the model. Our estimated radiative forcing of brown carbon amounts up to -3 W m^{-2} and 0.3 W m^{-2} at the surface and at the top of the atmosphere (TOA), respectively, over East Asia. Mean radiative forcing of brown carbon aerosol is -0.56 W m^{-2} and 0.07 W m^{-2} at the surface and at the TOA, accounting for about 20% of total radiative forcing by absorbing aerosols (BC + brown carbon aerosol), having a significant climatic implication in East Asia.

Keywords: black carbon aerosol; brown carbon aerosol; radiative forcing; East Asia; regional climate

LEXTRA -- AERIAL OBSERVATION OF AEROSOLS AND GASES OVER THE EASTA CHINA SEA IN MARCH-APRIL, 2008

Shiro HATAKEYAMA[1], Sayuri HANAOKA[1], Izumi WATANABE[1], Takemitsu ARAKAKI[2], Kaori KAWANA[3], Yutaka KONDO[3], Yasuhiro SADANAGA[4], Hiroshi BANDOW[4], Shungo KATO[5], Yoshizumi KAJII[5], Kei SATO[6], Atsushi SHIMIZU[6], and Akinori TAKAMI[6],

[1]Tokyo Univ. Agric. Technol., Fuchu, Tokyo, Japan, [2]Univ. Ryukyus, Nishihara, Okinawa, Japan, [3]Univ. Tokyo, Meguro-ku, Tokyo, Japan, [4]Osaka Pref. Univ., Sakai, Osaka, Japan, [5]Tokyo Metr. Univ., Hachioji, Tokyo, Japan, [6]Nat'l Inst. Environ. Studies, Tsukuba, Ibaraki, Japan, hatashir@cc.tuat.ac.jp

Abstract

Anthropogenic emission in East Asia has been increasing due to the rapid economic growth. Transformation of pollutants during the long-range transport is an important problem from a point of view of regional air quality and acid rain. In order to analyze the transport of atmospheric pollutants from the East Asia and the transformation processes during the transport aerial observation cmapaign, LEXTRA (Lagrangian EXperiment on long-range TRansported Aerosols), was carried out in March-April, 2008 over the East China Sea.

The aircraft employed was Beechcraft Kingair 200T chartered from Diamond Air Service, Inc. Items of observation were as follows. Gaseou species: O_3, SO_2, NOy, and CO. Partices: TSP (hi-volume tape sampler), BC (Cosmos), PM (particle mass monitor) and particle number conc. (particle counter). Temperature and relative humidity were aloso monitored on board.

Aerial experiments were made by setting its base on Fukue Island (Nagasaki Pref.), where a ground-based observation station is located. Round trip flights from Fukue to Cape Hedo, Okinawa (Fig. 1), where another ground-based observation station (CHAAMS) is located, were made on March 28, 31, and April 1. Level flights at 500 m for south bound flights and at 2000 m for north bound flights. Observations of vertical distribution of gases and aerosols were made above Cape Hedo on March 28 and above Fukue on April 2 by circular flights at altitudes of 500, 1000, 1500, 2000, and 3000 m.

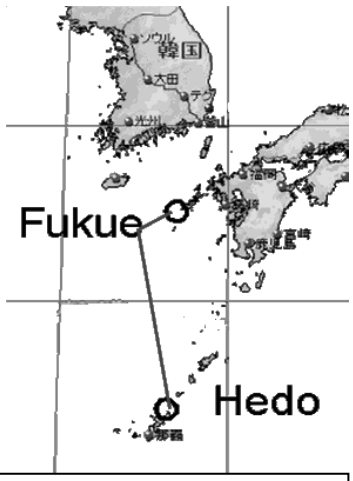

Fig. 1: Locations of ground-based observation sites and the flight track.

Ozone, SO_2, and PM concentrations showed similar spatial distribution over the East China Sea during the forward flight from Fukue to Okinawa at 500 m asl and backward flight at 2000 m asl. Namely, the concentrations increased from north to south. Such distribution was in accordance with CFORS Model prediction.

The value of $[SO_4^{2-}]/([SO_2]+[SO_4^{2-}])$ also went up from ~0.5 near Fuke to ~0.8 near Okinawa, which clearly showed the oxidative aging of the air pollutants during the transport from north to south over the East China Sea.

Keywords: long-range transported aerosols, sulfate, SO_2, CFORS model analysis

SYNOPTIC-SCALE VARIATIONS OF AEROSOLS AROUND BEIJING IN THE SUMMER 2006

M. KOIKE,[1] H. MATSUI,[1] Y. KONDO,[2] N. TAKEGAWA,[2] and T. ZHU[3]

[1] Department of Earth and Planetary Science, Graduate School of Science, The University of Tokyo, Tokyo, Japan (koike@eps.s.u-tokyo.ac.jp)
[2] Research Center for Advanced Science and Technology, The University of Tokyo
[3] College of Environmental Sciences, Peking University

Abstract

Regional aerosol model calculations were made using the WRF-CMAQ and WRF-chem models to study spatial and temporal variations of aerosols around Beijing, China, in the summer 2006, when the CAREBEIJING-2006 intensive campaign was conducted. Model calculations captured temporal variations of primary (such as elemental carbon, EC) and secondary (such as sulfate) aerosols observed in and around Beijing. The spatial distributions of aerosol optical depth observed by the MODIS satellite sensors were also reproduced over the northeast China. Model calculations showed distinct differences in spatial distributions between primary and secondary aerosols in association with synoptic-scale meteorology. Secondary aerosols increased in air around Beijing with a scale of about 1000 × 1000 km^2, which slowly moved northward under the influence of anti cyclonic systems. This accumulation was resulted by continuous photochemical production from precursor species emitted from a high anthropogenic emission area (the Great North China Plain) extending south of Beijing. Subsequent cold front passages brought clean air from the north, and polluted air around Beijing was swept to the south of Beijing. These cycles were repeated about once a weak and were found to be responsible for observed enhancements/reductions of aerosols at intensive sites. In contrast to secondary aerosols, spatial distributions of primary aerosols (EC) reflected those of emissions, resulted in only slight variability in spite of the change in synoptic-scale meteorology. In accordance with these results, source apportionment simulations revealed that primary aerosols around Beijing were controlled by emissions within 100 km around Beijing within preceding 24 hours, while emissions as far as 500 km and the preceding 3 days were found to affect secondary aerosols.

Relationships between aerosol mass concentrations and optical properties are also discussed.

Keywords: primary aerosol, secondary aerosol, EC, sulfate

INTERNAL MIXING STATES OF ATMOSPHERIC AEROSOLS STUDIED BY A LASER IONIZATION SINGLE-PARTICLE MASS SPECTROMETER DURING SPRING TIME IN OKINAWA, JAPAN

Yutaka MATSUMI[1*], Akihiro YABUSHITA[2], Toshiya KUMAZAWA[1],
Jun MATSUMOTO[3], Masahiro NARUKAWA[1], Tomoki NAKAYAMA[1],
Kenshi TAKAHASHI[4],
[1] Solar-Terrestrial Environment Laboratory, Nagoya University, Nagoya 464-8601, Japan
[2] Department of Molecular Engineering, Kyoto University, kyoto 615-8510, Japan
[3] Center for Priority Areas Tokyo metropolitan University, Tokyo 192-0397, Japan
[4] Kyoto University Pioneering Research Unit, Kyoto University, Kyoto 611-0011, Japan
* matsumi@stelab.nagoya-u.ac.jp

Abstract

Atmospheric aerosols play a critical role in atmospheric sciences in view of solar radiation, heterogeneous reactions in the atmosphere, and human health. Hence, it is essential to understand the source, transport and transformation of atmospheric particles and their components. In terms of cross-border pollution, atmospheric acidification, and nutrient supply to the ocean, it is important to find out the mechanisms of transport of tracer compounds from the Asian Continent toward Japan, the Pacific Ocean, and North America. The identification of the chemical compositions of aerosols is essential for understanding the interactions between the aerosols and adsorbed pollutants.

To examine the internal mixed states, several techniques for analyzing single particles have been developed by using the combination of laser ionization and mass spectrometry Recently, we reported the first observation of Asian mineral dust far downstream of the Asian continental outflow. The uptake of sulfates and nitrates onto Asian dust particles during transport from the Asian continent to the Pacific Ocean was analyzed using a a laser-ionization single-particle aerosol mass spectrometer. It was found that sulfate-rich dust particles made their largest contribution during the 'dust event'. As a result of detailed analysis including backward trajectory calculations, it was confirmed that sulfate components originating from coal combustion in the continent were internally mixed with dust particles.

Using the laser-ionization single-particle aerosol mass spectrometer, observation of atmospheric aerosol particles was performed at Cape Hedo, Okinawa in spring, 2006. The instrument obtains both size and chemical compositions of the individual particles with a high time resolution (about 2 s at the maximum). The aim of this observation is to capture internal mixed states of submicron particles in the downstream of the continental outflow. During Kosa events, nitrate was detected for most of sea-salt particles. On the other hand, sulfate was mainly detected for the fine mode (Dp < 1μm) of dust and sea-salt particles. These results indicate that the uptake of anthropogenic nitrate and sulfate occurs on sea-salt particles as well as dust particles. We have also observed particles containing leed (Pb) element. Correlations among various components were explored to discuss the observed internal mixed states.

Keywords: aerosol, single particle analysis, laser ionization mass spectrometer, Okinawa, internal mixing

Modeling exploration of the relationships between meteorological parameters and homogeneous nucleation in the continental boundary layer over China

Enagnon A. GBAGUIDI[a, b], Zifa WANG[b], Jinnan CHEN[a] and Chao GAO[b]

(a) School of Chemical Engineering and Environment, Beijing Institute of Technology, Beijing100081, China

(b) LAPC/NZC, Institute of Atmospheric Physics, Chinese Academy of Sciences, Beijing 100029, China

Abstract

The influence of meteorological parameters (temperature, relative humidity, solar radiation and cloud cover) on homogeneous nucleation process in the Chinese continental boundary layer in January 2004 is examined using US/EPA Models-3 CMAQ (version 4.4) modeling system coupled with the Mesoscale Model MM5. Results indicate seven event days (23% of simulated days): 5^{th} , 6^{th} , 9^{th} , 13^{th} , 20^{th} , 26^{th} and 27^{th} detected in daytime essentially over southern and western China under specific meteorological conditions such as: temperature ≤288K, solar radiation ≥600W/m^2, 40≤ relative humidity ≤52% and 0≤ cloud fraction ≤0.25， and weak preexisting particles surface area concentration. Gas phase NH_3, H_2SO_4 and SO_2 also acted as chemical trigger in reinforcing the preponderant role of meteorological factors. The new particles formation process suggests a relative dominance of ternary nucleation (compared to binary nucleation) which increases significantly sulfate loading in the Chinese continental boundary layer. This highlights the key role of atmospheric ammonia in sulfate increasing over China. Estimating nucleation parameter values (nucleation meteorological probability) shows the importance of relative humidity, greater than water molecule in the nucleation process.

Key words: meteorological factors; binary and ternary homogeneous nucleation; nucleation parameter; continental boundary layer; China.

CCN IMPACTS ON MARINE STRATOCUMULUS CLOUD DEVELOPMENT AND THEIR NOCTURNAL/ DAYTIME CONTRASTS

Seong Soo YUM and Keunyong SONG
Department of Atmospheric Sciences, Yonsei University, Seoul, Korea
*ssyum@yonsei.ac.kr

Abstract

One of the largest uncertainties in assessing the human impact on climate is related to the role of aerosols and clouds. Anthropogenic aerosols in the atmosphere exert so called the indirect aerosol effects by acting as cloud condensation nuclei (CCN), thereby affecting the cloud droplet number concentration, and sizes, cloud albedo, radiation budget, cloud dynamics, precipitation efficiency, and lifetime of clouds.

The marine stratocumulus topped boundary layer, which prevails in the subtropical oceanic regions where the subsidence inversion associated with the descending branch of the Hadley-Walker cell dominates, is thought to be an important component of the climate system. High albedo (30-40%) of stratocumulus clouds compared to the ocean background (10%) gives rise to large deficits in the absorbed solar radiative flux at the top of the atmosphere. Since cloud radiative properties are highly dependent on cloud microphysical properties, which are in turn dependent on the cloud condensation nuclei (CCN) distribution, understanding the impact of anthropogenic CCN on cloud microphysics and dynamics is a key to accurately assess the climatic impact of marine stratocumulus clouds. This study employs a Large Eddy Simulation (LES) model with size-resolving microphysics. Three different CCN concentrations at 1% supersaturation of 163 (maritime), 1023 (continental) and 5292 (polluted) cm^{-3} are used as input to the model. Four different thermodynamic soundings are used. First we examine the microphysical and dynamical evolution of stratocumulus clouds under different CCN loadings. Secondly we compare the contrasting results of daytime and nocturnal conditions.

Commonly to all four thermodynamic soundings, cloud droplet number concentration, cloud optical depth and albedo increase but the cloud droplet effective radius decreases with the increase of CCN loading for both daytime and nocturnal conditions. Morevoer, for the daytime condition, decoupling of the cloud layer and the subcloud layer leads to shallower depths of cloud and the drizzle was minimal even for the maritime CCN concentration. In detail, however, different thermodynamic conditions result in significantly different microphysical and macroscale features of clouds. Details will be presented at the conference.

Keywords: stratocumulus cloud, Cloud Condensation Nuclei (CCN), cloud radiative forcing, Large Eddy Simulation (LES)

BLACK CARBON AGING AND ITS IMPACT ON AEROSOL PROPERTIES IN OUTFLOW FROM ANTHROPOGENIC SOURCES USING A MIXING STATE RESOLVED MODEL

N. OSHIMA,[1] M. KOIKE,[2] Y. ZHANG,[3] and Y. KONDO[1]

[1] Research Center for Advanced Science and Technology, The University of Tokyo, Tokyo, Japan.
[2] Department of Earth and Planetary Science, Graduate School of Science, The University of Tokyo, Tokyo, Japan.
[3] Department of Marine, Earth, and Atmospheric Sciences, North Carolina State University, Raleigh, North Carolina, USA.

Email: oshima@atmos.rcast.u-tokyo.ac.jp

The Model of Aerosol Dynamics, Reaction, Ionization, and Dissolution (MADRID) with resolution of a mixing state of black carbon (BC) (MADRID-BC) is developed in this study to accurately simulate the time evolution of the entire BC mixing states. We apply the MADRID-BC model to evaluate the influence of changes in BC mixing states on aerosol optical properties and cloud condensation nuclei (CCN) activities in air parcels horizontally transported out from an urban area in Japan within the planetary boundary layer (PBL) over the ocean. The evaluation shows that the coatings on BC particles enhance light absorption at a wavelength of 550 nm by 38% in air leaving the source region and by 59% after their transport over the ocean for half a day. When the model treats aerosols using the conventional size-resolved sectional representation that does not resolve BC mixing states, the simulated absorption coefficients and single scattering albedos are given greater by 35-44% and smaller by 7-13%, respectively, than those from the simulation that resolves BC mixing states. These results indicate that it is essential to take into account BC-free particles in atmospheric models for accurate predictions of aerosol optical properties, because the conventional representation cannot separately treat BC-containing and BC-free particles in each size section. The evaluation also shows that the BC-containing particles having 55% and 83% of the BC mass can act as CCN at a supersaturation of 0.05% when they left the source regions and after transported for half a day, respectively. These results suggest the importance of the uplifting of BC particles from the PBL near source regions for their efficient long-range transport in the free troposphere.

Keywords: aerosol modeling, black carbon, mixing state, aerosol optical properties, and cloud condensation nuclei

The effect of traffic restriction on air quality in Beijing

Qizhong Wu[1,2], Zifa Wang[1]
1 LAPC/NZC, Institute of Atmospheric Physics, Chinese Academy Sciences, Beijing, 100029, China
2 Graduate University of Chinese Academy of Sciences，Beijing 100049, China

Abstract

An assessment of the impact of vehicles traffic restriction implemented within pre-Olympics environmental measures on Beijing air quality is performed through numerical analysis using Nested Air Quality Prediction Modeling System (NAQPMS) with high resolution emission inventory covering the period 17-20 August 2007. Two scenarios (baseline-emissions and traffic control emissions) are simulated to analyze the potential reduction of PM_{10} and NO_2 concentrations during this campaign. Results indicate the traffic restriction efficiency by reducing emissions of NO_x and NO_2 by 28% and 21% respectively in urban Beijing. PM_{10} and HNO_3 are reduced by about 11% and 8.5% respectively. Both simulated results and observed data indicate the most significant reduction of pollutants in urban Beijing, illustrating traffic restriction success since the restriction has been mainly imposed in urban Beijing. Such sectoral environmental measure may contribute to regional acid rain phasing out, reduction of photochemical pollution and population health risks.

Key words: traffic control, air quality, NO_2, PM_{10}, Beijing

Multi-models Ensemble Air Quality Forecasting System for Beijing Olympics

Zifa Wang, Qizhong Wu, Xiao Tang, Alex Gbaguidi, Wei Wang, Pingzhong Yan
LAPC/NZC, Institute of Atmospheric Physics, Chinese Academy of Sciences, Beijing, 100029 (zifawang@mail.iap.ac.cn)

Abstract

We test over Beijing, the performance of a multi-models ensemble air quality forecasting system through analysis of some indicative results of a framework conceived during the Olympics with the US/EPA Community Multiscale Air Quality (CMAQ) modeling system, the three dimensional Comprehensive Air Quality Model with extensions (CAMx) and the Nested Air Quality Prediction Modeling System (NAQPMS), using same meteorological field and same emissions inventory provided respectively by the fifth-generation NCAR/Penn State Mesoscale Model (MM5) and the Sparse Matrix Operator Kernel Emissions (SMOKE). The multi-models averaging-ensemble results have some desirable features. It may significantly improve air quality forecasts by reducing models bias. Stations hourly ensemble-averaging results present better performance than daily trends and in general with greater accuracy than patterns obtained over whole Beijing. The ensemble-averaging performance may vary over different stations or with different pollutants, suggesting the complexity of the multi-models ensemble air quality approach.

Key words: multi-models ensemble; air quality forecast, ensemble-averaging; Beijing Olympics.

A LIDAR NETWORK FOR CLOUD AND AEROSOL OBSERVATIONS IN ASIA

Atsushi SHIMIZU, Ichiro MATSUI, Tomoaki NISHIZAWA and Nobuo SUGIMOTO
National Institute for Environmental Studies, Tsukuba, Japan
shimizua@nies.go.jp

Abstract

Since 2001 National Institute for Environmental Studies (NIES) and collaborating organizations have expanded a lidar network for continuous cloud/aerosol observations in East / South East Asia. Currently more than 20 lidars are in operation in Japan, Korea, China, Mongolia, and Thailand. All lidars detect backscatter intensity at wavelengths of 532/1064 nm and depolarization ratio at 532 nm. Systems are automated for unmanned continuous observation throughout the year regardless of weather conditions. Lidars obtain four vertical profiles per hour, and almost all results are transferred to NIES immediately, processed in a unified manner, and visualized on WWW server.

For Asian dust studies, four dimensional structure revealed by lidar network are very useful. For example Yumimoto et al. (2007) exhibited an improvement of dust layer extent calculated in their numerical model by 4DVAR data assimilation of lidar data, and slight change of estimated dust emission in the source region for particular Asian dust event.

Vertical structure of troposphere are also characterized by continuous lidar observation. The climatological distribution of mixing layer depth detected by lidar network is compared with the planetary boundary layer depth expressed in GCM to evaluate the performance of parameterization in models.

Another challenging target for lidar network is anthropogenic aerosols. Emitted pollutants are transported with chemical reactions, thus combined observations of gaseous species and small particles are important for total understanding of trans-boundary pollution. Though space-borne lidars are powerful to observe horizontal distribution of aerosols, it is little difficult to measure aerosol layers near the surface because clouds and upper aerosol layers obscure the lower layers. Ground based lidar network can contribute to illustrate four dimensional structure of fine particles in Asian region, and combined analyses with other observational data and chemical reaction models are planned.

Keywords: lidar, dust, anthropogenic aerosols, clouds

TOWARDS THE UNDERSTANDING OF ASIAN DUST: ITS PHYSICS, MODELING, AND ROLES IN THE ATMOSPHERE AND CLIMATE SYSTEM.

Masao MIKAMI
Meteorological Research Institute, Tsukuba, Japan
mmikami@mri-jma.go.jp

Abstract

Mineral dust in the atmosphere plays an important role in the global and local climate through radiative perturbations and it is also the greatest atmospheric environmental problem in East Asia. More recently, it is pointed out that dust impacts on atmospheric dynamics and precipitation via its radiative and cloud microphysical processes.

Based on such a background, we, Japanese group, started a research program for the advancement of the dust model (Kaken-Hi Kiban-A) from April 2008 as three-years project. This project consists of monitoring of dust emission in Mongolia, CALIPSO/CALIOP data analysis, data assimilation of dust model using UnKF method, and development and validation of global dust model, MASINGAR.

In this paper, we will present a review of the recent progress of dust research and will introduce preliminary results of our project.

Keywords: dust, aerosol, data assimilation, climate impact

TEMPORAL AND SPATIAL DISTRIBUTIONS AND OCCURRENCE CAUSES OF DUST EVENTS IN GOBI DESERT DURING 1999-2007

Liu YANG* and Kenji KAI

Graduate School of Environmental Studies, Nagoya University, Nagoya, Japan
kai@info.human.nagoya-u.ac.jp
* Present address: Weather News Inc., Chiba, Japan

Abstract

Dust events are frequently observed during springtime in arid and semi-arid regions in East Asia. The Gobi Desert spreading in Mongolia and Northern China is one of main source regions of dust events. The occurrence of dust events is closely related to local climate conditions (strong wind, precipitation *etc*.) as well as surface features including snow and vegetation covers. Recently, anthropogenic process such as deforestation and over-grazing also affect the occurrence of dust events. The characteristics of temporal and spatial distributions and occurrence causes of dust events in Gobi Desert during 1999-2007 are investigated in this study, by analyzing SYNOP and NDVI data.

In the analyzed period, the dust events (including dust storm, blowing dust and floating dust) frequently occurred in 2000-2002 and 2006, especially in spring (Mar - May). The dust storm mainly occurred in the north of Gobi Desert, but the blowing dust was observed almost the whole region. The floating dust was transported to the southern region of the Gobi Desert because of the prevailing northwest wind.

Because the Gobi Desert is influenced by the Altai-Sayan cyclone, the strong wind tends to occur frequently in spring. The temporal and spatial distributions of strong wind have a high correlation with dust outbreak.

In the Gobi Desert, the annual precipitation is less than 400 mm during 1999-2007. Because of the dry condition, soil particles can be lifted up to the atmosphere easily. The precipitation falls as snow in March because the temperature is still below 0 ℃. The dust outbreak decreases as the snow cover provides a 'shield' for soil particles from wind erosion. The vegetation cover has the same function as the snow cover and control the occurrence of dust outbreak. In May, as the vegetation begins to grow in the east of Gobi Desert, the frequency of dust outbreak decreases.

Finally factors controlling the dust outbreaks are discussed by analyzing anomalies of strong wind days, precipitation and NDVI during 1999-2007. Main results are as follows.

(1) There are a positive anomaly of strong wind days and negative anomalies of precipitation and NDVI in 2001 when the dust outbreaks most frequently occurred during the studied period.
(2) There are a negative anomaly of strong wind days and positive anomalies of precipitation and NDVI in 2003 when the dust outbreaks fewest occurred during the studied period.
(3) Either of strong wind days and precipitation contributes the dust outbreak in 1999, 2004 and 2005.

It is concluded that the factors controlling the dust outbreaks are the strong wind, the precipitation and the vegetation cover in the Gobi Desert.

Keywords: dust event, Gobi Desert, strong wind, precipitation, NDVI

CHARACTERISCICS OF THE DUST OVER THE TAKLIMAKAN DESERT IN SPRING AND ESTIMATION OF THE TOTAL AMOUNT OF THE DUST

Yudai UENO[1)*], Kenji KAI[1)] and Hongfei ZHOU[2)]

1) Graduate School of Environmental Studies, Nagoya University, Nagoya, Japan
kai@info.human.nagoya-u.ac.jp
*Present address: Kyushu Railway Company, Fukuoka, Japan
2) Xinjiang Institute of Ecology and Geography, CAS, Urumqi, China
zhouhf@ms.xjb.ac.cn

Abstract

Dust storms frequently occur during March and May in the arid and semi-arid regions of East Asia, and emit a large amount of the dust into the atmosphere. The dust has an effect not only on the human health but also on the global climate by altering the radiation budget. To evaluate the influence of the dust on the climate, it is important to estimate the mass concentration and total amount of the dust. However, there have been few studies to estimate the total amount of the dust in source regions.

The Taklimakan Desert is one of the main sources of the dust outbreaks in East Asia. In the present study, lidar observations, satellite remote sensing and ground base observations of the dust at Aksu, Xinjiang, China are used to estimate the dust concentration and total amount of the dust in the Taklimakan Desert in April 2002 and 2004.

A dust storm occurred due to a strong easterly wind in the Taklimakan Desert during 6 and 7 April 2004. A vertical scale of the dust reached to 5 km (ASL) and a horizontal scale was about 1000 km, occupying 70 % of the Taklimakan Desert.

Firstly, a mass extinction conversion factor (MECF), which is a ratio of lidar-derived extinction to the mass concentration of the dust measured by Andersen sampler, is estimated for the background condition and for the dust event. Using two MECFs, the dust concentration is estimated 0.2 mg/m^3 during the background condition and 3.8 mg/m^3 during the dust event.

Secondly, a relationship between the aerosol optical thickness (AOT) derived from the lidar and TOMS Aerosol Index (AI) is determined. It is a linear relationship with a correlation coefficient of 0.95

Thirdly, using the MECFs, TOMS Aerosol Index and lidar observations, the total amount of the dust in the Taklimakan Desert is estimated 200 Gg during the background condition, and 400 - 800 Gg during the dust event in April 2004. The monthly averaged total amount of the dust during April is 320 Gg.

In April 2002, the total amount of the dust ranges from 400 - 1000 Gg because of frequent and heavy dust events. The monthly averaged total amount of the dust is 602Gg.

Keywords: dust storm, lidar, mass extinction conversion factor, Taklimakan Desert

ASIAN DUST PARTICLES ARRIVING AT JAPAN: CHANGES AND SUBSEQUENT EFFECTS DURING THE TRANSPORT

Daizhou ZHANG[1], Hiroko OGATA[1], Maromu Yamada[1], Yutaka TOBO[2], Atsushi Matsuki[2], Bin CHEN[3], Zongbo SHI[4], Guangyu SHI[3] and Yasunobu IWASAKA[2]

1 Prefectural Uinvesity of Kumamoto, Kumamoto, Japan
2 Kanazawa University, Kanazawa, Japan
3 Institute of Atmospheric Physics, CAS, Beijing, China
4 Leeds University, UK
(Email: dzzhang@pu-kumamoto.ac.jp)

Abstract

As an approach of identifying atmospheric aerosol particles, individual particle analysis is able to provide accurate information on the shape, size, composition, and other properties of particles. Compared to bulk sample analysis which can show quantitatively the characteristics of total collected particles on a filter (called bulk sample or integrated sample), this approach provides the virtual physical and chemical natures of a single atmospheric particle. On the other hand, due to the tremendous consuming of time and fund and the lack of suitable standards, it is very hard to obtain quantitative data in good qualities although this situation is gradually improved by the increasing commercial use of aerosol time-of-flight mass spectrometry (ATOFMS) in a limited series of field studies. In the past several years, our group has been working at Asian dust with individual particle analysis and a number of new results were obtained. In this presentation, major results obtained by our group and together with other groups are summarized in the point of view of particle changes due to the formation of sulfate, nitrate, and chloride and the adhering of sea salt during their transport in the atmosphere. The subsequent effects on dust particle properties and fate due to these changes are introduced. Finally, some important lacks and undergoing subjects corresponding to individual particle analysis and the potential subsequent effects are briefly described.

Keywords: Asian dust particles, Aging and mixing

DEVELOPMENT OF AN AEROSOL MODULE IN AN EARTH SYSTEM MODEL FOR GLOBAL WARMING PREDICTION

Taichu Y. TANAKA, Tomonori SAKAMI, Seiji YUKIMOTO, Makoto DEUSHI and MRI Earth System Modeling Group
Meteorological Research Institute, Japan Meteorological Agency, 1-1 Nagamine, Tsukuba City, Japan
Email: yatanaka@mri-jma.go.jp

Abstract

In order to reduce uncertainties and to improve accuracy for the global warming projection, we are developing an integrated global climate model called "MRI Earth System Model (MRI-ESM)", which consists of a state-of-the-art atmosphere-ocean coupled general circulation model (MRI-CGCM3), carbon cycle processes model in land and ocean, global chemical model (MRI-CCM2) with reactions of trace gases including ozone, and global aerosol model (MASINGAR mk-2). All of the components are interactively integrated into the Earth system model. The model components are interactively connected using a coupler library called Simple coupler (Scup). Scup is a simple and easy-to-use general-purpose coupler for coupling component models. Scup uses the Message Passing Interface (MPI) for data exchange of each model component, which enables flexible cofigurations and and efficient computing.

In the aerosol model MASINGAR mk-2, sulfate, black and organic carbon, sea-salt, and mineral dust are simulated. The emission flux of mineral dust, sea-salt, and dimethylsulfide are calculated based on the surface properties calculated by the MRI-CGCM3. The calculated aerosols species are coupled with the radiative transfer processes in the atmospheric circulation model to incorporate the direct radiative effect of aerosols. For the effects of aerosols on the microphysics of the clouds, number concentration of cloud particles are evaluated with aerosols, for both water and ice clouds. The production of sulfate aerosol is calculated with hydroxyl radical, ozone, $O(^3P)$, $O(^1D)$ and hydrogen peroxide, which are calculated by the MRI-CCM2. The calculated surface area density of sulfate aerosol is coupled to the heterogeneous chemical reactions in MRI-CCM2. In this presentation, we will present an evaluation of the effects of the aerosol species on global climate and chemical fields using MRI-ESM.

Keywords: aerosol, numerical model, climate simulation, radiative effects of aerosols

DUST TRANSPORT MODEL WITH 4D-VAR DATA ASSIMILATION METHOD: INVERSE MODELING USING GROUND-BASED LIDAR AND SATELLITE OBSERVATIONS

Keiya YUMIMOTO[1], Itsushi UNO[1], Atsuchi SHIMIZU[2], and Nobuo SUGIMOTO[2]
[1]Research Institute for Applied Mechanics, Kyushu University, Fukuoka, Japan
[2]National Institute for Environmental Studies, Tsukuba, Japan
yumimoto@riam.kyushu-u.ac.jp

Abstract

During the last decade, hindcast analyses and predictions of Asian dust have been performed using numerical dust models. These analyses have reproduced many important observational facts and revealed various characteristics of Asian dust outflows. However, great uncertainties remain in initial condition, emissions and parameterized processes (e.g. dry and wet depositions). Results of the recent dust model inter-comparison project (DMIP: Uno et al., 2006) suggested that variability in dust emission, which reflects differences in dust emission scheme and surface boundary data (e.g., soil texture, soil wetness and land-use data) during models, dominates the model uncertainty, necessitating further improvement and refinement.

Yumimoto et al. (2007) developed a regional dust transport model with a four-dimensional (4D-Var) data assimilation system (RAMS/CFORS-4DVAR: RC4). The RC4 consists of a successful regional dust model (RAMS/CFORS: Uno et al., 2004) and its adjoint model, and an optimization process. RC4 has been used for adjoint inversions of Asian dust with ground-based Lidars (Uno et al., 2008; Hara et al., 2009) and MODIS AOT (Yumimoto et al., 2008). In this study, we perform two inverse modelings for an extreme dust phenomenon during 20 March-4 April 2007 using NIES Lidar observation network (Sugimoto et al., 2006) and MODIS aerosol optical thickness (Remer et al., 2005), and compare both inversion results. In the inverse modeling with ground-based Lidars, vertical profiles of the dust extinction coefficients are directory assimilated. On the other hand, MODIS AOT based inversion assimilates horizontal distribution of MODIS coarse-mode AOT over ocean twice a day (TERRA and AQUA satellites). Both inversion results mitigate underestimation of dust concentrations and show better agreement with Lidar and MODIS observations. Independent validation with OMI/AURA aerosol index also shows that both inversions lead to significant improvement. Optimized dust emissions by NIES Lidar and MODIS observations result in considerably greater dust emissions over the Gobi Desert and Mongolia. Especially, optimized emissions are as 6.8 and 8.1 Tg for 29 March and 20.4 and 19.5 Tg for 30 March. Consistency between inversion results underscores that the combined inversion, which simultaneously assimilates observations provided by Lidar and satellite platforms, is promising for additional improvement of the dust adjoint modeling.

Keywords: dust, data assimilation, 4D-Var, inverse modeling

DATA ASSIMILATION OF CALIPSO AEROSOL OBSERVATIONS USING AN ENSEMBLE KALMAN FILTER

T. T. SEKIYAMA [1], T. Y. TANAKA [1], A. SHIMIZU [2], and T. MIYOSHI [3]
[1] *Meteorological Research Institute, Tsukuba, Japan;* [2] *National Institute for Environmental Studies, Tsukuba, Japan;* [3] *University of Maryland, USA*
Correspondence to: Thomas T. Sekiyama (tsekiyam@mri-jma.go.jp)

Abstract

We have developed an advanced data assimilation system for a global aerosol model with a four-dimensional ensemble Kalman filter (4D-EnKF) in which the Level 1B data from the Cloud-Aerosol Lidar and Infrared Pathfinder Satellite Observations (CALIPSO) were successfully assimilated for the first time, to the best of the authors' knowledge. The aerosol observations were ingested in this data assimilation system where they were processed with an ad hoc observational operator specifically designed for attenuated backscattering coefficients and volume depolarization ratios.

A one-month data assimilation cycle experiment for dust, sulfate, and sea-salt aerosols was performed in May 2007. The results were validated via two independent observations: 1) the ground-based lidar network in East Asia, managed by the National Institute for Environmental Studies of Japan (NIES), and 2) weather reports of aeolian dust events in Japan. Detailed four-dimensional structures of aerosol outflows from source regions over oceans and continents for various particle types and sizes were well reproduced. The intensity of dust emission at each grid point was also rationally corrected. These results are valuable for the comprehensive analysis of aerosol behavior as well as aerosol forecasting.

Keywords: aerosol, assimilation, CALIPSO, ensemble Kalman filter

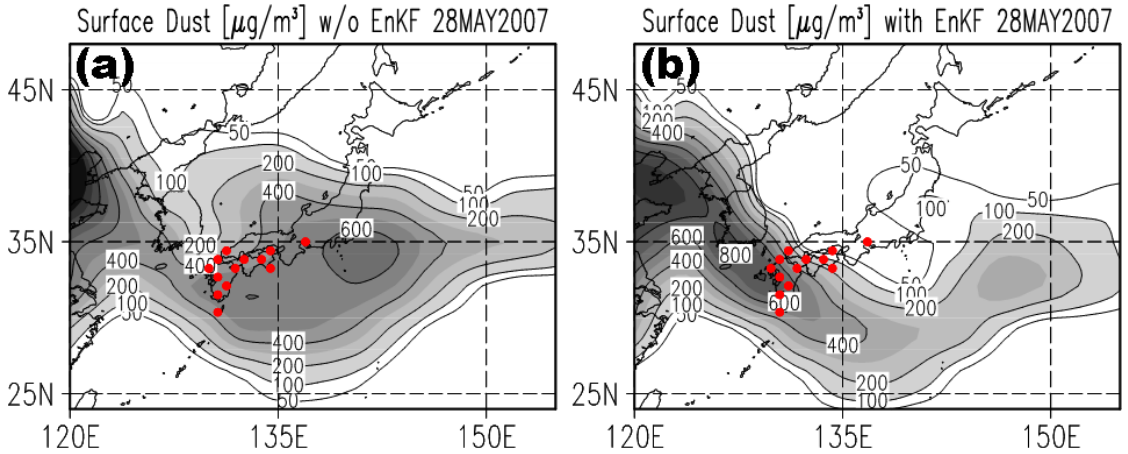

Comparison of simulated surface dust concentrations on 28 May 2007 (contours and gray shades; daily mean) and the weather stations (red circles) that observed aeolian dust events, so-called *Kosa*, on the same day (plotted only in Japan). (a) Reference model run without assimilation and (b) 4D-EnKF assimilation results.

Experience of emission control from the Beijing Green Olympic Games

Xin LI

Chief of Science Technology and International Cooperation Division

Beijing Environmental Protection Bureau, Beijing, China

Since 1998, Beijing had implemented a series of measures for pollution control, particularly after winning the bid for the 29th Olympic Games in 2001, Beijing takes the opportunity to accelerate the city's environmental improvement process. During the Olympic Games period, temporary and strict measures had been implemented collaborating with neighboring cities and provinces such as odd/even plate number traffic restriction for whole city, operation stop for all construction sites, therefore, daily emission of SO_2, NOx, PM_{10}, CO, VOCs in Beijing decreased sharply respectively, NOx and VOCs emission reduction is up to above 60%, and daily emission of SO_2, NOx, PM_{10}, VOCs in neighboring cities and provinces decreased by 10-40%. The ambient concentration of SO_2,NOx, PM_{10}, CO decreased by 50% based on comparing to the same period in last year. The good air quality was deeply impressed to people who had participated the Games, clearly indicating that the 29th Olympic Games has left rich environmental legacy for Beijing, China and the world. In this talk, it will be generally introduced about the strategy that was put in place to monitor and assess air quality in Beijing 2008 for the Olympics. It will also examine whether these measures have had a lasting impact on the city's air quality. Specifically, we will include an assessment of the problem, providing some background on the scope of the challenges and the impact that recent policy measures have had on public health and the environment. In conclusion, we will discuss the lessons that other large cities in China and elsewhere could learn from the experience in Beijing.

OZONE, CO, and AEROSOLS OBSERVED in A RURAL AREA in THAILAND: INCREASING INFLUENCES OF TRANSPORT FROM CHINA

Kazuyuki KITA[1], Seiichiro Yonemura[2], Haruo Tsuruta[3] Pakpong Pochanart[4], Akkaneewut Chabangborn[5], Boossarasiri Thana[5] and Michio Hashizume[5]

1:Colledge of Sciences, Ibaraki University, Mito, Japan
2: National Institute for Agro-Environmental Sciences, Tsukuba, Japan
3: CCSR, University of Tokyo, Kashiwa, Japan
4: FRCGC, JAMSTEC, Yokohama, Japan
5: Faculty of Science, Chulalongkorn University, Bangkok, Japan

kita@mx.ibarakki.ac.jp

In Southeastern Asian region, as Thailand, both industrial activities and biomass burning may significantly contribute source of precursors of ozone and aerosol. Because this region locates just south of China, where industrial activity glows rapidly, influence of long-range transport of pollutants can be significant.

Since 2007, surface ozone and carbon monoxide (CO) concentrations have been observed at Phimai, a rural area in central Thailand. Aerosol components, such as elemental carbon (EC), organic carbon (OC), sulfate (SO_4^{2-}), and nitrate (NO_3^-), were also sampled there 6 days per month.

Ozone and CO concentrations show obvious seasonal variation: they were low in wet season (June-September) and they repeated high and medium in early dry season (November-January), and they were significantly high during late dry season (local summer) during February to April. EC and OC concentrations were tightly correlated with CO concentration, while correlation between these components and sulfate concentration was not very tight. The variation of ozone, CO, EC and OC can be connected with the variation of air masses transported to central Thailand. During early dry season, for example, two type air masses were transported: air masses from East China Sea and air masses from Southern China. In the latter air masses, concentrations of ozone, CO, EC and OC were significantly higher than those in the former air masses.

Comparison of the ozone and CO concentrations with those measured by Pochanart et al. (2000, 2001, 2003) at Srinakarin, remote area in Thailand suggests the variation of these concentrations during this decade. They were often higher in 2007-08 than those in 1997-98. Ozone and CO concentrations in the air masses from South China significantly increased in 2007-08 in comparison with those in 1997-98, while these concentrations in the air masses from the East China Sea in 2007-8 were similar to those in 1997-98. This result shows that the transport of air masses from South China significantly affect ozone, CO and other concentrations in Southeast Asia during early dry season, and those concentrations in these air masses obviously increased during this decade, suggesting more influence of trans-boundary pollution.

Keywords: Ozone, Carbon Monoxide, Elemental Carbon aerosol, Thailand, China

Impact of Chemical Production and Transport on Summertime Diurnal Ozone Behavior at a Mountainous Site in Central Eastern China

Jie Li[1, 2], Pakpong Pochanart[1], Zifa Wang[2], Yu Liu[1, 2], Kazuyo Yamaji[1], Masayuki Takigawa[1], Yugo Kanaya[1], Hajime Akimoto[1]

[1] *Frontier Research Center for Global Change, JAMSTEC, Yokohama, Japan*
[2] *Nansen-Zhu International Research Centre, LAPC, Institute of Atmospheric Physics, CAS, Beijing, China*

Abstract:

The impact of chemical production and transport on diurnal ozone behavior in June 2006 at a mountainous site (Mt. Tai) in Central Eastern China (CEC) was studied by regional chemical transport coupled with process analysis and tagged tracer technology. The observed diurnal variation in the morning minimum-afternoon maximum was reproduced well. The results showed that regional transport contributed ~60 ppbv to "background" ozone, with no significant diurnal variations (<7 ppbv), while the chemistry (~25 ppbv) in the surrounding region (an area of 150,000 km2) which demonstrated an afternoon-maximum explained the causes of diurnal ozone behavior. Process analysis also suggested that in-situ chemistry accounted for most of the increase in ozone from morning to mid-afternoon (rather than the ozone concentration itself), with a minor contribution from vertical transport. A comparison was conducted between Mt. Tai and a mountainous site in Japan (Happo) to determine the regional variability in photochemistry and transport over Eastern Asia. The results showed that photochemical activities around Mt. Tai were stronger than those around Happo, where dynamic processes, rather than in-situ chemistry, played a dominant role in the diurnal behavior of ozone at midnight (0:00-3:00 local time (LT) and at the maxima-minima before noon (11:00 LT).

Observation study on ozone dry deposition over grass land in suburban area of Beijing

$Xiaole\ Pan^{1,3}, Zifa\ Wang^{1,2}, Xiquan\ Wang^{1,2}, Huabin\ Dong^{2,3}$

1 Nansen-Zhu International Research Center,Institute of Atmospheric Physics, Chinese Academy of Sciences, Beijing 100029

2 State Key Laboratory of Atmospheric Boundary Layer Physics and Atmospheric Chemistry, Institute of Atmospheric Physics, Chinese Academy of Sciences, Beijing, China

3 Graduate University of Chinese Academy of Sciences, Beijing, China

Abstract: The field experiment of ozone dry deposition on grassland was performed by using the concentration gradient method in the suburban area of Beijing which is often situated downwind of urban plumes and then influenced by high ozone concentration episode. The vertical profiles of ozone concentration and meteorological parameters were measured in late summer in a "V"-shape mountain valley of "Mangshan" Forest Park($40^o15'29''N, 116^o16'34''E$, 250 m above sea level). Strict QA/QC was conducted on the collection of data to guarantee the adequate analysis and credibility. Results show that:（1）Both ozone flux and dry deposition velocity were characterized by strong diurnal variation, with daily mean value of -0.40 $\mu g \cdot m^{-2} \cdot s^{-1}$ (minus sign refers the down-ward to the ground) and 0.55 $cm \cdot s^{-1}$ respectively. （2）Owing to the influences of topographic wind, strong ozone dry deposition flux occurs in the valley breeze (9:00-15:00) with mean value of -0.67 $\mu g \cdot m^{-2} \cdot s^{-1}$, then followed by that of mountain-valley wind shift period (08:00 in the morning and 16:00 in the afternoon), averagely -0.44 $\mu g \cdot m^{-2} \cdot s^{-1}$. When observation site is predominated by mountain breeze, ozone down-ward flux is only -0.26 $\mu g \cdot m^{-2} \cdot s^{-1}$. Daily average ozone dry deposition velocity displays the same feature with 0.74 $cm \cdot s^{-1}$, 0.50 $cm \cdot s^{-1}$, 0.47 $cm \cdot s^{-1}$ respectively for these periods.（3）Canopy resistance (Rc) calculated with the resistance model indicates the mean value of 184.0 $cm \cdot s^{-1}$ for the whole observation period. During the daytime, due to the gas-phase exchanges near leaf stomatal and the strong photosynthesis effects, canopy resistance (109.0 $cm \cdot s^{-1}$) is relatively low than that of night (217.7 $cm \cdot s^{-1}$) when the plant physiological activities drop off.

Keywords: ozone, deposition flux, dry deposition velocity, gradient method, canopy resistance

E-mail: xlpanelf@gmail.com

Correspondence to: Zifa Wang (zifawang@mail.iap.ac.cn)

Monte Carlo sensitivity analysis of the relationship between O_3 and its precursor emissions during high summer ozone in Beijing

Xiao Tang[1,2], Zifa Wang[1], Jiang Zhu[1], Qizhong Wu[1,2], Jie Li[1], Alex Gbaguidi[1], Tong Zhu[3]

[1] LAPC and NZC, Institute of Atmospheric Physics, Chinese Academy of Sciences, Beijing, China

[2] Graduate University of Chinese Academy of Sciences, Beijing, China

[3] College of Environmental Sciences and Engineering, Peking University, Beijing, China

Abstract. Through Monte Carlo method combined with Latin hypercube sampling and multi-linear regression method, this paper investigates high summer ozone concentrations sensitivity to NO_x and NMVOC emissions in the central urban of Beijing during CAREBEIJING-2006. The results show that current high averaged ozone concentrations are strongly stimulated by emissions of NMVOC and inhibited by NO_x emissions in Beijing. Among the NMVOC, formaldehyde (HCHO), ethylene (ETH) and olefins (OLET, OLEI) emissions show the greatest impact on average ozone concentrations. Daytime ozone maximum is even inhibited by the emissions of NO and NO_2, indicating that current atmosphere is in NO_x oversaturated conditions. The roles of NMVOC and NO_x emissions in ozone production under three emissions scenarios (reference emission and successive reductions of NOx emissions by 50% and 75%) are analyzed through Monte Carlo simulations. The 50% reduction of NO_x emissions triggers an increase of ozone concentrations sensitivity to HCHO emissions while excessive NO_x emissions still prevent ozone production. The reduction of 75% NO_x emissions however engenders a decrease of ozone concentrations sensitivity to HCHO emissions, changing NO_x sensitivity into a positive sensitivity during daytime. This suggests that ozone concentrations are sensitive to both NMVOC and NO_x emissions in this scenario. Therefore, in a condition of NO_x reduction lower than 50%, reducing NMVOC emissions (especially HCHO, ETH, OLET, and OLEI) is the most efficient measure for ozone control, while NO_x removal reinforces ozone pollution. Over 75% NO_x reduction, reducing NO_x emissions may be efficient for ozone concentration decreasing.

***Keywords*:** Monte Carlo method; Sensitivity analysis; Ozone production; Precursor emissions;

SOURCE ATTRIBUTION OF SURFACE OZONE OVER EAST ASIA WITH TRACER TAGGING METHOD

Tatsuya NAGASHIMA[1,3], Toshimasa OHARA[1,3], Kengo SUDO[2,3], Hajime AKIMOTO[3]
[1]National Institute for Environmental Studies, Tsukuba, Japan,
(corresponding author: nagashima.tatsuya@nies.go.jp)
[2]Nagoya University, Nagoya, Japan
[3]Frontier Research Center for Global Change, Yokohama, Japan

Long-term monitoring have shown that both NOx and NMHC at surface over Japan have been steadily decreasing in the last two decades, which is regarded as a result of emission controls for both substances. Because these substances are the precursors of tropospheric ozone, reduction of surface ozone over Japan is consequently expected. However, surface ozone at monitoring stations as well as remote sites over Japan have been increasing. Increase in emissions of ozone precursors in Asia and the transport of produced ozone from those area to Japan is a probable cause of the ozone growth in Japan. However, there are other factors which would have much effects on the air quality over Japan, such as ozone precursor emissions from Japan itself or long range transport from the farther remote regions than Asia. Therefore, it is quite important to estimate how much effect does each emission source region have on the surface ozone concentration over Japan; The estimation of source-receptor (S-R) relationship of ozone with Japan as the receptor region.

In order to estimate the S-R relationship of ozone, we use tracer tagging method with a chemistry-transport model (CHASER). This model can divide the ozone concentration over Japan into the ozone created over 20 different source regions. The model calculations were performed from the year 2000 to 2005, and the model meteorology (U, V, T) was assimilated into the NCEP/ NCAR reanalysis 6-hourly data of the corresponding year. The emission data used in the calculation is REAS 1.1 for Asian emissions and EDGAR FT2000 for the other region. RETRO fires data are adopted for biomass burning emissions both in Asia and the rest of the world

The model could well simulate the monthly mean surface ozone over Japan observed at EANET monitoring sites. The results show that, except for the southern island region, the ozone created in Japan has the largest contribution on the surface ozone in the annual-mean basis, but there is a large seasonality. In general, the contributions of ozone created in the farther remote regions than Asia are large from late Fall to early spring. In this time of year, contributions from Europe, Central Asia, and North America are noticeable, the total contribution of these three regions could be greater than contributions of Korea or China in some stations. On the other hand, the contiributions from relatively close regions to Japan, such as China or Korea, could be great in the warm season. The contributions from each source region can be different between the high ozone concetration case and the low ozone concentration case, even in the same season.

Keywords: surface ozone, source-receptor relationship, chemistry-transport model

FUTURE PROJECTION OF SURFACE OZONE AND ITS IMPACT ON CROP YIELD LOSS OVER EAST ASIA IN 2020

Masayuki TAKIGAWA, Masaaki TAKAHASHI, Hajime AKIMOTO,
and Kazuyuki KOBAYASHI
Japan-Agency for Marine-Earth Science and Technology, Yokohama, Japan
takigawa@jamstec.go.jp

Abstract

To evaluate the impact of emission change in East Asia on the surface ozone concentration and crop yield loss especially for wheat and rice, we developed a one-way nested global-regional chemical transport model, and conducted 1–year calculations with emission inventories for 2000 and 2020. The model consisted of global and regional CTMs. The global CTM was based on the chemical atmospheric general circulation model for study of atmospheric environment and radiative forcing (CHASER) model, while the regional part is based on the Weather Research and Forecasting (WRF) /Chem model. We have been also implemented a model which estimates stomatal ozone flux into agricultural crops following to EMEP (European Monitoring and Evaluation Programme) Unified Model, to evaluate exceedance of flux-based critical levels for ozone. The anthropogenic emissions in East Asia were taken from the Regional Emission inventory in ASia (REAS). Phenological data for spring wheat, single rice, and double rice in China, Korea, and Japan are taken from statistical data for each country. Comparison of the modeled surface ozone with ground–based observations in China in 2007 and 2008 showed that the model generally reproduced the seasonal and diurnal variations of ozone at the canopy height. For the horizontal distribution of surface ozone concentration, comparison between 2000 and 2020 revealed an ozone increase of 5-20 ppbv in the North China Plain, where the increase of ozone precursors was most remarkable. Remarkable increase of accumulated ozone flux into wheat during its growing season can be seen in the southern part of China. The maximum increase of AFst6 (accumulated stomatal flux of ozone above threshold of 6 nmol PLA/m^2/s) was 2.4 mmol/m^2 in Kanton Province. Crop yield loss caused by high ozone concentration was also estimated by using AFst6 and AOT40 (accumulated ozone concentration over threshold of 40 ppbv). Both estimates showed that crop yield loss might increase from 7% to 15% in East Asia.

Keywords: chemical transport model, surface ozone, future projection (**within 5 words**)

OBSERVATION OF RADON-222 IN THE WESTERN NORTH PACIFIC WITH A NEW RADON MEASURING SYSTEM

Akira WADA[1], Shohei MURAYAMA[2], Hidekazu MATSUEDA[3], Yousuke SAWA[3] , Hiroaki KONDO[2], Shoichi TAGUCHI[2] and Kazuhiro TSUBOI[4]

1 Meteorological College, Kashiwa, Japan
2 National Institute of Advanced Industrial Science and Technology (AIST), Tsukuba, Japan
3 Meteorological Research Institute, Tsukuba, Japan
4 Japan Meteorological Agency, Tokyo, Japan

E-mail: awada@mc-jma.go.jp

Abstract

Atmospheric radon-222 (Rn) is a useful chemical tracer for understanding transport mechanism of continental air masses. For continuous observations of the atmospheric Rn, a compact Rn measuring system with a higher sensitivity is required, especially at remote sites with low background level of the atmospheric Rn. For this purpose, we developed an automated Rn measuring system based on an electrostatic method. This system allows more precise measurement of low-level Rn concentrations with better detection limit than that of a commercially available instrument. The new Rn measuring system was installed at Minamitorishima (24.3 ºN, 154.0 ºE), about 2000 km southeast of Tokyo and at Yonagunijima (24.5 ºN, 123.0 ºE), about 100 km east of Taiwan. Very small Rn peaks were able to be observed at Minamitorishima to detect signals of the long-range transport from the Asian continent. On the other hand, relatively larger Rn peaks associated with synoptic weather changes were observed at Yonagunijima. It was clearly shown by the surface weather charts that the enhanced Rn peaks were brought by the passages of cold fronts associated with the migrating cyclonic development. When we simulated atmospheric Rn concentration using a 3D chemical transport model (NIRE-CTM-96) developed by the AIST, it well reproduced observed Rn concentrations at Minamitorishima station. The model results indicate that air masses with high concentration of Rn widely spreaded out from Asian continent to the western North Pacific Ocean through the boundary layer. In addition, we found tight relationships between atmospheric Rn and trace gases such as carbon monoxide, carbon dioxide, methane, and ozone observed simultaneously at Minamitorishima and Yonagunijima. This result indicated that polluted air masses were transported by the same transport mechanism of Rn. In this presentation we will discuss the Asia continental outflow by detailed analyses of observed and simulated Rn.

Keywords: radon, atmospheric observation, Asian outflow, chemical transport model

INTERCOMPARISON OF CIRRUS OPTICAL DEPTHS RETRIEVED FROM SPACE-BORNE CALIOP AND GROUND-BASED LIDAR IN SEOUL

Yumi Kim, Sang-Woo Kim and Soon-Chang Yoon
School of Earth and Environmental Sciences, Seoul National University, Seoul, Korea
Email: yumi1224@snu.ac.kr, kimsw@air.snu.ac.kr, yoon@snu.ac.kr

Cirrus clouds play a significant role in the radiative balance of the Earth's atmospheric system. A clear understanding of their properies at different geographical locations is highly essential for climate modeling studies. Lidars are regarded as one of the leading techniques for remotely studying the characteristics and properties of cirrus clouds. Especially, space-borne active remote sensing [e.g. LITE (Lidar In-space Technology Experiment), GLAS (Geoscience Laser Altimeter System) and CALIPSO (Cloud-Aerosol Lidar and Infrared Pathfinder Satellite Observations)] of atmospheric aerosols and clouds is the key to providing global observations.

This study presents to evalutate the benefits of applying two methodologies for retrieving optical properties of cirrus clouds to the space-borne lidar Cloud-Aerosol Lidar with Orthogonal Polarization (CALIOP) onboard CALIPSO and the ground-based lidar at Seoul National University (SNU; 37.4579° N, 126.9520° E, 116 above mean sea level), Seoul, South Korea, as well as to investigate the limits of their applicability. The main objective is to compare cirrus optical depth (τ_{cirrus}) from CALIOP profiles with measurements collected by SNU lidar and to investigate seasonal geometrical and optical properties of cirrus using long-term observation by SNU lidar.

The retrieval of τ_{cirrus} is performed using two methods, taking into account multiple scattering effect. Most of the methods that have been developed to retreive the optical properties of cirrus clouds depend on the solution of the standard lidar equation. Klett method, one of them, shows that a backward solution of backscatter coefficient was inherently stable. The second method is the transmittance method that determined by comparing the backscattering signal just below and above the cloud in the case whence lidar signals correctly represent the scattering medium. But the last method had some limitation. When lidar signal was too noisy at the top of the cloud, or there were some lower layers that cannot be distinguished, the applying fit can lead to erroneous values of the optical depth.

On 25 November 2006, the CALIOP (a day time flight, 04:50 UTC) and the SNU lidar detected cirrus clouds simultaneously. For cirrus clouds measured according to CALIPSO track (37-39° N), the two sets of cirrus optical detph are in good agreement, with correlation coefficient of 0.95 for CALIPSO level 2 data/Klett method results comparison. At coincident point, the top and base heights for cloud layer estimated from CALIOP and SNU lidar (in parenthesis) are 11.44 (11.53) km and 10.54 (10.81) km. The τ_{cirrus} from CALIPSO level 2 and Klett method for CALIOP profiles is each 0.209 and 0.215. And that from the Klett method and the transmittance method for SNU lidar profiles is respectively 0.219 and 0.234.

Keywords: Cirrus, Cirrus optical depth, CALIPSO, CALIOP, Lidar

LONG TERM OBSERVATION OF AEROSOL OPTICAL PROPERTIES AND THEIR RADIATIVE FORCING AT GOSAN, KOREA

Sang-Woo Kim, In-Jin Choi, and Soon-Chang Yoon
School of Earth and Environmental Sciences, Seoul National University, Seoul, Korea
Email: kimsw@air.snu.ac.kr, choiij@air.snu.ac.kr, yoon@snu.ac.kr

In the past several ten years, North East Asia has been experiencing a considerable increase in anthropogenic pollution aerosols. In addition, North East Asia is one of major source regions of wind-blown mineral dust aerosols. These aerosols significantly influence the solar and terrestrial radiation budgets. Thus far, numerous intensive regional-scale short-term field campaigns, such as ACE-Asia and ABC-EAREX 2005, have been conducted over East Asia to quantify these aerosol-induced radiative flux changes and revealed very high values of aerosol direct radiative forcings (ADRFs).

Seven-year analysis of clear-sky column-integrated aerosol optical properties and ADRF at Gosan in Korea is presented in this paper; the Gosan site is heavily impacted by aerosols emitted from the Asian continent. We investigate columnar optical and physical properties of aerosols and evaluate the ADRF as well as atmospheric heating rate using AEROENT sun/sky radiometer measurements of aerosol properties and column radiative transfer model calculations. In particular, we investigate the intra-seasonal, seasonal, and annual variations in the optical properties of aerosols and the associated radiative effects, as such seasonal variations in the regional-scale atmospheric circulations can lead to different patterns of aerosol transports.

MODIS and AERONET Sun/sky radiometer measurements showed significant seasonal and geographical variability aerosol optical depth (AOD), with high AODs over the east coastal industrialized regions of China in spring and summer. The monthly mean AOD at 675 nm ranged between 0.11 and 0.38. High AODs were observed from March to June (>0.3), while low-to-moderate monthly mean AODs were apparent during the remaining months. The single scattering albedo (SSA) exhibited relatively low values from February to June (<0.95), indicating the presence of light-absorbing aerosols, whereas high values of SSA (>0.95) were observed during the remaining months. The annual average clear-sky direct forcing (forcing efficiency) at the surface was –21.25 W m^{-2} (–92.37 W m^{-2} τ^{-1}) and at the top of the atmosphere (TOA) was –11.08 W m^{-2} (–48.17 W m^{-2} τ^{-1}), thereby leading to an atmospheric absorption of 10.17 W m^{-2}. From March to June, the surface aerosol radiative forcing (forcing efficiency) ranged between –28.79 (–87.32) and –41.05 W m^{-2} (–121.22 W m^{-2} τ^{-1}), the TOA ranged between –14.86 (–45.06) and –20.62 W m^{-2} (–54.71 W m^{-2} τ^{-1}), and the atmospheric forcing ranged between 13.93 and 24.74 W m^{-2}. The atmospheric forcing (i.e., atmospheric absorption) cause an increase in atmospheric heating (about 1.5 to 3.5 K day^{-1}). The strongest radiative heating was observed from April to June (>2.5 day^{-1}).

Keywords: AERONET Sun/sky radiometer, Gosan, Asian aerosols, aerosol optical depth, aerosol radiative forcing

AEROSOL RADIATIVE PROPERTIES AND SHORTWAVE RADIATION BUDGET OVER EAST ASIA

Tadahiro HAYASAKA[1], Kazuaki KAWAMOTO[2], Kazuma AOKI[3] and Guang-Yu SHI[4]

[1]Tohoku University, Sendai, Japan; [2]Nagasaki University, Nagasaki, Japan;
[3]Toyama University, Toyama, Japan; [4]Institute of Atmospheric Physics, Beijing, China
Corresponding author: Tadahiro HAYASAKA
E-mail:tadahiro@m.tains.tohoku.ac.jp

Abstract

Shortwave radiative forcing is dominated by an average condition of the atmosphere; for example, aerosol change affects the irradiance under the clear sky condition while cloud optical thickness change affects it under the cloudy sky condition. We quantified relative contributions of cloud amount, cloud optical thickness, aerosol optical thickness and precipitable water to the change of surface shortwave irradiance over East Asia by using ISCCP cloud and radiation data, and MODIS aerosol data. It is shown from the analysis that a change in aerosol optical thickness contributes to the inter-annual change of surface shortwave irradiance in the same order as that in cloud amount or cloud optical thickness over the East Asia region. Aerosol and radiation measurement facilities so called SKYNET are operated around East Asia. Aerosol optical thickness, size distribution and single scattering albedo are retrieved from skyradiometer measurements in SKYNET stations. The results from the skyradiometer analysis show that one of the conspicuous properties of aerosols in this region is strong absorption of shortwave radiation as a result of mixture of carbonaceous and soil dust particles. It is also indicated from the pyranometer and ISCCP data analyses and radiative transfer calculation that absorbing aerosols affect the surface shortwave irradiance not even under the cloudy sky condition as well as clear sky condition. As a result, the absorbing aerosols in this region contribute to warming of lower atmosphere and climate changes such as temperature and precipitation changes. In addition to the aerosol direct effect, large emission of anthropogenic aerosols affect cloud properties such as droplet size distribution and cloud lifetime, i.e., indirect effect. The indirect effect is recognized over China from a comparison of satellite remote sensing of clouds and aerosol chemical transport model.

Keywords: aerosol, shortwave irradiance, East Asia

INCREASING TRENDS IN ANGSTROM EXPONENT OVER EAST-ASIAN WATERS OBSERVED IN SEAWIFS AND AQUA/MODIS

Hajime FUKUSHIMA[1], Kazunori OGATA[1], and Liping LI[2]

[1)] School of High-technology for Human Welfare, Tokai University, Numazu, Japan
E-mail: hajime@wing.ncc.u-tokai.ac.jp
[2)] College of information science and technology, Ocean University of China

Abstract

Monthly mean data of Angstrom exponent (AE) and aerosol optical thickness (AOT) from Sea-viewing Wide Field-of-view Sensor (SeaWiFS) measurements over East Asian waters were analyzed. Increasing trend of the AE from 1998 through 2006 was found while AOT mean was observed stable. Statistical tests for the increase were made for three data sets covering different lengths of the study period of (a) 98-04, and (b) 98-06. The results showed statistically significant uptrend in AE over three (98-04) to all (98-06) of the six study areas around Japan, after eliminating seasonal dependency. In consideration to the calibration ambiguity for 2005 and for 2006 SeaWiFS data, 98-04 data set was taken to evaluate the uptrend, which showed 1% statistical significance of the increase in AE over North Japan Sea (North East Sea), East China Sea, and East of Japan with annual increase in AE of 0.08-0.14. These increase can be interpreted as increase in submicron fraction (SMF, the contribution of sub-micron particles to AOT) of 3-5% over a decade.

We also conducted similar data analysis with the Aqua/MODIS standard product on aerosol characteristics, where similar increase in AE was found to be statistically significant with 5 % significance. Although the absolute values for monthly mean AOT and AE were found to be different between SeaWiFS and MODIS, the AE time series anomaly, as well as that of AOT, over 2002-2006 showed very good agreement.

Keywords: aerosol, submicron particles, satellite, remote sensing

HINDCAST SIMULATION OF AEROSOL GLOBAL DISTRIBUTION AND RADIATIVE FORCING WITH AEROSOL CLIMATE MODEL

Toshihiko TAKEMURA
Research Institute for Applied Mechanics, Kyushu University, Fukuoka, Japan
toshi@riam.kyushu-u.ac.jp

In this study the global distributions, radiative forcing, and climate effects of aerosol particles from the year 1980 to the present are simulated and discussed with the global aerosol climate model, SPRINTARS. The model is coupled with MIROC which is a general circulation model (GCM) developed by Center for Climate System Research (CCSR)/University of Tokyo, National Institute for Environmental Studies (NIES), and Frontier Research Center for Global Change (FRCGC). The horizontal and vertical resolutions are T106 (approximately 1.1˚ by 1.1˚) and 56 layers, respectively. SPRINTARS includes the transport, radiation, cloud, and precipitation processes of all main tropospheric aerosols (black and organic carbons, sulfate, soil dust, and sea salt). The model treats not only the aerosol mass mixing ratios but also the cloud droplet and ice crystal number concentrations as prognostic variables, and the nucleation processes of cloud droplets and ice crystals depend on the number concentrations of each aerosol species. Changes in the cloud droplet and ice crystal number concentrations affect the cloud radiation and precipitation processes in the model. The emissions of soil dust, sea salt, and dimethylsulfide (DMS) from oceanic phytoplankton and land vegetation are calculated within the model. The other historical emissions, that is consumption of fossil fuel and biofuel, biomass burning, aircraft emissions, and volcanic eruptions are prescribed from the standard database provided by the Aerosol Model Intercomparison Project (AeroCom). The simulated results are compared and discussed with observations on the aerosol surface mass concentration and optical properties from surface and spaceborne sensors over multiple years. It is especially important to discuss variations of the simulated surface radiation budget for last several decades considering the aerosol effects on the climate system in comparison with “dimming” and “brightening” from observations. Detailed analysis of changes in the aerosol effects on the climate system for last few decades including year-by-year variations from the simulation will be useful for their near-term (~ a few decades) projection.

Keywords: aerosol, cloud, radiative forcing, climate model

Challenges for long-term global warming projection using an earth system model

Frontier Research Center for Global Change /
Japan Agency for Marine-Earth Science and Technology
Michio Kawamiya
(kawamiya@jamstec.go.jp)

The protocol for global warming projection being discussed for IPCC AR5 has two target time scales, that is, decadal and centennial. For the decadal time scale, global models with a high horizontal resolution of ~50-150km for the atmosphere will be desirable. The model integration will start from particular years blending observed data into the ocean component using an assimilation method. For the centennial time scale, on which the main focus will be put in the presentation, GCM-based earth system models with a moderate horizontal resolution of ~250km for the atmosphere will be adopted in order to consider interactions between climate change and biogeochemical processes significant for this time scale.

Models for the latter time scale should include carbon cycle with a capability of the "quasi-inversion" approach for stabilization scenarios. Preliminary experiments have been performed based on this approach for estimating allowable carbon emission to stabilize CO2 concentration according to SP450, SP550 and SP1000 scenario. Results show that climate – carbon cycle feedback significantly reduces allowable emission for all the scenarios. For example, the “ultimate” emission, i.e., emission allowed even after stabilization of atmospheric CO2, is approximately halved for all the scenarios. It is also demonstrated that the ultimate allowable emission can be positive due to long-lasting ocean uptake, although it might appear counterintuitive that CO2 can be emitted while retaining atmospheric concentration constant.

From an observational point of view, a recent report on the airborne fraction, i.e., fraction of anthropogenic CO2 remaining in the atmosphere, suggests that it is gradually increasing, which is possibly an indication that climate – carbon cycle feedback is already activated. One of the feedback mechanisms that the report proposes associates stratospheric ozone depletion with the reduced efficiency in natural carbon sinks, illustrating the necessity of a chemistry component in comprehensive models for investigating global change. Indeed, JAMSTEC is developing an earth system model with a fully coupled chemistry component with help of National Institute of Environmental Research and University of Tokyo, etc., which may enable us to make a quantitative examination of the mechanism proposed above.

A problem with studying climate – carbon cycle feedback is, however, that its magnitude is strongly model dependent as has been demonstrated by IPCC AR4. Efforts to constrain model results from observational evidence, and/or to indentify main factors to create the differences, are underway and some of them will be introduced in the presentation. Other challenges for the centennial time scale include projection of land-use and vegetation change, estimation of biogeochemical feedback loops and their incorporation into models, and uncertainty estimation for the projections including those of CO2 and other GHG concentrations. Ongoing efforts in Japan and the international community will be introduced and possible outcomes of the next IPCC assessment round will be discussed.

CLIMATE2030: A Japanese Project for Decadal Climate Prediction

Masahide Kimoto[1], Masayoshi Ishii[2], Takashi Mochizuki[2], Yoshimitsu Chikamoto[1], Masahiro Watanabe[1], Toru Nozawa[3], Takashi T. Sakamoto[2], Hideo Shiogama[3], Toshiyuki Awaji[2,4], Nozomi Sugiura[2], Takahiro Toyoda[2], Sayaka Yasunaka[1], Hiroaki Tatebe[1], and Masato Mori[1]

1) Center for Climate System Research, University of Tokyo, Kashiwa, Japan.
2) Frontier Research Center for Global Change, JAMSTEC, Yokohama, Japan.
3) National Institute for Environmental Studies, Tsukuba, Japan.
4) Department of Geophysics, Kyoto University, Kyoto, Japan.

Abstract

Active discussions are under way in the international climate science community on the design of the next coordinated experiment for climate projection, CMIP5, to contribute to the fifth assessment report of IPCC envisioned to be published in 2013. One of the highlights of CMIP5 is a new category of experiments aimed at near-term prediction up to 2030. In order to make political decisions against climate change over the coming decades, we need to take into account the large–scale climate changes associated with internal variability in the climate system in addition to global warming. While global climate change is the main subject in centennial–scale warming studies, a globally averaged surface air temperature (SAT) forecast up to 2030 depends little on socioeconomic scenarios or models used in centennial climate projection experiments. On decadal timescales, SAT changes due to internal climate variability are comparable to those associated with global warming in magnitude and major uncertainties are closely related to the predictability of internal climate variations rather than global warming. Therefore, in addition to natural and anthropogenic climate forcings, near-term climate prediction models are initialized, like in daily weather forecasting, by observational data of recent decades to incorporate actual evolution of natural modes of climate variability. In other words, the climate projection experiment for the first time becomes a mixed boundary-initial value problem. Whether such an attempt is successful or not is not known and poses a significant scientific challenge.

In parallel to international discussion, Japanese community has been discussing the possibility of near-term high-resolution experiments and the CLIMATE2030 project has been started since April 2007 under so-called KAKUSHIN Program (the Innovative Program of Climate Change Projection for the 21st Century) supported by the Ministry of Education, Culture, Sports, Science and Technology (MEXT). In the CLIMATE2030 project, we update the coupled ocean-atmosphere climate model, MIROC, and develop an initialization scheme for decadal predictions by using historical subsurface ocean data. In addition to limited number of high-resolution (60 km atmosphere + 20x30 km ocean) ensemble predictions, a comprehensive suite of hindcast and forecast experiments are conducted by using a medium resolution (280 km atmos. + 140 km ocean) version of MIROC in order to explore impact of initialization and to assess predictability of natural climate variations. The system for assimilation and prediction by MIROC is called SPAM and is being tested not only for decadal prediction but also for seasonal to interannual predictions.

An initial result of SPAM on decadal prediction is reported. It is found in the hindcast experiments that there is useful decadal predictability in one of the well-known natural decadal modes, called the Pacific Decadal Oscillation (PDO), which is known to affect the pan-Pacific climate and ecosystems. In a prediction experiment started in year 2005, the PDO signal is expected to suppress the present global warming trend in the coming decade albeit with enhancement in some regions including the East Asia. The initial tendency of PDO polarity change has been successfully verified by observations.

PROJECTION OF PRECIPITATION EXTREMES IN THE ASIAN MONSOON REGION

Akio KITOH, Kenji KAMIGUCHI, Osamu ARAKAWA and Shoji KUSUNOKI
Meteorological Research Institute, Tsukuba, Japan
kitoh@mri-jma.go.jp

Abstract

Three 25-year time-slice experiments are conducted using high-resolution global atmospheric models, focusing on the future changes in weather extremes. Four resolutions are used: 20-km, 60-km, 120-km and 180-km. First, we conducted an AMIP-type experiment for the period 1979-2003 using the observed sea surface temperature and sea ice concentration. It is confirmed that representation of large-scale features does improve, although not so much, by increasing horizontal resolution of the model. Topography is better represented by high-resolution model, leading to good representation of orographic precipitation. Close comparison is made with daily gridded precipitation dataset over East Asia, Middle East and Russia provided by the APHRODITE (Asian Precipitation - Highly-Resolved Observational Data Integration Towards Evaluation of Water Resources) project. There is resolution dependency for various extremes indices in the present-day climate. For the future climate projections, we added CMIP3 model ensemble mean changes in their SRES A1B experiments of sea surface temperature and sea ice concentration to the present values, and conducted the 2015-2039 and 2075-2099 simulations. An increasing precipitation is projected over Asian land areas in summer, while a decreasing precipitation is projected over Southeast Asia in winter. Resolution does not affect much on future projected changes in seasonal mean precipitation, but does affect in extremes. The 20-km mesh model projects larger increase in precipitation extremes such as the maximum 5-day precipitation total. An issue on resolution and ensembles is also discussed.

Keywords: high-resolution model, GCM, precipitation, extremes

ENSO CHANGES DUE TO GLOBAL WARMING: FOCUS ON THE OCEAN CHANGE

[1]Yoon-Kyoung LEE, [1]Jong-Ghap JHUN and [2]Byung-Kwon MOON
[1]School of Earth and Environmental Sciences, Seoul National University, Seoul, Korea
yklee77@snu.ac.kr, jgjhun@snu.ac.kr
[2]Division of Science Education/Institute of Science Education, Chonbuk National University, Jeonju, Korea, moonbk@chonbuk.ac.kr

Abstract

The El Nino and Southern Oscillation (ENSO) is the largest and best known mode of climate variability that affects weather, ecosystem and societies in large parts of the world. The period and intensity of ENSO changed. For example, after 1976/77 climate shift, the period and intensity of ENSO became longer and stronger. It is very important task to understand how the ENSO will be changed under the on-going global warming. In order to understand characteristic change of ENSO which appears in the future, several studies about understanding the role of tropical mean field change have been suggested (Timmermann et al., 1999; Collins, 2000; Guilyardi, 2006; Meehl et al., 2006). But exact understanding about relationship between the change of mean field and ENSO is not sufficient.

The role of the oceans in determining the rate of warming induced by greenhouse gases has been the subject of several studies. These studies indicate that oceans have a major influence upon the rate and the distribution of climate change. Other studies described that the ENSO will be strong, or be not changed, or even weaken. But the most previous studies did not concentration on the oceanic changes.

A vertical baroclinic mode is due to the vertical temperature distribution of the ocean. It was found that the vertical baroclinic mode is related with the El Nino change (using the observation data, SODA) (Moon et al., 2004). Yeh et al. (2006) investigated that ENSO amplitude changes in climate change commitment to atmospheric CO2 doubling. In this study, we will find the ENSO changes in the global warming using IPCC model results by focusing on the oceanic changes.

We analyzed monthly model data from 11 CGCMs (CCCMA-CGCM-3.1; Canada, GISS-E-R; USA, ECHO-G; Germany/Korea, CNRM-CM3; France, GFDL-CM2.0; USA GFDL-CM2.1 ; USA, INMCM3.0; Russia, INGV-ECHAM4; Italy, IPSL-CM4; France, MIROC3.2(medres); Japan, MRI-CGCM2.3.2; Japan,) that are in the multi-model ensemble collected by the Program for Climate Model Diagnosis and Intercomparison (PCMDI) for assessment in the Intergovernmental Panel on Climate Change (IPCC). 3 experiments used in this study. The first one is Pre-industrial experiment (PIcntrl) and the others are CO2 doubling (1pctto2x) and quadrupling (1pctto4x) experiments.

Keywords: ENSO, Vertical baroclinic mode, CGCM

MULTI-MODEL BASED PROJECTION OF TROPICAL CYCLONE GENESIS FREQUENCY OVER THE WESTERN NORTH PACIFIC BASIN USING CMIP3 ARCHIVE

Satoru YOKOI[1], and Yukari N. TAKAYABU[1, 2]
1: Center for Climate System Research, the University of Tokyo, Kashiwa, Japan
2: Japan Agency for Marine-Earth Science and Technology, Yokosuka, Japan
yokoi@ccsr.u-tokyo.ac.jp

Abstract

There have been a number of studies that assessed global warming impacts on tropical cyclone (TC) number with the use of their own high-resolution general circulation model or regional model. Most of the recent studies that dealt with global TC number projected decrease trends. On the other hand, there seems almost no consensus on regional trends. This study performs multi-model based projection of TC genesis frequency to achieve projections that are common among the models analyzed. Target domain is the western North Pacific (100°E–180°, 0°–40°N).

For this purpose, this study analyzes outputs of 20th-century-climate experiment and Special Report on Emissions Scenarios (SRES) A1B, A2, and B1 experiments performed by climate models that participiated in the third phase of Climate Model Intercomparison Project (CMIP3). TC-like disturbances are detected from daily-mean outputs of these experiments archived at the Program for Climate Model Diagnosis and Intercomparison (PCMDI). At first, this study examines performance of eight CMIP3 models that have atmospheric horizontal resolution of T63 or greater in simulating TC genesis characteristics, and finds that five models reproduce realistic horizontal distribution and gross summer-to-winter contrast of TC genesis frequency.

Comparison between 20th-century-climate and SRES experiments reveals that all of the five "high-performance" models project increase trends of TC genesis frequency over the central North Pacific, and decrease trends over the South China Sea and areas to the east of the Philippines. The former increase trends are primarily attributable to projected intensification and eastward extension of the monsoon trough, while the latter decrease trends may be associated with projected weakening in activity of tropical depression-type disturbances that can later be developed into TC. In contrast, all five models project increase trends of environmental potential indices of cyclogenesis proposed by previous studies all over the western North Pacific basin, which is inconsistent with the distribution of TC genesis frequency trends. It seems necessary to take into account, at least, the monsoon trough behavior and activity of pre-TC disturbance to design a potential index in order to make it applicable for the global warming problem.

Keywords: tropical cyclone, climate change, CMIP3, western North Pacific

POTENTIAL INTENSIFICATION OF TROPICAL CYCLONES APPROACHING JAPAN DERIVED FROM MULTI-MODEL CLIMATE EXPERIMENTS

Junichi TSUTSUI
Central Research Institute of Electric Power Industry, Abiko, Chiba, Japan
tsutsui@criepi.denken.or.jp

Abstract

The intensities of the tropical cyclones (TCs) that approach or make landfall in Japan and the possible changes in these intensities due to global warming were investigated based on the theoretical model of Holland (1997, *J. Atmos. Sci.*). This theoretical model calculates the maximum potential intensity (MPI) of a TC as a lower limit of central sea level pressure for a given upper-air temperature profile and underlying sea surface temperature (SST). This study uses the climatology of the JRA-25 long-term reanalysis for the present environment, along with global warming anomalies derived from CMIP3 multi-model climate experiments, which are added to the reanalysis climatology to form a warmed environment. A characteristic of the tropical atmosphere is that warming anomalies are amplified toward the upper troposphere, so that TC intensification due to a rise in SST is suppressed to some extent by greater warming aloft. This study evaluated uncertainty ranges for the MPI changes considering inter-model differences in the warming structure.

The MPI-SST relationship in the present climate was consistent with the historical minimum surface pressure in the western North Pacific, when the eyewall relative humidity (RH), one of the model's key parameters, was set at 88%. The average change in the MPI due to a 1 degC rise in the SST was -6.7 hPa [-0.6 to -12.0 hPa], where a negative change indicates intensification and the estimated range in brackets reflects the uncertainty in the warming structure. The error of these MPI changes was estimated to be about 15%, assuming that the likely range of the RH parameter was 88 +/- 2%. The fractional change in the surface pressure drop was 3.6%, 8.4%, and 19%, respectively, in response to a 0.5, 1.0, and 2.0 degC rise in SST, which was basically comparable to existing studies based on observations and numerical simulations. While TC intensification due to global warming tended to be greater for intense TCs at low latitudes, the tendencies at relatively high latitudes near the main islands of Japan suggested that TC development occurs in a broader region over a more prolonged season in a warmed environment.

Keywords: tropical cyclone, potential intensity theory, multi-model climate experiment, global warming, tropical atmosphere

GLOBAL WARMING PROJECTION WITH A SUPER-HIGH-RESOLUTION AGCM -- TROPICAL CYCLONES AND PRECIPITATION --

Jun YOSHIMURA
Meteorological Research Institute, Tsukuba, Japan
junyoshi@mri-jma.go.jp

Abstract

Influences of the global warming on the tropical cyclone climatology have been investigated by numerical experiments using a global atmospheric model with an approximately 20-km grid size. In this study, precipitation associated with tropical cyclone is analyzed. Results of the experiments suggest that precipitation near the centers of tropical cyclones (r = 100 km) tends to increase significantly under warmer climate condition. For more intense tropical cyclones, larger percent increase is simulated. Such changes can be attributed to increased moisture in the warmer atmosphere.

Keywords: global warming, climate model, tropical cyclones

GLOBAL WARMING AND TROPICAL CYCLONE ACTIVITY IN THE WESTERN NORTH PACIFIC

Johnny C L CHAN
Guy Carpenter Asia-Pacific Climate Impact Centre, City University of Hong Kong
Hong Kong, China
Email: johnny.chan@cityu.edu.hk

Abstract

The possible relationship between global warming and tropical cyclone (TC) activity in the western North Pacific is discussed in this paper. It is found that none of the time series of the annual number of TCs, annual number of intense TCs, track distributions and landfall locations shows a linear trend. Rather, all of them show large interannual and multi-decadal variations that can be explained to a large extent by similar variations in the planetary-scale variations in the atmospheric and oceanic conditions in the Pacific. These results suggest that global warming cannot be attributed to the observed variations in TC activity in the western North Pacific.

Keywords: global warming, tropical cyclone climate

Global Warming Effects on Wave Energy Generation in the Northern Hemispheric Winter

Toshiki IWASAKI, Yasushi MOCHIZUKI and Chihiro KODAMA
Graduate School of Science, Tohoku University, Sendai, Japan
iwasaki@wind.geophys.tohoku.ac.jp

Abstract

Many climate models have projected that the global warming may suppress stationary ultra-long waves and shift storm tracks northward with greater activity in the northern hemispheric winter. This is to study the physical mechanism of changes in stationary and transient waves through a comprehensive analysis of a thirty-year time-slice atmospheric GCM experiment.

The authors are developing a cascade-type energy conversion diagram based on mass-weighted isentropic zonal means (MIM), which facilitates to present the energy conversion from the zonal mean kinetic energy to wave energy through wave-mean flow interactions accurately. Both dynamic and dibatic wave energy generation rates are estimated from the time-slice GCM experiment.

Atmospheric wave energy changes are not caused directly from the CO2 increase but most of them are caused indirectly through the SST rise. The dynamic conversion from zonal mean kinetic energy are primarily resoponsible for the wave energy changes, while enhanced diabatic heating simply amplifies dynamically induced changes. The reduction of ultra-long stationary waves seems to result from the deceleration of low-level zonal mean zonal wind around 30 N induced by the changes in SST/SSI. The poleward shift of transient waves may also be understood in the context of changes in zonal mean states. To confirm this, we made an aqua-planet experiment and proved that the uniform SST rise induces the poleward shift of the wave energy through enhanced vertical shear in mid-latitude upper troposphere and the static stabilization in the subtropical troposphere. However, the uniform SST rise could not explain enhanced transient waves. The enhancement of transient wave energy is possibly related to the suppression of stationary wave energy, because the interannual variability of transient wave energy are negatively correlated to that of stationary wave energy.

Keywords: global warming, storm track, ultra-long wave, wave energy, mass-weighted isentropic zonal mean (MIM) (**within 5 words**)

REPRODUCIBILITY AND FUTURE PROJECTION OF THE MIDWINTER STORM-TRACK ACTIVITY OVER THE FAR EAST IN THE CMIP3 CLIMATE MODELS IN RELATION TO *HARU-ICHIBAN*

Kazuaki NISHII, Takafumi MIYASAKA, Yu KOSAKA and Hisashi NAKAMURA
Graduate School of Science, University of Tokyo, Tokyo, Japan
nishii@eps.s.u-tokyo.ac.jp

Abstract

A reanalysis dataset is used to establish the relationship between year-to-year fluctuations in midwinter storm-track activity over the Far East measured by poleward heat flux associated with subweekly disturbances and the occurrence of the first spring storm with strong southerly winds over Japan (*Haru-Ichiban*). Our analysis reveals that its early (delayed) occurrence tends to follow the enhanced (suppressed) winter storm-track activity with less (more) apparent minimum in midwinter in the course of the seasonal march. A metric is defined on the basis of the eddy heat flux to measure the reproducibility of the particular seasonal march of the storm-track activity over the Far East simulated by each of the Coupled Model Intercomparison Project Phase 3 (CMIP3) climate models under the present climate. Under a particular global warming scenario, ensemble projection based on several models that show the highest reproducibility of the storm-track activity based on the particular metric indicates that the future enhancement is likely in the midwinter storm-track activity associated with the weakening of the winter monsoon, implying that the earlier occurrence of *Haru-Ichiban* is likely in the late 21st century.

Keywords: storm track, mid-winter suppression, climate projection

Change of East Asian Summer Rainfall Interannual Variability in the Twenty-first Century

Yuanhai Fu and Riyu Lu
Center for Monsoon System Research, Institute of Atmospheric Physics, Chinese Academy of Sciences, Beijing, China
Email: fugreen1981@mail.iap.ac.cn

Abstract: The projected changes in interannual variability of East Asian summer monsoon rainfall (EASR) is investigated under the Intergovernmental Panel on Climate Change (IPCC) scenarios A1B and A2, respectively, by analyzing the simulated results of twelve Coupled Model Intercomparison Project Phase 3 (CMIP3) coupled models. The projection reveals a significant enhancement in EASR interannual variability, which is evaluated by the standard deviation of summer rainfall in East Asian and West North Pacific in the 21st century under both the SRES A1B and A2 scenarios. The models also project an enhanced interannual variability of the Western North Pacific Subtropical High (WNPSH) and the East Asian Upper-tropospheric Jet stream (EAJ). The EASR anomaly is significantly correlated with that in the WNPSH and the EAJ, and their relationships do not exhibit clear changes in the 21st century under both scenarios. Therefore, the enhancement of interannual variability of the WNPSH and the EAJ provides more evidence for the enhanced interannual variability of East Asia summer rainfall in the future, considering that the projection is likely more reliable for large-scale circulation than for precipitation.

Key Words: Climate Change; East Asian Summer Rainfall; Interannual Variability; IPCC AR4

AN UNCERTAINTY ASSESSMENT OF ANNUAL VARIABILITY OF PRECIPITATION SIMULATED BY IPCC AOGCMS IN EAST ASIA

Jinho Shin*, Hyo-Shin Lee, Minji Kim, and Won-Tae Kwon
Climate Research Laboratory, National Institute of Meteorological Research, Seoul, Korea
jshin@metri.re.kr

Abstract

Climate change is highly related to changes in hydrological system, which makes a long-term plan for future water resource management to be established. To provide reliable climate scenario for projecting the plan over East Asia, an uncertainty assessment for precipitation (PCP) datasets simulated by Atmosphere-Ocean Coupled General Circulation Model (AOGCM) participating in the International Panel on Climate Change (IPCC) Fourth Assessment Report (AR4) is conducted in this study. Most of results overestimate PCP compared to the observational data (wet bias) in spring-fall-winter, while they underestimate PCP (dry bias) in summer in East Asia. Higher spatial resolution model shows better performances in simulation of PCP. To assess the uncertainty of spatiotemporal PCP in East Asia, the cyclostationary empirical orthogonal function (CSEOF) analysis is applied. An annual cycle of PCP obtained from the CSEOF analysis accounts for the biggest variability in its total variability. A comparison between annual cycles of observed and modeled PCP anomalies shows distinct differences: 1) positive PCP anomalies of the multi-model ensemble (MME) for 20 models (thereafter MME20) in summer locate toward the north compared to the observational data so that it cannot explain summer monsoon rainfalls across Korea and Japan. 2) The onset of summer monsoon in MME20 in Korean peninsula starts earlier than observed one. These differences show the uncertainty of modeled PCP. Also the comparison provides the criteria of annual cycle and correlation between modeled and observational data which helps to select best models and generate a new MME, which is better than the MME20. The spatiotemporal deviation of PCP is significantly associated with lower-level circulations. In particular, lower-level moisture transports from the warm pool of the western Pacific and corresponding moisture convergence significantly are strongly associated with summer rainfalls. These lower-level circulations physically consistent with PCP give insight into description of the reason in the monsoon of East Asia why behaviors of individually modeled PCP differ from that of observation.

Keywords: uncertainty assessment, precipitation, IPCC, annual cycle, moisture transport.

Acknowledgments
This research was supported by a grant (code#1-9-3) from Sustainable Water Resources Research Center of 21st Century Frontier Research Program.

ASSESSMENT OF FUTURE CHANGES IN THE BAIU RAINBAND USING THE PSEUDO-GLOBAL WARMNING DOWNSCALING METHOD

H. Kawase[1], T. Yoshikane[2], M. Hara[2], F. Kimura[2, 3], B. Ailikun[4], T. Yasunari[2, 5]

1.National Institute for Environmental Studies, Tsukuba, Japan; 2.Japan Agency for Marine-Earth Science and Technology, Yokohama, Japan; 3.Tsukuba University, Tsukuba, Japan; 4.Institute of Atmospheric Physics, Chinese Academy of Science, Beijing, P.R., China; 5.Nagoya University, Nagoya, Japan

Email: kawase.hiroaki@nies.go.jp

Abstract

Changes in the Baiu rainband due to global warming are assessed by the Pseudo-Global Warming Downscaling method (PGW-DS). The PGW-DS is almost the same as the conventional dynamical downscaling method using a regional climate model (RCM), but the initial and boundary conditions of the RCM are obtained by adding the difference between the future and present climates simulated by coupled general circulation models (CGCMs) into six-hourly reanalysis data in a present control period, e.g., the 1990s. The daily atmospheric variation is similar to that of the control period, but the climate mean is comparable to the future climate. We conducted the PGW-DS runs using the CGCMs with better reproducibility around East Asia in June. We also conducted the PGW-MME run that was the PGW-DS run using multi-selected CGCMs ensemble mean. The PGW-MME and PGW-DS runs show an increase in precipitation over the southern part of the present Baiu rainband. The PGW-MME run has a good similarity to the average of all PGW-DS runs. This indicates that an average of the multiple PGW-DS runs can be replaced by a single PGW-DS run using the multiple CGCM ensemble mean, reducing the significant computational expense. The comparison between the PGW-DS runs and the CGCM projections indicates that the PGW-DS runs reduce the inter-model variability of changes in the Baiu rainband caused by the CGCMs themselves.

Keywords: dynamical downscaling, Baiu rainband, future projection, regional climate modeling

CHANGE IN THE EAST ASIA SUMMER MONSOON PROJECTED BY AN ATMOSPHERIC GLOBAL MODEL WITH 20-KM GRID

Shoji KUSUNOKI[1)], Ryo MIZUTA[2)], Mio MATSUEDA[2)]

1) Meteorological Research Institute, 1-1 Nagamine, Tsukuba, Ibaraki 305-0052, JAPAN, E-mail : skusunok@mri-jma.go.jp
2) Advanced Earth Science and Technology Organization, Japan

Abstract

We have conducted global warming projection with 20-km grid Atmospheric General Circulation Model (AGCM). We especially focus on the change in rain band in the East Asia summer monsoon season which is called the Mei-yu in China, the Changma in Korea and the Baiu in Japan. This study is supported by the Innovative Program of Climate Change Projection for the 21st Century (KAKUSHIN). The Earth simulator was used for calculation.

The global atmospheric model has the 20-km grid spacing with 60 vertical levels. This is a hydrostatic model and a prognostic Arakawa-Schubert scheme is used for cumulus convection. For present-day climate, observed historical sea surface temperature (SST)s were prescribed from 1979 to 2003 (25 years). For future climate from 2075 to 2099 (25 years), changes in the multi-model ensemble of SSTs projected by atmosphere–ocean general circulation models (AOGCMs) of the Coupled Model Intercomparison Project 5 (CMIP5) were superposed to the observed historical SSTs. Intergovermental Panel on Climate Change (IPCC) A1B emission scenario was assumed for green house gases in the future climate.

In June and July, precipitation increases over the most regions of East Asia with statistically significance. Some regions show decrease of precipitation, but their changes are not statistically significant. In June and July, the intensity of precipitation also increases over the most regions of East Asia with statistically significance. Over Japan area, the termination of rainy season tends to delay until August.

To quantify the uncertainty of projction, we have conducted a set of ensemble simulations with 60-km grid AGCM giving different SSTs and different atmospheric initial conditions. General increase of precipitation over East Asian regions and delay of rainy season over Japan are also found by the 60km AGCM ensemble simulations.

Keywords: Global warming projection, East Asia summer monsoon, 20-km mesh AGCM

PRESENT CLIMATE VERIFICATION AND FUTURE CLIMATE PROJECTIONS OVER SOUTHEAST ASIA BY AN MRI 20KM-MESH AGCM

Yasuo SATO[1)], Md. Mizanur RAHMAN[2)], Nazlee FERDOUSI[2)], Erwin Eka Syahputra MAKMUR [3)], Analiza Solmoro SOLIS[4)], Winai CHAOWIWAT [5)], Tran Dinh TRONG [6)], Shoji KUSUNOKI[1)], Akio KITOH[1)]

1) Meteorological Research Institute, Tsukuba, Japan, kitoh@mri-jma.go.jp
2) SAARC Meteorological Research Centre, Dhaka, Bangladesh
3) Indonesia Meteorological and Geophysical Agency, Jakarta, Indonesia
4) PAGASA-DOST, Quezon City, Philippines
5) Chulalongkorn University, Bangkok, Thailand
6) Vietnam Institute of Meteorology, Hydrology and Environment, Hanoi, Vietnam

Abstract

Time slice climate simulations by an MRI 20 km-mesh AGCM firstly made possible to obtain climate change projections on extreme weather events and for the globe, especially countries such as Philippines and Indonesia etc. where they have complex land-sea contrast and narrow and steep mountaines, apart from another way by a high-resolution RCM. However, finer resolution of model does not straightforwardly assure the advance in accuracy of climate simulation, especially in the tropics.

The study states preliminary analyses of model verification of present climate and future climate projections using the output of the MRI/JMA 20 km- and 60 km- mesh AGCM simulations under the SRES-A1B emission scenario and station climate data over Southeast Asia: Bangladesh, Indonesia, Philippines, Thailand, Vietnam. Analysed variables mainly are monthly-mean surface air temperature and precipitation.

On Bangladesh climate, seasonal variation of surface air temperature was captured well within the 1.8 deg C negative bias by the model, whereas that of precipitation was delayed about one-month and also the model calculated half amount of precipitation in the monsoon season compared with observation.

In Indonesian future climate, the model projected that precipitation in rainy season (DJF) would increase in the end of the 21st century (2075-2099), whereas precipitation in dry season (JJA) would decrease. The results may force some adaptation in agricultural irrigation in Indonesia.

In Philippine present climate, the model well simulated interannual variations of seasonal precipitation except the southwest monsoon season (July, August, September), which may be partly explained by having specified an observed SST in the model.

In Thailand, correlation coefficients of interannual variation between observations and the model showed comparatively high correlations in precipitation and temperature. The model projected a precipitation increase in most areas, whereas a decrease in the mountainous area of Northern region and parts of Northeast region.

In Vietnam, the correspondences between the station observations and the model are quite good, especially in temperature, and the model projected 2-2.5 deg C temperature increase in the North in the end of the 21st century, whereas 2.5-3.0 deg C in the South.

Keywords: 20km-mesh AGCM, projection, verification, station data, Southeast Asia

SIMULATION OF REGIONAL CLIMATE CHANGE UNDER IPCC A2 SCENARIO IN SOUTHEAST CHINA

Zhihong JIANG[1], Weilin CHEN[1],Laurent LI[2], Pascal YIOU[3]

1, Nanjing University of Information Science and Technology, Key Laboratory of Meteorological Disaster of Ministry of Education, Nanjing, China
2, Laboratoire de Météorologie Dynamique, IPSL/CNRS/UPMC, Paris, France
3, LSCE/IPSL, CNRS/CEA, Saclay, France
First author email: zhjiang@nuist.edu.cn

Abstract A variable-grid atmospheric general circulation model, LMDZ, with a local zoom over southeast China is used to investigate climate changes in terms of both means and extremes in southeast China. Two time slices of 30 years are chosen to represent respectively the end of the 20th century and the middle of the 21st century. The boundary conditions were taken from the outputs of three global coupled climate models: Institut Pierre-Simon Laplace (IPSL), Centre National de Recherches Météorologiques (CNRM) and Geophysical Fluid Dynamics Laboratory (GFDL). Some preliminary results from a two-way nesting system between LMDZ-global and LMDZ-regional are also presented. The evaluation of simulated temperature and precipitation for the current climate shows that LMDZ reproduces generally well the spatial distribution of mean climate and extreme climate events in southeast China, but the model has systematic cold biases in temperature and tends to overestimate the extreme precipitation, the two-way nesting model can reduce the "cold bias" to some extent compared to the one-way nesting model. Scenario results using A2 emissions show that in all seasons there is a significantly increase for mean, daily-maximum and minimum temperature in the entire region, associated with a decrease in the number of frost days and with an increase in the heat wave duration. The magnitudes and main spatial patters of the changes in temperature extremes show a quite good consistency among the three global scenarios and between the one-way and two-way nesting models. A warming environment will also give rise to changes in extreme precipitation events. Precipitation extremes are projected to increase over most of southeast China, and this in a quite consistent manner among the three global scenarios.

Keywords: climate change, climate extremes, variable-grid model, southeast China

THORPEX PACIFIC ASIAN REGIONAL CAMPAIGN FOR TYPHOON TARGETING IN 2008 OVER THE WESTERN NORTH PACIFIC

T. NAKAZAWA[1], P. HARR[2], J. MOORE[3], M. WEISSMANN[4], S. MAJUMDAR[5], C. REYNOLDS[2], C.-C. WU[6], H.-S. Lee[7], H.-M. KIM[8] and K. BESSHO[1]

[1]MRI/JMA, Tsukuba, Japan
[2]NPS, Monterey, USA
[3]NCAR, Boulder, USA
[4]DLR, Wessling, Germany
[5]University of Miami, Miami, USA
[6]NTU, Taipei, China
[7]NIMR/KMA, Seoul, Republic of Korea
[8]Yonsei University, Seoul, Republic of Korea

THORPEX is a 10-year international global atmospheric research program under the World Meteorological Organization (WMO)/World Weather Research Program (WWRP) to accelerate improvements in the accuracy of 1-day to 2-week high-impact weather forecasts and in society's utilization of weather products. The program was established in May 2003 by the 14th WMO Congress (see http://www.wmo.int/pages/prog/arep/thorpex/index_en.html).

The THORPEX Pacific Asian Regional Campaign (T-PARC) was conducted in 2008 over the western North Pacific, aiming at our understanding of (i) tropical cyclogenesis, (ii) recurvature, (iii) extra-tropical transition (ET) of tropical cyclones. T-PARC is based on the societal needs to improve prediction of (i) the lifecycle of western Pacific and Asian typhoons from genesis to extratropical transition/decay, and (ii) high-impact weather events, over North America, the Arctic and other locations, whose dynamical roots and/or forecast errors are driven by upstream typhoons and other intense cyclogenesis events over east Asia and the western Pacific.

The following aircrafts have been operated during the campaign period from August 1 to October 5.

- DLR Falcon 20
- WC-130J (from USAF under the program of TCS-08)
- P-3 (from NRL under the TCS-08)
- ASTRA (from DOTSTAR)

In addition, the Driftsonde operation was conducted by US, the special upper-sounding operations were made by KMA and JMA and the rapid-scan operations by MTSAT-2 were also performed by JMA.

During the campaign, totally eleven tropical circulation systems were observed; four named tropical storms, one tropical depression, one ex-tropical storms and five others.

In this paper we document the overview of the campaign and show the preliminary results on targeted observation to improve typhoon track forecasts. .

Keywords: THORPEX, typhoon, targeting, western Pacific

DROPSONDE OPERATION OF FALCON IN T-PARC AND THE ANALYSES OF SURROUNDING ENVIRONMENT OF TYPHOONS

Kotaro BESSHO*[1], Tetsuo NAKAZAWA[1] and Martin WEISSMANN[2]
[1] Meteorological Research Institute, Tsukuba, Japan
[2] Institut für Physik der Atmosphäre, DLR Oberpfaffenhofen, Wessling, Germany

Abstract

From 23 August to 4 October 2008, missions of German Aerospace Center aircraft Falcon was executed under T-PARC with collaboration of Meteorological Research Institute / Japan Meteorological Agency (JMA). Falcon observed the atmospheric profiles in and out of clouds surrounding typhoons using its dropsonde system to achieve the target observation. In the missions, Falcon had 25 flights around Japan islands and its total flight times were 85 hours. The total number of dropsondes in its flights was 328. The observational targets were mainly recurvatures and extratropical transitions of Typhoon Sinlaku and Jangmi.

In early autumn, there is Autumn Rain Front (ARF) near Japan islands. ARF usually brings light rain, not heavy rainfall like Baiu-Meiyu-Chagma front in early summer. Sometimes it causes big disasters such as floods combined with typhoons moved to mid-latitude. Because of difficulty of catching the rare case of heavy rainfall in ARF, there was no observational experiment for ARF. In T-PARC, Falcon had many chances to observe the detailed structures of ARF affected by typhoons.

And from the point of view of typhoon structure, Falcon also got suitable dropsonde data set for Delta Rain Shield (DRS) located on the northern side of typhoon approaching mid-latitude frontal zones. DRS is often accompanied by heavy rain.

ARF with typhoons and DRS within typhoons were not investigated by using observational equipments still now. But it is important to clear their structures for understanding the impact of extratropical transition of typhoons to the forecast because ARF and DRS have big roles as heat source. In this presentation, outline of Falcon mission in T-PARC focused on dropsonde operation will be presented. And the preliminary results of analyses of ARF with typhoon and DRS from the dropsonde observations by Falcon and other aircrafts with JMA special and operational data will be shown.

Keywords: THORPEX, T-PARC, Falcon, dropsonde, typhoon

JMA SINGULAR VECTOR GUIDANCE FOR T-PARC 2008

Takuya KOMORI [1]*, Ryota SAKAI [1], Hitoshi YONEHARA [1], Kiyotomi SATO [1], Takashi KADOWAKI [1], Takemasa MIYOSHI [2], Munehiko YAMAGUCHI [3], Tetsuo NAKAZAWA [4], Kotaro BESSHO [4], Naoko KITABATAKE [4]

1: Numerical Prediction Division, Japan Meteorological Agency, Tokyo, Japan
2: University of Maryland, Maryland, USA
3: University of Miami, Florida, USA
4: Typhoon Research Department, Meteorological Research Institute, Tsukuba, Japan
Email: komori@met.kishou.go.jp

Abstract

The Japan Meteorological Agency (JMA) performed special observations and sensitivity analysis of tropical cyclones (TCs) as a part of the THORPEX Pacific Asian Regional Campaign (T-PARC). To provide guidance for the special targeted observations, sensitivity analysis was performed using a total energy singular vector (TESV) method; the activities are presented.

For effective decision making of targeted observations using the information of sensitive area, a 2day lead-time was needed for each observation. Accordingly, the sensitivity analysis was performed for the forecast fields (T+24h and T+48h) of operational Global Spectral Model (GSM) at a TL959L60 resolution. In addition to daily sensitivity analysis for three fixed target areas (named as GUAM, TAIWAN and JAPAN), JMA conducted another sensitivity analysis for an adaptive target area (named as MVTY) in the vicinity of the TC location because an adaptive target area is preferable when targeting a TC although a fixed target area is useful for inter-comparison of the sensitive area calculated by each provider. The MVTY target region was automatically defined according to the TC position forecasted by the operational GSM. The optimization time of SV was chosen to be 48 hours for the GUAM, TAIWAN and JAPAN regions and 24 hours for the MVTY region.

The TESVs calculated for all target areas were called moist TESVs, because moist processes including both large-scale condensation and deep convection were implemented in the tangent linear and adjoint models at a T63L40 resolution for the global domain. In addition to impact of the moist processes, JMA TESVs calculated using tangent linear and adjoint models with different resolutions are compared and discussed.

Keywords: T-PARC, tropical cyclone, singular vector, sensitivity analysis

ADAPTIVE OBSERVATION GUIDANCE AND OBSERVATION SYSTEM EXPERIMENTS FOR TROPICAL CYCLONES DURING T-PARC 2008

Hyun Mee KIM, Byoung-Joo JUNG, and Sung Min KIM
Atmospheric Predictability and Data Assimilation Laboratory,
Department of Atmospheric Sciences, Yonsei University
Shinchon-dong 134, Seodaemun-gu, Seoul, 120-749, Republic of Korea
khm@yonsei.ac.kr

Abstract

Tropical cyclones in the western North Pacific (i.e., typhoons) are affected by complex dynamical systems over the area. To improve short-range typhoon forecasts, observation field experiments as T-PARC (THORPEX-Pacific Asian Regional Campaign) have been implemented in the western North Pacific. During these field experiments, additional (or adaptive) dropsonde observations are deployed over the sensitive regions where the observations may have the most impact in typhoon forecasts.

In this study, the characteristics of total energy singular vectors of typhoons that occurred during T-PARC period (1 August ~ 4 October 2008) are evaluated using a mesoscale model and its tangent linear and adjoint models with a Lanczos algorithm. In addition, the impact of the additional dropsonde observations to typhoon track forecasts is investigated by implementing observation system experiments for typhoons observed during T-PARC experiments. As the model and data assimilation system to assimilate the dropsonde data, the Weather Research and Forecasting (WRF) model and the corresponding three dimensional variational (3DVAR) data assimilation system are used. The characteristics of adaptive observation guidance and the results of observation system experiments will be presented in the conference.

Keywords: T-PARC, adaptive observations, observation system experiments, typhoon forecasts, data assimilation system

AN OBSERVING SYSTEM EXPERIMENT OF SPECIAL OBSERVATIONS OF T-PARC FOR SINLAKU AND JANGMI USING THE OPERATIONAL NWP SYSTEM AT JMA

Koji Yamashita[1], Yoichiro Ohta[1] and Tetsuo Nakazawa[2]
[1]Numerical Prediction Division, Japan Meteorological Agency, Tokyo, Japan
[2]Meteorological Research Institute, Tsukuba, Japan
kobo.yamashita@met.kishou.go.jp

Abstract

A special observation experiment project that examines the effectiveness of next generation forecast technology, "Interactive forecast system", has been performed under THORPEX Pacific Asian Regional Campaign (T-PARC) for track forecasts of three typhoons in the summer of 2008 at JMA. Special observations for T-PARC2008 are dropwindsonde observations, extra radiosonde observations at JMA observatories and ships observations. Meteorological Satellite Center (MSC) of JMA produced MTSAT-2 Rapid Scan Atmospheric Motion Vector (MTSAT-2-RS-AMV) for T-PARC2008.

In the project, we conducted three kinds of numerical experiments which are different in use of the special observations and typhoon bogus data using the JMA operational NWP system: (I) special observations are assimilated (TEST); (II) special observations are not assimilated (CNTL); (III) typhoon bogus data (BOGUS) are assimilated instead of special observation. If conventional observations are not sufficient in the vicinity of a typhoon, the bogus data are assimilated to generate a realistic typhoon structure in an analysis field in the operational system. The purpose of the third experiment is to evaluate the effect of the bogus technique. These typhoon track forecasts are compared with the observed typhoon track.

The typhoons of SINLAKU and JANGMI, which came to the vicinity of Japan, have been taken up to investigate through an Observing System Experiment (OSE) using the special observational data, typhoon bogus data and MTSAT-2-RS-AMV data.

Comparing the result of TEST to CNTL in the two typhoons without bogus data, their track errors of TEST in the before-recurvature stage were reduced by about 23-40 % within 12-hour forecasts. Their intensity forecast errors were also reduced considerably around 23-50 % in improvement rate at least within 48-hour forecasts. These results suggest that the special observations contributed significantly to enhance accuracy of the analysis fields. On the other hand, in the after-recurvature stage, their track and intensity forecast errors of TEST have remained almost the same as those of CNTL.

The results of OSE with BOGUS in early hours of forecasts were close to the observed typhoon tracks and intensities in the before-recurvature stage compared with no BOGUS.

These results will be reported in detail. We also will make further experiments and will present as much as possible about the results of OSEs including sensitivity analysis.

Keywords: Typhoon, Special Observation, OSE, T-PARC

OBSERVATION AND SIMULATION OF THE GENESIS OF TYPHOON FENGSHEN (2008) IN THE TROPICAL WESTERN PACIFIC

Hiroyuki YAMADA[1], Wataru YANASE[2], Ryuichi SHIROOKA[1],
Kunio YONEYAMA[1], Masaki SATOH[1,2], and Masanori YOSHIZAKI[1]
[1]Japan Agency for Marine-Earth Science and Technology, Yokosuka, Japan;
[2]Center for Climate System Research, University of Tokyo, Kashiwa, Japan
Email: yamada@jamstec.go.jp

Abstract

The formation of an incipient vortex and its rapid growth into Typhoon Fengshen (2008) were successively observed during a field campaign using ground-based and ship-borne Doppler radars in the tropical Western Pacific. In addition, the rapid growth was numerically simulated using a global cloud-resolving model (NICAM). In the present study, the multi-scale structure and evolution of this tropical cyclone in its genesis stage are examined based on the observational evidence and simulation results. The goal of the study is to reveal the mechanisms governing tropical cyclogenesis over a monsoon trough in the Western Pacific. The initial vortex formed when an off-equatorial westward-propagating tropical disturbance approached the monsoon trough. This vortex was marked by the stagnation over the trough with diurnal convective activity for the first three days. The Doppler radars observed many mesoscale convective vortices near the circulation center in this period. Gradual deepening of a near-surface layer with positive vorticity was observed by an upper-air sounding array. Rapid intensification of the vortex into a typhoon occurred when another cloud system with strong upward motion approached the vortex center from southeast. This seems to have caused the vertical stretching of the whole circulation, leading spin-up of the cyclone. The cloud-resolving simulation succeeded to reproduce the rapid intensification. The rainfall distribution and low-level flow structure were similar to the observed ones, showing a good reproducibility. These results may provide information necessary to understand the mechanisms associated with tropical cyclogenesis.

Keywords: tropical meteorology, typhoon, cyclogenesis

Development of a typhoon genesis in the early stage simulated in hydrostatic- and non-hydrostatic atmospheric models

Mayumi K. YOSHIOKA, Kazuhisa TSUBOKI and Atsushi SAKAKIBARA
Hydrospheric Atmospheric Research Center (HyARC), Nagoya University, Nagoya, JAPAN
yoshioka@rain.hyarc.nagoya-u.ac.jp

Abstract

A typhoon generated from a typhoon genesis (tropical cyclogenesis) grows up with enhancement by active cumulus convections in a favorable environment in the western north Pacific in the tropics.

In this study, typhoon genesis developed from low level vortexes were investigated in the quite early stage with hydrostatic and non-hydrostatic atmospheric numerical models.

Two atmospheric numerical models were utilized in this study: (1) AFES (AGCM For the Earth Simulator), a hydrostatic model, was performed at a high resolution of T639L96, of which the horizontal resolution is about 20km at the equator. AFES at the high resolution enabled to describe both typhoon structures of several hundred kilometers and their environmental atmospheric field. (2) CReSS (Cloud Resolving model for Storm Simulator), a regional non-hydrostatic model including cloud physics, was applied for the regions of about 2000km around the center of the early low level vortexes (typhoon genesis) which were detected in the global field simulated by the AFES. CReSS performed at 2km resolution describes isolated strong cumulus convections.

Two typhoon genesis were analyzed, which were detected in the AFES simulations performed for October 8-15 in 2004. One decayed within a day and the other lived long over several days. Regional simulations for the typhoon genesis were performed by CReSS for 1 day from their detections.

The developing typhoon genesis had some strong cumulus convections surrounded of several kilometers in the spiral structure and moist westerlies in the southern part in the environment. The typhoon genesis of early decay was weakened by strong cumulus of no spiral structure around the center, besides weak moist westerlies in the southern part. In the time development, the strength of the tropical storm (e.g., tangential wind and central sea level pressure) tends to be suppressed more in the CReSS than in the AFES.

Keywords: tropical cyclogenesis, typhoon, AGCM, cloud resolving model

Comparison of three western North Pacific Tropical Cyclone best track datasets in seasonal context

Ming YING[1] and Eun-Jeong CHA[2,*]
1. Laboratory of Typhoon Forecast Technique, Shanghai Typhoon Institute, China Meteorological Meteorological Administration, Shanghai, China
2. National Typhoon Center/Korea Meteorological Administration, Seogwipo, Jeju, Korea
Email cha@kma.go.kr

Abstract

The quality of tropical cyclone (TC) best track data has received increasingly more attention in climate research in recent years because of interest in the possible effects of global warming on TC activity. In this paper, three best track datasets for the western North Pacific TCs are compared in a seasonal context. Although their power spectra are different in decadal and longer-timescale variations, they show consistent annual cycles. The medians of pentad-by-pentad storm frequencies (PSFs) reveal that the annual cycle in the JMA data is the most intense on average, but those in the JTWC and CMA-STI data are quite similar, while the interannual variability of PSFs is weaker in the CMA-STI than in the JMA or JTWC. An inhomogeneity is also identified for the JTWC data around 2003~2004 by both the outliers and by a detailed comparison with the JMA and CMA-STI data.

K-means cluster analysis demonstrated that due to difference in interannual variabilities, both the JMA and JTWC data are clearly affected by the outliers, while the CMA-STI data can effectively resist the effects of the outliers. However, after excluding the outliers, the results from the JMA and JTWC data are more consistent than are the CMA-STI data. The JTWC data also tend to be distinctly affected by the wind conversion with different averaging time intervals, whereas the representation of the annual cycle is important for the CMA-STI data.

Key Words: Tropical cyclone, Best track, the western North Pacific, Annual cycle, Data comparison

CLIMATOLOGY OF MULTI-TROPICAL CYCLONE ACTIVITIES IN THE WESTERN NORTH PACIFIC

YING, Ming
Laboratory of Typhoon Forecast Technique, Shanghai Typhoon Institute of China Meteorological Administration, Shanghai, China
yingm@mail.typhoon.gov.cn

Abstract

Multi-tropical cyclone (MTC) events always indicate intense tropical cyclone (TC) activities. The climatological characteristics of MTC events in the western North Pacific (WNP) are investigated using the CMA-STI TC best track data from 1949 to 2006. The frequency of MTC events are decreasing exponentially when TC number increases, which demonstrates they are extreme climatic events. The duration of a MTC event is generally about two to seven days. The differences of intensities between every two TCs are commonly less than 20 ms^{-1}, while their distances are between 1700 to 4000 Km. Both the TC pairs close to each other and those pairs rotating anticlockwise about each other tend to occur in the west and south part of the WNP.

Some properties of MTCs, such as the distances and its accumulated changes between the TC pairs, suggest that MTC activities may have two different regimes. The two regimes are indicated by the MTC-associated abnormal wave chains in the 500 hPa geographical height fields as well. A PJ-like wave chain is associated with the chain-like MTC patterns, which usually exist at 2- and 3-TC events and some 4-TC events; while a zonal wave chain from the East Asia to the North America commonly appears during the block-like MTC events, which mainly exist at 5- and 6-TC events and other 4-TC events. These findings suggest that MTC events may have feedbacks on their embedded air circulation, and may be useful in further studies on the relationship between them.

Keywords: multi-tropical cyclone, climatology, anomalous wave chain, the western North Pacific

Acknowledgements: This research is sponsored by the Shanghai Typhoon Research Foundation under Grant #2004STB03 and the National Natural Science Foundation of China under Grant #40805040.

INTERDECADAL VARIABILITY OF TROPICAL CYCLONE LANDFALL IN THE PHILIPPINES FROM 1902 TO 2005

H. KUBOTA[1], and J. C. L. CHAN[2]
[1] Institute of Observational Research for Global Change, Japan Agency for Marine-Earth Science and Technology (IORGC, JAMSTEC), Yokosuka, Japan, kubota@jamstec.go.jp
[2] Guy Carpenter Asia-Pacific Climate Impact Centre, City University of Hong Kong, Hong Kong, China

Abstract

Recently, the variability of Tropical Cyclone (TC) activity has become a great concern because it may be linked to global warming. The activity of TC has interannual and interdecadal variabilities. To discover the variability, long term TC track data is necessary. At present, TC track data is available from 1945 by Joint Typhoon Warning Center (JTWC) over the western North Pacific (WNP). In this study, historical observation record of TC track is collected by Monthly Bulletins of Philippine Weather Bureau (MBP) over the WNP of 1901 to 1940. A dataset of tropical cyclone landfall numbers in the Philippines (TLP) is created from a combination of historical observation record of the MBP and JTWC best-track data for the period of 1902 to 2005. Interdecadal variability of TLP is found to be related to different phases of El Niño/Southern Oscillation (ENSO) and Pacific Decadal Oscillation (PDO). The annual TLP has an apparent oscillation of about 32 years before 1939 and about 10-22 years after 1945. No long-term trend is found. During the low PDO phase, the annual TLP decreases (increases) significantly in El Niño (La Niña) years. During the high PDO phase, however, the difference in annual TLP between different ENSO phases becomes unclear. These results suggest that natural variability is prevailed in the interdecadal variability of TLP. Then, we will expand the analysis of interdecadal variability of TC to the WNP.

Keywords: tropical cyclone, interdecadal variability, Philippine

INTERCOMPARISON OF DVORAK PARAMETERS IN THETROPICAL CYCLONE DATASETS OVER THE WESTERN NORTH PACIFIC

Shunsuke HOSHINO and Tetsuo NAKAZAWA
Meteorological Research Institute, Tsukuba, Japan
shoshino@mri-jma.go.jp

Abstract

A study to compare Dvorak parameters (T-number and CI-number) for tropical cyclones over the western North Pacific in both JMA and JTWC datasets from 1987 to 2006 is presented to show if there is a difference between two datasets. The study shows that the Dvorak parameters by JTWC are generally higher than these by JMA during the period of 1992-1997 and 2002-2005. The major reasons for stronger cases in JTWC are "faster intensification before the mature stage and slow/delayed start of weakening after the mature stage".

Keywords: tropical cyclone

Projection of changes in tropical cyclone activity and its cloud height due to a greenhouse warming: a global-cloud-system-resolving approach

Yohei Yamada[1]*, Kazuyoshi Oouchi[1], Masaki Satoh[1,2],

Hirofumi Tomita[1] and Wataru Yanase[3]

[1]Research Institute for Global Change, Japan Agency for Marine-Earth Science and Technology, 3173-25 Showamachi, Kanazawa-ku, Yokohama-Shi, Kanagawa 236-0001, Japan,
[2]Center for Climate System Research, the University of Tokyo, 5-1-5 Kashiwanoha, Kashiwa-Shi, Chiba 277-8568, Japan
[3]Ocean Research Institute, the University of Tokyo, 1-15-1 Minamidai, Nakano-ku, Tokyo 164-8639, Japan

Email yoheiy@jamstec.go.jp

Abstract

Change of tropical cyclone (TC) activity in greenhouse-warmed (GW) climate has been traditionally investigated using general circulation models (GCMs). However, GCMs involve uncertainty in treating the ensemble effects of deep convections. Here we sidestep the uncertainty using a global cloud-system-resolving model (GCSRM) of 14-km mesh, and assess the future TC changes based on the time slice experiment for the present-day control (CTL) and future GW experiments spanning 5 months each. Comparison between the two cases reveals the change of TC in favor of the statement in Intergovernmental Panel on Climate Change (IPCC) Fourth Assessment Report in that reduction of global frequency (by about 25%) and increase of more intense TCs. The frequency reduction is notable over the North Atlantic, which is explained by intensified vertical shear in the subtropical main development region flanked by the weakened shear region equatorward, as revealed from recent observations. The GCSRM runs also demonstrate that the cloud height becomes taller for more intense TC, and the relationship is strengthened in GW

Keywords: tropical cyclone, global warming, global cloud-system-resolving

RESPONSE OF TROPICAL CYCLONE POTENTIAL INTENSITY TO A GLOBAL WARMING SCENARIO IN THE IPCC AR4 CGCMs

Jinhua Yu[1,2], Yuqing Wang[2,1], and Kevin Hamilton[2]

[1] KLME, Nanjing University of Information Science and Technology, Nanjing 210044, China

[2]International Pacific Research Center and Department of Meteorology, School of Ocean and Earth Science and Technology, University of Hawaii at Manoa, Honolulu 96822, US

Abstract

This paper reports on an analysis of the tropical cyclone (TC) potential intensity (PI) and its control parameters in transient global warming simulations. Specifically the TC PI is calculated for Coupled Model Intercomparison Project/CMIP3 integrations during the first 70 years of a transient run forced by 1% per year CO_2 increase. The linear trend over the period is used to project a 70-yr change in relevant model parameters. The results for a 15-model ensemble mean climate projection show that the thermodynamic potential intensity (THPI) increases on average by 1.0%~3.1% over various TC basins, which is mainly attributed to changes in the disequilibrium in enthalpy between the ocean and atmosphere, in the transient response to increasing CO_2 concentrations. This modest projected increase in THPI is consistent with that found in other recent studies.

In this paper we also quantify the effects of evolving large-scale dynamical factors on the projected TC PI using the empirical formulation of Zeng et al. (2007, 2008), which takes into account the effects of vertical shear and translational speed based on a statistical analysis of present day observations. Including the dynamical efficiency in the formulation of PI leads to larger projected changes in PI relative to that obtained using just THPI in some basins and smaller projected changes in others. The inclusion of the dynamical efficiency has the largest relative effect in the main development region (MDR) of the North Atlantic where it leads to a 50% reduction in the projected PI change. Results are also presented for the basin-average changes in PI for the climate projections from each of the 15 individual models. There is considerable variation among the results for individual model projections, and for some models the projected increase in PI in the Eastern Pacific and South Indian Ocean regions exceeds 10%.

Keywords: global warming, tropical cyclone potential intensity, IPCC AR4 models

MULTISCALE INTERACTIONS ON THE LIFECYCLE OF TROPICAL CYCLONE SIMULATED BY GLOBAL CLOUD-SYSTEM-RESOLVING MODEL

Hironori FUDEYASU[1], Yuqing WANG[1], Masaki SATOH[23], Tomoe NASUNO[3], Hiroaki MIURA[3] and Wataru YANASE[2]
1 International Pacific Research Center, University of Hawaii, Honolulu, USA
2 Center for Climate System Research, University of Tokyo, Kashiwa, Japan
3 Japan Agency for Marine-Earth Science and Technology, Yokohama, Japan
Email: fudeyasu@hawaii.edu

Abstract

The global cloud-system-resolving model, NICAM, successfully simulated the lifecycle of Tropical Storm (TS) Isobel that formed over the Timor Sea in the austral summer 2006. The multiscale interactions on the lifecycle of the simulated storm have been analyzed in this study as the large-scale and meso-scale aspects. The westerly wind burst accompanied by the onset of a Madden-Julian Oscillation (MJO) event over the Java Sea enhanced the cyclonic shear and convergence in the lower troposphere, providing the pre-conditioned large-scale environment for the genesis of Isobel. In the subsequent evolution, five stages are identified for the simulated Isobel, namely, the initial eddy, intensifying, temporary weakening, re-intensifying, and decaying stages.

At the initial eddy stage, small-/meso-scale cyclonic vortices (eddies) developed in the zonally-elongated rainband organized in a convergent shear-line in the lower troposphere over the sea north of Java. As the MJO propagated eastward, the cyclonic eddies moved southeastward with intensifying convective activities, showing the signal of cyclogenesis over the Timor Sea. As a result of multi-vortex interaction/merging in an environment with enhanced low-level cyclonic vorticity and weak vertical shear, a typical tropical cyclone structure developed, leading to the birth of Isobel (intensifying stage). An approaching subtropical high from the southwest exposed Isobel to a large-scale stretching deformation field with strong vertical shear. This change led to the development of asymmetric structure in the inner core of Isobel and interrupted its intensification, causing a temporary weakening (temporary weakening stage). As the vertical shear weakened and changed the direction in response to the upper-level northerlies, Isobel re-intensified in response to the reformation of its eyewall as a result of the inward spiraling rainband that was formed on the downshear left side (re-intensifying stage). Finally Isobel decayed due to the land effect as it approached the land and made landfall in northwest Australia (decaying stage).

A multiscale interaction associated with the genesis of Isobel has been investigated. It is clear that the large-scale cyclonic shear closely related to the WWB in the MJO provided a favorable condition for deep convection over the sea north of Java. The deep convection was accompanied by small-scale high low-level cyclonic potential vorticity with diameters less than 40 km, very similar to the so-called vortical hot towers discussed by previous studies (e.g., Montgomery et al. 2006). Isobel thus formed as a result of the following events: increased cyclonic shear due to the WWB, collective heating from the vortical hot towers, the merging and strengthening of low-level potential vorticity of the hot towers, and eventually the axisymmetrization of meso-scale features by the storm-scale low-level cyclonic circulation over the sea south of Java.

Keywords: TC lifecycle, multiscale interactions, vortical hot towers, MJO, NICAM

SIMULATIONS OF TROPICAL CYCOGENESIS USING MODELS WITH DIFFERENT RESOLUTIONS

Masato SUGI[1], Sachie KANADA[2] and Kengo MIYAMOTO[2]
1 Research Institute for Global Change, JAMSTEC, Yokohama, Japan
2 Advanced Earth Science & Technology Orgainazation, Tsukuba/Tokyo, Japan

msugi@mri-jma.go.jp

Abstract

What resolution is required to simulate tropical cyclogenesis? Can we simulate tropical cyclogensesis properly by using low resolution models with cumulus parameterization? To answer these questions, a series of forecast experiments of the genesis period of Typhoon SAOMAI (T0608) in August 2006 have been conducted. Models used for the experiments are the JMA global model (GSM) with resolution of 60km and 20km, and JMA/MRI non-hydrostatic model (NHM) with resolutions of 20km, 5km and 2km. Note that the NHM with 2km resolution does not use cumulu parameterization, while all other models use cumulus parametrizaion. In the forecast experiments, the genesis process of the typhoon has been simulated very well by all the models with different resolutions ranging from 60km to 2km.

In low level vorticity field of the high resolution models (5km and 2km resolution NHM), we can see a lot of small scale intense positive and negative vortices over the active convection regios (Fig.1). When we apply smoothing over these regions we have weak vorticity field similar to that of 20km resolution model. This indicates that these convection scale vortices do not play an essential role in the tropical cyclogensesis process, because the 20km resolution model which does not have such small scale vortices can simulate the genesis process as well as 2km resolution model.

Keywords: tropical cyclogensis, typhoon, cumulus parameterization

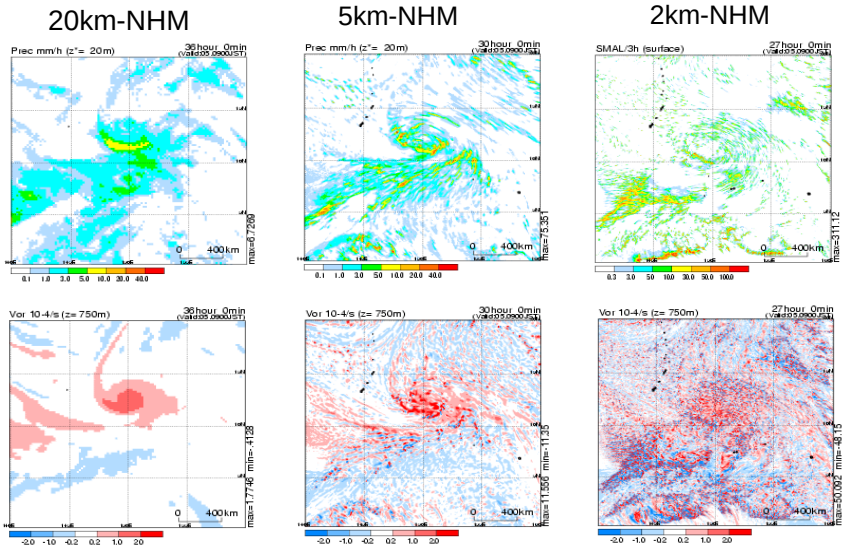

Fig.1 Simulations of genesis process of T0608.
Top: 3-hrly precipitation. Bottom: Vorticity at 750 m altitude.

AN EXPERIMENT WITH THE HIGH RESOLUTION GLOBAL ICOSAHEDRAL GRID POINT MODEL FOR THE PREDICTION OF TROPICAL CYCLONES OVER THE NORTH INDIAN OCEAN

Yogesh KUMKAR, Purnendranath SEN, Ok-Yeon KIM and *Jai-Ho OH
Integrated Climate System Modeling Lab, Busan, South Korea.
jhoh@pknu.ac.kr

Abstract

In this paper an attempt has been made to conduct a numerical experiment with the high resolution Global GME model to predict the tropical storms in the North Indian Ocean during the year 2007. Numerical integrations using the Icosahedral Hexagonal Grid Point Global Model (GME) were performed to study the evolution of tropical cyclones viz; Akash, Gonu, Yemyin and Sidr over North Indian Ocean during 2007. It has been observed that the GME model forecast underestimates Cyclone's intensity, but the model can capture the evolution of Cyclone's intensity; especially it's weakening during landfall, which is primarily due to the cutoff of the water vapor supply in the boundary layer as Cyclones approach the coastal region. A series of numerical simulation of tropical cyclones have been performed with GME to examine model capability in prediction of intensity and track of the cyclones. In the North Indian Ocean, Tropical cyclones form mainly during the Pre – Monsoon and the Post Monsoon Seasons[12, 13]. During the South West Monsoon period four to five low pressure systems develop over the North Indian Ocean, but very rarely do they intensify into Tropical Cyclone stage. The model has been able to simulate the cyclonic storm 'Akash' reasonably well. But it has underestimated the central pressure and the wind speed in the case of Super Cyclonic storm Gonu. In the case of the cyclone Yemyin it has overestimated the parameters. In the case of Sidr the model has been able to simulate the track of the cyclone reasonably well. The model is also simulating the accumulated rainfall reasonably well. Thus the GME model has a tendency to underestimate the central pressure or winds for a very intense system over the Bay of Bengal. However the model is capable to simulating a tropical storm of moderate intensity reasonably well, keeping in mind that GME is a Global model. Therefore, we can conclude that in spite being a global model GME is capable of simulating the tropical storms over the North Indian Ocean reasonably well.

Keywords: Tropical Cyclones, GME, Icosahedral-hexagonal grids

***Correspondence with:**

Prof. Jai Ho Oh

LARGE-SCALE ENVIRONMENTAL FIELD ASSOCIATED WITH TROPICAL CYCLOGENESES OVER THE BAY OF BENGAL

Wataru Yanase[1], Hiroshi Taniguchi[2] and Masaki Satoh[2,3]
1 Ocean Resarch Institute, The University of Tokyo, Tokyo, Japan
2 Frontier Research Center for Climate Change,
Japan Agency for Marine-Earth Science and Technology, Kanagawa, Japan
3 Center for Cliamte System Research, The University of Tokyo, Chiba, Japan
E-mail: yanase@ori.u-tokyo.ac.jp

Abstract

In May 2008, Cyclone Nargis caused catastrophic destruction in Myanmar. From late April to early May including the period of Nargis's life-cycle, the large-scale westerly wind in the lower troposphere over the Bay of Bengal shifted from the equator to ~10^{o}N. The shift of westerly flow had longer time scale and larger horizontal scale than those of a tropical cyclone, which seems to be related to the seasonal transition and boreal summer intra-seasonal oscillation (BSISO) in the Asian monsoon. During the northward shift of the westerly flow, based on the genesis potential analysis (Emanuel and Nolan, 2004), the Bay of Bengal was characterized by an environment favorable for the tropical cyclogenesis. Therefore, in the present study, the climatological relation between environmental field and tropical cyclogeneses over the Bay of Bengal between 1982 and 2008 was analyzed using best-track and JCDAS reanalysis datasets.

The composite analysis showed that signal of high genesis potential shifted northward from the equator to the Bay of Bengal with time-scale of ~40 days during the period including tropical cyclogeneses, which resembles the characteristic of the BSISO. The high genesis potential was attributed to the high vorticity in the lower tropsphere, weak vertical shear, and high relative humidity in the middle tropsphere. Thus, the modulation of large-scale environmental field influenced the tropical cyclogeneses over the Bay of Bengal. In additional analysis based on the the phase of BSISO, the frequency of tropical cyclogenesis over the Bay of Bengal was apparently modulated by the BSISO. These results are important for the probablistic prediction of tropical cyclogeneses in the region.

Keywords: tropical cyclogenesis, genesis potential, monsoon, intra-seasonal oscillation, the Bay of Bengal

NUMERICAL STUDY ON THE RAPID DEVELOPMENT OF THE DEEP CONVECTION TO THE NORTH OF TYPHOON BEBINCA

Arakane, S., M. Satoh and W. Yanase
Center for Climate System Research, The University of Tokyo.
Kashiwa, Japan
arakane@ccsr.u-tokyo.ac.jp

Abstract

The satellite imagery showed that Typhoon Bebinca (T0616) in October 2006 had deep convection to the north of typhoon center rather than near the center, which differed from a typical cloud pattern with spiral bands and a cloud free eye. This study performed a numerical simulation of Typhoon Bebinca, using the stretched Nonhydrostatic ICosahedral Atmospheric Model (NICAM), whose finest grid interval is about 24 km around the typhoon.

The NICAM simulation reproduces the deep convection to the north of Typhoon Bebinca. The formation mechanism of the deep convection was analyzed in detail. A sensitivity experiment modifying the water vapor field indicates that the low-level water vapor mainly transported by the cyclonic circulation generates latent instability in the convective area. The Q-vector analysis (Hoskins and Pedder, 1980) shows that synoptic-scale dynamical ω-forcing occurs around the convective area on the eastern side of the upper-trough. In addition, a sensitivity experiment using a enhanced bogus vortex suggests the structure of Bebinca, which has a weak Ekman convergence, is preferable for the excitation of the deep convection in the north area.

Keywords: typhoon, deep convection, ω-forcing

Mechanisims of Warm Core Formation and Pressure Fall of a Developing Typhoon Simulated by the Cloud-Resolving Model

Tomohito Hioki, and Kazuhisa Tsuboki
Hydrospheric Atmospheric Research Center, Nagoya University, Nagoya, Japan
hioki@rain.hyarc.nagoya-u.ac.jp

Abstract

Warm core and eyewall are characteristic structures of a typhoon and are related to the central pressure fall. Focusing on a structure of the inner core of a typhoon, we performed a numerical simulation with very high resolution using a cloud-resolving model, CReSS (the Cloud Resolving Storm Simulator). Purpose of the present study is to reveal the origin of air which composes the warm core and the path of airparcels removed from the center of typhoon.

The result of the simulation shows that the track and the central pressure drop of the simulated typhoon are similar to those of the observed typhoon. Typical structures and dynamical characteristics such as warm core, the eyewall, lower level inflow, updraft in the eyewall, and upper level outflow, were successfully simulated. The maximum of the warm core is formed at an altitude of 15 km. At this height, potential temperature perturbation was larger than 14 K.

We performed a backward trajectory analysis to find the origin of airparcels within the maximum of the warm core. The backward trajectory analysis revealed two major pathes of airparcels toward the warm core. One is the path of airparcels which come inward in the lower troposphere and ascend in the eyewall. The other is that of airparcels descending form the lower stratosphere. When the airparcels ascends in the eyewall cloud, potential temperature increases greatly owing to the condensation diabatic heating. This indicates that one of the heat sources of the warm core is the diabatic heating in the eyewall clouds.

We also performed a forward trajectory analysis of airparcels with the origin in the lower troposphere to find the path of airparcels. This shows that most airparcels flow outward at the upper troposphere by the centrifugal force which is larger than the pressure-gradient force, and a small number of airparcels come into the warm core by the pressure-gradient force which is larger than the centrifugal force.

We also performed a forward trajectory analysis of airparcels in the center of typhoon to reveal the path of airparcels removed form the center of typhoon. The forward trajectory analysis reveal that airparcels of the center of typhoon move into the eyewall at all levels of the troposphere. After entering into eyewall, airparcels ascend in the eyewall and flow outward in the upper troposphere. As a result the central pressure decreases.

POSSIBLE CONTROL OF NEAR-SURFACE WIND DISTRIBUTIONS IN TYPHOONS BY ENVIRONMENTAL VERTICAL WIND SHEAR

Mitsuru UENO and Masaru KUNII
Meteorological Research Institute, Tsukuba, Japan
mueno@mri-jma.go.jp

Abstract

Azimuthal wavenumber-one structures of near-surface winds are investigated attempting both theoretical and statistical approaches. In the theoretical approach, a set of analytical formulae that relate the asymmetries of radial and tangential winds to convective asymmetry in the eyewall region are derived by applying a scaling argument to the result from a numerical simulation of Typhoon Chaba (2004). The formulae predict that the maximum in storm-relative tangential wind occurs 90 degree azimuthally downwind of the enhanced updraft region. On the other hand, the statistical approach is based on the operational mesoscale analyses from the Japan Meteorological Agency (JMA) for the four typhoon seasons from 2004 to 2007, and QuikSCAT data from 1999 to 2008. The statistical approach reveals that the azimuthal location of tangential wind maximum relative to storm direction is determined by the directional difference between environmental vertical wind shear and storm motion, under relatively strong shear conditions, and the wind maximum, contrary to the majority of cases, tends to occur to the left of motion in cases where the directional difference is very small. Considering the strong dependence of convective asymmetry in the inner-core region on the shear, the results are in line with expectations from the analytic theory.

Keywords: typhoon, wind, asymmetry, shear

ON OCEAN EVIRONMENTAL FACTORS AFFECTING TYPHOON INTENSITY: RESULTS FROM THE COUPLED TYPHOON-OCEAN MODEL

IL JU MOON, SUNG HUN KIM, MIN YOUNG KIM, and YOUNG YUN JUNG
Graduate Course of Marine Meteorology, Cheju National University, Jeju, Korea
ijmoon@jejunu.ac.kr

Abstract

One of crucial factors influencing the tropical cyclone (TC) intensity and its intensification is the ocean thermal energy in the upper ocean. It has also been known that TCs leave a wake of cold surface water behind them that results from rapid turbulent entrainment of cold water into the oceanic mixed layer (Fig. 1). The TC-induced sea surface temperature (SST) cooling, called by SST feedback, plays an negative role on the TC intensity.

A series of numerical experiment was performed with the coupled typhoon-ocean model to investigate systematically oceanic factors determining the effect of the SST feedback under typhoon conditions. In these experiment, various oceanic and atmospheric conditions have been tested using different initial SST, mixed layer depth (MLD), topography, ocean warm core, storm traslantion speed, and recurvature angle, with a special forcuse on the interactions between typhoons and the Changjing diluted water. The resutls will be discussed.

Keywords: the coupled typhoon-ocean model, SST feedback, TC intensity

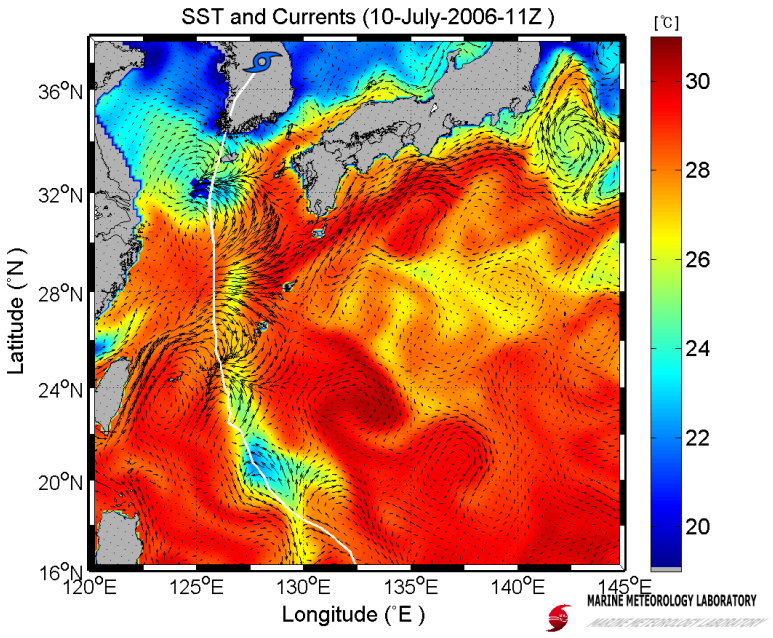

Fig. 1 Distribution of surface temperature and current during the passage of typhoon Ewiniar (2006)

NUMERICAL SIMULATION OF MYANMAR CYCLONE NARGIS AND ITS ASSOCIATED STORM SURGE

Tohru KURODA, Kazuo SAITO, Masaru KUNII, Nadao KOHNO and Hiromu SEKO
Meteorological Research Institute , Japan
Email: tkuroda@mri-jma.go.jp

Abstract

On 2 May 2008, cyclone Nargis made landfall in southwestern part of Myanmar and caused the worst natural disaster in the country which claimed more than one hundred thousand people by storm surge. If an appropriate warning was issued about 2 days before the landfall, the number of casualties might have been reduced drastically. In order to show the performance of the downscale NWP using NHM and JMA data, we performed a forecast experiment of Nargis. We also simulated the storm surge with the Princeton Ocean Model (POM) using the NHM forecast data.

We conduct a regional forecast with NHM, using the JMA global analysis (horizontal resolution is about 20 km) as the initial condition and the GSM global forecast GPV as the boundary condition. NHM is executed with a horizontal resolution of 10 km for a square region of 3400 km around the Bay of Bengal. Considering the lead time for waning, the initial time is set to 12 UTC 30 April, 2008. In the JMA analysis, Nargis was expressed as a weak depression of 999 hPa in the center of the Bay of Bengal, and its position was deviated eastwardly about 0.7 degree in longitude compared with the best track. After 42 hour (06 UTC 2 May), the depression developed to a 974 hPa cyclone and reached southwestern part of Myanmar in the NHM forecast.

Using the NHM forecasted data (surface wind and pressure), we conducted a numerical simulation of the associated storm surge with POM. The horizontal resolution is about 3.5 km and vertically 12 layers sigma coordinates are employed. The domain size is 451x391 which covers eastern part of the Bay of Bengal. In the simulation, the initial state is assumed to be static, and the astronomical tide and wind waves are not considered. In the simulation, we can see a rise of sea-level due to low pressure near cyclone center and southerly sea surface current generated by surface wind flows into mouths of rivers in southern Myanmar. At points in these river mouths, water levels become highest (maximum height is about 3.2m) at the times when the southerly winds are strongest. This correspondence between peaks of wind speed and water level suggests that surface current generated by wind is the major cause of water level rising in these areas.

A mesoscale ensemble forecast experiment of Nargis with 20 members was conducted to consider forecast errors of the cyclone. Initial and boundary perturbations are given by JMA's operational one-week EPS. The center positions of Nargis were distributed in an elliptic area with 200-300 km distant from the control run. Storm surge simulation is also performed using surface wind forecasts by the mesoscale EPS. 13 members predict high tide levels higher than 3 m, while the timings are dispersed from FT=32 to FT=60. Application of NHM-LETKF to modify its intensity is also underway.

Keywords: Myanmar cyclone, Nargis, storm surge, ensemble prediction, (**within 5 words**)

ESTIMATES OF THE AIR-SEA EXCHANGE COEFFICIENTS FOR HIGH WIND REGIME IN A TROPICAL CYCLONE USING AN ADJOINT METHOD

Kosuke ITO, Yoichi ISHIKAWA, and Toshiyuki AWAJI
Department of Geophysics, Kyoto University, Kyoto, Japan
Email: itokosk@kugi.kyoto-u.ac.jp

Abstract

The transfer of momentum and heat between the atmosphere and the ocean is a crucial subject in tropical cyclone intensity prediction [Emanuel, 1986]. The momentum and heat exchanges are usually parameterized using a state-dependent drag coefficient (C_d) and heat coefficient (C_k) that increase approximately linearly with wind speed. The behavior of C_d and C_k are actually determined on the basis of the extrapolations from the measurements in weak-to-moderate wind regimes. More recently, a field measurement of Powell et al. (2003) showed that the C_d decreases at wind speed exceeding 30 m s^{-1}. This feature of the C_d was qualitatively consistent with a coupled wave-wind model study of Moon et al. (2004), though their estimates are far from quantitative agreements. On the other hand, there is, even qualitatively, no consensus on the behavior of the C_k for high wind regime. The uncertainty in these coefficients likely causes the errors in the hurricane modeling.

The adjoint method is a promising candidate for reducing such uncertainty. It is one of the sophisticated data assimilation methods, which combines observations with a dynamical model using a variational approach. The adjoint assimilation technique is often used for the accurate estimates of initial states, but it can be applied to improvement of physical parameter values. In this study, the estimates of the C_d and C_k are obtained to minimize a cost function by incorporating the observational data.

As a first step toward this goal, we employ a simple atmosphere-ocean coupled model, and perform an identical twin experiment. The atmospheric model is a nonhydrostatic, axisymmetric tropical cyclone model originally made by Rotunno and Emanuel (1987). The model is coupled to the one-dimensional ocean model developed by Schade (1997). A "true" case with the particular setting of the $C_{d,true}$ and $C_{k,true}$ is generated by the numerical integration of the coupled model, and an "observation" is generated by adding Gaussian noise to dynamical variables in the true run. The simulation run is initiated with the the particular setting of $C_{d,sim}$ and $C_{k,sim}$, and the observations are incorporated through the adjoint method.

Our result showed that the air-sea exchange coefficients are successfully corrected toward the true values as long as the observations are sufficiently assimilated. The quantity of observations required for the estimates of initial states and physical parameter values will be discussed in terms of the recent observational projects such as THORPEX Pacific Asian Regional Campaign (T-PARC) and A Global Array for Temperature /Salinity Profiling (ARGO) Floats.

Keywords: data assimilation, air-sea interaction, adjoint method, parameter estimation

LATENT HEAT FLUX VARIATIONS DURING TROPICAL CYCLONES IN THE SOUTH CHINA SEA

Weibiao LI[1] Shumin CHEN[1], Youyu LU[2], Dongxiao WANG[3]

1. Department of Atmospheric Sciences, Sun Yat-Sen University, Guangzhou, 510275, China

2. Bedford Institute of Oceanography, Department of Fisheries and Oceans, Dartmouth, Nova Scotia, B2Y 4A2, Canada

3. LED, South China Sea Institute of Oceanology, Chinese Academy of Sciences, Guangzhou 510301, China
Email: eeslwb@mail.sysu.edu.cn

Abstract

Air-sea fluxes of heat and momentum play important roles in the formation and development of tropical cyclones (TCs). Usually, the latent heat flux transferred from ocean to atmosphere increases during the development and intensification stages of a TC. However, through analyzing a number of TC cases over the South China Sea, it is found that the latent heat flux changes exhibit a distinct behavior during the intensifying stage of the TCs, depending upon their traveling pathways. The air-sea latent heat flux increases while the TCs are developing and intensifying in open sea areas of the South China Sea; and decreases while the TCs are travelling over the narrow area between the Indo-China Peninsula and the Hainan Island, even though the TCs are in their intensifying stage. For the later case, the decrease in latent heat flux is accompanied by the decrease in low layer wind due to the terrain friction while these TCs are traveling over the narrow area between the Indo-China Peninsula and Hainan Island.

Keywords: Tropical Cyclone, the South China Sea, Latent Heat Flux

HIGH RESOLUTION NUMERICAL SIMULATION OF CONVECTIVE CELLS IN THE RAINBAND OF CYCLONE SIDR

Nasreen AKTER and Kazuhisa TSUBOKI
Hydrospheric Atmospheric Research Center, Nagoya University, Japan
Email: akter@rain.hyarc.nagoya-u.ac.jp

Abstract

Tropical cyclone Sidr, which hit Bangladesh on 15 November 2007, is one of the most ten fierce cyclones for the last 131 years from 1876 to 2007 in this region. The hazardous consequence by its strong wind, flash flooding and intense rain made the evidence of high death rate and damages of the socio-economic condition of the country. The numerical model CReSS (Cloud Resolving Storm Simulator) has been used to simulate Sidr for the period of 48 hr from 0000 UTC of 14 to 0000 UTC of 16 November 2007. For the simulation, the domain size of 84.5-96.7E and 12-26.4N are considered with grid resolution of 1 km in horizontal and 0.5 km in vertical. Initial and boundary conditions are taken from 6 hourly JMA (Japan Meteorological Agency) - GSM (Global Spectral Model) data with 0.5 degree resolution. From the simulation it has been observed that convective cells in the rainband of Sidr are produced owing to the convergence effect of strong moist southerly. Veering of wind at low level also produces horizontal vorticity in the convergence region. The value of wind shear and CAPE (instability) are found to be the modest. The purpose of the study is to find out the characteristics of the convective cells in the rainband of Sidr. Considering this, a few cells are analysized to be acquainted with their evolution, structural organization, maintance process and strength. The moist, intense convective updraft (15 ~ 25 m/s) of the cells extended upto 10 to 12 km in height are tilted by the shear and make the horizontal vortex into the vertical cyclonic and anticyclonic vortex couplets of mesocyclone. Maximum vorticies of 1 x 10^{-2} /sec (approx.) are noticed around at the level of 9 to 11 km. After 30-40 minutes of formation, cells are split into two mesocyclone pairs. The pattern of the clockwise curved hodogragh also signifies the strong right and weak left moving supercells. The horizontal diameter of each cell is about 15-20 km. The longivity of the supercell is more than 90 minutes. Obviously this long lived high precipitation supercell (precipitation more than 200 mm/hr at mature stage) formed in the rainband of Sidr results the cruelty after landfall.

Keywords: supercell, rainband

STRUCTURE AND MODIFICATION OF A SPIRAL RAINBAND ASSOCIATED WITH A TYPHOON OBSERVED BY DOPPLER RADARS

Tetsuya SANO[1] and Kazuhisa TSUBOKI[2]

1. International Research Center for River Basin Environment, University of Yamanashi, Kofu, Japan.
Email: tsano@yamanashi.ac.jp

2. Hydrospheric Atmospheric Research Center, Nagoya University, Nagoya, Japan.
Email: tsuboki@rain.hyarc.nagoya-u.ac.jp

Abstract

A spriral rainband associated with a typhoon is one of the elements which causes heavy rainfall and a violent wind. The structure and modification of the spriral rainband associated with Typhoon 0712 (T0712), which approached to Miyako Islands in Okinawa on September 18, 2007, was investigated by using the observational data of two Doppler radars installed in Tarama Island and Shimoji Island.

On the first quagrant of T0712, the spiral rainband moved to a counterclockwise direction at about 100 km from the center at 0430 Japan Standard Time (JST) (Fig. 1). Many precipitating cells developed in a line on the upwind side of the spiral rainband. Stratiformed rainfall area within a few weakening cells extended on the downwind side.

As one of the composing precipitating cells, the time variation of structure of Cell A was investigated by using dual Doppler analysis. Cell A having the core under about 6 km above mean sea level (ASL) developed by lifting the air at lower layer on the outer side at 0430 JST (Fig. 2). At 2 ~ 4 km ASL, the inflow from the inner side of Cell A appeared with developing downdraft. The horizontal momentum at the middle layer was being transported to the lower layer by the convective effect of Cell A.

At 0454 JST (Fig. 3), Cell A moving to a counterclockwise direction weakened and stratiformed rainfall area extended to the inner side. At 3 ~ 6 km ASL, the strong inflow from the inner side intruded to Cell A and the stratiformed rainfall area and downdraft developed. Under the downdraft, the radial airflow toward the center of T0712 developed more than the tangential airflow at the lower layer. The airflow resulted from the formation of meso high by the downdraft associated with evaporative cooling.

We consider that the structure of spiral rainband with T0712 was modified by the development and weakeness of composing precipitating cells. The modification brought the difference to the formation processes of rainfall and a violent wind in a typhoon.

Keywords: Spiral rainband, Precipitating Cell, Typhoon and Doppler radar.

Acknowledgment: This study was supported by a Grant-in-Aid for Scientific Research from the Japan Society for the Promotion of Science.

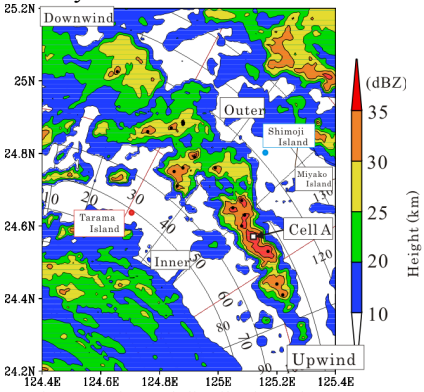

Fig. 1 Horizontal distribution of reflectivity at 2.5 km ASL observed by Doppler radars at 0430 JST. Dots indicate the position of precipitating cells. Polar coordinate at the center of T0712 is used.

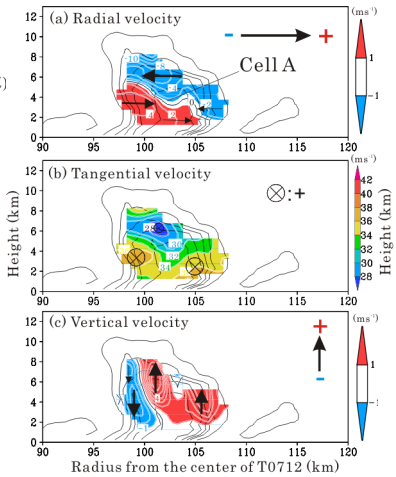

Fig. 2 Velocities in vertical section of cell A at 0430 JST along 54 degree in azimuth. Black contours are reflectivity with 10, 20, 25, 30 and 35 dBZ.

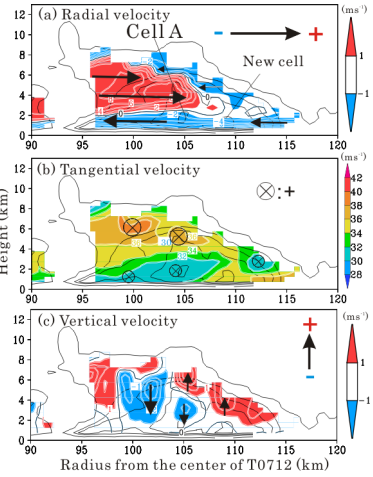

Fig. 3 Same as Fig. 2 except at 0454 JST along 30 degree in azimuth.

STRUCTURE OF TYPHOON KROSA RAINBAND WITH DUAL-DOPPLER RADAR

ZHOU Haiguang
State Key Laboratory of Severe Weather, Chinese Academy of Meteorological Science, 100081, Beijing, P.R.China
zhg@cams.cma.gov.cn

Abstract

The typhoon Krosa lands on the vicinity region between Zhejiang province and Fujian province at 1530 LST 7 October 2007 for the third time. An outer spiral rainband in the mature phase was passing through the dual-Doppler radar observation domain. Three dimensional wind field was retrieved by the dual-Doppler radar data. The mesoscale structure of the spiral rainband was investigated by the 3D wind. It shown that there were some strong reflectivity areas in the low level of the rainband region. The inflow in the upstream of the rainband outside was weak. On the other hand, the inflow in the downstream of the rainband outside was strong. There was outflow in the inside of the rainband at the low level. In the vertical cross-section, there was inflow in the low level of the outside rainband. The inflow entered the rainband at low level from the outside rainband. On the contrary, there was outflow in the inner side of the rainband. These flows converged at the low level of the rainband center region. The tangential component of the wind decreased with height and the maximum wind region was at 2km level.

Keywords: typhoon, spiral rainband, dual-Doppler weather radar, wind retrieval, three dimensional structure

Satellite and Modeling Analysis of Elliptical Eye of Devastating Cyclone Nargis

Ryuji Yoshida, Yuichiro Oku, Tetsuya Takemi, Hirohiko Ishikawa
Disaster Prevention Research Institute Kyoto University, Kyoto, Japan
yoshida@storm.dpri.kyoto-u.ac.jp

Abstract

In 27 April 2008, Cyclone Nargis, category 4 cyclone, was organized in the Bay of Bengal. The cyclone approached the coast of Myanmar on May 2, and killed more than 60,000 people. On the other hand, it is remarkable that satellite images pronounce the cyclone does not have a complete circular eye, but an almost elliptical eye. Mitsuta and Yoshizumi (1973) documented the elliptical eye rotates counterclockwise, and the distribution of surface precipitation concentrates the head of major axis of the elliptical eye. Therefore, researching of the structure of elliptical eye is important to prevent disaster. We analyze the eye of Nargis in detail using satellite data and high resolution meteorological data simulated by a mesoscale model.

Hourly infrared equivalent black body temprerature (TBB) data observed from the Chinese meteorological satellite (FY-2C) were utilized to identify the eyewall shape of Nargis. Nargis's eyewall shapes extracted from satellite images pronounce not complete circular, but almost elliptical in some times. It suggests that Nargis has an elliptical eye.

In order to obtain high resolution meteorological data, we simulated Nargis using the Weather Research and Forecast (WRF) version 3. Domains were multinested in three levels. The model was initialized at 0000UTC 30 April 2008, and then integrated 4days.

Eye shapes of the simulated cyclone identified by SLP pronounce almost elliptical. In addition, its elliptical eye rotates counterclockwise at about 4.5 hours period; the rotation speed is much slower than the wind speed there, and this is consistent with Kuo et al (1999).

Figure 1 shows a distribution of a surface rainfall intensity around the identified elliptical eye, which is obtained from compositing for 2 hours and 40 minutes. It is clearly that the simulated cyclone has an elliptical eye, and a strong surface precipitation distributes around the outer area of the identified eye, especially at the head of major axis of ellipse. In addition, this strong preciptation area rotates with the eye rotation. These results are consistent with Mitsuta and Yoshizumi (1973), and suggests possibility that the real Nargis may have a same unique distribution of a surface precipitation.

Therefore, it is suggested that an observation of a tropical cyclone eye shape and its rotation is important to prevent disaster such as a flood. In this presentation, we are also discussing a distribution of a surface wind intensity.

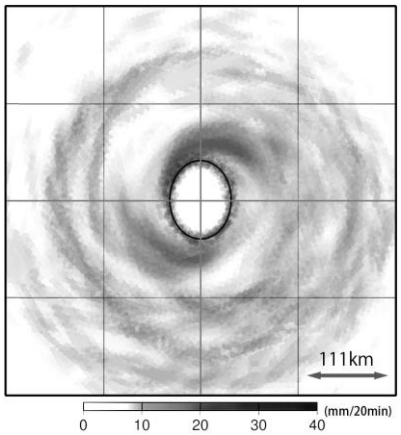

Fig.1. Composite of surface rain fall intensity.

Keywords: tropical cyclone, elliptical eye, Cyclone Nargis, WRF

SPECTRAL ANALYSES OF THE PENTAGONAL EYE OF TYPHOON SINLAKU

Toshihisa ITANO and Muneyuki HOSOYA
Dept. of Earth and Ocean Sciences, National Defense Academy, Yokosuka 239-8686, Japan
itano@nda.ac.jp

Abstract

Typhoon Sinlaku(T0216) had a clear pentagonal eye when it passed over the Okinawa main island, Japan(Fig.1). In order to reveal structure and behavior of this polygonal eye, we objectively anlyze the shape of the Sinlaku's eye appeared on radar images with the Fourier and the time-space cross spectral methods.

In the Fourier analysis, it was revealed that the most dominant peturbation was, unexpectedly, that with wave number-2 structure in the azimuthatl direction while the perturbation with wave number-5 is the second dominant structure. It was also shown that the shape of the eye was successively synthesized with those two perturbations alone. The perturbations with wave number 2 and 5 were both rotated cyclonically, but their angler velocity was diferent with each other, i.e. 80 and 130 degrees per hour, respectively.

The time-space cross spectra supported the above results(Fig.2). The perturbations with various wave numbers, including those with 2 and 5, fundamentally rotated cyclonically. And prominant peaks of spectra were seen around 50-85 degrees per hour in wave number-2 and 130 degrees per hour in wave number 5.

Keywords: typhoon, polygonal eye, the Fourier analysis, the time-space cross spectra

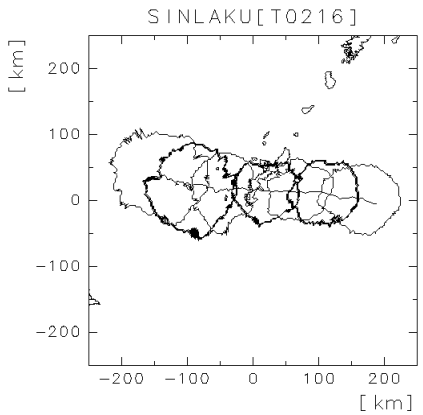

Fig.1 Path of typhoon Sinlaku and outlines of its eye at selected times form 15:37JST on Sep.4 to 11:17JST on Seo.5, 2004.

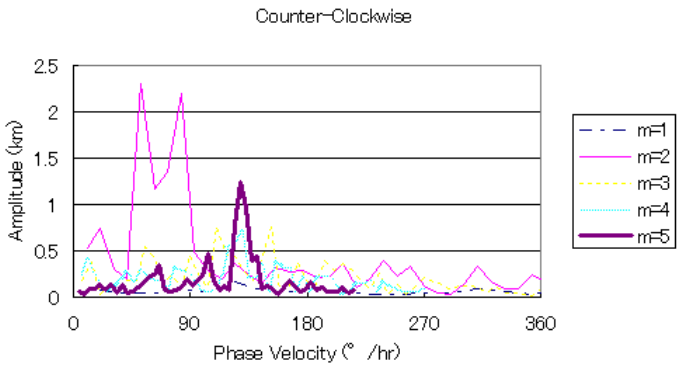

Fig.2 Time-space cross spectrum of the polygonal eye of typhoon Sinlaku for a cyclonic rotation.

SPATIAL AND TEMPORAL CHARACTERISTICS OF LIGHTNING IN TYPHOON

Fujiyuki NAKANO, Takeshi MORIMOTO, Tomoo USHIO and Zen KAWASAKI
Graduate School of Engineering Osaka University, Yamada-Oka 2-1, Suita, Osaka, 562-0871,Japan
nakano@comf5.comm.eng.osaka-u.ac.jp

Abstract

Lightning is an electrical discharge in thunderclouds. A typhoon consists almost entirely of thunderstorms. However, lightning flash rate in typhoon's thunderstorms is a remarkable low frequency compared to that in typical thunderstorms. Why the thunderstorm in typhoons produces little lightning flash is still mystery. It is important to know the feature of lighting flahes in typhoons to solve this problem.

In this paper, we used the Lightning Imaging Sensor (LIS) on board Tropical Rainfall Measuring Mission (TRMM) satellite to analyze the strom-relative and radial distribution of lightning flashes, the seasonal variation of lightning flashes, and the lightning activity per typhoon's life stages, namely the developing stage, the mature stage, and the dissipating stage. Lightning flashes in 218 typhoons from January 1998 to December 2007 were examined.

Remarkable features of lightning flashes in typhoons are the following: (a) High flash rate regions in typhoons are most commonly found in the left of the strom motion. (b) A radial distribution of lighting flashes in the peak season (July-September) had two maximums. The first maximum appears in the outer rainband region. The second maximum appears in the eyewall region. A clear minimum appears in the inner rainband region. This radial distribution in lightning flashes consistent with previous studies of lightning flashes in hurricanes [Molinari et al., 1994; Molinari et al.,1999]. However, a radial distribution of lightning flashes in the late season (October-December) had the maximum in the eyewall regon. It is interesting to note that lighting flashes in the outer rainband region decreased remakably. (c) Most vigorous lightning activity occurred in the dissipating stage. It is suggested that the distribution of lightning flashes in peak season shows the typical pattern of lightning flahses in typhoons.

Keywords: typhoon, lightning, TRMM, LIS

CONVECTIVELY FORCED MESOSCALE FLOWS IN A SHEAR FLOW WITH A CRITICAL LEVEL

Ji-Young HAN and Jong-Jin BAIK
School of Earth and Environmental Sciences, Seoul National University, Seoul, Korea
han0@snu.ac.kr

Abstract

Convectively forced mesoscale flows in the presence of basic-state shear with a critical level are theoretically investigated by obtaining analytic solutions for a hydrostatic, nonrotating, inviscid, Boussinesq airflow system. In the surface pulse heating case, the magnitude of the maximum upward motion observed at the center of the moving mode becomes constant after some time, whereas the vertical displacement and perturbation horizontal velocity near the center of the moving mode increase linearly in magnitude with time, regardless of whether the basic-state wind is uniform with height or has a constant vertical wind shear and whether the airflow system considered is 2D or 3D. In a unidirectional shear flow with finite-depth steady heating, there always exits a low-level upward motion near the heating center whatever the intensity of vertical wind shear and the heating depth are. For thermal forcing located across a critical level, a low-level upward motion near the heating center shows no change in its magnitude, although the heating top height increases This is because downward-propagating gravity waves, which come directly from the heat source above and not near the critical level, have almost no influence upon the flow response field below the critical level. When the basic-state wind backs with height, the vertex of V-shaped upward or downward motion above the heating top points to the direction rotated a little clockwise from the basic-state wind direction. This is because V-shaped feature at a certain height above the heating top is induced by upward-propagating gravity waves that have passed through the layer below where the basic-state wind direction is clockwise relative to that above.

Keywords: convection, mesoscale flows, basic-state shear, critical level, gravity waves

RELATIONSHIP BETWEEN SURFACE WIND FIELDS AND THREE-DIMENSIONAL STRUCTURES OF TROPICAL CYCLONES LANDFALLING IN THE JAPAN MAIN ISLANDS

Naoko KITABATAKE and Fumiaki FUJIBE
Meteorological Research Institute, Tsukuba, Japan
nkitabat@mri-jma.go.jp

Abstract

Seventy tropical cyclones (TCs) that made landfall in the southern Japan main islands during 1979-2004 were classified into 5 clusters on the basis of the surface wind fields within 200 km from the cyclone center, and their three-dimensional structures were presented in both the cyclone phase space and the composite analyses using the Japanese 25-year Reanalysis (JRA-25) dataset. The average TC of each cluster exhibits peculiar features associated with thermally symmetric/asymmetric, warm-/cold- core structures related to the weakly/strongly baroclinic environments in the midlatitude. The strong winds on the left side of a storm are likely to be related to the slow translation speed of the storm with a relatively symmetric structure or, alternatively, to the thermally asymmetric structure of the storm undergoing extratropical transition. It is also implied that other disturbances including a midlatitude trough and another TC may have contributed to the occurrence of strong winds or gusts near the cyclone center.

Keywords: tropical cyclone, structure, extratropical transition

LARGE ENVIRONMENTS AND MESOSCALE SYSTEMS ATTENDING CHINA MCC GENESIS AND DEVELOPMENT

Jing Xi[1, 2], Li Mingjuan[3], Li Shehong[2], Tu Nini[4], Jing Yu[5], Du Jiwen[3]
(1.Laboratory of Severe Weather, CMA, Beijing, 10081; 2. Shaanxi Yulin meteorological bureau, Shaanxi,Yulin,China,719000, Email:jingxiailihua@126.com; 3. Shaanxi provincial meteorological Bureau, Xi'an, China, 710015, Email:qxt – djw@sina.com; 4. Institute of plateau meteorology, CMA,Chengdu, China, 610071, Email:tunini80@yahoo.com.cn; 5. College of atmospheric science, Lanzhou university, Gansu, Lanzhou, China,730000,Email: jingyu.1128@163.com)

Abstract

Using various synoptic data as satellite image, Doppler radar data and sounding data, we studied 25 MCCs in China occurred between 2005 and 2007. Results indicate that: (1) China MCCs generated mostly between June and August in three regions, Yunnan-Guizhou-Guangdong-Guangxi region, Sichuan region and Huabei(north of China) region. Night is a favorable period for its development, and midnight the best; (2) China MCCs occurred in different background environments, which can be classified different types by lower troposphere, 500 hPa level, and 200 hPa level，its circulation characteristic is outstanding on 200 hPa level and it may be divided into 4 types， flow-splitting divergence at synoptic-scale jet exit, flow splitting with strong divergence ahead of short-wave trough, anticyclonic circulation developing in south side of macro-scale jet stream, anti-cyclonical circulation developing in front of deep trough, and these types are deferent from the type summarized by Maddox; (3) Its water vapor is transferred in two ways: direct and indirect; (4) MCC genesis is attended by northern frontogenesis and narrowing processes of spatial high-energy tube; (5) Besides, the triggering systems consist of low-vortex shear in lower troposphere coupled with high-value center of θse , and strong divergence at 200 hPa level; (6) The tri-dimensional dynamic structure is different between MCC accompanied by precipitation above or beneath torrential rain.

Key words: MCC China environmental conditions

STRUCTURE OF A PRECIPITATION SYSTEM DEVELOPED AROUND AICHI PREFECTURE, JAPAN ON AUGUST 28-29, 2008

Taro SHINODA, Masaya KATO, Yukari SHUSSE, Mitsuharu NOMURA,
Mariko OUE, Takeharu KOUKETSU, Kazuhisa TSUBOKI and Hiroshi UYEDA
Hydrospheric Atmospheric Research Center (HyARC), Nagoya University, Nagoya, Japan
shinoda@rain.hyarc.nagoya-u.ac.jp

Abstract

A precipitation system brought about heavy rainfall around Aichi Prefecture on August 28-29, 2008. Total rainfall amounts in these two days were 304.5 mm at Okazaki, 240.0 mm at Ichinomiya, and 202.0 mm at Nagoya. Hourly rainfall amounted to 146.5 mm at Okazaki from 01 to 02 Japan Standard Time (JST) on August 29. In this study, we examine the structure of the precipitation system using a new X-band polarimetric radar situated at Nagoya University and the Cloud Resolving Storm Simulator (CReSS).

From the observation using the polarimetric radar, a line-shaped precipitation system from south-southwest to north-northeast propagates southeastward slowly (at about 7 m/s). Southeastern and northwestern regions of the precipitation system in the lower troposphere are occupied by southeasterly and northwesterly winds, respectively; thus, the low-level convergence between these low-level winds should maintain the precipitation system. The differential reflectivity (Z_{DR}) observed by the polarimetric radar shows the existence of large raindrops whose median volume diameter (D_0) is larger than 2.7 mm. The observation of the ground-based drop size distribution (DSD) using the Disdrometer also shows the existence of large raindrops whose D_0 is larger than 2.3 mm; thus, many of large raindrops were formed in the precipitation system and should contribute to the heavy rainfall.

Global Spectral Model (GSM) data provided by the Japan Meteorological Agency (JMA) are used as the initial and boundary conditions of a simulation with a horizontal grid resolution of 2 km using the CReSS. The simulation reproduces well the generation location, propagation direction, and speed of the precipitation system; and the maximum hourly precipitation amount around Aichi Prefecture. The simulation also reproduces the low-level convergence between the southeasterly and northerly winds below the precipitation system. The southeasterly is a high equivalent potential temperature (warm and moist) airmass induced by a synoptic-scale situation. On the other hand, the northerly is a relatively low equivalent potential temperature airmass, whose relative humidity is greater than 75%, induced by the downdraft in the precipitation system. Since evaporation cooling is quite limited in a moist environment, the temperature decrease at the surface is only about 2-3℃. Although the propagation of the precipitation system shows a gravity-current-like structure by the relatively cool and dry airmass located in the northwestern side of the system, the propagation speed to the southeastward is slow, because the difference in density of the airmasses between both sides is quite less. The minute effect of evaporation cooling in the precipitation system is the predominant structure under the high humid environment.

Keywords: precipitation system, heavy rainfall, polarimetric radar, CReSS, moist environment

Initial check-out results of TANSO calibration

Kei SHIOMI, Shuji KAWAKAMI, Tomoko KINA, Makiko MUKAI,
Daisuke SAKAIZAWA, and Takashi MORIYAMA
Earth Observation Research Center, Japan Aerospace Exploration Agency,
2-1-1 Sengen, Tsukuba, Ibaraki 305-8505, Japan
shiomi.kei@jaxa.jp

Abstract

The GOSAT sattelite has been launched on January 23, 2009. Initial check-out is scheduled to be operated in 3 months after the launch. Initial calibration and validation are follows in 3 months. GOSAT Level 1 products, which containts observed digital number and converted equivalent spectral radiance, are implemented as released version.

The GOSAT carries the 2 science instuments, Fourier Transform Spectrometer (TANSO-FTS) and Cloud and Aerosol Imager (TANSO-CAI). On-orbit sensor characterizations are evaluated after the initial check-out activity. Radiometric, geometric, and spectral accuracies are evaluated after the initial calibration activities and the Level 1 products will be improved. The first light has been obtained successfully on February 7, 2009 over Japan. This paper shows the mission plan and initial results of TANSO calibration activities.

Keywords: GOSAT, TANSO, calibration

FIRST HIGH SPECTRAL RESOLUTION OBSERVATION FROM SPACE WITH TANSO-FTS ON GOSAT

Akihiko KUZE, Hiroshi SUTO, Masakatsu NAKAJIMA, and Takashi HAMAZAKI
Japan Aerospace Exploration Agency,
2-1-1 Sengen, Tsukuba-city, Ibaraki, 305-8505, Japan
kuze.akihiko@jaxa.jp

Abstract

The Greenhouse gases Observing SATellite (GOSAT) is a satellite to monitor the carbon dioxide (CO_2) and the methane (CH_4) globally from space. It is a joint project of Japan Aerospace Exploration Agency (JAXA), Ministry of the Environment (MOE) and National Institute for Environmental Studies (NIES). GOSAT is placed in a 666 km sun-synchronous orbit of 13:00 local time, with an inclination angle of 98 deg. It was launched on January 23, 2009 from Tanegashima Space Center. There are two instruments on GOSAT. The Thermal And Near infrared Sensor for carbon Observation Fourier-Transform Spectrometer (TANSO-FTS) detects the Short wave infrared (SWIR) reflected on the earth's surface as well as the thermal infrared (TIR) radiated from the ground and the atmosphere. TANSO-FTS is capable of detecting wide spectral coverage; three narrow bands (0.76, 1.6, and 2 micron) and a wide band (5.5-14.3 micron) with 0.27 cm^{-1} spectral resolution. The TANSO Cloud and Aerosol Imager (TANSO-CAI) is a radiometer of ultraviolet (UV), visible, and SWIR to correct cloud and aerosol interference. The first high spectral resolution SWIR spectra by TANSO-FTS and the image by TANSO-CAI were acquired on Feb. 7, 2009. The presentation includes the instrument design, pre-launch test results, onboard calibration schemes, and the initial on-orbit results.

Keywords: GOSAT, TANSO, Fourier Transform Spectrometer, Carbon Dioxide, Methane

RETRIEVAL OF CARBON DIOXIDE AND METHANE FROM SHORT-WAVELENGTH INFRARED SPECTRA OBTAINED FROM GREENHOUSE GASES OBSERVING SATELLITE (GOSAT)

Yukio YOSHIDA[1], Yoshifumi OTA[1], Nawo EGUCHI[1], Tomoaki TANAKA[1], Nobuhiro KIKUCHI[2], Koji NOBUTA[2], Tatsuya YOKOTA[1]
1) National Institute for Environmental Studies
2) Fujitsu FIP Corporation
16-2 Onogawa, TSUKUBA, Ibaraki 305-8506, Japan
yoshida.yukio@nies.go.jp

Abstract

Greenhouse gases Observing SATellite (GOSAT) is a satellite to monitor global distribution of carbon dioxide and methane from space, and it was launched on January 23, 2009. Two types of sensors are installed on GOSAT. Thermal And Near infrared Sensor for carbon Observation-Fourier Transform Spectrometer (TANSO-FTS) detects the signal of reflected solar light on the earth's surface as well as that of thermal emitted radiance from the surface and the atmosphere. TANSO-Cloud and Aerosol Imager (TANSO-CAI) is a radiometer to obtain the information on cloud and aerosols that contamintate the FTS signals. TANSO-FTS has three short-wavelength infrared (SWIR) bands at 0.76, 1.6, and 2.0 μm. Column abundances of carbon dioxide and methane are retrieved globally from SWIR spectra obtained from TANSO-FTS, except for the cloudy regions detected by TANSO-CAI and TANSO-FTS itself. Figure 1 shows an observed spectrum at 1.6 μm-band obtained from GOSAT during its initial functional check period. The observed spectrum agrees well with the simulated one, and TANSO-FTS is considered to show the expected performance as designed. From the end of April to July, the initial calibration and validation will be carried out. Some preliminary results will be presented.

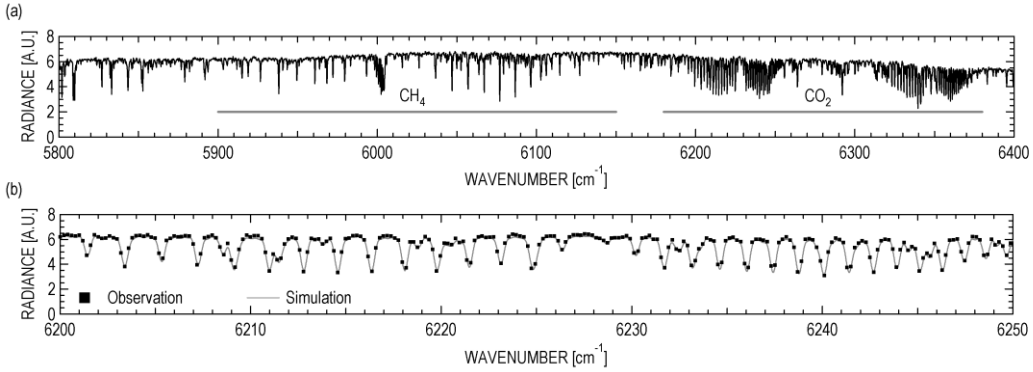

Figure 1. (a) Example of observed spectrum at 1.6 μm-band from TANSO-FTS on February 7, 2009. (b) Comparison between the observed and simulated spectra around the absorption band of carbon dioxide.

Keywords: GOSAT, carbon dioxide, methane

Comparison analysis of CO2 simulation between NIES Transport Model and GEOS-5 for GOSAT CO2 retrieval

Nawo Eguchi[1,2], Lesley E. Ott[2,3], Ryu Saito[1], Zhengxin Zhu[3,4], Tatsuya Yokota[1], Steven Pawson[3] and Shamil Maksyutov[1]
1) National Institute for Environmental Studies, Tsukuba, Japan
2) NASA/GSFC, GEST, UMBC, USA,
3) NASA/GSFC, GMAO, Greenbelt, USA,
4) SSAI, USA
eguchi.nawo@nies.go.jp

Abstract

GOSAT (Greenhouse gases Observing SATellite) was launched on Jan 23, 2009. The Thermal And Near infrared Sensor for carbon Observation Fourier-Transform Spectrometer (TANSO-FTS) which is the main instrument on board GOSAT has four spectral bands including three narrow bands (0.76, 1.6, and 2 micron), which detect light reflected from the earth's surface, and a wide band (5.5-14.3 micron), which detects thermal radiation from the ground and the atmosphere, with 0.2 cm^{-1} spectral resolution. The column abundances and profiles of CO_2 and CH_4 will be retrieved from the narrow band data and the thermal band data, respectively. The pre-calibrated spectral data (Level 1B) has been released since the end of April 2009.

A priori profiles of CO_2 and CH_4 for the retrieval with Maximum A Posteriori (MAP) method will be prepared by using field simulated by the NIES TM (National Institute for Environmental Studies Transport Model) with forecasting meteorological parameters and climatological CO_2 and CH_4 flux data. The a priori covariance matrices are also derived from the NIES TM. It is known generally that the model-simulated seasonal cycle of CO_2 tends to have biases. For example, the simulated amplitude of seasonal cycle in Northern mid-latitudes tends to be smaller than the observed amplitude [Yang et al., 2007]. However, the discrepancy between model and observation is not fully understood. The effort of the present study is to reduce the uncertainty of NIES TM (NIES05 [Maksyutov et al., 2008]) though the comparison with the other simulated data (GEOS-5) and observational data (e.g., WDCGG and GlobalView).

The CO_2 time series at each global grid point in 2002 and 2003 are simulated by GEOS-5 and NIES05 along the protocol of TransCom continuous experiment (TransCom04) [NIES05 results were published by Law et al., 2008]. Climatological fluxes of CO_2 (e.g. fossil98, Takahashi02 and CASA) are imposed in the simulations. The seasonal and diurnal cycles of both models show similar features and both have smaller variability than the ground-based observations, especially at ocean sites. It is found that the vertical transport processes are quite different between GEOS-5 and NIES05, especially in the convective regions, due to the difference of the convective behavior. These differences have a clear signature in the CO_2 covariance matrices computed using the two models.

CURRENT STATUS OF SUPERCONDUCTING SUBMILLIMETER-WAVE LIMB-EMISSION SOUNDER (SMILES)

Masato SHIOTANI, Masahiro TAKAYANAGI and JEM/SMILES Mission Team
Kyoto University, Kyoto, Japan
shiotani@rish.kyoto-u.ac.jp

Abstract

The Superconducting Submillimeter-Wave Limb-Emission Sounder (SMILES) was designed to be aboard the Japanese Experiment Module (JEM) on the International Space Station (ISS) as a collaboration project of Japan Aerospace Exploration Agency (JAXA) and National Institute of Information and Communications Technology (NICT). Mission Objectives are: i) Space demonstration of super-conductive mixer and 4-K mechanical cooler for the submillimeter limb-emission sounding in the frequency bands of 624.32- 627.32 GHz and 649.12- 650.32 GHz, and ii) global observations of atmospheric minor constituents in the stratosphere (O_3, HCl, ClO, HO_2, HOCl, BrO, O_3 isotopes, HNO_3, CH_3CN, etc), contributing to the atmospheric sciences.

The main part of the SMILES payload consists of the Submillimeter Antenna (ANT), Submillimeter Receiver (SRX), Intermediate Frequency Amplification Section (IFA), and Radio Spectrometer (AOS). The SMILES is equipped with a heterodyne superconductor-insulator-superconductor (SIS) receiver to be operated in the 625/650 GHz band as a limb-emission sounding radiometer. The SMILES has a mechanically scanning elliptical offset-Cassegrain antenna with diameters of 40 cm x 20 cm to achieve an altitude resolution of about 3 km at the tangential height ranging from upper troposphere (10 km) to lower mesosphere (60 km) from the orbit of the ISS. The envelope of the SMILES payload mainframe structure has a dimension of 1.85 m x 1 m x 0.8 m. The total mass of the payload is less than 500 kg. The electrical power consumption of the payload is less than 900 W for normal operation.

One of the most unique characteristics of the SMILES observation is its high sensitivity in detecting atmospheric limb emission of the submillimeter wave range (640 GHz). The ISS has a circular orbit with an inclination angle of 51.6 degrees and with an orbital period of 93 minutes. In order to measure high-latitude regions, the antenna beam is tilted 45 degrees left from the direction of orbital motion, enabling SMILES to observe latitudes from 38S to 65N. With its high sensitivity the SMILES observation will provide superior global data on several radical species crucial to the ozone chemistry (O_3, HCl, ClO, HOCl, BrO, HO_2 etc.).

We have done several functional tests. Noise and gain performances of SRX are found good within the specification. Calculated and phase-retrieved far-field beam patterns at 637.32 GHz indicate close match with each other. Results from gas cell measurements for several species at several conditions are also very good. All these results confirm expected performance for each of the elements. SMILES will be scheduled for the launch using H-II Transfer Vehicle (HTV) in 2009 summer.

Keywords: satellite measurement, ISS, middle atmosphere, ozone

CAPABILITY STUDY FOR ATMOSPHERIC MINOR SPECIES WITH JEM/SMILES

Chikako. TAKAHASHI, Chihiro. MITSUDA, Makoto. SUZUKI, Yoshitaka. IWATA,
Hiroo. HAYASHI, Koji. IMAI, Takuki. SANO, Masahiro. TAKAYANAGI
and SMILES mission team
Japan Aerospce Exploration Agency, Sagamihara, Japan
takahashi.chikako@jaxa.jp

Abstract

In this work, we clarified the capability of atmospheric minor species with the JEM/SMILES (Japanese Experiment Module / Superconduting Submillimeter-wave Limb Emission Sounder). The JEM/SMILES will be launched in 2009 and observe limb emission from atmospheric minor species in the stratosphere, such as O3, ClO, HCl, HNO3, HOCl, CH3CN, HO2, BrO, O3 isotopes etc. The measurement bands are band A (624.3-625.5 GHz), band B (625.1-626.3 GHz), and band C (649.1-650.3 GHz) in the altitude range between 10 and 60 km and the nominal latitude coverage from 65N to 38S. The major feature is the high-sensitive observation with low system noise temperature approximately 700 K to carry 4 K cooled SIS mixer.

A level 2 data processing system (DPS-L2) for the SMILES, which converts emission spectra (Level 1B data) into vertical profiles of the atmospheric minor species concentrations in near-real time, is underdeveloped. Since the SMILES is the high sensitive sensor comparing with existing similar sensors, such as Aura/MLS and Odin/SMR, the development of the high accurate algorithm of the DPS-L2 is important to take advantage of the SMILES. Furthermore the processing speed is also important for the near-real time operational data processing.

The launch ready algorithm was developed and it was confirmed to meet these requirements. According to the algorithm, a preliminary error analysis on random and systematic errors are performed. It is clarified that the minimum precision of the retrieved vertical profile of ozone, HCl, and ClO is approximately 0.5%, 1%, and 3% at 30 km with 3 km height resolution, respectively, and that the systematic errors are kept at low level comparable with the retrieval precision

Keywords: JEM/SMILES, retrieval, stratosphere

Observation Capabilities of Superconductive Submillimeter-Wave Limb-Emission Sounder (SMILES) onboard International Space Station(ISS)

Y. KASAI[1], P. Baron[1], J. Mendrok[1], S. Ochiai[1], J. Moller[2], J. Urban[2], P. Eriksson[2], D. Murtagh[2], T. Manabe[3], K. Kikuchi[4], T. Nishibori[4], T. Sano[4], S. Buehler[5], W. U. Dong[6], and JEM/SMILES Mission Team[1, 4]

[1]National Institute of Information and Communications Technology (NICT)
4-2-1 Nukui-kita, Koganei, Tokyo 184-8795, Japan
[2]Chalmers University, Sweden
[3]Osaka Prefecture University, Japan
[4]Japan Aerospace Exploration Agency (JAXA), Japan
[5]Lulea University of Technology, Sweden
[6]NASA/JPL, USA

Email ykasai@nict.go.jp

Abstract

A new generation of sub-millimeter-wave receivers employing sensitive SIS (Superconductor-Insulator- Superconductor) detector technology will provide new opportunities for precise remote sensing measurements of minor constituents in atmosphere. Superconductive Submillimeter-Wave Limb-Emission Sounder (SMILES) was designed to be onbord the Japanese Experimental Module (JEM) on the International Space Station (ISS) as a collaboration project of Japan Aerospace Exploration Agency (JAXA) and National Institute of Information and Communications Technology (NICT). SMILES scheduled to launch in September 2009 by the H-II Transfer Vehicle (HTV). Mission Objectives are: i) Space demonstration of superconductive mixer and 4-K mechanical cooler for the submillimeter limb emission sounding, and ii) global observations of atmospheric minor constituents. JEM/SMILES will allow to observe the atmospheric species such as O_3, $H^{35}Cl$, $H^{37}Cl$, ClO, BrO, HOCl, HO_2, HNO_3, CH_3CN, Upper Tropospheric Humidity (UTH) and Cirrus Cloud with the precisions in a few to several tens percents from upper troposphere to the mesosphere. We have estimated the observation capabilities of JEM/SMILES. This new technology may allow us to shade new light the open issue in atmospheric science.

Keywords: Cirrus cloud, Upper Tropospheric Humidity (UTH), Ozone, SMILES, ISS

DEVELOPMENT OF JEM/SMILES LEVEL 2 DATA PROCESSING SYSTEM

Chihiro MITSUDA, Chikako TAKAHASHI, Makoto SUZUKI,
Hiroo HAYASHI, Takuki SANO, Masahiro TAKAYANAGI,Yoshitaka IWATA,
Hirotomo TANIGUCHI, Koji IMAI and SMILES mission team
Fujitsu FIP Corporation, Tokyo, Japan
c.mitsuda@fip.fujitsu.com

Abstract

The Superconducting Submillimeter-wave Limb-Emission Sounder (SMILES) is planned to be launched in 2009 and will be on board the Japanese Experiment Module (JEM) of the International Space Station (ISS). The SMILES carries 4 K cooled Superconductor-Insulator-Superconductor mixers to carry out high-sensitivity observations for submillimeter limb-emission sounding. Since the system noise temperature of the SMILES is less than 700 K, the sensitivity of the SMILES is a few times higher than that of similar sensor in orbits, such as Aura/MLS and Odin/SMR. The SMILES measures the atmospheric limb emission from stratospheric minor constituents in the submillimeter-wave range. The target species of the SMILES are O_3, ClO, HCl, HNO_3, HOCl, CH_3CN, HO_2, BrO, and O_3 isotopes (^{18}OOO, ^{17}OOO and $O^{17}OO$).

As a part of the ground system for the SMILES, a level 2 data processing system (DPS-L2) has been developed. It retrieves the density distributions of the target species from calibrated spectra in near-real-time (53 seconds). Since DPS-L2 must provide the most accurate basis for results and be implemented under limited computing resources, DPS-L2 algorithm for an operational code has to be accurate and fast.

Hence, the algorithm is improved as follows; (1) designing accurate instrument functions such as the instrumental field of view, sideband rejection ratio of sideband separator, and spectral responses of Acousto-Optic Spectrometer, (2) absorption line selection, (3) optimization of the Voigt algorithms, (4) frequency and height grids selection.The accuracy of this algorithm is less than 1%, and the processing time for single-scan spectra using a 3.16-GHz Quad-Core Intel Xeon processor is less than 1 min per core. Thus, this algorithm is suitable for the SMILES observation.

Keywords: SMILES, ISS, JEM, retrieval, data processing system

REGIONALIZATION OF LAND SURFACE HEAT FLUXES OVER HETEROGENEOUS LANDSCAPE OF THE TIBETAN PLATEAU BY USING THE SATELLITE AND IN-SITU DATA

Yaoming MA[1]; Lei ZHONG[1]; Hirohiko ISHIKAWA[2]; Osamu TSUKAMOTO[3]; Massimo MENENTI[4]; Zhongbo SU[5]; Kenichi UENO[6]

[1]Laboratory of Tibetan Environment Changes and Land Surface Processes, Institute of Tibetan Plateau Research, the Chinese Academy of Sciences, Beijing , China, E-mail: ymma@itpcas.ac.cn; [2]Disaster Prevention Research Institute, Kyoto University, Kyoto, Japan; [3]Department of Earth Sciences, Okayama University, Okayama, Japan; [4]Laboratoire des Sciences de l'Image, de l'Informatique et de la Te´le´de´tection, Universite´ Louis Pasteur, Strasbourg, France; [5]International Institute for Geo-Information Science and Earth Observation, Enschde, the Netherlands; [6]Department of Environmental Sciences, University of Tsukuba, Tsukuba, Japan

Abstract

The exchange of energy and water vapor between land surface and atmosphere over the Tibetan Plateau area play an important role in the Asian monsoon system, which in turn is a major component of both the energy and water cycles of the global climate system. The study on the regional distribution of land surface heat fluxes of paramount importance over heterogeneous landscape of the Tibetan Plateau. Therefore, here the parameterization methods based on satellite data (NOAA/AVHRR, Landsat-7 ETM, ASTER and MODIS) and Atmospheric Boundary Layer (ABL) observations have been proposed and tested for deriving surface reflectance, surface temperature, NDVI, MSAVI, vegetation coverage, LAI, net radiation flux, soil heat flux, sensible heat flux and latent heat flux over heterogeneous landscape. As cases study, the methods were applied to the Tibetan Plateau area. Five scenes of Landsat-7 ETM data, four scenes of NOAA/AVHRR data, three scenes of ASTER data and four MODIS data were used in this study. To validate the proposed methods, the ground-measured surface reflectance, surface temperature, net radiation flux, soil heat flux, sensible heat flux and latent heat flux are compared to satellite derived values. The results show that the derived surface variables and land surface heat fluxes over the study area are in good accordance with the land surface status. These parameters show a wide range due to the strong contrast of surface features. And the estimated land surface variables and land surface heat fluxes are in good agreement with ground measurements, and all their absolute percent difference is less than 10% in the validation sites. It is therefore concluded that the proposed methods are successful for the retrieval of land surface variables and land surface heat fluxes over heterogeneous landscape of the Tibetan Plateau area. Further improvement of the methods and its applying field were also discussed.

Key Words: regional land surface heat fluxes; Tibetan Plateau; satellite data

DEVELOPMENT OF LAND SURFACE TEMPERATURE RETRIEVAL ALGORITM FROM GEOSTATIONARY SATELLITE DATA

Jeon-Ho Kang, Myoung-Seok Suh, Ki-Ok Hong
Department of Atmospheric Science, Kongju National University,
182 Shinkwan-dong, Gongju-city 314-701, ChungCheongnam-do, Korea
e-mail: jtiger02@gmail.com

ABSTRACT

The Japanese geostationary satellite, MTSAT-1R carries the high resolution meteorological imager, which has two thermal infrared channels. And Korean Meteorological Administration plans to launch his first geostationary satellite, COMS (Communication, Oceanic, and Meteorological Satellite) at the end of this year. In this study, we developed split-window type of land surface temperature (LST) retrieval algorithms to retrieve the LST over East Asian region from MTSAT-1R and COMS data, on the basis that the spectral emissivities of land surface are known. The coefficients of split-window algorithms for retrieval of LST were obtained by means of a statistical regression analysis from radiative transfer simulations using MODTRAN 4.0 for a wide range of atmospheric profiles (TIGR data over MTSAT-1R coverage area), satellite zenith angle and near surface lapse rate conditions including surface inversions. The space and time varying spectral emissivities of land surface were calculated by vegetation coverage method using the IGBP land cover map over East Asia and bi-weekly normalized difference vegetation index. The LST over the East Asian region under the various conditions, especially for the day/night and seasons, have been retrieved and validated. The cloud is masked by multi-channel dynamic threshold method developed by Chung et al. The validation results with MODIS LST showed that the correlation coefficients and RMSE are about 0.83~0.98 and 1.38~4.06, respectively. And the validation results with air temperature data showed that the correlation coefficients and RMSE are about 0.29~0.68 and 3.38~6.47, respectively. The performance of LST retrieval algorithm is clearly dependent on the retrieval time, land cover type and seasons. In general, the performance of LST algorithm is significantly better during nighttime (and winter) than daytime (and summer). And it is clearly better in the vegetated area than barren area or semi-desert. The validation results showed that the LST retrieval algorithm developed in this study could be used for the operational retrieval of LST from MTSAT and COMS data with some modifications.

Keywords: Land surface temperature, MODTRAN4, MTSAT-1R, COMS, Split-window

Characteristics of Brightness Temperature from MTSAT-1R on Lightning Events over South Korea

Hyo-Sik Eom and Myoung-Seok Suh
Dept. of Atmospheric Science, Kongju Nat'l Univ., Kongju, 314-701, South Korea
sms416@kongju.ac.kr

Abstract

This study investigates the characteristics of brightness temperature (BT) of WV and IR1 from MTSAT-1R when lightning strikes in South Korea. Lightning data was provided by 24 sensors consisting of total lightning detecting system (TLDS) of KMA. An analysis domain is defined between 33^{o}N, 124^{o}E and 39^{o}N, 130^{o}E due to 90% lightning detection efficiency of TLDS. For temporal and spatial collocations, lightnings, occurred only within ±5 minutes from the six minutes added official satellite observation time (e.g., not 0600 UTC but 0606 UTC, considering the real scan time over South Korea), were selected. And the BTs corresponding to lightning spots were determined using the nearest pixel within 5 km.

The brightness temperature difference (BTD, defined as WV – IR1) between two channels is negatively large when no lightning occurrs, whereas it increases up to positive values (sometimes, +5 K) and the largest frequency distributes around 225 K and 205 K in lightning cases. The probablistic approach for lightning frequency forecast, presented by Machado et al. (2008) in Southern America, was applied over South Korea and new exponental equations, with high coefficients of determination around 0.98 to 0.99, were developed using two channels' BTDs when lightning strikes. Moreover, a case study on 10th June, 2006, the largest number of lightning occurred between 2002 and 2006, was made. The major finding is that lightning activity is closely related to the dramatic decreases in BT and the increases in BTD (esp., equal to or larger than 0 K). Lightning frequency increases exponentially when BTD increases up to 0 K. Therefore, lightning forecast skill will be improved when the integrated strategy (synoptic background and satellite-based BT and BTD) is applied. It is believed that this study contributes to the application of the Korean first geostationary satellite (COMS), scheduled to launch at the end of this year, to severe weather detections.

Keywords: MTSAT-1R, BT, BTD, lightning, South Korea

VISIBLE CHANNEL CALIBRATION BASED ON DEEP CONVECTIVE CLOUD TARGETS OVERSHOOTING THE TTL

Byung-Ju SOHN[1], Seung-Hee HAM[1], and Ping YANG[2]

[1]School of Earth and Environmental Sciences
Seoul National University
Seoul, 151-747, Korea

[2]Department of Atmospheric Sciences
Texas A&M University
College Station, TX 77843, USA

Abstract

Deep convective clouds (DCCs), clouds that overshoot the Tropical Tropopause Layer (TTL), are identified to calibrate satellite measurements at solar channels. DCCs are identified in terms of the MODIS 10.8 μm brightness temperature (TB_{11}) on the basis of a criterion specified by $TB_{11} \leq 190$ K. To determine the characteristics of these clouds, the MODIS-based cloud optical thickness (COT) and effective radius (r_e) for a number of identified DCCs are analyzed. It is found that COT values for most of 4249 DCC pixels observed in January, 2006 are close to 100. Based on the MODIS quality-assurance information, 90% and 70.2% of the 4249 pixels have COT larger than 100 and 150, respectively. On the other hand, the r_e values distributed between 15 and 25 μm show a sharp peak centered approximately at 20 μm. Radiances are simulated at the MODIS 0.646-μm channel by using a radiative transfer model under homogeneous overcast ice cloudy conditions for COT = 200 and r_e = 20 μm. These COT and r_e values are assumed to be typical for DDCs. A comparison between the simulated radiances and the corresponding Terra/Aqua MODIS measurements for six months in 2006 demonstrates that, on a daily basis, visible-channel measurements can be calibrated within an uncertainty range of ±5%. Because DCCs are abundant over the tropics and can be identified from IR measurements, the present method can be applied to the calibration of a visible-channel sensor aboard a geostationary or a low-orbiting satellite platform.

CLOUD-TOP HEIGHT ESTIMATION BY GEOSTATIONARY SATELLITE SPLIT-WINDOW MEASUREMENTS USING CLOUDSAT MEASUREMENTS

Atsushi HAMADA* and Noriyuki NISHI†

* Research Institute for Humanity and Nature, Kyoto, Japan
† Graduate School of Science, Kyoto University, Kyoto, Japan
E-mail: hamada@chikyu.ac.jp

Abstract

Estimation tables for cloud-top height and visible optical thickness of upper-tropospheric clouds by the infrared brightness temperature (T_B) at 10.8 μm (T_{11}) and its difference from T_B at 12 μm (ΔT_{11-12}) measured by a geostationary satellite were presented. These tables were constructed by regressing the cloud radar measurements by the CloudSat satellite over the infrared measurements by the Japanese geostationary satellite MTSAT-1R. Uncertainties in the estimates were also displayed as the dispersions of measurements around the estimates. For the upper-tropospheric clouds with $T_{11} < 240$ K, the standard deviations of measurements were less than 1 km.

The dependences of the estimates of cloud-top height at each point in T_{11}-ΔT_{11-12} space on latitude, season, satellite zenith angle, day-night, and land-sea differences were examined. It was shown that these dependences were considered as being uniform in tropics, except for the region with large satellite zenith angle.

The presented tables can provide hourly estimates of cloud-top height and optical thickness at a specified location, and are fairly useful in comparing them with ground-based observations such as vertical profiles of humidity and/or wind.

Keywords: cloud-top height, geostationary satellite, split-window, CloudSat

CLOUD AND PRECIPITATION OBSERVATION MISSION IN JAPAN: CURRENT AND FUTURE

Nobuhiro TAKAHASHI* and Riko OKI**
*National Institute of Information and Communications Technology, Koganei, Japan
** Japan Aerospace Exploration Agency, Tsukuba, Japan
ntaka@nict.go.jp

Abstract

The global warming and the global water issue are two of the most serious social issues to be urgently solved and the cloud and precipitation is key parameter for these issues. Satellite observation helps to measure cloud and precipitation globally and quantitatively especially by the spaceborne radars. In this paper, Japanese satellite missions to observe cloud and precipitation by radar is mainly introduced and foresees the possible future missions.

The Tropical Rainfall Measuring Mission (TRMM) is Japan-US joint satellite mission which equips world first spaceborne precipitation radar (PR) as well as microwave imager (TMI) and has been producing very valuable precipitation data more than eleven years. This long term precipitation record from TRMM made it possible to provide not only the precise global precipitation amount but also improve the understanding the mesoscale tropical and sub-tropical weather system revolutionary. For example, diurnal cycles of rainfall is revealed by several studies using PR data both land and ocean. It is worth to note that the mesoscale climatology developed from PR data is used to evaluate the global cloud resolving model such as NICAM. The follow-on mission of TRMM which is called the global precipitation measuring (GPM) mission is planned to start in 2013. GPM mission is consist of Core satellite which equips dual frequency (14 GHz and 35 GHz, the former is same frequency as TRMM/PR) radar to improve the estimation accuracy of rainfall and to observe the light rain and snowfall and constellation satellites which equip microwave radiometer to gain the sampling of precipitation. On the other hand, satellite cloud remote sensing started with optical sensors to estimate the effective radius of cloud and so on. In 2006, NASA's CloudSat satellite was launched to observe the cloud structure using 95-GHz cloud radar. CloudSat has been providing the vertical structure of clouds and even light rain and enables us to see the cloud and precipitation properties at the same time. In Japan, spaceborne cloud radar similar to the CloudSat but upgraded in terms of sensitivity, long life time and the additional Doppler capability is being developed for EarthCARE mission which is JAPNA-ESA joint program aiming to reveal the aerosol-cloud processes to realize more precise Earth radiation budget estimation using cloud radar and lidar (laser radar). Beyond the GPM and the EarthCARE it is foreseen that more collaborative satellite observation to see the cloud and precipitation simultaneously and the development processes of cloud-precipitation system is desired. For this purpose, several missions are studied and proposed. One of the consensuses of the proposed missions is that multiple satellite system is the most probable solution.

Keywords: TRMM, GPM, EarthCARE

MISSION AND DEVELOPMENT OF CLOUD PROFILING RADAR ON EARTHCARE SATELLITE

Toshiyoshi KIMURA [1)], Nobuhiro TAKAHASHI [2)]
and JAXA/NICT EarthCARE/CPR Project Team
1) Japan Aerospace Exploration Agency,Tsukuba, Japan, kimura.toshiyoshi@jaxa.jp
2) National Institute of Information and Communications Technology, Koganei, Japan

Abstract

Cloud and aerosol contribution to Earth radiation budget are not well understood, still. European Space Agency (ESA) and JAPAN; Japanese Aerospace Exploration Agency (JAXA) and National Institute of Information and Communications Technology (NICT), are developping a satellite named EarthCARE (Earth Cloud, Aerosol and Radiation Explorer). EarthCARE satellite aims to observe cloud and aerosol profile in global scale with simultanious radiative flux at top of atmosphere. JAXA and NICT are responsible for the development of Cloud Profiling RADAR (CPR), which is a core instrument together with Atmospheric LIDAR (ATLID) by ESA. Synergy obervation with multiple intruments on EarthCARE, materializes the consistent evaluation from small to large partile, in other words, from aerosol, cloud to light rain. Additionally, new CPR capability of Doppler measurement in cloud layer will add new knowledge for cloud formation system and dynamics. EarthCARE is planned to be launched in 2013.

Keywords: Aerosol, Cloud, Radiation budget, Satellite, RADAR

SATELLITE-BORNE CLOUD RADAR CALIBRATION USING AIRBORNE CLOUD RADAR AND GROUD MEASUREMENTS

Yuichi OHNO, Kenji SATO, Hiroaki HORIE, Nobuhiro TAKAHASHI and Hiroshi KUMAGAI
National Institute of Information and Communications Technology, Koganei, Japan

Abstract

Cloud is one of the most important factors for the global warming prediction model. CloudSat satellite was launched by NASA in April 2006. It carrys a first satellite-borne cloud profiling radar (CPR) that can measure vertical distribution of cloud. It has been operational since June 2006 and brings new knowledge about the global cloud aspects. NICT tried a few experiments to calibrate the CloudSat CPR. In April 2007, we conducted synchoronized airplain observations using the airborne cloud radar (SPIDER). We can directly compare the SPIDER results with CloudSat CPR since it has almost the same transmit frequency and it can observe the cloud from the same direction. Figure 1 shows CloudSat CPR reflectivity factor section across Niigata and Tokyo (top) and the SPIDER observation of the same section (bottom). Figure 2 shows the both radar reflectivity profiles at the center. It shows very good agreement. We also made a experiment to receive the CloudSat radio on the ground. Radar beam pattern of CPR was obtained with this experiment. Similar calibration methods will be used for EarthCARE CPR calibration in future.

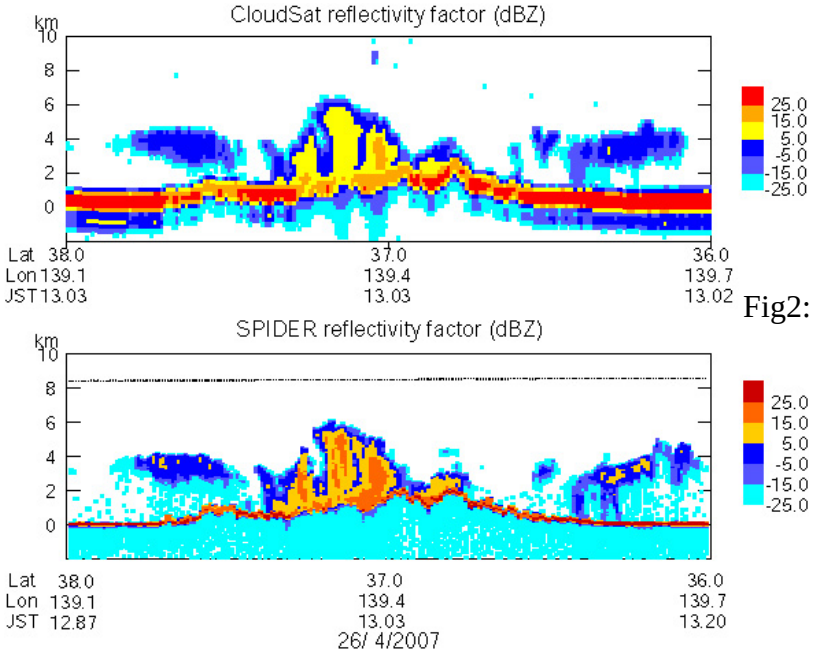

Figure 1: Radar reflectivity section observed CloudSat CPR (top) and SPIDER (bottom)

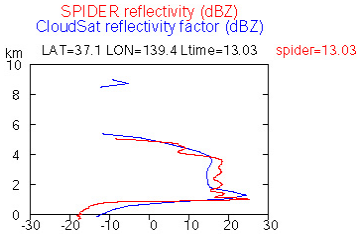

Fig2: Radar reflectivity profiles of CloudSat & SPIDER

Keywords: CloudSat, cloud radar, calibration

GLOBAL ANALYSIS OF CLOUD PROPERTIES FROM CLOUDSAT AND CALIPSO

Hajime Okamoto, Kaori Sato, Yuichiro Hagihara and Ryo Yoshida
Center for Atmospheric and Oceanic Studies, Graduate School of Science, Tohoku University,

Sendai, Miyagi
okamoto@caos-a.geophys.tohoku.ac.jp

Abstract

We developed the cloud mask schemes for CloudSat and CALIPSO and global distribution of clouds for CloudSat-only, CALIPSO-only and the synergy products were examined during September to November 2006. The CALIPSO mask was compared with CALIPSO vertical feature mask (VFM) developed at NASA-Langley. The fraction of clouds for the VFM was significantly larger than that for our CALIPSO mask results, especially below 3km and also over ocean. This was due to the misclassification of aerosols and noises into clouds in the VFM. Comparisons of cloud cover at three height categories between the CloudSat and CALIPSO synergy products and MODIS were performed. In the tropics, good agreement was obtained for low cloud amount between MODIS and our CloudSat-CALIPSO synergy products, while the VFM gave about 15% larger values compared with MODIS. VFM shows much high values than our CALIPSO product. In mid- and high clouds, the differences between our CALIPSO products and VFM were smaller than in the low clouds and MODIS mostly shows the lowest values.

Cloud particle type discrimination was also performed for CALIPSO data from depolarization ratio and extinction on the basis of backward Monte Carlo simulations. This allowed to infer water, super cooled water, 3d-ice and horizontally oriented crystals (2d-plate). Global analyses showed that the ratio of water to ice decreased as temperature decreased for all latitudes, however temperature dependence on the ratio of water and ice differed for latitudes. In sub-tropics and high latitudes, the ratio of water is higher for the same temperature. 2d-plate existed in the temperature between -10 to -20 degree C for all latitudes. We compared phase discrimination for CALIPSO with that of MODIS. CALIPSO tends to detect more clouds for both water and ice but general agreements for the phase were obtained.

The global distribution of ice microphysics detected by CloudSat and CALIPSO were presented. We first developed the new radar-lidar algorithm that can treat specular reflection that is frequently observed in CALIPSO data. Effective radius in the specular reflection ranges from 100 μm to 200 μm. Both effective radius and IWC increases as altitude (temperature) decreases (increases). Since effective radius becomes large in the specular reflection region, the extinction is low and thus lidar can see the thick cloud layer.

Keywords: ClouSat, CALIPSO, EarthCARE, cloud

DIURNAL VARIATION IN SUMMER PRECIPITATION OVER THE CENTRAL TIBETAN PLATEAU

PRASAMSA SINGH, and KENJI NAKAMURA
Hydrosophere and Atmosphere Research Center, Nagoya University,
Nagoya, Japan
nakamura@hyarc.nagoya-u.ac.jp

Abstract

The diurnal cycle of rainfall over the central Tibetan Plateau was investigated by examining data acquired by the Tropical Rainfall Measuring Mission (TRMM) Precipitation Radar (PR) during the summer monsoon season (June −August) of 1998−2007. High spatial resolution data (0.05^o x 0.05^o grid: ~ 5 km x 5 km) were used to identify the role of topographic features over the complex region of the plateau. Diurnal variations in rainfall amount, frequency of rainfall, rain conditioned rain rate, and storm- height were analyzed to determine the characteristics of precipitation. The results are interpreted as precipitation characteristics in a rather dry region with weak prevailing winds. Distinct diurnal variation was seen over hilly regions, valleys and lakes.

The central Tibetan Plateau receives less than 300 mm of rainfall per year, with more than 70 % occurring during June, July, and August. In summer, precipitation activity over the region is generally strongest during the late afternoon, and diurnal variation is found to be most prominent in the month of July. During July, the late afternoon convective rain maximum is followed by persistent rainfall. However, valleys and lakes show dominant late-evening peaks, and a secondary morning rainfall peak is distinctly evident over large lakes. The shift in rainfall from the large lakes and mountain ridges to the deep valley regions appears clearly during the daytime. However, the strength of the diurnal variation appeared weak for averaged rainfall over large lakes. The local time of peak rainfall is delayed as the size of the lake increases.

Keywords: TRMM, Tibetan Plateau, precipitation, diurnal variation

SHALLOW AND DEEP LATENT HEATING MODES OVER TROPICAL OCEANS OBSERVED WITH TRMM PR SPECTRAL LATENT HEATING DATA

Yukari N. Takayabu(1), Shoichi Shige(2), Wei-Kuo Tao(3), and Nagio Hirota(1)

(1) CCSR, University of Tokyo, Kashiwa, Japan
Email yukari@ccsr.u-tokyo.ac.jp
(2) Osaka Prefecture University, Osaka, Japan
(3) Goddard Space Flight Center, Maryland, USA

Abstract

Three-dimensional distributions of Q1-QR estimated from Tropical Ranfall Measuring Mission Precipitation Radar (TRMM PR) utilizing the Spectral Laten Heating (SLH) algorithm are analyzed. Mass-weighted and vertically integrated Q1-QR averaged over the tropical oceans is estimated as ~72.6 J s^{-1} (~2.51 mm day^{-1}), and that over tropical land is ~73.7 J s^{-1} (~2.55 mm day^{-1}), for 30N-30S. It is shown that non-drizzle precipitation over tropical and subtropical oceans consists of two dominant modes of rainfall sytems, deep systems and congestus. A rough estimate of shallow mode contribution against the total heating is about 46.7 % for the average tropical oceans, which is substantially larger than 23.7 % over tropical land.

While cumulus congestus heating linearly correlates with the SST, deep mode is dynamically bounded by large-scale subsidence. It is notable that substantial amount of rain, as large as 2.38 mm day^{-1} in average, is brought from congestus clouds under the large-scale subsiding circulation. It is also notable that even in the region with SST warmer than 28 degreeC, large-scale subsidence effectively suppresses the deep convection, remaining the heating by congestus clouds.

Our results support that the entrainment of mid-to-lower-tropospheric dry air, which accompanies the large-scale subsidence is the major factor suppressing the deep convection. Therefore, representation of the realistic entrainment is very important for proper reproduction of precipitation distribution and resultant large-scale circulation.

Keywords: meteorology, shallow convection, deep convection, TRMM, Latent Heating

EVALUATION OF THE EFFECTS OF THE ORBIT BOOST OF THE TRMM SATELLITE ON PR RAIN ESTIMATES

Shuji SHIMIZU, Toshio IGUCHI, Riko OKI, Tetsuya TAGAWA and Masafumi HIROSE
Earth Observation Research Center, Japan Aerospace Exploration Agency, Tsukuba, Japan
shimizu.shuji@jaxa.jp

Abstract

The Precipitation Radar (PR) on the Tropical Rainfall Measuring Mission (TRMM) satellite, which was launched on 28 November 1997, has been collecting global rainfall data for more than 10 years. The monthly surface rainfall amounts estimated by PR (e_SurfRain) have decreased on average since the satellite altitude was changed from 350km to 402.5km in August 2001 to extend its lifetime. There is no significant decrease in e_SurfRain in the five angle bins around the nadir (near-nadir) or in rainfall amounts at a 2km height. The major causes of the changes in rain estimates due to the orbit boost are (1) sensitivity degradation, owing to the increase of satellite altitude, (2) an increase in the range of surface clutter owing to the increase in the footprint size, and (3) a mismatch between the transmission and reception angles of the radar beams, affecting one in every 32 pulses.

The decrease in the echo from a distributed target near the surface attributable to the change of the satellite altitude from 350km to 402.5km is 1.21dB (= 20log(402.5/350)). From a simulation result, we estimate a decrease of 0.5% in surface-rainfall estimates due to the sensitivity degradation. Because the height of the clutter-free bottom increases at off-nadir angles due to the increase in the footprint size from 4.3km to 5.0km, the sampling range bins for near-surface rain have been raised, causing the PR to miss low-rain systems more often after the boost than before the boost. Although a beam-mismatch correction is executed in the current 1B21 algorithm, the correction algorithm still typically results in a negative bias in rain-rate estimates near the surface in the second half of the PR scan. The changes in the surface-rainfall estimates after the boost due to the second and third causes can be estimated as –2.5% and –2.9% by comparing the estimates at off-nadir bins with those at near-nadir bins with the assumption that the true rain rates measured at all angle bins should be the same, on average. It is concluded that the total effect of the orbit boost is a decrease of 5.9% (= 0.5 + 2.5 + 2.9%) in the estimated surface-rainfall amounts in PR version 6 products.

Keywords: TRMM, PR, rain, orbit boost

DIFFERENCES BETWEEN PRECIPITATION RADAR AND MICROWAVE IMAGER RETRIEVED RAIN RATES

Eun-Kyoung Seo
Department of Earth Science Education, Kongju National University
182 Sinkwan-Dong, Kongju 314-701, Chungnam, Republic of Korea
ekseo@kongju.ac.kr

Abstract

Analysis of the collocated rain rate retrievals from Tropical Rainfall Measuring Mission's precipitation radar and microwave radiometer reveals that their difference depends on the intensity of rain rates and the type of rain – the radiometer-derived rain rates vary from higher to lower than the radar-derived ones as rain rate or convective fraction increases. To better understand how this difference occurs, the relations between the two leading EOFs (Empirical Orthogonal Functions) of the observed brightness temperatures and the radiometer- or radar-derived rain rates were examined for convective, mixed and non-convective rain categories. In all types of rain, the two EOFs respond to the variation of the radiometer- and radar-derived rain rates in a similar fashion in low rain rates, while they respond quite differently in high rain rates.

Keywords: TRMM, TMI, PR, rain, retrieval

NEAR-REAL-TIME GLOBAL RAINFALL MAP USING MULTI-SATELLITE DATA BY JAXA AND ITS VALIDATION

Takuji KUBOTA, Misako KACHI, Riko OKI,
Earth Observation Research Center, Japan Aerospace Exploration Agency, Tsukuba, Japan
Email: kubota.takuji @jaxa.jp
Tomoo USHIO,
Osaka University, Osaka, Japan,
Shoichi SHIGE,
Osaka Prefecture University, Osaka, Japan,
Kazumasa AONASHI,
Meteorological Research Institute, Japan Meteorological Agency, Ibaraki, Japan
and Ken'ichi OKAMOTO
Tottori University of Environmental Studies, Tottori, Japan

Abstract

Japan Aerospace Exploration Agency (JAXA) has developed and operated near-real-time data processing system with passive microwave radiometer (PMW) data (i.e., TRMM TMI, Aqua AMSR-E, and DMSP SSM/I) and GEO IR data and distributed rainfall products via the Internet (http://sharaku.eorc.jaxa.jp/GSMaP/). Core algorithms of the system are based on the combined PMW-IR algorithm developed under the Global Satellite Mapping of Precipitation (GSMaP) project. Horizontal resolution of GSMaP_NRT is 0.1-degree latitude/longitude grid and temporal resolution is 1 hour. The datasets are provided in near real time (about four hours after observation). By the use of the GSMaP_NRT data, accumulated rainfall amount can be obtained, for example, for the cyclone "Sidr" during 10-16 November 2007, and the cyclone "Nargis"during 27 April-3 May 2008, and we can see differences of rainfall distibutions between both tropical cyclone.

Daily product of the GSMaP is utilized for the International Precipitation Working Group (IPWG) satellite precipitation validation/intercomparison studies. Currently GSMaP_NRT, as well as other satellite-based rainfall products, are compared to regional ground rain gauge and radar network data in near-real-time basis over United States (University of Maryland), South America (University of Maryland), Australia (Bureau of Meteorology), and Japan (Osaka Prefecture University).

The GSMaP rainfall products during 1998-2006 were produced by the post-processing system. We analyzed six high resolution satellite rainfall estimates from various centers and universities with reference to the gauge calibrated ground radar data provided by the Japan Meteorological Agency (JMA Radar-AMeDAS precipitation analysis) during the period from January to December 2004 and strengths and limitations of the satellite estimates are examined around Japan.

Keywords: rainfall map, validation, microwave radiometer, near-real-time

THE GSMaP PRECIPITATION RETRIEVAL ALGORITHM FOR MICROWAVE SOUNDERS: OVER-OCEAN ALGORITHM

Shoichi SHIGE, Tomoya YAMAMOTO, Takeaki TSUKIYAMA, Satoshi KIDA, Hiroki ASHIWAKE
Osaka Prefecture University, Sakai, Japan
Email: shige@aero.osakafu-u.ac.jp

Takuji KUBOTA
Earth Observation Research Center, Japan Aerospace Exploration Agency, Tsukuba, Japan

Shinta SETO
University of Tokyo, Tokyo, Japan

Kazumasa AONASHI
Meteorological Research Institute, Japan Meteorological Agency, Ibaraki, Japan

and Ken'ichi OKAMOTO
Tottori University of Environmental Studies, Tottori, Japan

Abstract

Global precipitation maps have been retrieved from passive microwave radiometers currently in orbit such as the TMI, AMSR-E and SSM/I using the GSMaP_MWR algorithm. Despite the improved rainfall estimates from the passive microwave radiometers, the challenge remains to further fill in information gaps through more frequent satellite observations. In this study, we develop an over-ocean rainfall retrieval algorithm for the AMSU based on the GSMaP microwave radiometer algorithm. This algorithm combines an emission-based estimate from Tb at 23 GHz and a scattering-based estimate from Tb at 89 GHz depending on an SI computed from Tb at both 89 and 150 GHz. Precipitation inhomogeneity is also taken into account.

The GSMaP-retrieved rainfall from the AMSU is compared with NOAA standard algorithm retrieved data using the TRMM data as the reference. Rain rates retrieved from GSMaP_AMSU have better agreement with TRMM estimates over mid-latitudes during winter. Better estimates over mid-latitudes over winter are given by the use of Tb at 23 GHz in the GSMaP_AMSU algorithm. On the other hand, GSMaP_AMSU overestimates rain rates over the subtropical regions. This is probably because GSMaP_AMSU is developed based on the AMSU/TRMM matched-up cases, most of which are organized rain systems.

Comparisons using 75 AMSU/TRMM matched cases show that the GSMaP_AMSU as higher rain detection than NOAA_AMSU. Therefore, using the estimates retrieved by the GSMaP_AMSU may lead to better GSMaP_MVK estimates. It was also shown that physically consistent algorithms, which share a database or lookup table, should be applied to passive microwave imagers and sounders because consistency in the rain products from passive microwave imagers and sounders is very important in combining them.

Keywords: Microwave radiometer, microwave sounder, precipitation, rain-rate retrieval

DEVELOPMENT OF A RETRIEVAL ALGORITHM FOR THE GPM DUAL-FREQUENCY PRECIPITAION RADAR (DPR)

Shinta SETO[1)], Toshio IGUCHI[2)], and Taikan OKI[1)]
1) Insitute of Industrial Science, University of Tokyo, Tokyo, Japan
2) National Institute of Information and Communications Technology, Koganei, Japan

Email: Seto@rainbow.iis.u-tokyo.ac.jp

Abstract

As a successor of the Tropical Rainfall Measurement Mission (TRMM), the core satellite of the Global Precipitation Measurement (GPM) mission will be launched with a Dual-frequency Precipitaion Radar (DPR) on board in July 2013 (as planned). A precipitation retrieval algorithm for the GPM/DPR is introduced in this presentation. The algorithm is under development, and is planned to be composed of five modules: a vertical profile module, a texture module, a drop size distribution (DSD) module, a surface reference technique (SRT) module, and a solver module.

The solver module retrieves a vertical profile of DSD (and rain rate) from observations at two frequencies of radar reflectivity factor (Zm) and path integrated attenuation (PIA). The SRT module estimates the PIA by comparing surface backscattering cross sections ($\sigma 0$) under rainfall and under no-rainfall. In the DSD module, DSD is approximated by a parametric function and constrained on DSD according to the rain-type (convective, stratiform, …) and the particle type (rain, snow, …) that are judged by the vertical profile and texture modules. The vertical profile module has another role of correcting for the attenation in Zm and $\sigma 0$ caused by non precipitating particles (cloud, water vapor, and oxygen). The main role of the texture module is to get information about the non-uniformity of precipitation within a radar beam, which strongly affects the retrieval results.

After a general explanation of the above modules, we may focus on some hot topics related to PIA; 1) How accurately can the SRT module estimate the PIA? and 2) What accuracy of PIA is required in the solver module to retrieve the rain rate with a desired accuracy.

Keywords: GPM, DPR, TRMM, DSD, SRT

ANALYSIS OF THE LAND SURFACE HETEROGENEITY AND ITS IMPACT ON ATMOSPHERIC VARIABLES AND THE AERODYNAMIC AND THERMODYNAMIC ROUGHNESS LENGTHS

Yaoming MA[1], Massimo MENENTI[2], Hirohiko ISHIKAWA[3], Reinder FEDDES[4]
[1]Laboratory of Tibetan Environment Changes and Land Surface Processes, Institute of Tibetan Plateau Research, the Chinese Academy of Sciences, Beijing , China, E-mail: ymma@itpcas.ac.cn; [2]Laboratoire des Sciences de l'Image, de l'Informatique et de la Te´le´de´tection, Universite´ Louis Pasteur, Strasbourg, France; [3]Disaster Prevention Research Institute, Kyoto University, Kyoto, Japan; [4] Department of Environmental Sciences, Wageningen University, Wageningen, the Netherlands

Abstract

The land surface heterogeneity has a very significant impact on atmospheric variables (air temperature T_a, wind speed u, and humidity q), the aerodynamic roughness length z_{0m}, thermodynamic roughness length z_{0h}, and the excess resistance to heat transfer kB^{-1}. First, in this study the land surface heterogeneity has been documented through the comparison of surface reflectance r_0, surface temperature T_0, net radiation flux R_n, and sensible heat flux H partitioning over the different land cover types in the experimental areas of the Global Energy and Water Cycle Experiment (GEWEX) Asian Monsoon Experiment on the Tibetan Plateau (GAME/Tibet), the Coordinated Enhanced Observing Period (CEOP) Asia-Australia Monsoon Project on the Tibetan Plateau (CAMP/Tibet), the Heihe Basin Field Experiment (HEIFE), the Arid Environment Comprehensive Monitoring Plan, 95 (AECMP'95), and the Dun Huang Experiment (DHEX). The results show that the surface heterogeneity was very significant in the areas of the HEIFE, the AECMP'95, and the DHEX and that it was less significant in the areas of CAMP/Tibet and GAME/Tibet. Second, the vertical profiles of T_a, u, and q in the near-surface layer and above the blending height z_b have been analyzed using the atmospheric boundary layer (ABL) tower data, radiosonde data, and tethered balloon data observed during the HEIFE, the DHEX, and the CAMP/Tibet. The results show that the land surface heterogeneity leads in the near-surface layer to different vertical profiles of u, Ta, and q overlying the surfaces of the Gobi and the oasis in the areas of the HEIFE and DHEX. The values of u, T_a, and q become well mixed above a height of about 300 m at the HEIFE and 150 m at the DHEX. z_{0m}, z_{0h}, and kB^{-1} over the different land surfaces have also been determined in this study. The results show that the land surface heterogeneity leads to different aerodynamic and thermodynamic parameters over the areas of the HEIFE, the AECMP'95, and the GAME/Tibet.

Key Words: land surface heterogeneity; atmospheric variables; aerodynamic and thermodynamic parameters

Local circulation and its possible relationship to local climate and so that to CO2 flux observation over complex terrain on Tibetan Plateau

Mingyuan Du*, Seiichiro Yonemura(NIAES)，Yingnian Li, Song Gu, Liang Zhao, Xianzhou Zhang and Jingshi Liu(CAS),

* National Institute for Agro-Environmental Sciences, 3-1-3 Kannondai, Tsukuba, Japan

Email: dumy@affrc.go.jp

Abstract

The Tibetan Plateau (TP) is the highest (averaging >4000m) and largest plateau on Earth. The TP is characterized by very complex terrain and 1/3 of the plateau is over 4800m. However, all the meteorological observatories on the Tibetan Plateau are biased to the populated lower-elevation area (<4800m) in the eastern and southern Tibetan Plateau. Ten simple automatic meteorological systems were set on a mountain slope from 4300m to 5530m a.s.l. in the central part of the TP and 7 simple automatic meteorological systems were set on a mountain slope from 3200m to 4380m a.s.l. in the east part of the TP. The observation results show the lapse rate in summer time is similar to that of averaged over the TP, while that in winter is much less than the averaged one. There is a temperature inversion layer on the slope due to the local cooling system there. The YSA's (Yamada Science and Art) A2C atmospheric modeling solutions (NEW HOTMAC/RAPTAD model) is used for illustrate this local circulation system.

On the other hand, TP has been considered to be one of the most ecologically fragile and sensitive ecosystems on the earth. Grassland occupies about 50% of the Tibetan Plateau. A more than three times increasing in livestock production in the Tibetan Plateau has occurred since 1978. An increase in air temperature on the Tibetan Plateau, greater than for whole China and East Asia has occurred within the same period based on meteorological observations. This paper will try to clarify mutual relationship between this circulation and local climate and so that CO2 flux observation in Tibetan Plateau.

Keywords: Local circulation, Temperature inversion, Complex terrain, Tibetan Plateau.

THE MERGER OF MULTIPLE VOTICES IN DUST DEVIL GENERATION

Hiroshi OHNO, Tetsuya TAKEMI
Disaster Prevention Research Institute, Kyoto University, Kyoto, Japan
ohno@storm.dpri.kyoto-u.ac.jp
takemi@storm.dpri.kyoto-u.ac.jp

Abstract

Dust devils often occur in arid areas when environmental wind is weak and heat flux at the surface is high. Although dust devils lift a significant amount of dust to the atmosphere from the surface even if environmental wind is weak, global models and regional models cannot include the effects because of their coarse resolution. In order to know in detail the effects on a global transport of dust, we need in advance to reveal the process of generation and enhancement of dust devils.

In this research, a large eddy simulation of a highly developed convective boundary layer under no mean wind condition was conducted with the Weather Research and Forecasting model in order to investigate the physical processes of dust devils. Many vertical vortices with both signs of vorticity were generated in the lower region of the simulated convective boundary layer. By performing composite analysis for intense vortices, it was found that most of the intense vortices are enhanced through the merger of multiple vortices. It was also found that the most intense vortex generated in this simulation had a two-cell structure whose vertical velocity at the center was negative. Moreover, such a significantly intense vortex was maintained and enhanced by additionally merging small-scale vortices and tilting horizontal vortices at the boundaries of the convective cells.

Keyword: Dust devil, large eddy simulation, convective boundary layer, vortex merger, horizontal vortices

MICROSCALE VORTICES IN CONVECTIVE BANDS OVER WARM OCEAN IN WINTER

Tetsuya TAKEMI[1)], Hanako INOUE[2)], Kenichi KUSUNOKI[2)], Wataru KATO[3)], Keiji ARAKI[4)], Kotaro BESSHO[2)], Masahisa NAKAZATO[2)], Shunsuke HOSHINO[2)], Wataru MASHIKO[2)], Syugo HAYASHI[2)], Yoshihiro HONO[3)], Toshiaki IMAI[4)], Toru SHIBATA[4)]

1) Disaster Prevention Research Institute, Kyoto University, Kyoyo, Japan
2) Meteorological Research Institute, Ibaraki, Japan
3) East Japan Railway Company, Saitama, Japan
4) Railway Technical Research Institute, Tokyo, Japan

1) takemi@storm.dpri.kyoto-u.ac.jp

Abstract

Recent observational studies of cold outbreaks in a coastal region in northern Japan in winter have revealed that there are unexpectedly frequent occurrences of microscale vortices (i.e., misocyclones) embedded in winter convective storms that develop over the Japan Sea. These vortices in some instances evolve into well-defined tornadoes. The present study investigates the development and evolution of microscale vortices in convective bands by conducting 120-m grid simulations with the Weather Research and Forecasting (WRF)-Advanced Research WRF (ARW) model. A case on 2 December 2007 over the Shonai Plains, Yamagata, Japan is chosen for the present analysis.

The control simulation well represents well-defined multiple vortices (with the vorticity of 0.06 s^{-1} and the size of 500 m) embedded in a precipitating convective band. The microscale vortices are generated at the leading edge of a weak cold-air outflow where horizontal wind shear is significant. The vortices extend vertically up to the 1.5-km level and are seen to be enhanced by the convective clouds that develop at the leading edge of cold outflow. Interestingly, the height of the cloud top is only at most 5 km. Considering that the low-level vertical shear as well as the cold outflow is weak, the source of the vortices seems to be not in the vertical shear but in the horizontal shear. Since the environmental low-level atmosphere is very unstable owing to cold air over the warm sea surface temperature (SST), the strength of convective clouds is significant enough to enhance the vortices, in spite of relatively low cloud-top height than that for cumulonimbus clouds.

A sensitivity simulation with SST uniformly decreased by 5 K is also performed in order to examine the effects of warm SST. The strength of convective updrafts is significantly reduced and thus the strength of microscale vortices is also reduced. Therefore, warm SST plays an important role in the development of convective clouds and hence the associated microscale vortices.

The present 120-m grid simulation captures observed high wind speeds due to the strong vortices, which indicates that resolving microscale disturbances is important for the representation of strong wind events in numerical weather prediction models.

Keywords: atmospheric vortex, misocyclone, winter convective storm

SELF-SIMILARITY OF HORIZONTAL CONVECTIONS CAUSED BY THERMAL FORCING AT THE BOTTOM

Atsushi Mori, Hiroshi NIINO
J. F. Oberlin University / Ocean Research Institute The University of Tokyo, Tokyo, Japan
moriat@obirin.ac.jp / niino@ori.u-tokyo.ac.jp

Abstract

Horizontal convection is one of the most important physical processes in the ocean and the atmosphere. Land and sea breeze circulations and heat or cool island circulations are typical examples. However, the physical processes of those horizontal convections had not drawn attention so much until recently.

In order to clarify the physical processes of the horizontal convections, we have been studying time-evolution of two-dimensional nonlinear horizontal convections due to thermal contrast at the bottom of a stably stratified Boussinesq fluid. In the case of cooling with fixed temperature on the semi-infinite part of the bottom, we have shown that there exist three types of self-similar solutions(Mori and Niino, 2002). And the time-evolution of the horizontal convections was found to be successfully described by those solutions and the transitions between them. The validity of each of the solutions was proved according to a set of nondimensional parameters and the elapsed time. The solutions can be interpreted by diffusive processes, propagations of gravity current and internal gravity wave, respectively. And thus, we have classified the flow regimes into three regimes: diffusion regime, gravity current regime, and gravity wave regime.

We have found that the discussions can be extended to other types of boundary conditions. There exist three types of self-similar solutions, when the temperature at the semi-infinite part of the bottom is proportional to t^q, where t is the elapsed time and q is a certain non-negative constant. If the temperature deviation of the thermal forcing is constant in time, the corresponding value of q is zero. And similarly, constant heat flux condition corresponds to $q=1/2$. According to the extended theory, we have found that the classification of the flow regimes can be described in a more generalized way (fig.1).

Those results can be used to interpret the formation mechanism and the structure of steady horizontal convections. We have shown that the ideal steady heat island circulations which are caused by the temperature difference at the bottom can be re-interpreted by those solutions(Mori and Niino, 2002 and Niino, et al., 2006).

Keywords: self-similarity, horizontal, convection, gravity wave, gravity current

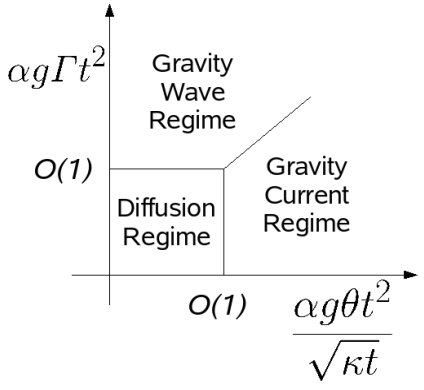

α : coefficient of thermal expansion
g : gravitational acceleration
Γ : strength of stratification
κ : thermal conductivity

θ : temperature deviation imposed on the lower boundary, $\theta \propto t^q$

fig.1: Regime diagram of horizontal convections

APPLICATION OF DYNAMICAL DOWNSCALING IN WIND RESOURCE ASSESSMENT OVER EAST CHINA

Yi-Xiong LU, Jianping TANG and Yuan WANG
School of Atmospheric Sciences, Nanjing University, Nanjing, P.R. China
luyixiong@hotmail.com

Abstract

For the sake of wind power exploitation, the mesoscale meteorological model MM5 has been applied to downscale 2.5° reanalysis data provided by NCEP/NCAR onto a 3.3 km grid covering the Jiangsu region, East China. The simulated low-level winds are compared with observations at 64 surface stations in 2000. In addition to conventional scores (mean absolute error, anomaly correlation), a spectral analysis is carried out in order to explore the physical aspects of the model performance. Conventional scores indicate that the downscaling has been successful. Scores show that there are significant features that errors are smaller where observed wind speed is higher. The utilization of spectral analysis enables a more physical insight into the model performance. It can be seen that the simulated synoptic oscillations agree well with the observed and the seasonal oscillations are slightly overestimated by the model. Otherwise, the biweekly osillations cannot be replicated by the model so well. As an illustration, it is indicated that the simulated wind power density can be comparable to the observed obtained by using the Weibull distribution function at Xi-Lian Island.

Keywords: wind resource assessment, dynamical downscaling, spectral analysis

LARGE EDDY SIMULATION OF PARTICLE SETTLING IN THE ATMOSPHERIC BOUNDARY LAYER

H. J. Ko, and Y. Noh
Department of Atmospheric Sciences, Yonsei University, Seoul 120-749, Korea
kohj@yonsei.ac.kr

Abstract

Settling of heavy particles in the turbulent flow was investigated by analyzing the Lagrangian motion of a large number of particles in the atmospheric boundary layer simulated by large eddy simulation (LES). Both convective and shear-driven turbulent boundary layers were considered, and particles were initially introduced to the height above the boundary layer with uniform horizontal concentration. It was investigated how vertical profiles of particle concentration evolves with time under the influence of turbulence in the boundary layer. The sedimentation rate were evaluated under different conditions of particles and the atmospheric boundary layer, and compared with the existing empirical formula for its prediction. Furthermore, the probability distribution function of particles to the given turbulence fields, such as vertical velocity and vorticity, were investigated together with the preferential concentration in order to understand how turbulence affects the particle settling process.

Keywords: large eddy simulation (LES), atmospheric boundary layer, settling velocity, Lagrangian particles, aerosol

OBSERVATION OF ^{222}Rn CONCENTRATION AT THE MRI TOWER AND ANALYSIS OF ITS VARIATION

Hiroaki KONDO[1], Shohei MURAYAMA[1], Yousuke SAWA[2], Hidekazu MATSUEDA[2], Kentaro ISHIJIMA[3] Hirofumi SUGAWARA[4] and Akira WADA[5]

1 National Institute of Advanced Industrial Science and Technology (AIST), Tsukuba, Japan
2 Meteorological Research Institute, Tsukuba, Japan
3 JAMSTEC, Yokohama, Japan
4 National Defense Academy of Japan, Yokosuka, Japan
5 Meteorological College, Kashiwa, Japn

Abstract

Time variation of ^{222}Rn concentration was observed at 1.5m and 100m or 200m above the ground using observational tower (36°3'9"N, 140°7'25"E) of the MRI (Meteorological Research Institute), Japan with a newly developed equipment to measure ^{222}Rn cocentration (Wada et al., 2009) from 13 Nov. to 27 Nov., 2006. Wind and turbulence were measured at 10m and 25m level at the tower and temperature profile was measured with a temperature profiler at the same time. Rn efflux from soil was measured at one point in the MRI campus and was estimated from observation of soil water content at other five points near the tower.
The relation of Rn concentration and stable stratification at night was mainly analyzed. In this period strong inversion layer appeared two nights asocciated with persistent temperature rise above 300m throughout the night. However concentration near the surface was not corelated with the intesity of the inversion layer. The layer that Rn was accumulated was approximately one third of inversion layer height. From the increment of Rn concentration before sun rise, efflux from soil was estimated, which agreed with direct observation. The effects of MRI main buildings on the results were detected in the variaition of TKE and Rn concentration.

Acknowledgement
This study was supported by KAKENHI (17201009).

Reference:
Wada, A., S. Murayama, H. Kondo, H. Matsueda, Y. Sawa, K. Tsuboi, 2009: Development of a compact and sensitive Radon-222 measuring system for use in atmospheric observation. submitted to Journal of Meteor. Soc. of Japan

Keywords: ^{222}Rn, stable boundary layer, meteorological tower

corresponding author: Hiroaki Kondo, kondo-hrk@aist.go.jp

ANALYSES OF THE WATER AND ENERGY CYCLES IN THE UPPER TONE RIVER BASIN WITH THE AIDS OF A DISTRIBUTED BIOSPHERE HYDROLOGICAL MODEL (WEB-DHM) AND MODIS LAND SURFACE TEMPERATURE

Lei WANG[1], Toshio KOIKE[1], Kun YANG[2]

[1]Dept. of Civil Eng., the University of Tokyo, Bunkyo-ku, Tokyo 113-8656, Japan
[2]Institute of Tibetan Plateau Research, Chinese Academy of Sciences, Beijing 100085, China

Email: wang@hydra.t.u-tokyo.ac.jp

Abstract

Land surface temperature (LST) is a key parameter in land-atmosphere interactions. The recently released Moderate Resolution Imaging Spectroradiometers (MODIS) LST Version 5 products have provided good tools to evaluate water and energy budget modeling for regions without flux observations. In this study, a distributed biosphere hydrological model (WEB-DHM; so-called water and energy budget-based distributed hydrological model) that couples a biosphere scheme (SiB2) with a geomorphology based hydrological model (GBHM), is applied to the upper Tone River Basin where flux observations are not available. The model facilitates a better understanding of the water and energy cycles in this region. After being calibrated with discharge data, WEB-DHM is assessed against observed streamflows at 4 major gauges and MODIS LST. Results show that long-term streamflows including annual largest floods are well reproduced. As well, both daytime and nighttime LSTs simulated by WEB-DHM agree well with MODIS observations for both basin-averaged values and spatial patterns. The validated model is then used to analyze water and energy cycles of the upper Tone River Basin. It was found that from May to October, with relatively large leaf area index (LAI) values, the simualted daily maximum LST is close to soil surface temperature (T_g) since T_g is much greater than canopy temperature (T_c) in their peak values; while the daily minimum LST appears similar to T_c. For other months with relatively small LAI values, the diurnal cycles of LST closely follow T_g.

Keywords: land surface temperature, distributed biosphere hydrological model, streamflow, flood

THE CHARACTERISTICS OF SNOW OBSERVATION BY NEW WEIGHT MEASUREMENT ROUNDED PLATE

Bu-Yong Lee, Hyun-Chul Kim
Dept. of Environmental Science, Catholic University of Daegu, Kyeongsan-shi, Korea
bylee@cu.ac.kr

Abstract

Nowdays the trend of temperature is increasing world wide. This can cause much of snowfall to rain every where. It is the serious problems water supplies from winter snowfall. Snow fall can store on the ground but rain goes to the river away. We still do not have a much infromation of snow because there is many difficulties in field observations.

There is two methods of observation of snowfall by length and mass unit. The length measurement of sonic can get only the depth of snow fall not mass of snow cover. We need water equivalent unit data of snow cover for the purpose of accurate estimate of precipitation. We use snow pillows for measuring mass of snow cover. The principle of this instrument measuring pressure of snow cover not mass unit. This kind of instruement measure the most hightest preassure on the pillow side this can cause wrong data. Parcel melting of sonw can gives high pressure on small area, then instruemt indicate high amount of snow fall because instrument only indicate the pressure by the mass.

This study developed new method of snow cover by weight unit. This instrument use strain-gauge loadcell for measuring weight not pressure with rounded shape. The size of instrument is 100 cm diameter and measuring area of snow fall is 80 cm inside.

Field test of instrument carried out at Daegwallyeong Observation Station in Korea from 20 to 23 January 2008 druing heavy snowfall day. There is 74 cm snow depth and 54.6 mm precipitation by Daegwallyeong Observation Station. But this study recorded 71.0 mm of precipitation amount. There is 15.4 mm difference between diffenent observation method. From the observation data snow cover density calculated from 0.09 to 0.15 g/cm3 during observation period. And have a good relations between manual observation and automatic observation from this study with slope of 1.35 to 1.39.

Keywords: snow, snow cover, precipitation, automatic observation

ESTIMATE OF THE UPTAKE AND STORAGE OF ANTHROPOGENIC CO_2 IN THE PACIFIC OCEAN

Yongfu XU, Yangchun LI
LAPC, Institute of Atmospheric Physics, Chinese Academy of Sciences, Beijing, P. R. China
xyf@mail.iap.ac.cn, lych@mail.iap.ac.cn

Abstract

Atmospheric CO_2 is up almost 40% since the industrial revolution because of the consumption of a large amount of fossil fuels. The increased CO_2 amount is often called anthropogenic (or excess) CO_2. So far, there has been no doubt about that the increasing atmospheric CO_2 is caused by human activities. However, there is some controversy about how the biogeochemical system corresponds to and adapts to the increase of atmospheric CO_2. It has been estimated that the ocean absorbed 2.0 PgC/yr of atmospheric CO_2 for the period 1980-1989 but with an uncertainty of 30-40%. There is even much larger uncertainty about how much anthropogenic CO_2 has been and will be taken up by the Pacific Ocean. We have an attempt to use a basin-wide ocean general circulation model (OGCM) of the Pacific Ocean to study the storage and uptake of anthropogenic CO_2 in the Pacific Ocean. Two approaches are used in this work, including a perturbation approach (model) and an ocean biogeochemistry general circulation model (OBGCM). The simulated results show that the surface distribution and inventory of anthropogenic CO_2 from the perturbation model is in good agreement with data-based estimates. The simulated vertical distributions at several sections are also consistent with those obtained by data-estimates. The model estimates that the Pacific Ocean contained 44.7 PgC of anthropogenic CO_2, including 16.7 PgC in the North Pacific. In 1980s, the Pacific Ocean absorbed 0.77 PgC/yr of anthropogenic CO_2, and this figure was increased to 0.87 PgC in 1990s, including 0.31 PgC in the North Pacific. The simulated distributions of anthropogenic CO_2 from the OBGCM are in agreement with those from the perturbation model. However, both the concentration and penetration depth from the OBGCM are larger than those estimated by the perturbation model. It is known from the exchange flux that the OBGCM enhances the anthropogenic CO_2 uptake in the North Pacific but weakens the anthropogenic CO_2 uptake in the South Pacific, compared with the estimate by the perturbation model.
Keywords: anthropogenic CO_2, Pacific Ocean, perturbation approach, biological processes

CHANGE IN THE ENSO TELECONNECTION CHARACTERISTICS IN THE BOREAL WINTER

kunihiko KODERA
The Solar-Terrestrial Environment Laboratory, Nagoya University,
Nagoya, Japan
kodera@stelab.nagoya-u.ac.jp

Abstract

Substantial change was found in the El Niño/Southern Oscillation (ENSO) teleconnection during the boreal winter after the regime shift of the late 1970's. The ENSO teleconnection pattern of the earlier period is characterized by a wave-train-like structure over the Pacific/North American sector that also propagates into the stratosphere. In contrast, the recent ENSO-related extratropical circulation anomalies are characterized by changes in the tropospheric subtropical jet. The interaction of zonal winds with large-scale topography creates meridional dipole-type height anomalies downstream of the Rockies and the Tibetan Plateau, which may characterize the recent ENSO teleconnection pattern..

Keywords: ENSO, Decadal change, Climate change, teleconnection

SIMULATING SURFACE ENERGY FLUX AND SOIL MOISTURE AT THE WENJIANG PBL SITE USING THE LAND DATA ASSIMILATION SYSTEM OF THE UNIVERSITY OF TOKYO

Hui LU[1], Toshio KOIKE[1], Kun YANG[2], Xiangde Xu[3], Xin LI[4], Hiroyuki TSUTSUI[1], Yueqing LI[5], Xingbing ZHAO[5], and Katsunori TAMAGAWA[1]

[1]Dept. of Civil Eng., Univ. of Tokyo (Bunkyo-ku, Tokyo 113-8656, Japan)
[2]Inst. of Tibet Research, China Academy of Sciences (Beijing 100085, China)
[3]Chinese Academy of Met. Science., China Met. Admin. (Beijing 100081, China)
[4]Cold and Arid Regions Envi. and Eng. Research Inst., CAS (Lanzhou 730000, China)
[5]Institute of Plateau Meteorology, China Met. Admin. (Chengdu 610071, China)
Email: lu@hydra.t.u-tokyo.ac.jp

Abstract

This paper reports an application of a Land Data Assimilation System (LDAS) to the Wenjiang site located near Chengdu, China, for the period from January to March, 2008. The LDAS was first driven by in-situ observed micrometeorological data. Simulated energy fluxes were compared to hourly direct measurements and simulated soil moisture content was compared to the in-situ soil moisture observations at a depth of 4 cm. The results show that the LDAS well simulated those variables and thus validated the capability of LDAS. To check the possibility of applying LDAS globally and simulating surface energy and water budget worldwide, two sets of model output data were used as the driving data of the LDAS: the Japan Meteorology Agency (JMA) Model Output Local Time Series (MOLTS), and the Modified JMA MOLTS. The LDAS performance was not so good when driven by the original JMA MOLTS data, but improved after we used modified MOLTS data with some simple linear regression equations. This result demonstrated the feasibility of reliably simulating land surface fluxes with a LDAS driven by model outputs.

Keywords: Land Data Assimilation System, Energy Fluxes, Soil Moisture, Field Experiments

STRUCTURE AND MECHANISMS OF THE SOUTHERN HEMISPHERE SUMMERTIME SUBTROPICAL ANTICYCLONES

Takafumi MIYASAKA and Hisashi NAKAMURA
University of Tokyo, Tokyo, Japan
miyasaka@eps.s.u-tokyo.ac.jp

Abstract

Three-dimensional structure and dynamics of the climatological-mean summertime subtropical anticyclones in the Southern Hemisphere (SH) are investigated. As in the Northern Hemisphere (NH), each of the surface subtropical anticyclones in the South Pacific, South Atlantic and South Indian Oceans is accompanied by a meridional vorticity dipole aloft, exhibiting barotropic and baroclinic structures in its poleward and equatorward portions, respectively, in a manner dynamically consistent with the observed mid-tropospheric subsidence. Their dynamics is also similar to their NH counterpart. It is demonstrated through our numerical experiments that each of the SH surface anticyclones observed over the relatively cool eastern oceans can be reproduced in response to a local near-surface cooling-heating couplet. The cooling is due mainly to radiative cooling associated with low-level maritime clouds, and the heating to the east is associated with sensible heat flux over the dry, heated continental surface. Since the low-level clouds act to maintain the coolness of the underlying ocean surface, which is also maintained by the alongshore surface southerlies, the presence of a local atmosphere-ocean-land feedback loop is suggested as in the NH in association with the summertime subtropical anticyclones and continental cyclones to their east. Both our model experiments and diagnosed upward flux of Rossby wave activity suggest that the land-sea heating contrasts across the west coasts of the three continents, in addition to the continental deep convective, can contribute to the formation of the summertime planetary-wave pattern observed in the entire subtropical SH, characterized by the zonal wavenumber-3 component.

Keywords: subtropical anticyclone, planetary wave, climatology

AN EXTRATROPICAL AIR-SEA INTERACTION OVER THE NORTH PACIFIC IN ASSOCIATION WITH A PRECEDING EL NIÑO EPISODE IN EARLY SUMMER

Yafei WANG

State Key Laboratory of Severe Weather, Chinese Academy of Meteorological Sciences,

Beijing, China

yfwang@cams.cma.gov.cn

Abstract

Using data for the month of June from 1951 through 2000, this study examined an air-sea interaction over the North Pacific after El Niño had matured in the preceding November in each of the respective years. The principal findings are: (1) A coherence area near the International Date Line in the extratropical North Pacific revealed an area of significant negative correlation (SNC) between the sea surface temperature (SST) in the Niño-3 region in the preceding November and the SST in the North Pacific in June. The coherence area is very close to and has a common point with the area of SNC between an index of the Okhotsk High and the SST in June. Two indexes of the Okhotsk High in June are positively correlated with the SST in the Niño-3 region in the preceding November. (2) The strong southeastward wave activity flux from the upstream area of the Okhotsk Sea scattered over most parts of the North Pacific in the middle latitudes is associated with a strong preceding El Niño event, the development of the Okhotsk High, and a negative 500 hPa geopotential height / SST anomaly around the coherence area. The scattering stationary wave propagation plays a strong part in suppressing the northward progress of the subtropical high. The above process is one of the ways that bridges the Central Pacific warming and the East Asian summer monsoon circulation, which is a supplement to the physical explanation by Wang et al. (2000). (3) A wave train-like anomaly of the SST tilted northwest-southeast was established and maintained for more than two months in the North Pacific in the summer of 1998; this occurrence coincided with the direction of the atmospheric Rossby wave propagation as the strong wave activity flux southeastward was scattered over most areas of the North Pacific in middle latitudes. This event provides solid evidence that such an atmospheric Rossby wave propagation plays an important role in forming an oceanic temperature wave train on extratropical Pacific through a barotropic process.

Keywords: blocking, wave train, air-sea interaction

NUMERICAL SIMULATION OF WIND HOLE CIRCULATION AT ICE VALEY IN KOREA USING A SIMPLE 2D MODEL

H. L. Tanaka, H.-R. Byun, D. Nohara, and N. Mura

Center for Computational Science, University of Tsukuba,
Tsukuba Japan (First Author)
tanaka@ccs.tsukuba.ac.jp

Abstract

In this study, numerical simulations of the summertime ice formation at Ice Valley in Korea are conducted using a simple 2D model, which is driven by the observed air temperature. The Ice Valley in Korea is a famous summer resort, as the Natural Monument where natural ice forms in spring, and remains till summer along the slope, and the ice disappears in fall to winter. It is interesting to note that the hotter the outside air is, the larger the ice grows in spring. The mysterious behavior of the summertime ice has been partly explained by a series of numerical experiments in terms of the convection theory, which is explained by the seasonally reversing wind-hole circulations. The numerical model in this study is updated from our former versions considering the new finding by the in situ observations. The result of the simulation is compared with the observations at the Ice Valley in Korea, and Nakayama in Japan.

According to the result of the numerical simulation, the summertime wind-hole circulation activates the downward flow when the outside air is getting hot. The downward flow transfers the cold accumulated in the talus during the previous winter toward the outlet of the cold wind hole. As a result, the intensified cold advection grows the ice when the outside air is getting hot. The wind hole circulation appears to be about 17 mm/s in April, and the residence time of the air in the talus is estimated as 2.8 hours for this case. It is shown that the seasonal reversal of the wind hole circulation is the essential mechanism of the summertime ice at the Ice Valley, acting as a natural thermal filter which effectively accumulates only the winter cold in the talus.

Keywords: Ice Valley, Cold wind hole, Warm wind hole, Convection

A Proposal of Standard Calibration Laboratory for RICs

Yizhuo Sha, Xigui Fu, Xiaolei He, Lekun Zhu
(National Centre for Meteorological Metrology,
Meteorological Observation Centre, CMA, Beijing, China)

Abstracts

According to WMO, considered the need for regular calibration and maintenance of meteorological instruments to meet the increasing needs for high quality meteorological and hydrological data, the requirements of Members for standardization of meteorological instruments, the need for international instrument comparisons and evaluations, it was recommended to establish Regional Instrument Centres.

But up to now, there are no detail proposals for establishing a standard calibration. This paper will give three proposals to establish a standard meteorological metrology calibration laboratory for RICs.

Key words: Meteorology, Calibration, Standard, Laboratory, Proposal

SEASONAL START OF THE ANTARCTIC OZONE HOLE DERIVED BY THE OBSERVATIONS WITH DOBSON SPECTROPHOTOMETERS

Shigeru CHUBACHI
Meteorological Research Institute, Tsukuba, Japan
schubach@mri-jma.go.jp

Abstract

The Antarctic ozone hole appears in the Antarctic spring, just after the polar night period when sunlight is not available on the surface. Because we are not able to have a large solar elevation angle in the Antarctic winter and spring, it is hard to make observations of total ozone amounts with TOMS or Dobson spectrophotometer using sunlight. Because of this reason, there is not enough information about the total ozone amounts over the Antarctic just before and after the seasonal appearance of the Antarctic ozone hole.

We have made an analysis of the total ozone amounts with Dobson spectrophotometer with moonlight as well as sunlight at the three Antarctic stations and Macquarie Island. The results derived from the analysis are as follows. The author hopes that these results will be useful for better understanding of the Antarctic ozone hole.

1. Decrease of the deviation of total ozone amounts from polar night mean (the mean value between 1st June and 10th July) leading to the Antarctic ozone hole started in the beginning of August at around 69 degrees south at first and then took place at the higher latitudes later in the period from 1993 to 2005.

2. The total ozone amounts at the higher latitudes on the Antarctic show the smaller value as a latitudinal gradient of about 1.6 DU per degree in the period from 1993 to 2005.

Keywords: ozone hole, seasonal start, Antarctica

Study on the relationships among SO-NO-AAO-NPO

Peng Jingbei Zhang Qingyun Chen Lieting
(Institute of Atmospheric Physics, Chinese Academy of Sciences, Beijing, 100029)

Abstract

The connections among the Southern Oscillation (SO), the Northern Oscillation (NO), the Arctic Oscillation (AAO) and the North Pacific Oscillation (NPO) which are all over the Pacific Ocean (hereafter the four oscillations) were studied by using the monthly mean sea level pressure (SLP) from NCEP/NCAR reanalysis data set and the International Comprehensive Ocean–Atmosphere Data Set (ICOADS) for the period of 1951–2006. Main conclusions are as follows:

1) Interannual variabilities of the four oscillations were identified in distinct 3–7 years.

2) In the interannual time scale, the leading modes of SLP over the North and South Pacific were NO and SO, respectively. The second modes were NPO and AAO.

3) The four oscillations were not independently. They connected with each other. NO and NPO in the interannual scales were significantly in-phase with SO and AAO, NPO and AAO were highly correlated with NO and SO at a quarter-cycle phase lag, respectively.

4) One oscillation conversed to another according to $SO^- \rightarrow AAO^+ \rightarrow SO^+ \rightarrow AAO^- \rightarrow SO^-$（$NO^- \rightarrow NPO^+ \rightarrow NO^+ \rightarrow NPO^- \rightarrow NO^-$）. The beginning and the end of the transition of oscillations in South and North Pacific was roughly at the same time. The period of the transition was about 4~6 years.

5) Examining the evolving SLP anomaly (SLPA) during transition of the four oscillations infers SLPAs propagated from west to east in the tropic Pacific. The SLPAs moved to the North, towards the Aleutian region, after they reached the eastern Pacific. That leaded to the transition between NO and NPO. The SLPAs in the mid- and high-latitude of the South Pacific which were out of phase with those in the tropical Pacific Ocean also propagated eastward, causing the transition between SO and AAO.

The interannual variations of SO and NO related to the El Niño/La Niña closely. Thus, the transition of the four oscillations may also relate to the ENSO cycle. The relationship between the ENSO cycle and the transition of the four oscillations should be studied in the future.

SPATIAL DISTRIBUTION OF SOLAR RADIATION FLUX ACCOUNTING TOPOGRAPHICAL SHADE AND REFLECTION FRACTION BY SEA SURFACE: A CASE OF CHEJU-DO, KOREA

Yousay HAYASHI*, Fumichika UNO*, Soo-jin HWANG**, Jin-Il YUN***
and Hae-Dong KIM****

* University of Tsukuba, Tsukuba, Japan
**Pusan National University, Pusan, Korea
***Kyung Hee University, Yongin, Korea
****Keimung University, Taegu, Korea

hayyou@geoenv.tsukuba.ac.jp

Abstract

Solar radiation is an important input for many aspects of hydrology, meteorology and climatology, biology and agricultural land use. Although its computaion is relatively straightforward for a gently undulated surface using inclination and aspect, in many physical situations the influence of shading effect by steep topography and reflection fraction of direct solar radiation need to be taken into account. Especially for research subjects focused in the present study, which treats geographical conditions of a location of orchard zone facing open sea, summation of global solar radiation and reflected solar radiation by sea surface is essential for the flux estimation.

Modelling and measurement of a single surface solar radiation is relatively uncomplicated, but to be of worthwhile application to large-scale processes there is a need for models to be able to predict efficiently and accurately over a wide area. Basically, over complex terrain areas where shading is commonplace, it is imperative to be able to differentiate between global radiation (downward) and reflected radiation (upward) as their relative importance on orchard cultivation throughout the growing season. Practically, large percentage of photosynthetically acitve radiation energy is contained in reflected fraction. The present research attempts to calculate the incoming solar radiation flux using digital elevation map and discuss significance of solar radiation flux on the area categorized by agricultural land use.

A methodology for predicting global solar radiation into any meshed surface based on comparison of the elevation angle of the ridgeline and the sun track is descibed. The model is based on individual calculations of direct, diffuse and reflection components, enabling its application under a wide range of sky conditions. An algorithm accounting for the effect of topographical shading is also included and this enables accurate estimations of spatially distributed global solar radiation over complex terrain of Cheju-do (island), Korea. The model is then applied to the summer and winter solstices. Spatial distribution pattern of the solar radiation flux is strongly affected also by weather conditions. In winter, a zone occupied by orchard receives larger amount of the flux than is expected on horizontal surfaces. This is emphasizing an importance of the spatial distribution of the agro-climatic resources over an isolated island of Cheju-do.

Keywords: agro-climatic resources, Cheju-do, reflection fraction, shading effect, spatial distribution

VERIFICATION OF T213 ENSEMBLE FORECASTING BASED ON TIGGE DATASET

Xiao-Wen TANG, Yuan WANG

NanJing University, NanJing, China

xwtang@smail.nju.edu.cn

Abstract

In the recent decade, developing and utilizing ensemble weather forecasting system has become the most important task in many operational NWP centers. The use of ensemble weather forecasting has shown promising results, so WMO launched the TIGGE project which intends to establish an interactive grand global ensemble forecasting database facilitating the global ensemble forecasting research. Through recent years of preparation, the TIGGE dataset is now available to meteorological researchers and many significant works have been done based on this dataset.

The T213 ensemble predicting system (EPS) of CMA (China Meteorological Administration) is based on the sophisticated T213 which had been used operationally as deterministic forecasting model for many years. T213 EPS had become one member of the TIGGE dataset since the project established. Unlike ensemble forecasting of other numerical centers, the performance of T213 EPS has not been systematically analyzed and verified. This article devoted to discuss the performance of T213 EPS both in deterministic and probability way. Results show that by mean of ensemble forecasting T213 EPS gives much better results than deterministic forecasting, and can be further improved by mean of multi-center grand ensemble. At the same time, we can see that the T213 EPS is still fall behind of ECWMF and NCEP in either deterministic or probabilistic forecasting.

Keywords: TIGGE, ensemble forecast, probability verification

ENSEMBLE KALMAN FILTER APPLIED ON TYPHOON WUKONG (2006) PREDICTION

Jong Im PARK and Hyun Mee KIM
Atmospheric Predictability and Data Assimilation Laboratory,
Department of Atmospheric Sciences, Yonsei University
Shinchon-dong 134, Seodaemun-gu, Seoul, 120-749, Republic of Korea
khm@yonsei.ac.kr

Abstract

Ensemble Kalman Filter (EnKF) based on ensemble assimilations of observational data has been applied to the initialization of atmospheric and oceanic models. The EnKF estimates flow- and location- dependent background error covariance from short-range ensemble forecasts. This flow- and location- dependent error covariance may produce a better analysis than the analysis produced by a fixed error covariance. While applications of the EnKF on large-scale weather prediction have achieved a big progress, the EnKF began to apply to meso-scale and regional-scale weather prediction recently.

In this study, we applied the EnKF on the prediction of typhoon Wukong (2006). Typhoon Wukong was formed in the western Pacific on 13 August 2006 and did not weaken after landfall on the Kyushu island on 18 August 2006. Wukong stayed around 28 hours on Kyushu from 18 to 19 August 2006, which makes difficult to predict the track of Wukong. To investigate the performance of the EnKF with Weather Research and Forecasting Model (WRF) on the prediction of this irregular typhoon, 6- and 12-hour cycles were used to assimilate sounding observations from 17 to 20 August 2006. Overall, the EnKF reults in low root mean square error and typhoon track error in the analysis. More detailed characteristics of performance of the EnKF will be presented in the conference.

Keywords: Ensemble Kalman Filter, ensemble forecasts, typhoon forecasts

Forecast study of the cause of the cold December 2005 in Japan

Morio INABA[1] and Kunihiko KODERA[2,1]

[1] Climate Research Department Meteorological Research Institute, Japan

[2] The Solar-Terrestrial Environment Laboratory, Nagoya University, Japan

Japan experienced unusually heavy snow fall and low temperature during December 2005 due to the cold air advected from Siberia. Owing to this strong and sustained cold surge, a continuous and record-breaking snowfall occurred along the coast of the Sea of Japan. To determine the cause and also to examine the ability of the numerical forecasts of such a unusual climate, ensemble one-month forecasts of December 2005 were conducted by changing the lower boundary conditions such as the sea surface temperature (SST) and the sea ice coverage (SIC). Forecasts were initiated everyday between 1 November and 1 December to investigate the dependency on the initial atmospheric conditions. Little impact of the SST and the SIC are found on the forecast of the cold December in Japan. Instead, high sensitivity on the atmospheric initial condition is found. Forecast started before 15 November 2005 usually failed, but that initiated after 17 November successfully predicted cold December.

From the difference between the members forecasted cold and warm Decembers, we could identify the processes producing cold December 2005. A blocking develops over North Atlantic in mid-November 2005. When it decays Rossby waves are emitted and the waves propagate along the subpolar jet across Siberia, which induce a cold surge over Japan. Also Rossby waves propagating over the Indian sector along the subtropical jet, give rise to intense convections over the Bay of Bengal and the South China Sea, which also lead to a deepening of the trough over Japan. Unusual climate condition in December could be due to the simultaneous occurrence of these two processes.

Comparison of medium-range ensemble forecast skill using the TIGGE database

Mio MATSUEDA[1,2](mimatsue@mri-jma.go.jp)
1: Advanced Earth Science and Technology Organization, Tsukuba, Japan
2: Meteorological Research Institute, Tsukuba, Japan

More than 2 years have passed since the THORPEX Interactive Grand Global Ensemble (TIGGE) portals came into operation started in October of 2006. In this study, forecast performance of medium-range ensemble forecasts: BoM, CMA, CMC, ECMWF, CPTEC, ECMWF, JMA, KMA, NCEP, and UKMO, were investigated for 500hPa height over the Northern Hemisphere (20-90N) from December 2006 to May 2009.

In addition, Multi-Center Grand Ensemble (MCGE) was constructed by combining five operational medium-range ensemble forecasts: CMC, ECMWF, JMA, NCEP, and UKMO with equal weights and no bias correction. The ECMWF has the best forecast performance in the world. The CMC, JMA, NCEP, and UKMO ensembles have a superior forecast skill in all available medium-range ensemble forecasts. The forecast performance of the MCGEs relative to the ECMWF ensemble was investigated using the seasonal Root Mean Square Error (RMSE) and the seasonal Ranked Probability Score (RPS) for 500hPa height over the Northern Hemisphere (20-90N) from December 2006 to February 2008.

Weekly Forecast Experiments of NICAM; using the Global Gaussian Analysis Data for Vertical Levels of Eta of the JMA

Kazuhiro Mori and Hiroshi L. Tanaka

Centar for Computational Science, University of Tsukuba,
Tsukuba Japan(Last Author)
s0921052@u.tsukuba.ac.jp

Abstract

A new type of ultra-high resolution atmospheric global circulation model is developed by the Center for Climates System Research, University of Tokyo and Frontier Research Center for Global Change/Japan Agency for marine-Earth Science and Technology. The new model is designed to perform " cloud resolving simulations " by directly calculating deep convection and meso-scale circulations; which play a key role not only in the tropical circulations but also in the global circulations of the atmosphere. Since deep convection cores are only a few kms in its horizontal length, they have not directly been resolved by existing atmospheric general circulation models (AGCMs). In order to drastically enhance horizontal resolution, a new framework of the global atmospheric model is required; they adopted nonhydrostatic governing equations and icosahedral grids to the new model, and call it Nonhydrostatic ICosahedral Atmospheric Model (NICAM).

In this study, we implemented the use of the global gaussian analysis data for vertical levels of eta (made by JMA) as the initial data of NICAM, and investigated the results of the forecast skill for NICAM. The results show that the annual mean of the deterministic predictability of NICAM is 5.75 days, whereas the annual mean of the JMA-GSM is over 8.00 days.

The results show the present forecasting skill of NICAM, where the physical process are still under development. However, it is proposed that the forecast skills for NICAM will achieve the same level as the JMA-GSM if the dataset suited best for NICAM is found.

Key Words: NICAM, The global gaussian analysis data for vertical levels of ita, predictability

Applying a Local Ensemble Transform Kalman Filter to the Nonhydrostatic Icosahedral Atmospheric Model (NICAM)

Keiichi KONDO [1] and Hiroshi L. TANAKA[2]

1: Graduate School of Life and Environmental Sciences, University of Tsukuba, Japan

2: Center for Computational Sciences, University of Tsukuba, Japan

tanaka@ccs.tsukuba.ac.jp

Abstract

A new type of ultra-high resolution atmospheric general circulation model is developed by the Center for Climate System Research, University of Tokyo and Frontier Research Center for Global Change/Japan Agency for Marine-Earth Science and Technology. The new model is designed to perform cloud-resolving simulations by directly calculating deep convection and meso-scale circulation, which plays a key role not only in the tropical circulations but also in the general circulation of the atmosphere. The model is called the Nonhydrostatic Icosahedral Atmospheric Model (NICAM).

In this study, we apply a Local Ensemble Transform Kalman Filter (LETKF) to the NICAM (NICAM-LETKF) because an assimilation system of the NICAM has not been constructed and the optimum initial condition for the NICAM does not exist. We investigate the NICAM-LETKF performance by tuning the localization scale and changing the observational elements under the perfect model assumption.

According to the results, the NICAM-LETKF works stably even if the ensemble size is 20, and the analysis RMSEs are smaller than the observational errors. If the horizontal localization scale is 500 km and the vertical localization scale is 3.0 grid points in the tropics and 4.0 grid points in the Northern and Southern Hemisphere, the NICAM-LETKF shows the best performance. The ensemble spread corresponds to the analysis RMSE. Moreover, the performance is comparable for the cases with and without assimilating water vapor.

It is concluded from the results that the NICAM-LETKF works appropriately under the perfect model configuration.

Keywords: Data assimilation, Ensemble Kalman Filter, NICAM

INTERCOMPARISON OF ENSEMBLE PREDICTION SYSTEMS IN THE WWRP B08RDP PROJECT

Masaru KUNII, Kazuo SAITO, Masahiro HARA and Hiromu SEKO
Meterological Research Institute, Tsukuba, Japan
mkunii@mri-jma.go.jp

Abstract

WWRP Beijing 2008 FDP/RDP is a WWRP (World Weather Research Program) 's short range weather forecasting research project which is conducted corresponding to the Beijing Olympic Games of August 2008. The project is divided into 2 components. One is the FDP component, which is the forecast demonstration for FT=0-6 hours based on nowcasting. Another is the RDP component, which is the research and development on the mesoscale ensemble prediction for FT=6-36 hours. Including MRI/JMA, six organizations (MRI/JMA (Japan), NCEP (USA), MSC (Canada), ZAMG&Meteo-Fr. (Austria and France), NMC (China), CAMS(China)) participated in the RDP component.

Figure 1 shows threat scores for 6 hour precipitation and surface (2m) temperature of the control run. MRI/JMA is superior to others in forecasts of weak to moderate rains and temperature, which results from the use of the 4-dimensional mesoscale data assimilation system over Beijin area.

Figure 2 shows Brier scores and ROC curves for 6 hour precipitation of ensemble prediction. Despite the small number of ensemble members (11) MRI/JMA's system showed the second best Brier score after MSC (20 members) for weak to moderate rains, and ensemble mean of temperature and humidity was best among the participants. In the area of ROC, detection rate of precipitation of MRI system was insufficient, which suggests the importance of number of EPS members and physical perturbations.

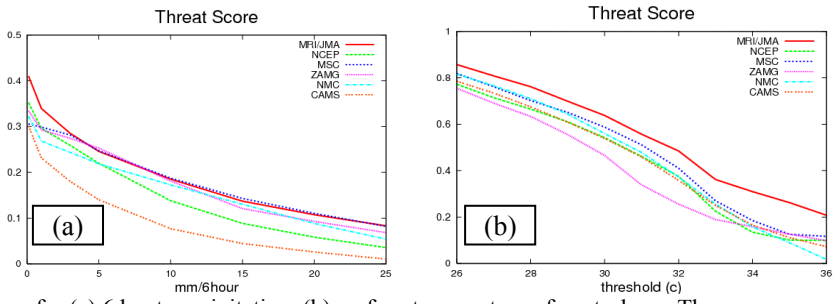

Fig.1 Treat scores for (a) 6 hout precipitation, (b) surface temperature of control run. The scores are averaged from 25 July to 23 August.

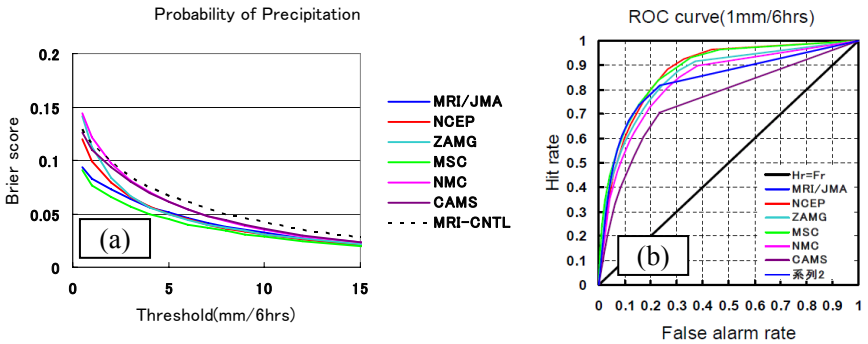

Fig.2 (a) Brier scores (b) ROC curve for all participants. The scores are averaged from 25 July to 23 August.

Keywords: WWRP, ensemble prediction, verification

An Evaluation of High-Impact Weathers over Korea Simulated by the Two Non-Hydrostatic Regional Models

Eun-Chul Chang[1], Kyo-Sun Sunny Lim[1], Yoo-Bin Yhang[1], Jung-Eun Kim[1], Song-You Hong[1], Jong-Il Han[2], and Hann-Ming Henry Juang[2]

[1]Department of Atmospehric Sciences and Global Environment Laboratory, Yonsei University, Seoul, Korea

[2]Environmental Modeling Center/NCEP/NOAA, Maryland, USA

(ecchang@yonsei.ac.kr)

Abstract

Most regional models employ the non-hydrostatic dynamics as a dynamical core. Although the non-hydrostatic forcing is assumed to become important at higher resolution when dynamical and thermodynamical forcing are strong, much of previous non-hydrostatic works have focused on dry-dynamics, for example, mountain-induced waves. It is however recognized that much uncertainty exists in dealing with the physics forcing interacted with the dynamical forcing when the non-hydrostatic assumption is introduced. This study attempts to clarify the advantages of non-hydrostatic dynamical forcing in simulating high-impact weathers that are forced by strong diabatic forcing. Simulated morphology of high-impact weathers and associated precipitation are investigated. The NCEP Regional Spectral Model (RSM) and NCAR Weather Research and Forecasting (WRF) are utilized. Results from the two models with hydrostatic and non-hydrostatic options for a heavy snowfall and rainfall over Korea are compared and evaluated over available observations at various horizontal resolutions from 50 km to 1 km are selected.

Keywords: nonhydrostatic, dynamical core, RSM, WRF, high-impact weather, East Asia

Questioning the Reliability of Sensitivity Experiments in Determining Urban Effects on Precipitation Patterns

Key Words:
Numerical model, Precipitation, Chaos, Decisiveness, Ensemble experiment

Hiroyuki Kusaka, Keiko Nawata, Fujio Kimura, Yukako Miya, and Yuko Akimoto

Abstract

Positive impacts of urbanization on convective rainfall are considered to be seen in the Tokyo Metropolitan area when comparing control runs (with urban areas) to experimental runs (without urban areas). The present study discusses whether the standard sensitivity experiment is reliable in determining urban effects on a realistic convective rainfall event, analyzing several cases in the Tokyo Metropolitan area. Similar to previous studies, we produced results showing the positive impact of urbanization. However, negative or neutral impacts have also been found when the experimental design had been marginally changed by adopting a different physics scheme, spatial resolution or domain size. In addition, the ensemble average of the urban impact showed that the rainfall in the urban area was found to be inhomogeneous. Furthermore, the enhancement of rainfall was unrelated to the location of the urban areas, with positive and negative impacts found in the countryside far from metropolitan area. Our results indicated that the standard sensitivity experiment over the urban area surrounded by complex terrain is not reliable due to the weak urban forcing and strong Chaos influence in rainfall simulation.

SENSITIVITY OF THE WRF MICROPHYSICS TO THE SNOWFALL SIMULATION IN THE COASTAL AREA OF JAPAN SEA

Manami OHYA and Hiroyuki KUSAKA
Center for Computational Science, University of Tsukuba,
Tsukuba, Japan (Last Author)
s0921025@u.tsukuba.ac.jp

Abstract

Recently, the Weather Research and Forecasting model (WRF) is used all over the world for weather forecasting and academic researches. The WRF Version3.1 was released in April 2009. The WRFV3.1 adopts twelve kinds of bulk microphysics models. Some of them, WSM and WDM Microphysics were developed only for the WRF.

There are two patterns for heavy snowfall case in coastal area of Japan Sea, Yamayuki type and Satoyuki type. In Yamayuki type, heavy snowfall is brought in mountain area of Japan Sea side. In Satoyuki type, it is brought in the coastal plain area of Japan Sea. We first simulated these 2 types of snowfall case and estimated precipitation with using 3 microphysical models in WRF. We use WSM5, WSM6 and Morrison for this research. WSM5 has 6 prediction parameters; mixing ratio of water vapor, cloud water, rain, cloud ice and snow. WSM6 is added mixing ratio of graupel. Morrison predicts number concentration of water substance with mixing ratio. We pick up the event on December 22nd, 2005 for Yamayuki case, and January 23th, 2004 for Satoyuki case.

Precipitation distribution was well reproduced in both cases with 3 models, but in Yamayuki case, 3 models estimated larger precipitation impact than observation. On the other hand, models tend to estimate smaller in Satoyuki case. Precipitation of WSM6 was large in mountain slope of Japan Sea side where graupel is produced a lot. Prediction of number concentration reduces large estimation of precipitation in large mixing ratio area, so Morrison expressed this effect.

Compared WSM5 to WSM6 in conversion process of water substances, there was large difference in Yamayuki case. WSM5 expressed diffusional growth from water vapor to snow in mountain slope of Japan Sea side. However in WSM6, it expressed diffusional growth and riming from water vapor and supercooled cloud water to snow and graupel. WSM5 carried more water substances to inland mountain region than WSM6. Because, WSM5 wasn't express graupel, and precipitation was less then WSM6 in mountain slope. In Satoyuki case, there were little graupel in WSM6, so differences of conversion process ware quite small between WSM5 and WSM6. Precipitation of WSM6 was large in mountain slope of Japan Sea side where graupel is produced a lot in both cases.

We will also introduce the preliminary results of the WDM simulations and other snowfall events at the conference.

Acknowledgments: This work was supported by the Global Environment Research Fund (S-5-3) of the Ministry of the Environment.

Keywords: Microphysical parameterization, Microphysical model, WRF model, snowfall simulation, Japan Sea

INTERDECADAL SHIFT IN THE ASSOCIATION BETWEEN ENSO AND NORTHWARD PROPAGATING INTRASEASONAL OSCILLATION IN THE EASM

Kyung-Sook YUN, Kyong-Hwan SEO, and Kyung-Ja HA*
Division of Earth Environmental System, Pusan National University, Busan, Korea

*Corresponding Author: kjha@pusan.ac.kr

Abstract

We investigate the interdecadal change in the relationship between El Nino/Southern Oscillation (ENSO) and the northward propagating intraseasonal oscillation (NPISO) in the East Asian summer monsoon (EASM). To find the long-term change in the relationship, the outgoing long-wave radiation data are obtained from ERA-40 for 44 year (1958 to 2001 year). Its interdecadal variability is significantly shown in between two epochs of 1958-1979 and 1980-2001 years. Since the late 1970s, the preceding winter ENSO influences the summertime NPISO activity. Because of an enhanced Walker-Hadley circulation, the Indian Ocean sea surface temperature (IOSST) warming is significantly maintained until the concurrent summer season, which in turn promotes a strong suppressed convection anomaly over the Philippine Sea. Consequently, ENSO is intimately linked to the suppressed convection anomalies over the Philippine Sea and in turn western North Pacific subtropical high (WNPSH). The mechanism was suggested as follows: ENSO-related IOSST warming – the suppressed convection over the WNP – WNPSH – the reinforced NPISO activity. However, before the late 1970s, a weak positive correlation is found during earlier summer (i.e., May to June). The relationship between NPISO and ENSO is immediately shown by the springtime IOSST warming, not through the summer WNPSH.

Keywords: East Asian summer monsoon, northward propagating ISO, ENSO

THE SHIFT IN THE EARLY 1980S OF SPRING PRECIPITATION IN KOREA

Ji-Sun LEE, Ki-Seon CHOI, Do-Woo KIM, Su-Bin OH and Hi-Ryong BYUN
Pukyong National University, Busan, South Korea
hrbyun@pknu.ac.kr

Abstract

This study investigate a regime shift in the spring precipitation in Korea around 1980-1981 during the period 1954-2008, which is revealed by the Change-Point Analysis. The spring precipitation in the post-1980 period showed a distinct decrease compared to the pre-1980 period. This phenomenon was particularly dominant in the southwestern regions of the Sobaek Mountain Range in Korea. The same phenomenon was also noticed in the mid-latitude East Asia including China, except south China, and Japan.

One of the major causes for this decrease in spring precipitation was found to be the increased snow depth in the mid-latitude East Asian continent. As a result, cold anticyclone was strengthened over East Asian continent while subtropical anticyclone was weakened relatively in the western North Pacific. It forced the continuation of the typical winter pressure pattern of 'high-West and low-East' in East Asia from winter into spring.

The strengthened northerlies from this zonal pressure pattern played a significant role in restricting the northern movement of the subtropical anticyclone from traveling north, preventing the inflow of warm and humid air into the mid-latitude East Asian region. This in turn reduces the spring precipitation in Korea.

Keywords: Change-point analysis, Interdecadal variation, Regime shift,
Spring precipitation in Korea, Snow

20－TH CENTURY WINTER TEMPERATURES NEAR JAPAN: ITS RELATIONSHIP TO THE DECADAL OSCILLATION OF THE ALEUTIAN LOW AND SIBERIAN HIGH

Minoru TANAKA
Meteorological Research Institute, Tsukuba, Japan
Mtanaka@mri-jma.go.jp

Abstract

Winter temperatures near Japan are dominated by the East Asian winter monsoon which is modulated by the change in intensity of the Siberian high and Aleutian low. The data over the Pacific Ocean are found to be reliable after 1914. Therefore, a 93-year period from 1914 to 2006 is analyzed over the East Asia and Pacific Ocean domain. The monthly data used in this paper are Global Historical Data Network (GHCN), World Weather Records, World Monthly Surface Station Climatology, Hadley SST2, Hadley SLP2, NCAR SLP grids. These data are station and 5 degree latitude-longitude grid data of temperature, SST and SLP.

January-February temperatures near Japan are found to be dominated by decadal-scale change in intensity of the Aleutian low and Siberian high. Corresponding SST variations over the Pacific Ocean are found to lag SLP change by 1 to 3years. These shifts in the temperature, SST and SLP regimes are abrupt with shifts around 1925-26, 1948-49, 1977, and 1987-90. 1925, 1948, and 1977 shifts are very similar to the well known regimes shifts of the Pacific Decadal Oscillation (PDO). An example for Miyako shows cold temperature regimes from 1884-1893, 1925-1945, and again from 1977-1986, and warm temperature regimes from 1896-1923, 1948-1974, and 1987 to present. The decadal-scale SLP patterns show unique statistically significant change in the SLP over the Aleutian low region for each regime shift. The Siberian high tends to change in opposite direction. These decadal-scale relationships to change in intensity of the Aleutian low were not observed in December.

The impacts of these regime shifts extend beyond Japan into adjacent Korea in 1948 shift, and Korea, China and adjacent Siberia in 1987 shift. During these regime shift, statistically significant decadal temperatures rise were observed in Japan and above regions.

Keywords: meteorology, winter monsoon, temperature in Japan, PDO

SHIFT OF PEAK IN SUMMER MONSOON RAINFALL OVER KOREA AND ITS ASSOCIATION WITH ENSO

Sun-Seon LEE[1], P. N. VINAYACHANDRAN[2], Kyung-Ja HA[1]*, and Jong-Ghap JHUN[3]

[1] Division of Earth Environmental System, Pusan National University, Busan, Korea
[2] Centre for Atmospheric and Oceanic Sciences, Indian Institute of Science, Bangalore & APEC Climate Center, Busan, Korea
[3] School of Earth and Environmental Sciences, Seoul National University, Seoul, Korea

*Corresponding Author : kjha@pusan.ac.kr

Abstract

The annual cycle of rainfall over the Korean Peninsula is marked by two peaks, one during July and the other during August. Since the mid 1970s, the maximum rainfall over the Korean Peninsula has shifted from July to August. This shift in rainfall peak was caused by a significant increase of August rainfall after 1970s.

The basic reason for this shift has been traced to a change in teleconnection between El Niño and August rainfall. The relationship between August rainfall over Korea and El Niño changed from 1954-1975 (PI) to 1976-2002 (PII). The interannual variability of August rainfall was significantly associated with SST variation over the eastern equatorial Pacific during PI, but this relationship is absent during the period PII. The strong (weak) low-level southerly and westerly winds around the East China Sea related to August rainfall closely corresponded to strong El Niño (La Niña) during the PI. During the PII period, however, southerly-westerly wind anomalies around East China Sea were responsible for the high August rainfall over the East Asian region, even though La Niña SST conditions were in effect over the eastern Pacific. These results suggest that the manner in which ENSO affects the Korean rainfall has changed since 1970s.

Keywords: shifting peak, EASM, August rainfall, ENSO

VARIATION OF CARBONACEOUS AEROSOLS IN POLLUTED AIR MASS TRANSPORTED FROM EAST ASIA

Kojiro SHIMADA[1], Akirori TAKAMI[2], Shungo KATO[3], Yoshizumi KAJII[3], and, Shiro HATAKEYAMA[1*]
[1]Tokyo Univ. Agric. Techlnol., Fuchu, Tokyo, Japan, [2]Nat'l Inst. Environ. Studies, Tsukuba, Ibaraki, Japan, [3]Tokyo Metr. Univ., Hachioji, Tokyo, Japan
* Email:hatashir@cc.tuat.ac.jp

Abstract

Rapid economic development in East Asia has brought about increased energy consumption along with a high rate of emission of particulate and gaseous pollutants. In this study, long-range transport of carbonaceous aerosols and gaseous species from East Asian countries to the East China Sea has been analyzed. Particularly, seasonal variation and source type of carbonaceous aerosols were evaluated. Mass concentrations of EC, OC, $PM_{2.5}$ and mixing ratio of carbon monoxide (CO) and ozone (O_3) were measured at the Cape Hedo Atmosphere and Aerosol Monitoring Station (CHAAMS) in Okinawa, Japan from spring to winter, 2004-2008.

The concentrations of EC, OC, $PM_{2.5}$, CO, and O_3 were simultaneously high in spring but low in summer. This difference was mainly caused by air mass history in each season. Atmospheric pollutants are often transported to CHAAMS by migratory high or low pressure systems from Asian Continent in spring, whereas oceanic clean air masses are transported from the Pacific in summer.

Identification of source type of carbonaceous aerosol was examined by evaluating OC/EC ratio, and correlation analyses of EC and OC with CO. As usual, EC to OC ratios have been used to distinguish between coal combustion (OC/EC ~2.7) and biomass combustion (OC/EC ~12.3). At Cape Hedo the OC/EC ratio was low (median: 4.1-6.7) in spring and in winter but high (median: 6.6-13) in summer (Fig. 1). It was interpreted that EC and OC of anthropogenic origin were not transported to CHAAMS from the Pacific in summer. Mono-carboxylic acid which was used as a tracer of marine biogenic species was reported to be detected in TSP samples in CHAAMS, which also supports above contention.

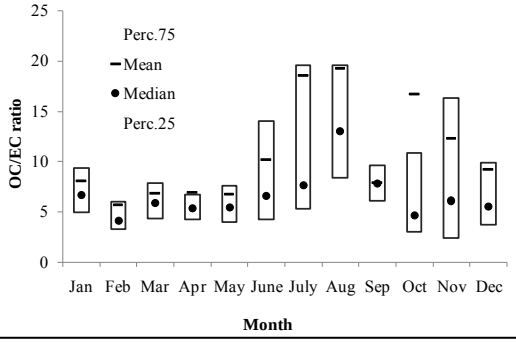

Fig.1 Monthly mean and median of OC/EC ratio.

In winter, the air mass with OC/EC<3 passed over a mega city in China judging from back trajectory analyses. The contribution of coal combustion was expected. On the other hand, the air mass with OC/EC>15 mainly passed over Korea or Japan or North China. The air mass from Japan or Korea was suggested to contain much VOCs and organic aerosols. Thus, increased secondary organic aerosol formation from gaseous organic substances could result in the high OC/EC ratio. Correlation with CO will also be discussed.

Keywords: CHAAMS, Seasonal variation, Source type of carbonaceous aerosols

WEEKLY PERIODICITIES OF METEOROLOGICAL VARIABLES AND THEIR POSSIBLE RELATION TO AEROSOLS IN KOREA

Min-Hyeok Choi, Byung-Gon Kim*
Department of Atmospheric Environmental Sciences Kangnung-Wonju National University, Gangnung, Korea
*bgk@nukw.ac.kr

Abstract

Weekly periodicities of meteorological variables such as temperature (T_{max}, T_{min}, T_{mean}), diurnal temperature range (DTR), cloud amount, insolation, precipitation, precipitation frequency (total rain, rain<5mm), and relative humidity (RH), as well as particle mass concentrations (PM_{10}) have been examined to understand anthropogenic influence on the regional climate. We used surface measurements data of 10 stations operated by Korea Meteorological Administration along with air pollution monitoring stations. The meteorological variables and their anomalies for each weekday have been analyzed as the departure from its weekly mean value. Here, we employed a similar method to that of Baumer and Vogel (2007). The negative anomaly of T_{min} in the first-half of the week and the positive anomaly of T_{min} in the second half were shown as significant different for 8 of 10 stations, except for Gwangju and Gangnung. Accordingly, DTR averaged over all analyzed stations in Korea also showed a clear dependency on the weekday, but with the reverse pattern against T_{min}. The weekly cycle of cloud amount was reverse to DTR and insolation (direct and diffuse radiation) such as more cloudiness (less radiation) from Wednesday to Saturday and less cloudiness (more radiation) from Monday to Tuesday. Meanwhile, the PM_{10} anomaly was positive for Tuesday through Thursday, and clearly negative at Sunday only. A remarkable decrease in PM_{10} anomaly on Sunday is thought to due to human-induced influence. It is interesting to see that weekly periodicities in meteorological variables were clearly significant especially in autumn, with their amplitudes almost 2~3 times greater than those for the annual mean. Enhancement in weekly variations and periodicities of meteorological variables in autumn is quite notable. This is, the anthropogenic influence is clearly discernible in autumn probably because the natural climate variability in autumn is relatively less prominent in comparison with the other season.

Keywords: weekly periodicities, meteorological variables, aerosols, cloud.

LIDAR NETWORK FOR OBSERVING TROPOSPHERIC AEROSOLS IN EAST ASIA

Nobuo SUGIMOTO[1], Ichiro MATSUI[1], Atsushi SHIMIZU[1], Tomoaki NISHIZAWA[1], Yukari HARA[1], Itsushi UNO[2], Zifa WANG[3], Weipeng WANG[4], Chenbo XIE[5], Jun ZHOU[5], Soonchang Yoon[6], and Dulam JUGDER[7]
1 National Institute for Environmental Studies, Tsukuba, Japan
nsugimot@nies.go.jp
2 Kyushu University, Fukuoka, Japan
3 Institute of Atmospheric Physics, Beijing, China
4 Sino-Japan Friendship Center for Environmental Protection, Beijing, China
5 Anhui Institute of Optics and Fine Mechanics, Hefei, China
6 Seoul National University, Seoul, Korea
7 Institute of Meteorology and Hydrology, Ulaanbaatar, Mongolia

Abstract

A network of two-wavelength (1064nm, 532nm) polarization (532nm) lidars is operated continuously in cooperation with various research institutes and universities in the east Asian region. Currently, 22 lidars are operated in Japan, China, Korea, Mongolia, and Thailand. The primary purpose of the network is to study distributions, characteristics, and transport of Asian dust and anthropogenic aerosols. Some of the lidar stations are operated in Asian dust monitoring project with Ministry of the Environment of Japan (JME), and some of the stations co-located with skyradiometers are operated in GEOSS/SKYNET. Other stations are operated in the research programs on Asian dust and regional air pollution. The data from the stations, where connected online, are transferred to the National Institute for Environmental Studies (NIES) and processed in realtime, and the attenuated backscattering coefficient at 532nm and 1064nm, the total depolarization ratio at 532nm, and the estimated extinction coefficient at 532nm for Asian dust and spherical aerosols are derived as the data product. The extinction coefficient data for Asian dust are provided to JME in realtime for Asian dust information www page to general public. In the study of Asian dust, a regional 4DVAR assimilation system using the lidar network data was developed by Kyushu University. Studies on data assimilation of Asian dust using the ensemble Kalman filter method have been carried out by Institute of Atmospheric Physics of China and Meteorological Research Institute of Japan. The use of the lidar network data in assimilation of aerosol climate model is also being studied. Recently, a global aerosol lidar observation network named GALION (GAW Aerosol Lidar Observation Network), which combines existing regional lidar networks, was formed. Our lidar network will play a role as an East Asian component of GALION.

Keywords: aerosol, lidar, observation network, Asian dust, data assimilation

ATMOSPHERIC AEROSOL CHARACTERIZATION IN EAST ASIA

Akinori Takami,
NIES, Tsukuba, Japan
takamia@nies.go.jpl

Abstract

Due to the rapid economic growth and energy consumption, emission in East Asia has increased recently. In order to understand the long term trend of aerosol mass and the variation of its chemical compositions in this region, we have measured the aerosol chemical composition using aerosol mass spectrometer in both Fukue, Nagasaki and Cape Hedo, Okinawa since 2003. We analyze these data and the followings are discussed.

1. Sulfate and organic aerosol are major species and they are mixed during transport. At Fukue, organics are major while sulfate are major at Cape Hedo. These differences are influenced by the air mass origin and transport time.
2. In spring time transport are determined by the synoptic scale weather system. When the low pressure system is passed in the East China Sea area and the high pressure system is moved to the Chinese costal area, air mass is transported from the Shanghai and Shangdon area to Okinawa, which leads to the high sulfate event.
3. Nitrate species are found in the coarse particles in contrast to sulfate. During the transport, ammonium nitrate is evaporated and nitrate is deposited on the coarse particle. Due to the difference of the particle size, the transported abundances of nitrate are different from sulfate species.
4. Organics are well oxidized during transport. For the air mass from the Chinese continent, black carbon is covered (internally mixed) by the sulfate and organics, which may influence the optical properties of the black carbon.

Keywords: CHAAMS, Fukue, Q-AMS

INCREASING TREND ON VOLUME CONCENTRATION OF LOWER TROPOSOHERIC SUBMICRON AEROSOL PARTICLES AT MOUNT TATEYAMA, JAPAN

K. OSADA[1*], T. OHARA[2], I. UNO[3], M. KIDO[4], and H.IIDA[5]
1: Nagoya University, Nagoya, Japan
2: NIES, Tsukuba, Japan
3: RIAM, Kyusyu University, Fukuoka, Japan
4: Toyama Prefectural Environmental Science Research Center, Imizu, Japan
5: Tateyama Caldera SABO Museum, Tateyama, Japan
*E-mail: kosada@nagoya-u.jp

Abstract

Number-size distribution (0.3−1.0 μm) of atmospheric aerosol particles were measured by an OPC (RION KC-01D) at Murododaira (36.6°N, 137.6°E, 2450 m a.s.l.) on the western flank of Mount Tateyama in central Japan from January 1999 to February 2009. Nighttime data from 2400 to 0500 hours (local time) were used to analyze free-tropospheric aerosol condition. 90 monthly data (> 50% coverage of daily night time data in a month) were obtained for this period (122 months). Monthly volume concentrations of submicron aerosols were high in spring to early summer and low in winter. Increasing trends were found in the submicron volume concentrations for December−January and March−April. Monthly SO_4^{2-} concentrations at Mt. Tateyama were simulated from results of regional aerosol modeling with SO_2 emission inventory up to 2005. The results showed seasonal variation and winter−spring increasing trends similar to those of observed aerosol concentration. According to the model analyses, the contribution of Chinese SO_4^{2-} concentration was high in winter–spring (ca. 80% of total SO_4^{2-} at Mt. Tateyama). This accords with the increasing trend observed in winter–spring, suggesting that increasing SO_2 emission in China engender enhancement of submicron aerosols over Japan, especially during winter–spring.

Keywords: Submicron aerosol particles, free troposphere, Increasing Trend, Asian dust

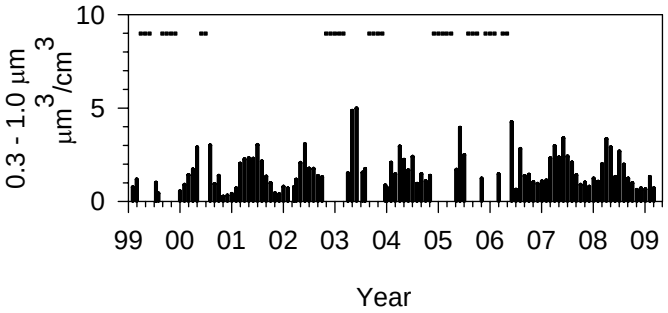

Figure 1 Monthly average of volume concentrations at Mt. Tateyama, Japan. Horizontal bar in the panel indicates months of insufficient data number.

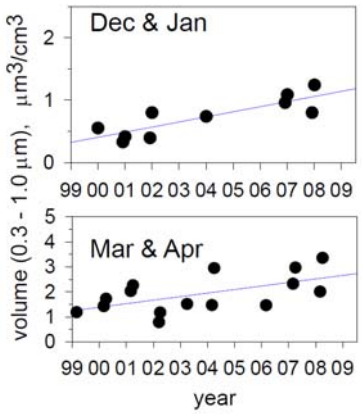

Figure 2 Increasing trends in monthly submicron aerosol volume.

DIURNAL CHANGES OF WIND AND AEROSOL CONCENTRATION AT MT. FUJI, JAPAN

Hiroshi Takahashi[1]*, Yasuhito Igarashi[1], Hiroshi Kobayashi[2], and Hiroaki Naoe[1]
[1] Meteorological Research Institute, Tsukuba, Japan
[2] Yamanashi University, Kofu, Japan
*Email : htakahas@mri-jma.go.jp

Abstract

It is present an urgent target in atmospheric sciences to improve our understanding on the atmospheric aerosol processes in both the free troposphere and atmospheric boundary layer as well as on the human-induced air quality change over the Asia and western North Pacific regions. Mt. Fuji (elevation 3776 m, 35°22′N, 138°44′E), the highest peak in Japan, is located downwind of the Asian industrial region. It is expected that the utilization of Mt. Fuji as an 'observation tower' for atmospheric chemistry could offer vertical information on aerosols and precursor species and their changes along with the long-range transport and mixing of air masses. It is important to evaluate that the data acquired there have sufficient spatial representability as of remote one. However, features of the local atmosphere enveloping the mountain, which could have a large impact on the data quality, have not been well investigated so far.

The objective of this study is to explore the system of the local wind circulations and its impact on the change of observing air mass using meteorological and aerosol observation, and to evaluate the periods when the free tropospheric air dominates on the mountain. We carried out an intensive observation at the mountain during the period of July – August 2007, and assessed the diurnal changes of the wind and aerosol concentration.

While the wind data at two slope sites (elevations of 3220 m and 1300 m) showed diurnal changes in the direction composed of daytime upslope and nocturnal downslope winds, the wind data at the summit well correlated to wind profiler (WPR) data near the mountain which showed almost no diurnal changes. Since the WPR system is capable of retrieving the upper wind in the free troposphere with high accuracy, the wind at the summit could be covered with free tropospheric air to a certain extent. However, the diurnal change of aerosol number concentration at the summit fluctuated with the magnitude of 10^0 – 10^3 times between day and night on some occasions in summer. The diurnal cycle of upslope and downslope winds and the atmospheric stabilities should mainly control the vertical transport of aerosols along the slope. An evident decrease of temperature lapse rate associated with stationary front approaching northern Japan in 8 August coincides with an increase of the amplitude of the diurnal change in aerosols concentration. The fact indicates that the enhanced vertical transport of aerosols was associated with the reductions in atmospheric vertical stability.

Keywords: mountain, wind, aerosol, free troposphere, boundary layer

CHEMICAL COMPOSITION OF FOG WATER AT MT. TATEYAMA

Koichi WATANABE[1*] and Hideharu HONOKI[2]
[1] Toyama Prefectural University, Kurokawa, Imizu, Toyama, 939-0398, Japan.
[2] Toyama Science Museum, Nishinakano-machi, Toyama 939-8084, Japan.
*E-mail: nabe@pu-toyama.ac.jp

Abstract

To investigate atmospheric environment on the mountainous sites, Hokuriku district, along the Japan Sea coast in central Japan, we have measured trace gases, aerosol particles and fog and rain water chemistry at Mt. Tateyama located near the cost of Japan Sea. Fog water was sampled at at Murododaira (2450m a.s.l.), the western slope of Mt. Tateyama, during the autumn. Fog water was collected by a passive sampler and was usually recovered every 3- 5 days. The pH and major ions were measured. In addition to the regular sampling, intensive fog water sampling was made. We collected fog water every 2-4 hours as a part of the intensive sampling. The concentrations of major ions and peroxides were measured during the intensive observation.

The weighted mean concentrations of major ions in fog water obtained by the regular sampling in the autumn seasons from 2004 to 2007 are shown in Fig. 1. The mean pH of fog water in 2004, 2005, 2006, and 2007 was 4.5, 4.0, 5.0, and 4.6, respectively. Strong acidic fogs that contained high concentrations of SO_4^{2-} were frequently observed, especially in 2005. The air mass at Mt. Tateyama was derived primarily from the polluted regions of Asia in September and October 2005, and the trans-boundary air pollution might have contributed to fog water acidification at Murododaira. On the other hand, acidic fog might have been produced by pollutants from central and Western Japan in 2004 and 2007, and the ratio of NO_3^-/SO_4^{2-} in fog water was relatively high in 2004 and 2007. Meteorological conditions may significantly influence the chemical characteristics of fog at Mt. Tateyama. High concentrations of Ca^{2+} derived from dust particles were detected in 2006. Background Kosa particles might have been abundant in the free troposphere and neutralized acidic fog in the autumn of 2006. Similar results of chemical characteristics in autumn from 2004 to 2006 were also obtained by the intensive observations in September. Fog water chemistry at Murododaira is significantly affected by chemical substances derived from Asia as well as from Japan.

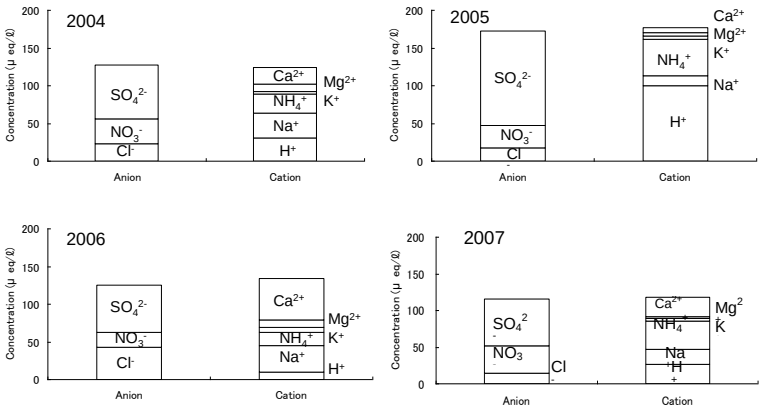

Fig. 1. Weighted mean concentrations of major ions in fog water at Murododaira, Mt. Tateyama obtained by the regular sampling in September and October from 2004 to 2007.

MIXING STATE OF CLOUD INTERSTITIAL PARTICLES AT MOUNT TATEYAMA, JAPAN: RELATIONSHIP WITH METEOROLOGICAL CONDITIONS

Sayako UEDA[1*], Kazuo OSADA[1] and Kikuo OKADA[2]
1: Nagoya University, Nagoya, Japan
2: Meteorological Research Institute, Tsukuba, Japan
*E-mail: ueda.sayako@d.mbox.nagoya-u.ac.jp

Abstract

Number concentrations of atmospheric aerosol particles with 0.1–0.5 μm in diameter were measured by an OPC (RION, KC18), at Tengudaira (36°24'N, 137°34'E, 2300 m a.s.l.), Mt. Tateyama in Japan, during 20-25 June 2007. At the same time, the fraction of less hygroscopic particles with 0.3–0.5μm in diameter (FLH) and soot concentration were measured using the OPC with a humidifier and impactors, and a particle soot photometer (Radiance Research, PSAP), respectively. Cloud interstitial samples of less-hygroscopic particles were collected for water dialysis by TEM analysis. During fog condition, aerosol number concentration decreased about one to two orders. At 22 June, high FLH was observed with high soot volume fraction. In sample B, most of less-hygroscopic particles were found as insoluble after water dialysis. Some of the residual particles showed chain-like shape characterizing as soot. At 21 and 25 June, low FLHs were observed under the fog condition. For samples A and C, most of less hygroscopic particles were partially water soluble after water dialysis. Relationship between the mixing states of interstitial particles and the meteorological conditions will be discussed at conference.

Keywords: atmospheric aerosol particles, electron micrograph, soot.

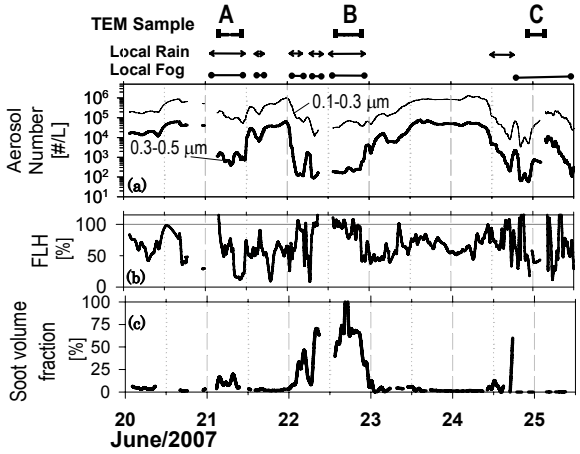

Figure 1 Temporal variation of (a) number concentrations of aerosols, (b) number fraction of less-hygroscopic particles for 0.3–0.5 μm in diameter, (c) ratio of soot volume (< 0.4 μm) per particle volume (0.1–0.5 μm).

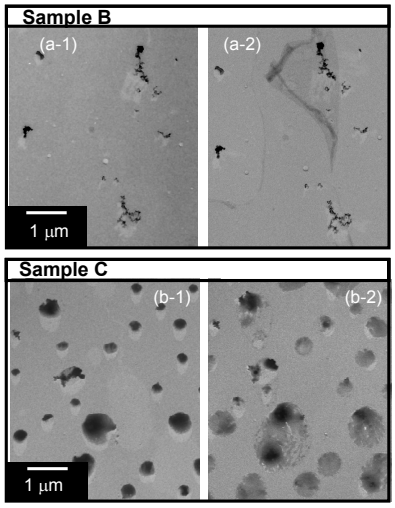

Figure 2 Electron micrograph of cloud interstitial samples B and C. (a-1) and (b-1) show before dialysis with water, and (a-2) and (b-2) show after that at the same place.

THRESHOLD FRICTION VELOCITY FOR SAND PARTICLES AT A GOBI DESERT AND A FALLOW FEILD

Masahide ISHIZUKA[1], Masao MIKAMI[2], Yutaka YAMADA[3] , John LEYS[4] and FanJiang ZENG[5]

[1]Kagawa University, Takamatsu, Japan
ishizuka@ eng.kagawa-u.ac.jp
[2]Meteorological Research Institute, Tsukuba, Japan
mmikami@mri-jma.go.jp
[3]RIKEN, Wako, Japan
yamadayu@riken.jp
[4]New South Wales government, Gunnedah, Australia
john.leys@environment.nsw.gov.au
[5]Chinese Academy of Sciences, Urumqi, R. P. China
fjzeng369@sohu.com

Abstract

The threshold friction velocity u_{*t} for sand particles at a gobi desert in the Taklimakan Desert are calculated to be 0.477 m/s in dry condition (volumetric soil water content θ = 0.002 m^3/m^3) and 0.564 m/s in wet conditions (θ = 0.009 m^3/m^3), respectively (Figure 1). Simultenously, the u_{*t} at a fallow wheat field in Austlaria are culculated to be 0.344 m/s and 0.398 m/s in dry and wet conditions, respectively. To calculate u_{*t}, we proposed a new method that minimizes the error objectively between the Owen's equation (1964) and observation data measured by a sand particle counter (SPC). The results show that 1) u_{*t} in a fallow field is lower than that in a gobi desert, 2) u_{*t} increases when soil moisture increases, 3) a simple relationship exists between saltation flux $q(z)$ at a reference height z and friction velocity u_* and $u_{*t}(\theta)$, and 4) the $q(z)$ is dependent on particle size D.

Keywords: threshold friction velocity, sand particles, mineral dust, gobi, fallow field

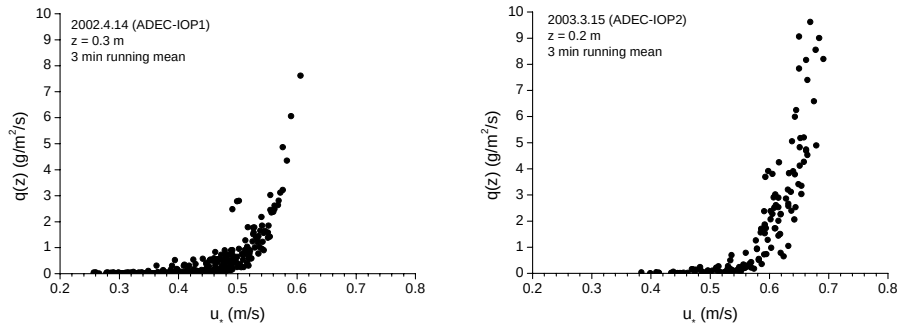

(a) 14 April 2002 (dry) (b) 15 March 2003 (wet)

Figure 1. Relationship between u_* and saltation flux $q(z)$ on 14 April 2002 (dry) and 15 March 2003 (wet) at a gobi desert in the Taklimakan Desert. The $q(z)$ was summed from 38 to 654 μm in diameter. The 3 minutes running mean data of u_* and $q(z)$ were used.

SPATIAL AND TEMPORAL VARIATIONS IN TRACE GASES AND AEROSOLS FROM BIOMASS BURNING IN SOUTHEAST ASIA AS MEASURED FROM SPACE

Yumiko HONDA[1], Sachiko HAYASHIDA[1],Makoto KUJI[1]
and Wataru TAKEUCHI[2]
[1]Nara Women's University, Nara 630-8263, Japan
[2]Institute of Industrial Science, University of Tokyo, Tokyo 153-8505, Japan
[1]yumi920@ics.nara-wu.ac.jp

Abstract

In Southeast Asia, slash-and-burn agriculture has been performed for centuries and is a traditional and eco-friendly farming method. However, recent development of large-scale plantations created using slash-and-burn has caused both deforestation and air pollution. The gases and aerosols generated by biomass burning contain greenhouse gases and their precursors. Carbon monoxide (CO) and aerosols are the main components generated by fire, and are used as an index of biomass burning. We have restricted this analysis to Indochina and the Indonesian islands, which are known to have extensive biomass burning. We examined the relation between CO and aerosols after fires.

Satellite observations allow both spatial and temporal distribution mapping with the same instrument. CO concentration measurements were obtained from the Measurements of Pollution in the Troposphere (MOPITT) data set and aerosol index (AI) measurements were from Ozone Monitoring Instrument (OMI) data. For fire occurrence, we analyzed the data of Takeuchi et al. [1], which were derived from thermal anomaly data from the Moderate Resolution Imaging Spectrometer (MODIS).

The spatial distributions of each data set were similar. Much biomass burning occurred in the mountains of northern Indochina, southern Borneo, and Sumatra in Indonesia, and these areas had high concentrations of CO and high AI values.

The time variation of each data set also similar, providing data on seasonal and latitudinal variation in fire caused by slash-and-burn agriculture just before the rainy season. Variations in CO were generally similar to variations in the AI in most burned areas.

In Northern Indochina, slash-and-burn agriculture is performed from February to April, corresponding to CO and AI increase in March or April. At Angkor in Southern Indochina, slash-and-burn agriculture is performed from January to March, but the AI was not high during this period. In Borneo, slash-and-burn agriculture is performed from September to November; in this area, the correlation between CO and fires was clear, because the background CO variation at low latitudes was small. The OMI AI also showed strong enhancement in Borneo around September and October.

[1] Takeuchi,W , Yasuoka,Y(2005)
Photogrammetry and Remote Sensing,45(5),59-63.

Keywords: biomass burning, Southeast Asia, aerosol, carbon monoxide

ANALYSIS OF METHANE CONCENTRATIONS OBSERVED BY SCIAMACHY CORRESPOND TO RICE PADDY EMISSIONS IN ASIA

Satomi ETO[1], Yuko ARIYAMA[1], Katsuyuki NOGUCHI[1], Sachiko HAYASHIDA[1] and Wataru TAKEUCHI[2]
[1]Nara Women's University, Nara 630-8506, Japan
[2]Institute of Industrial Science, University of Tokyo, Tokyo 153-8505, Japan
etoh@ics.nara-wu.ac.jp

Abstract

Methane (CH_4) is the second most important anthropogenic greenhouse gas after carbon dioxide (CO_2) in terms of radiative forcing. The concentration of CH_4 has doubled since the industrial revolution because of anthropogenic activities. However, sources and sinks of CH_4 remain largely uncertain. It is urgent to clarify the global CH_4 budget. Recently, the SCanning Imaging Absorption spectroMeter for Atmospheric CHartographY (SCIAMACHY) onboard the Environmental Satellite (ENVISAT) has enabled measurement of global CH_4 distribution from space. In this study, we analyzed the relation between CH_4 concentrations and areas of paddy rice, which are among the most important sources of CH_4 in Asia.

We analyzed SCIAMACHY data, including vertical column densities (VCD) of CH_4, which are retrieved using the IMAP-DOAS algorithm of Heidelberg University [1]. To convert the vertical column density into a mixing ratio, we used the CO_2 surface concentration of the NIES Transport Model [2]. We used the distribution data of rice paddies that Takeuchi et al. [3] derived from the spectrum of the MODerate resolution Imaging Spectroradiometer (MODIS).

The CH_4 emission from rice paddies depends largely on the season. When we compared rice paddy distributions and satellite observations, high CH_4 concentrations were observed over India, Bangladesh, Thailand, Vietnam, and China, where rice paddies are common. In India and the Indonesian Peninsula, satellite CH_4 concentrations were maximal in September and October, at the end of the rainy season, and then decreased. In China, high concentrations of CH_4 were observed throughout the year, except in July, and the peak in CH_4 concentrations continued until around December. This may be because of the high rate of double cropping, which ends around November in southern China.

[1] Frankenberg,C et al., J. Geophys. Res, 2006, Vol.111, D07303
[2] Maksyutov,S et al., Journal of the Earth Simulator, Volume 9, March 2008, 3-18
[3] Takeuchi,W et al., Photogrammetry and Remote Sensing, 2005, 43(6), 20-33.

Keywords: methane, rice, paddy, Asia

METHANE INVERSE MODELING USING NIES TRANSPORT MODEL: OPTIMIZATION OF THE SEASONAL FLUX BASED ON OBSERVATION DATA AND A PIROR FLUX

Heon-Sook Kim[1)], Shamil Maksyutov[2)], Tazu Saeki[2)] and Gen Inoue[1)]
[1)]Research Institute for Nature and Human, Kyoto, Japan
[2)]National Insititue for Envionmental Studies, Tsukuba, Japan
heonsook.kim@chikyu.ac.jp

Abstract

The dominant CH_4 fluxes from both natural and anthropogenic processes seem to be identified, but there are still large uncertainties in their individual magnitudes and temporal variabilities on the global and regional scales. In this study, we estimate the seasonal CH_4 flux in global scale through inverse modeling and optimize the monthly flux based on observation data and a prior flux. Our inverse model uses the TransCom 3 (level2) experimental framework, which is desinged to estimate seaonal CO_2 fluxes and seeks the linear combination of fluxes that yeilds modeled concentration fields that best mathch the observation data (Gurney et al., 2004).

Three inverseion are performed in this study: Case 1 uses obsevation data at all sites of GLOBALVIEW- CH_4 and a prior flux of Fung et al. (1991), Case 2 uses the selected observation data corresponding with 70% real data for 1992-1996 and a prior flux of Fung et al. (1991), and Case 3 use the selected observation data corresponding with 70% real data and the revised prior flux from Fung et al. (1991). Case1 and Case2 estimate large CH_4 emission from animals and small CH_4 emission from anthoropegenic sources. However, we have found that the predicted seaonslity of CH_4 concentrations in Case2 is better agreement with the observed seasonality. Case3 estimates resonable seasonal CH_4 flux, yeilding decreased animal flux and increased anthropogenic flux compared with Case1 and Case2. The predicted CH4 concentration in Case3 shows farily good agreement with the observed concentration except for some sites over tropical region.

Keywords: methane, inverse modeling,

IS-OROGRAPHIC-INDUCED PRECIPITATION RELATED TO AEROSOLS IN KOREA

Seung-Hee Eun and Byung-Gon Kim*
[1]Department of Atmoshperic Environmental Sciences, Kangung Wonju National University, Gangnung, Korea
Email : bgk@nukw.ac.kr

Abstract

Aerosols play as cloud condensation nuclei (CCN) and thus have a considerably effecet on cloud properties and the initiation of precipitation. The large concentrations of anthropogenic aerosols decrease the cloud droplet size per given liquid water content also decrease precipitation formation. Specially Givati et al. (2004) show that the suppression occurs mainly in the relatively shallow orographic clouds within the cold air mass of cyclones. This study analyzes long-term annual change of orographic precipitation in Korea with the similar method of analysis Givati et al. (2004), except for considering the synoptic wind direction such as westerly and easterly. We examined a precipitation data for 36 years from 1972 to 2007 obtained from 4 sites (Seoul, Wonju, Daegallyoung, Gangnung; from west to east) of the Korean Meteorological Administration (KMA). Er is defined as the ratio of precipitations between lowland and hill. Annual trend of precipitation at each station shows the increase of 0.32mm/year in Seoul, 0.30mm/year in Wonju, 0.60mm/year in Daegallyoung and 0.28mm/year in Gangnung, respectively, indicative of significant topographic effects on precipitation. Annual trend in Er between Daegallyoung and Wonju increased over 36 years, which is similar to between Daegallyoung and Gangnung. Additional analysis for the seasonal dependence clearly shows a significant increasing trend (R^2=0.36) between Daegallyoung and Gangnung especially in winter, which imply a significant increasing trend in the orographic ratio in winter. The present results sugguest that rainfall in hill has increased as compared to that on the lowland probably attributable to the topographic-enhanced precipitation, being independent of aerosols. In addition, orographic precipitation will be discussed together with urban dynamic effect and different synooptic wind effect on precipitation.

Keywords: orographic precipitation, aerosols, urban effect, Korea

CHARACTERISTICS OF AEROSOL TYPE INFERRED FROM AERONET SUNPHOTOMETER MEASUREMENTS

Jaehwa LEE[1], Jhoon KIM[1], Chul Han SONG[2], and Brent HOLBEN[3]
[1]Yonsei University, Seoul, Republic of Korea
[2]GIST, Gwangju, Republic of Korea
[3]NASA GSFC, Maryland, USA
jkim2@yonsei.ac.kr

Abstract

The aerosol classification algorithm is constructed by using Aerosol Robotic Network (AERONET) sunphotometer measurements. The aerosol types are classified into dust, non-absorbing water soluble fine mode aerosols which contain sulfate, nitrate, chloride, or mixing state of them, absorbing fine mode aerosol which contains black carbon, and mixture of coarse and fine mode aerosols based on its dominant size mode and radiation absorptivity determined by fine mode fraction and single scattering albedo, respectively. By applying this algorithm over the coverage of AERONET, aerosol types on a global map, frequency distribution and time series of aerosol types, and long-range transport of aerosols are analyzed. Classified aerosol types from AERONET represent regional characteristics of aerosol reasonably well. The frequency distribution and time series of aerosol types show regional differences depending on major source of aerosol and atmospheric conditions. The long-range transport of aerosol is inferred by the similarity of aerosol types over upwind and downwind region. The algorithm can be used for validating aerosol classification algorithm from satellite as well as analyzing aerosol characteristics in semi-global sense over land where the accuracy of satellite observation is poor.

Keywords: aerosol, aerosol type, aerosol optical properties, AERONET

SEASONAL AND SPATIAL COMPARISONS BETWEEN CLOUD AND AEROSOL OPTICAL PROPERTIES DERIVED FROM SATELLITE REMOTE SENSING IN NORTHEAST ASIA

You-Joon Kim[@], Byung-Gon Kim[@*], Chang-Hoi Ho[$]
[@] Department of Atmospheric Environmental Sciences, Kangnung-Wonju National University, Gangnung, 210-702, Korea (bgk@nukw.ac.kr)
[$] School of Earth & Environmental Sciences, Seoul National University

Abstract

Mainly MODIS/Terra level 3 and NCEP/NCAR Reanalysis long-term (2001-2008) daily data have been analyzed for the understanding aerosol-cloud interactions. The analysis is mainly confined to aerosol optical depth (AOD), liquid-phase cloud optical depth (COD), liquid-phase cloud effective radius (r_e), cloud fraction (CF), potential temperature (θ), vertical velocity (W) etc. in Northeast Asia. The analysis region is divided into 4 regions such as A1 (118-121E & 35-38N), A2 (122-125E & 35-38N), A3 (126-129E & 35-38N), and A4 (130-133E & 35-38N), since there seems to be strong horizontal gradient of AOD. The annual variations of AOD at 4 regions have overall similar annual trends with those of CF, impling more aerosols resulting in prolonging cloud lifetime (Albrecht, 1989). The monthly variation of AOD exhibits the highst values at late Spring and the lowest at late-Summer similar to those of other previous studies. Horizontal distributions and box plots of AOD for the different region showed the substantial horizontal gradient from China to Korea, especially with the strong difference between A1~A2 and A3~A4, which could represent the evidence of the anthropogenic influence downstream of China in the perspective of seasonal average. Meanwhile, CODs are highest over A3 in summer, and A4 in winter, respectively, which are probably attributable to the frequent deep convection over the Korea inland in summer and the warm current influence in East Sea in winter, respectively. This also implies that cloud properties could be firstly determined by regional climate variability. Specifically the relationship of AOD to r_e on the monthly-average basis has been examined, which showed the negative correlations, only in summer and most significant associations over the Yellow Sea (A2), but mostly ambiguous signals in the other seasons and/or regions.

RV is defined as normalized interquartile range being indicative of cloud variability. Note that relative variability in COD (RV_{COD}) is generally lowest whereas RV_{AOD} is higher in summer, such that the cloud variability in summer tends to be relatively suppressed and the long-term changes on aerosol loadings over the Yellow Sea is greatest. Especially, the highest ratio of RV_{AOD}/RV_{COD} in summer might indicate the favorable condition for the efficient aerosol-cloud interaction in the long-term spatial & temporal average. Vertical gradient of the potential temperature ($\Delta\theta$) between 700 and 1000hPa is overall higher in summer except for A1 and A2 in winter. This might be associated with the movement of subsidence zone of hadley cell.

Keywords: aerosol, cloud, optical depth, effective radius, relative variability (RV)

Seasonal variations of optical properties and hygroscopicity of atmospheric aerosol in Seoul, Korea

Jin Sang Jung[1], Mylene G. Cayetano[1], Tsatsral Batmunkh[1], Dam Duy An[1], Kwang Yul Lee[1], and Young J. Kim[1,*] Jhoon Kim[2]
[1]Advanced Environmental Monitoring and Research Center, Department of Environmental Science and Engineering, Gwangju Institute of Science and Technology, Gwangju, 500-712 South Korea
[2]Department of Atmospheric Science, Yonsei University, Seoul, Korea
yjkim@gist.ac.kr

Abstract

As a part of the IGAC Mega-cities program, aerosol optical and chemical properties were continuously measured from April 2007 to February 2008 at the urban site (37.57˚N, 126.94˚E) in Seoul, Korea. Light scattering coefficient of ambient particles in the total suspended particle regime (b_{scat}), light scattering coefficient of $PM_{2.5}$ dry particles (b_{scat}_dry$PM_{2.5}$), and light absorption coefficient in the fine regime (b_{abs}) were measured by an ambient nephelometer (OPTEC, NGN2), a $PM_{2.5}$ size-cut nephelometer (OPTEC, NGN3), and an aethalometer (Magee Scientific, AE16U), respectively. The carbonaceous aerosol was measured with a Sunset Laboratory semi-continuous organic carbon/elemental carbon (OC/EC) analyzer (Sunset Laboratory, RT3015) using thermal-optical transmittance (TOT) protocol for pyrolysis correction. Mass absorption efficiency, $\sigma_{abs}(=b_{abs}/EC)$ was determined based on thermally measured EC and light absorption coefficient. σ_{abs} at 550nm wavelength was determined to be 9.0±1.3, 8.9±1.5, 9.5±2.0, and 10.3±1.7 m^2 g^{-1} in spring, summer, fall, and winter, respectively. Single scattering albedo (SSA) of ambient aerosol was determined from the ratio of b_{scat} to b_{ext} (= $b_{scat}+b_{abs}$). Average SSA at 550nm was determined to be 0.88±0.07, 0.84±0.10, 0.82±0.09, and 0.84±0.06 in spring, summer, fall, and winter, respectively. Humidity dependent light scattering enhancement factor, *f*(RH) (=b_{scat}(RH)/$_{bscat}$(dry)) was obtained from light scattering coefficients of dry and ambient particles. *f*(RH) (=b_{scat} (80%)/b_{scat} (30%)) was determined to be 2.26±0.41, 2.02±0.36, 1.91±0.49, and 1.59±0.21 in spring, summer, fall, and winter, respectively.

Keywords: Mass absorption efficiency, Sing scattering albedo, f(RH)

Measurement of Optical Properties of Secondary Organic Aerosols

T. Nakayama[1]*, Y. Matsumi[1], A. Yamazaki[2], A. Uchiyama[2],
K. Sato[3], and T. Imamura[3]
[1] Solar-Terrestrial Environment Laboratory, Nagoya University, Nagoya, Japan
[2] Japan Meteorological Agency, Meteorological Research Institute, Tsukuba, 3020052, Japan
[3] National Institute for Environmental Studies, Tsukuba, 3058506, Japan
*nakayama@stelab.nagoya-u.ac.jp

Aerosol particles play an important role in radiation balance in the atmosphere by scattering and absorbing incident light. Therefore, accurate determination of the optical properties of atmospheric aerosols is essential. Although black carbon (BC) is the most potent absorber over the solar spectral, attention has turned recently to ″brown″ organic carbon as a source of significant absorption, particularly in the near-UV. Recently, light absorption by organic aerosol, especially from combustion and humic-like organic aerosols, has been studied in both field and laboratory studies. However, optical properties for secondary organic aerosol (SOA) have not been studied in detail.

In this study, we have determined the optical properties of the SOAs generated during (1) the photooxidation of toluene in the presence of NO_x, (2) the reactions of cyclohexadiene with O_3, and (3) the reactions of α-pinene with O_3. The SOAs were generated in a 6 m^3 teflon coated stainless-steel chamber in the absence of seed particles. Optical properties and size distributions of the SOAs were measured in real-time after a sufficient amount of aerosols (>130 $\mu g/m^3$) were generated. Extinction, scattering, and absorption coefficients of the SOAs were measured by an originally developed cavity ring-down aerosol extinction spectrometer (CRD-AES) (355, 532 nm), an integrated nephelometer (TSI) (450, 550, 700 nm), and a particle soot absorption photometer (PSAP, Radiance Research) (470, 522, 660 nm). Size distributions of the SOAs were measured by a scanning mobility particle sizer (SMPS, TSI). Using the obtained data, the extinction, scattering, and absorption efficiencies were calculated. Because the particle size of SOAs generated in the chamber increases with time due to condensation and coagulation, size parameter dependence of these efficiencies were obtained. The refractive index of SOAs was determined so that the measured size parameter dependence of these coefficients was reproduced by calculations using Mie scattering theory.

As a result, significant light absorption was found for the SOAs generated during the photooxidations of toluene in the presence of NO_x and the light absorption at 355 nm was larger than that at 532 nm. Small absorption was found for the SOAs generated during the reactions of cyclohexadiene with O_3. No significant absorption was found for the SOAs generated during the reactions of α-pinene with O_3. Using these results, mass absorption cross-sections of SOAs were calculated. In this presentation, the atmospheric implications of the light absorptions of SOAs will be discussed.

Keywords: aerosol optical property, light absorption, secondary organic aerosol (SOA), brown carbon, cavity ring-down spectroscopy

THE RECENT TRENDS OF AEROSOL OPTICAL PROPERTIES AND SURFACE RADIATIVE FORCING AT TSUKUBA, JAPAN

Rei KUDO, Akihiro UCHIYAMA, Akihiro YAMAZAKI, Eriko KOBAYASHI
Meterrological Research Institute, Japan Meteorological Research Agency
1-1 Nagamine, Tukuba-shi, Ibaraki-ken, 305-0052 Japan
reikudo@mri-jma.go.jp

Abstract

Solar radiation reaching the Earth's surface increases since the mid 1980's at widespread locations ("global brightening"). Since global brightening is seen under both cloudy and clear skies at numerous locations, the change in aerosol optical property is one of the key factors. The aerosol direct radiative forcing at the suraface is approximately determined by two optical properties: optical thickness (loading), and single scattering albedo (ratio of scattering to scattering + absorption).

We have developed a new method to estimate optical thickness and single scattering albedo from the direct and diffuse irradiances in visible and near infrared regions. The method assumes the external mixture of four typical aerosol components (water-soluble, soot, sea solt, and dust). The combination of four aerosols is optimized to the measured direct and diffuse irradiances. Optical thickness and single scattering albedo are calculated from the optimum combination. We applied this method to the measurements from 1998 to 2008 at Tsukuba, Japan. The daily mean global surface irradiances under clear sky increased by 5.9 Wm-2/decade. The daily mean aerosol surface radiative forcing decreased by 5.6 Wm-2/decade. The increase of the surface global irradiance was due to the decrease of the aerosol surface radiative forcing. Optical thickness had no tendency, but single scattering albedo increased by 0.1/decade. The aerosol surface radiative forcing was decreased by the increase of single scattering albedo, not by the decrease of optical thickness. Furthermore, the increase trend for single scattering albedo may be related to the reduced emission of black carbon in east Asia.

Keywords: aerosol, radiation, global brightening

The Comparison for Measurements of Diffuse Sky Radiation

MO Yueqin, YANG Yun, LV Wenhua, DING Lei and WANG Dong
Meteorological Observation Centre of CMA, Beijing, China 100081
myqaoc@cma.gov.cn

Abstract

With high-accuracy measuring system of solar radiation, sunlight is shaded by a sun-seeking disc, so the diffuse sky radiation is measured automatically. Contrast experiment is carried out to compare and analyze the data acquired by experimental and operational instruments. According to the contrast observation data, which is getting from the measurement by a sun-seeking disc system, it is shown that the current shadow bands coefficient is generally small in sunshine and big in overcast sky.

Keywords: diffuse sky radiation, sun-seeking disc, shadow band

A SENSITIVITY STUDY OF AEROSOL DIRECT RADIATIVE FORCING ON LARGE-SCALE CIRCULATION AND RAINFALL TREND IN ASIA DURING BOREAL SPRING

Maeng-Ki Kim and Woo-Seop Lee
Kongju National University, Gongju, Korea
mkkim@kongju.ac.kr

Abstract

A series of sensitivity studies were performed with the NASA finite-volume General Circulation Model (fvGCM) forced with monthly varying three-dimensional aerosol distribution from the Goddard Ozone Chemistry Aerosol Radiation and Transport model (GOCART). Result shows that radiative forcing of black carbon aerosol and sulfate aerosol leads to cooling of the land surface and reduction in rainfall over central East Asia. The maximum reduction in precipitation is shifted northward relative to the maximum aerosol loading region as a result of dynamical feedback, especially for sulfate aerosol. The anomalous thermal gradient by aerosol cooling near the land surface, reduces the baroclinicity of the atmosphere, leading to a deceleration of the upper level westerly flow. The westerly deceleration induces, through ageostrophic wind adjustment, anomalous meridional secondary circulation at the entrance region of the East Asian jetstream, with strong sinking motion and suppressed precipitation near 30^{o}N, coupled to weak rising motion and moderately enhanced precipitation over southern China and the South China Sea. The observed rainfall trends are more similar to the modeled rainfall anomaly induced by BC aerosol forcing than other aerosol forcings, especially over Bay of Bengal to Indochina peninsula. These results suggest that the radiative forcing of anthropogenic aerosol through induced dynamical feedback with the atmospheric water cycle may be a causal factor in the observed spring precipitation trend over Asia.

Keywords: Aerosol radiative forcing, rainfall trend, secondary circulation, dynamic feedback

STANRD GAS MISTURES OF KRISS SCALE FOR ATMOSPHERIC GREEN HOUSE GAS MONITORING

Jeongsoon LEE[1], Jin Bok LEE[1], Dong Min MOON[1], GawngSub KIM[1], TaeYoung GOO[2], Goan-Young PARK[2], and Jin Seog KIM[1]

[1]Korea Research Institute of Standards and Science (KRISS), Division of Metrology for Quality Life, P.O.Box 102, Yusong, Daejeon, Republic of Korea
[2] Korea Global Atmosphere Watch Center, Korea Meteorological Administration
leejs@kriss.re.kr

Abstract

Greenhouse gases (GHG), have been known as causing materials of the greenhouse effect, are carbon dioxide, methane, nitrous oxide, sulphur hexafluoride, hydrofluorocarbons, and perfluorocarbons. They has been paid attention since Kyoto protocol to the United Nations Framework Convention on Climate Change. Accurate monitoring data are vital for the study of the relationship between GHGs and global warming becouse of their tiny variation. For example, mixing ratio of carbon dioxide in the atmosphere, is reported to be growing by +1.7 ppm (parts per million)/year for recen 10 years according to GAW report.

For the purpose of accurate monitoring of GHGs, it is essential to have a accurate standard gas mixtures with high qualified and global scale. We have developed the standard gas mixtures by using a gravimetric method since 2002 and those of carbon dioxide, methane, nitrous oxide, sulphur hexafluoride, and 3 chloro-fluorocarbons are now available. Their specifications are presented here and some results monitored in Korea Global Atmosphere Watch (KGAW) Center are intorduced.

Keywords: greenhouse gas monitoring, standard gas mixtures, scale harmonization, KGAW station

CHANGES IN PRECIPITATION INTENSITY OVER THE EAST ASIA IN RESPONSE TO GLOBAL WARMING

Da-Hee CHOI, Won-Tae KWON, Hee-Jeong BAEK, and Yu-Mi CHA

Climate Research Laboratory, National Institute of Meteorological Research
Korea Meteorological Administration, Seoul, Korea
dhchoi@metri.re.kr

Abstract

This study investigates the possible changes due to global warming of summer precipitation over the East Asia with a high-resolution model. For this purpose, two 30-yr time-slice experiments for the present (1971-2000) and the future (2071-2100) climate simulations are performed with the high-resolution ECHAM4 T106 based on IPCC SRES A1B. The future climate simulation based on IPCC SRES A1B scenario shows that total precipitation, its intensity, and extreme events increase over the Yangtze River valley of China, Korea, and Japan. The future precipitation changes are affected to some extent by the change in the moisture flux and its convergence associated with the intensification of the monsoon flow and convective instability. The baroclinicity change regions coincide with the regions of increased precipitation intensity. The changes in the vertical structure for temperature and zonal wind due to global warming are responsible for increase of baroclinic instability in the lower troposphere. As a result, the future precipitation intensity changes are mainly attributable to the changes in the baroclinic instability.

Keywords: East Asian summer rainfall, precipitation intensity, climate change, time-slice experiments

Future change and its uncertainty in Northern Hemisphere wintertime atmospheric blocking

Mio MATSUEDA[1,2], Ryo MIZUTA[1,2], and Shoji KUSUNOKI[2]
1: Advanced Earth Science and Technology Organization, Tsukuba, Japan
2: Meteorological Research Institute, Tsukuba, Japan

In this study, the future change in the wintertime Northern Hemisphere atmospheric blocking was investigated using 20-km mesh Japan Meteorological Agency (JMA) / Meteorological Research Institute (MRI) Atmospheric General Circulation Model (AGCM). We focused on the frequency and the duration of the blocking for the Northern Hemisphere winter (December - February) in the present-day (1979-2003), the near future (2015-2039), and the future (2075-2099) climates under the Intergovermental Panel on Climate Change (IPCC) A1B emission scenario. Also, in order to estimate uncertainty in the future projection of the blocking, sea surface temperature (SST) and initial value ensemble simulations were conducted using a 60-km mesh AGCM.

In the near future climate, the Euro-Atlantic and the Pacific blocking frequencies are likely to decrease slightly. The decrease might depend on the climate sensitivity of AGCM. There is a possibility that the blocking frequencies do not change.

In the future climate, the Euro-Atlantic and the Pacific blocking frequencies are likely to decrease. In particular, the significant decreases tend to appear at the west of the peak of the Euro-Atlantic and the Pacific blocking frequencies. These decreases are consistent with the upper-level strong zonal wind in the future climate. The ensemble simulations have revealed that the more the global warming proceeds, the more the Euro-Atlantic and the Pacific blocking frequencies decrease. The number of the Euro-Atlantic blocking decreases in all categories of durations, whereas that of the Pacific blocking decreases particularly in categories of long durations.

Future changes of the midlatitude activities using the Dynamic State Index

Eiki Shindo
Meteorological Research Institute, 1-1 Nagamine, Tsukuba, Ibaraki
305-0052, JAPAN
Email:eishindo@mri-jma.go.jp

Abstract

We have conducted global warming projection with 20-km grid Atmospheric General Circulation Model (AGCM). We investigate the future changes of the midlatitude activities. Dynamic State Index (Nevir,2004) is used to evaluate the activities.

This study is supported by the Innovative Program of Climate Change Projection for the 21st Century (KAKUSHIN). The Earth simulator was used for calculation.

As is well known, in a non-dissipative fluid system, there exist the conserved quantities related to the vorticity and the energy based on the theory of Hamilton Fluid Dynamics. In a stationary, diabatic system, the conserved quantity composed of the potential vorticity, Bernoulli function and the potential temperature is exactly zero. This state is called Energy-Vorticity Equilibrium. This quantity is produced by the non-stationary, diabatic, dissipative processes, so it is useful to evaluate the activities of midlatitude disturbances.

In the presentation, another derivation of this conserved quantity based on the geometrical theory and the result of comparing to the analysis using the maximum Eady growth rate will also be shown.

Keywords: Global warming projection, 20km AGCM, Dynamic state index, midlatitude

FUTURE CHANGE OF NORTH ATLANTIC TROPICAL CYCLONE TRACKS: PROJECTION BY A 20-KM-MESH GLOBAL CLIMATE MODEL

Hiroyuki Murakami and Bin Wang
Advanced Earth Science & Technology Organization (AESTO), Tsukuba, Japan
himuraka@mri-jma.go.jp

Abstract

In this study, 25-year consecutive climate simulations for both a present-day and a future warmed environment based on an A1B scenario using a MRI/JMA 20-km-mesh high-resolution atmospheric general circulation model were conducted to explore changes in tracks of tropical cyclones (TCs) due to global warming. In this presentation, those changes over the north Atlantic (NA) will be presented.

Overall, TC tracks showed a significant eastward shift in future in the NA, resulting in a reduced probability of TC landfall over North America. The track changes were also caused by alternation in TC genesis locations rather than in TC steering flows. The reduction of genesis in the west NA was attributed to decreases in relative humidity and ascending motion caused by an enhanced large scale subsidence, whereas the increase of genesis in the southeast NA arised from increasing upward motion and convective available potential energy due to local ocean surface warming.

Keywords: tropical cyclone, high-resolution, future change, track change, genesis potential index

A STATISTICAL DOWNSCALING FOR REGIONAL-SCALE SOLAR RADIATION CHANGE OVER JAPAN BY USING GLOBAL REANALYSIS METEOROLOGICAL DATASETS

Motoki NISHIMORI and Toshichika IIZUMI
National Institute for Agro-Environmental Sciences, Tsukuba, Japan
mnishi@niaes.affrc.go.jp

Abstract

Statistical downscaling methods (SDMs) are useful tool that convert the large-scale circulation fields derived from GCMs to local-scale climate factors (surface air temperature: Tm; precipitation: Pr; global solar radiation: Sr, etc.) by using the statistical relationships between the large- and local- variables. Among of various climate factors, Sr is particularly important for agriculture. Furthermore, to overcome a poor spatial resolution problem of the current GCMs, we also start to adopt a SDM to the outputs of multi-RCMs that have relatively higher spatial resolution and are able to consider uncertainties in regional-scale climate projection. The purpose of this study is first to make further progress such the SDM developed by the authors, whom the daily timescale Sr change of Japan is to be consists with those of Tm and Pr. The SDM in this study is the combinational equations of canonical correlation analysis (CCA) and multiple linear regressions (Nishimori and Kitoh, 2006). However, it extended from monthly to daily timescale, and modified to analyze multi-predictors/ predictands. We used three general circulation factors, geopotential height at 700 hPa (Z700), zonal and meridional wind vector at 850 hPa (UV850), and sea level pressure (SLP) as predictor circulation variables derived from "Japanese 25-year Reanalysis" with a spatial resolution of 1.25º by 1.25º, and three climate elements, Tm, Pr and Sr derived from sunshine hours based on the AMeDAS dataset. Figure 1 shows the CCA-deduced spatial regression patterns of each pair of three elements (Z700/Tm, UV850/Pr and SLP/Sr). This CCA mode is predominated in summer, especially in the end of Baiu season. Positive (negative) phase showed warm (cold) summer days over Japan, dry (wet) spell and higher (lower) solar radiation in Kanto area associated with westward strengthened (eastward withdrew) North Pacific High, and heavy (light) rain in Hokkaido and Kyushu associated with strong (weak) southwest wet stream surrounding the High.

Keywords: statistical downscaling, solar radiation, Japan, canonical correlation analysis

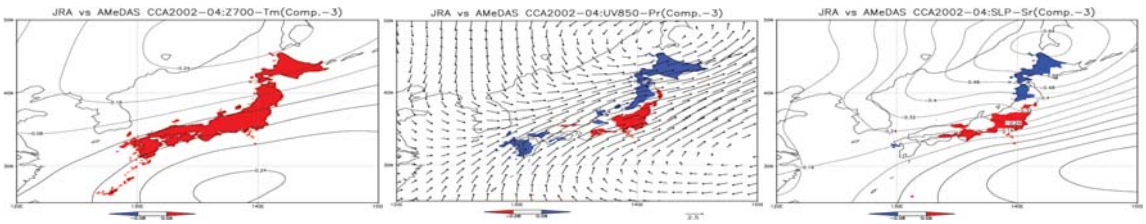

Fig.1. Spatial regression patterns of the third mode of the multi-factors CCA (Left) Z700/Tm, (center) UV850/Pr, and (right) SLP/Sr. Red (blue) shades show positive (negative) Tm and Sr and negative (positive) Pr anomaly values.

Acknowledgement: This work financially supported by 'The Global Environmental Research Funds (S-5-3 and S-4)' by the Ministry of the Environment of Japan.

PROJECTION OF THE CHANGES IN THE FUTURE EXTREMES OVER JAPAN USING A CLOUD - RESOLVING MODEL (JMA-NHM)

Masaomi NAKAMURA[1], M. NAKANO[2], S. KANADA[2],
S. HAYASHI[1], T. KATO[1], H.SASAKI[1], T.UCHIYAMA[1], K. ARANAMI [3],
Y. HONDA[3], K. KURIHARA[1] and A. KITOH[1]
1: Meteorological Research Institute(MRI), Tsukuba, Japan, manakamu@mri,jma.go.jp
2: Advanced Earth Science and Technology Organization (AESTO)
3: Japan Meteorological Agency (JMA)

Abstract

Regional climate projection experiments are being carried out focusing especially on the change in future extremes in the vicinity of Japan during the summer rainy season under the framework of the Innovative Program of Climate Change Projection for the 21st Century (KAKUSHIN program). The experiments by a semi-cloud resolving non-hydrostatic model (JMA-NHM) with a horizontal resolution of 5km (NHM-5km) have been conducted from June to October by nesting within the results of 20km-mesh-AGCM 10-year integrations for the present (1990-1999), near-future (2026-2035) and future climates (2086-2095).

In the future climate experiments, appearance frequency of daily precipitation amount exceeding 100 mm (heavy rain day), simulated by NHM-5km, increases more than 20%. The frequency of rain days (> 1.0 mm day^{-1}) decreases overall Japan, while the number of heavy rain day increases in western Japan in August and September and on the Pacific side of eastern Japan in July and August. The number of maximum consecutive dry days increases in most regions of Japan. Several extremely hot days (maximum daily temperature greater than 35 degrees centigrade) become to appear over some plain regions not only in July and August but also in future September.

In order to simulate precipitation extremes and horizontal distributions of precipitation strongly influenced by the complex topography over Japan, additional experiments are proceeding by using a model which has a horizontal resolution of 2km without cumulus parametarisation (NHM-2km). The results of preliminary experiments by NHM-2km, including those with perfect boundary conditions produced from objective analysis data, show good agreement with observational precipitation data and reproduce more detailed and realistic horizontal distributions of precipitation, compared with NHM-5km.

Keywords: regional climate, exteme event, global warming, cloud-resolving model

DIAGNOSIS OF CLIMATE-MODEL BIAS IN SUMMER TEMPERATURE AND WARM SEASON INSOLATION FOR SIMULATING REGIONAL PADDY RICE YIELD IN JAPAN

Toshichika IIZUMI, Motoki NISHIMORI, and Masayuki YOKOZAWA
National Institute for Agro-Environmental Sciences, Tsukuba, Japan
iizumit@affrc.go.jp

Abstract

Climate models, global and regional ones, have a systematic error (called bias) in their simulated meteorological elements. Bias is one reason that it is difficult to apply a climate-model output to impact application without bias correction. Although the importance of dealing with bias is widely recognized, the understanding on bias in impact model output and those in climate-model outputs is limited. Therefore, taking a large-scale crop model as an example, we investigated the nature of biases in regional paddy rice yields simulated by the crop model when the row daily climate-model outputs were used as the input of the crop model.

The following four sets of three meteorological elements (daily maximum and minimum temperatures and daily total insolation) from row and bias-corrected daily climate-model outputs were used as the inputs for the crop model: (1) row climate-model outputs of all meteorological elements; (2) a bias-corrected daily maximum and minimum temperatures and a row climate-model output of insolation; (3) a bias-corrected daily total insolation and a row climate-model outputs of daily maximum and minimum temperatures; and (4) a bias-corrected climate-model outputs of all meteorological elements. These four sets of meteorological inputs were provided by the outputs of the seven general circulation models (GCMs) and one regional climate model (RCM). The GCM outputs were the results of the 20 century climate in coupled climate model (20C3M) experiment, obtained from the WCRP CMIP3 Multimodel dataset (Meehl et al., 2007). The RCM output was the 20-km mesh size regional climate model (RCM20) outputs (JMA 2005). All the GCMs outputs included daily data on daily maximum and minimum temperatures and daily mean downward solar radiation for 20 years from 1981 to 2000. The RCM output include the daily data on daily maximum and minimum temperatures; however, the daily total insolation data were obtained form Iizumi et al. (2008), since the row data on daily mean downward shortwave radiation of the RCM were not released. We notice that the daily total insolation data were not row data of the RCM but statistically-downscaled data.

As a result, a linear relationship was found between the bias in regional yield and the bias in warm season insolation (May to October), while a cubic-function-like relationship was found between the bias in regional yield and the bias in summer season temperature (July and August). The relationship between the bias in regional yield and the biases in summer temperature and warm season insolation could be approximated by a cubic function reasonably.

Keywords: climate-model bias, crop model, impact application

Sensitivity experiments on FDDA options in WRF-based typhoon model

Sun-Hee Kim and H. Joe Kwon
Department of Atmospheric Science / Typhoon Research Center
Kongju National University, Kongju, Chungnam, 314-701 Korea
sunhkim@kma.go.kr

Abstract

Typhoon Research Center of Kongju National University in Korea have developed WRF(Weather Research and Forecast)-based typhoon model by implanting the GFDL(Geophysical Fluid Dynamic Laboratory)-type TC initialization scheme to the WRF (ARW) model. This WRF-based typhoon model uses two-way triple nests with the inner two nests moving automatically. The grid size of each domain is 5 km, 15 km, and 45 km, respectively.

Various sensitivity experiments on model physics have been conducted. We could recognize that microphysics affected not only track and intensity forecast but also precipitation. Track and intensity error were also smallest with Thompson graupel scheme in 2005 NABI case. In the sensitivity experiments on cumulus parameterization, predictability improvement is seen in the new Kain-Fritsch experiment over the Betts-Miler-Janjic experiment.

The initialization of tropical cyclone in its forecast is complex but very important. So the week vortex analyzed in the routine analysis cycle should be replaced with the realistic TC vortex in the initial field. GFDL-type TC initialization has been employed in this WRF-based typhoon model. Analysis nudging can be used to create dynamically consistent fore-dimensional dataset. In nudging FDDA, the model state is relaxed continuously at each time step toward the observed state by adding to the prognostic equations an artificial tendency term, which is based on the difference between the two states. Bogused vortex wind by GFDL-type TC initialization can be regarded as observed state. In the previous study (2008) analysis nudging was conducted just during 6 hour. In this study, however, the various sensitivity experiments will be conducted to optimize nudging coefficient and nudging time.

Keywords: WRF, GFDL, TC initialization, FDDA, analysis nudging

SEASONAL PREDICTION OF THE WNP TROPICAL CYCONE GENESIS FREQUENCY USING TELECONNECTION PATTERNS

Ki-Seon CHOI, Do-Woo KIM, Su-Bin OH, Ji-Sun LEE, and Hi-Ryong BYUN
Pukyong National University, Busan, South Korea
choiks@kma.go.kr

Abstract

This study developed a multiple linear regression model for the seasonal prediction of the summer TC genesis frequency (TCGF) in the WNP using the three teleconnection patterns. These patterns were composed of Siberian high Oscillation (SHO) in the East Asian continent, North Pacific oscillation (NPO) in the North Pacific, and Antarctic oscillation (AAO) near the Australia during the boreal spring (April-May).

This statistical model was verified through the two analyses: ⅰ) statistical method of cross validation was used. ⅱ) comparisons of the high TCGF years and low TCGF years that hindcasted by the statistical model were analyzed.

The high TCGF years were summarized as characteristics as follows; three anomalous teleconnection patterns such as anticyclone circulation (positive SHO phase) in the East Asian continent, pressure pattern like 'high-north and low-south' in the North Pacific, and cyclonic circulation (negative AAO phase) near the Australia was strengthened during the period from boreal spring to boreal summer. Thus, anomalous trade winds in the tropical western Pacific (TWP) were weakened by anomalous cyclonic circulations that located in the subtropical western Pacific (SWP) in both hemispheres. In consequence, this spatial distribution of anomalous pressure pattern suppressed convection in the TWP, strengthened convection in the SWP instead.

Keywords: Multiple linear regression model, TC genesis frequency, North Pacific Oscillation, Antarctic Oscillation, cross validation

THE CONTROLLING FACTORS OF TROPICAL CYCLONE INTENSITY CHANGE IN DIFFERENT INTENSITY PHASE

Li-Na BAI, Yuan WANG

NanJing University, NanJing, China

bailina@smail.nju.edu.cn

Abstract

By using tropical cyclone data from China Meteorological Administration (CMA), and the ERA daily reanalysis data for the period of 2000-2006, the statistical relationship between tropical cyclone (TC) intensity change and many influencing factors (including climatology/persistence factors, thermodynamic factors, dynamical factors and structural factors) is examined in western North Pacific. The TC life cycle is divided into three intensity phases: 1) formation; 2) intensification; and 3) decay. Research shows that the controlling factors of TC intensity change are different during its life cycle. In formation phase, the contribution of dynamical factors is a little larger than other factors, and the contribution of thermodynamic factors is nearly zero. In intensification phase, climatology/persistence factors are most important, the following is thermodynamic factors, structural factors and dynamical factors. In decay phase, the effect of thermodynamic factors and climatology/persistence factors are much larger than other factors. Furthermore, the analysis on standardized regression coefficient of these factors shows that strong vertical wind shear is negative to TC intensity change in formation phase, and sea surface temperature is one of the most important factors in intensification phase and decay phase, especially in decay phase.

Keywords: tropical cyclone intensity change, climatology/persistence factors, thermodynamic factors, dynamical factors, structural factors.

THE EFFECT OF ENVIRONMENTAL BAROCLINICITY ON STRUCTURE AND EVOLUTION OF SINGULAR VECTORS OF TROPICAL CYCLONES

Sung Min KIM and Hyun Mee KIM
Atmospheric Predictability and Data Assimilation Laboratory,
Department of Atmospheric Sciences, Yonsei University
Shinchon-dong 134, Seodaemun-gu, Seoul, 120-749, Republic of Korea
khm@yonsei.ac.kr

Abstract

In this study, the structure and evolution of total energy singular vectors (TESVs) of Typhoon Manyi (2007) and Typhoon Shanshan (2006) are evaluated using MM5 mesosclae model and its tangent linear and adjoint model with Lanczos algorithm. Compared to Shanshan influenced by the synoptic-scale environment with strong baroclinicity, Manyi developed in the environment with weak baroclinicity.

The horizontal structures of initial TESVs of Manyi are associated with the inflow toward the tropical cyclone along the edge of the subtropical high as approaching to typhoon recurvature, and are associated with the midlatitude trough after the recurvature. While the initial TESV structures of the Manyi are associated with the stretching deformation before the recurvature, those after the recurvature are caused by the thick shearing deformation. Due to weak baroclinicity and weak lower frontogenesis, the TESVs of Manyi in the midlatitude are located under the midlatitude trough with weak upshear tilted structures.

In contrast to Manyi, the TESV structures of Shanshan before the recurvature are associated with thin shearing deformation. In addition, because of strong baroclinicity and strong frontogenesis, the TESVs of Shanshan in the midlatitude are located under midlatitude trough with strong upshear tilted structures. The lower frontogenesis of Shanshan in the midlatitude is collocated with the region of conditional symmetric instability.

Keywords: tropical cyclones, singular vectors, environmental baroclinicity, deformation field, frontogenesis

THE WIND-PRESSURE RELATIONS OF TROPICAL CYCLONES IN THE WESTERN NORTH PACIFIC AND ITS RELATED CLIMATIC CHARACTERISTICS

Yuan Wang, Jin-Jie Song

Key Laboratory of Mesoscale Severe Weather / MOE, and Department of Atmospheric Sciences, Nanjing University
22 Hankou Road, Nanjing, P. R. China.
yuanasm@nju.edu.cn

Abstract

Three wind-pressure relations, which are equilibrium relationships of two forces, three forces and four forces, are compared in this paper. These forces include the pressure gradient force, centrifugal force, coriolis force, and friction. The relation between the tropical cyclone's maximum sustained wind (V) and minimum sea level pressure (p_c) is obtained as:

$$\alpha \cdot (p_0 - p_c) = \frac{V^2}{R} + fV .$$

The influence of coriolis force (fV) is considered in this formula, while the contribution of friction is neglected. It's superior to the equilibrium relationships of two forces and four forces. This formula is used to resolve the problem that the wind speed was highly estimated in the early period. Using the modified tropical cyclone record, the annual frequency of tropical storms is decreasing from 1949~2007, while the annual frequency of typhoons is increasing. And the intensity measured by the power-dissipation index is also increasing.

Key words: tropical cyclone, gradient wind equilibrium, frequency, intensity

EFFECTS OF TYPHOON RECURVATURE ON THE SEA SERFACE COOLING BY TYPHOONS

MIN-YOUNG KIM AND IL-JU MOON
Graduate Course of Marine Meteorology, Cheju National University, South Korea
nimbleyoung@hanmail.net

Abstract

Typhoons tend to move slowly during their recurvature. In the case of a slowly moving typhoon, the typhoon-induced sea surface cooling is strong, generally resulting in influencing the typhoon intensity. Therefore, this study investigates the effect of the typhoon recurvature on the sea surface cooling by typhoons. We have performed a series of experiment to find environmental factors affecting the SST cooling and its distribution during the recurvature period using the 1D and 3D POM model. In all experiments, symmetric typhoons with different translation speed are used. Ocean is initialized with horizontally-homogeneous temperature and salinity.

The experimental results show that typhoon with slow moving the smaller recurvature angle produced the larger SST cooling as well as the bigger SST difference between 3D and 1D model when other conditions are same. The reason will be discussed.

Keywords : typhoon, SST cooling, POM

EFFECTS OF THE CHANGJIANG DILUTED WATER ON TYPHOON INTENSITY

Sung-Hun Kim, Il-Ju Moon, Min-Young Kim and Young-Yoon Jung

Graduate Course of Marine Meteorology, Jeju National University
yah13@hanmail.net

Key words: Changjiang Diluted Water, typhoon intensity.

Abstract: The impact of Changjiang Diluted Water (CDW) on typhoon (TY) intensity is studied using the Princeton Ocean Model (POM).The results of the numerical experiment suggest that the CDW can prevent the SST cooling during the passage of a typhoon in the East China Sea (ECS) and affect the intensity of the typhoon. This is accomplished by the enhanced stratification in halocline due to the surface low salinity water originated from the CDW. Strong stratification layer tends to prevent the momentum transfer in the vertical, which produce weak vertical mixing. For an ideal typhoon with the 55-m/s maximum wind and 2.5-m/s translation speed, the stratification effects in the CDW contribute to a less surface cooling (maximum, 1.5oC) under the storm core than without the CDW. This implies that the CDW gives a positive role on the development of a typhoon in the ECS.

PRELIMINARY NUMERICAL EXPERIMENTS FOR TYPHOON HAI-TANG IN 2005 BY TYPHOON-WAVE-OCEAN COUPLED MODEL

Akiyoshi WADA[1*], Nadao KOHNO[2], Norihisa USUI[1] and Yoshimi KAWAI[3]
[1] Meteorological Research Institute, Tsukuba, Ibaraki, Japan
[2] Japan Meteorological Agency, Chiyoda, Tokyo, Japan
[3]Japan Agency for Marine-Earth Science and Technology, Tokosuka, Kanagawa, Japan
Email *awada@mri-jma.go.jp

Abstract

Recent developments of numerical modeling, observation and data assimilation technologies enable us to develop atmosphere-ocean prediction systems for weather forecasting. We aim at the improvement of the prediction of typhoons in the western North Pacific using a regional atmosphere-wave-ocean coupled model. The coupled model consists of NonHydrostatic atmospheric Model (NHM), Meteorological Research Institute the third generation ocean wave model (MRI-III) and slab mixed-layer ocean model. By using the coupled model, preliminary numerical experiments are performed for Typhoon Hai-Tang in 2005. The initial integration time is 1200 UTC 12 July in 2005. Three runs are performed: only atmosphere model(Atmos), atmosphere-ocean coupled model (Ocean) and atmosphere-wave-ocean model (Wave). Alternatively, two runs are performed by using different ocean conditions obtained by daily oceanic reanalysis data: daily reanalysis temperature and salinity in 1999 (99) and 2005 (05). Horizontal resolution of coupled model is 6 km and cumulus parameterization (Kain and Fritsch, 1990) is used for all runs.

Now we refer to predicted central pressures (CPs) as typhoon intensity in order to address the evolution of CPs. CPs in Atmos_99 and Atmos_05 are lower than those provided by Regional Specialized Meteorological Center Tokyo - Typhoon Center (best-track data), indicating that predicted CPs are much more stronger than those in best-track data without the effect of sea surface cooling (SSC). In contrast, CPs in Ocean_99, Ocean_05, Wave_99 and Wave_05 are higher than those in best-track data. Even though the negative impact on CPs seems to be significant compared with a difference in CPs between Atmos_99/Atmos_05 and best-track data, the impact of SSC is well reproduced by the coupled model.

The results suggest that oceanic environmental conditions such as sea-surface-temperature and sea-surface-height affect the intensity prediction during the intensification phase. The impact of ocean wave on the intensity prediction is different between ocean conditions in 1999 and 2005: The ocean wave helps intensification in 2005, while suppression in 1999. Therefore, oceanic environmental conditions play a crucial role in understanding typhoon-wave-interaction process and improving TC intensity prediction. We will disscuss the impact of diurnally-varying sea surface temperature on TC intensity prediction.

Keywords: Typhoon, Atmosphere-wave-ocean coupled model, Oceanic reanalysis data

A MECHANISM FOR HEAVY PRECIPITATION ASSOCIATED WITH TYPHOON MEARI (2004)

Akihiko MURATA
Meteorological Research Institute, Tsukuba, Japan
amurata@mri-jma.go.jp

Abstract

Heavy precipitation in the mountainous Kii Peninsula in Japan caused by typhoon Meari (2004) is investigated using a cloud-resolving model and observations. A marked characteristic of this heavy precipitation is its extreme rainfall rate. Several surface rain gauge measurements showed that 1-h accumulated rainfall amounts are extremely large: more than 100 mm. Another feature is that the area of precipitation is far from the storm center: more than 500 km.

From radar and surface observations, it was found that the precipitation systems were categorized as follows: A) the stationary system observed around Owase (34N, 136E), B) the moving system to the southwest of the system A, and C) the band-like moving system to the southwest of the system B.

The numerical simulation, using the Japan Meteorological Agency Nonhydrostatic Model with the horizontal grid spacing of 1 km, successfully reproduces the heavy precipitation. The simulated precipitation patterns are favorably compared with those in the observed one categorized on the basis of observations.

Detailed examination of the model fields and observations reveals that the predominant processes for the formation and maintenance of each precipitation system is as follows: system A) Elimination of vertical convective instability in the low-level warm and moist easterly on the slope of mountains located along the east coast of the Kii Peninsula, system B) Moisture supply due to higher-speed flow in the planetary boundary layer along the horizontal boundary between the low-level easterly and south-easterly flow, and lifting of slightly warmer south-easterly flow, and system C) Cold pool along the edge of the system and low-level inflow into the system like a tropical cyclone outer rainband.

Precipitation efficiency is calculated for elucidating the mechanisms of the heavy rains. One definition of the precipitation efficiency is the amount of rainfall reaching the ground divided by the sum of vertically accumulated condensation and deposition. The efficiency is higher in the heavy-precipitation period. The higher efficiency is attributed to the greater rate of conversion of cloud water to rainwater via accretion of cloud water by rain. In fact, the accretion efficiency, defined as the rainwater production rate for accretion of cloud water by rain divided by the sum of vertically accumulated condensation and deposition, is approximately equal to the rainfall efficiency and has a significantly larger value in the heavy-precipitation period. The relationship between the precipitation systems is responsible for the greater conversion of cloud water to rainwater. Clouds in the moving systems provide raindrops for the accretion of cloud droplets in clouds in the stationary system.

Keywords: tropical cyclone, typhoon, heavy rainfall, precipitation efficiency, cloud-resolving model

FORMATION AND EVOLUTION OF HEAVY RAIN CELLS IN CONVECTION BANDS WHICH ARE RELATED TO TOPOGRAPHY

WON-SU KIM, TAE-YOUNG LEE, and U-JU SHIN
Laboratory for Atmospheric Modeling Research, Global Environment Laboratory/
Dept. of Atmospheric Sciences, Yonsei University, Seoul 120-749, Korea
enemy@yonsei.ac.kr

Abstract

Convection band is one of the most frequent types of heavy precipitation systems (HPSs) comprising 27% of HPSs occurred during 2000-2006 over the Korean peninsula. This type can be characterized by line-shape, quasi-stationary behavior, rapid development, and movement of heavy precipitation cells along a convergence line. As a result of the quasi-stationary behavior of convection band and continued passage of convection cells along the band, rainfall becomes concentrated in a narrow zone, producing large amount of rainfall along the band. It sometimes causes enormous property loss or casualties. For this reason, it is very important to know about formation and evolution process of heavy rain cells in convection band. In many case, formation and evolution of heavy rain cells seems to be related to topography where the convection bands are located.

First of all, we have classified the type of disturbances that develop locally over the Korean peninsula in order to understand formation and evolution process of heavy raincells in convection bands, using PPI (Plan Position Indicator) radar images and AWS accumulated rainfall data during 1998 and 2000-2007. The types are classified as follows:

- Strengthening of heavy rain cells on the upwind side of mountains
- Development of heavy rain cells in the upstream portion of convection bands
- Strengthening and weakening of heavy rain cells on the upwind and downwind sides of mountains, respectively
- Deflection and blocking of heavy rain cells by mountains

According to the result of classification, 'Strengthening of heavy rain cells on the upwind side of mountains' type occurred most frequently. So we have carried out further study about this type of disturbance. The typical phenomena of this type occurred near Seoul during 21 LST 14 - 04 LST 15 July 2001. We have used SPRINT and CEDRIC program from NCAR in order to treat the radar data. Maximum accumulated reflectivity was appeared around the mountainous region. And vertical cross section analysis indicates that the heavy rain cells are strengthened as they get closer to the mountain peak and rainfall intensity is maintained continuously over the mountain.

Keywords: topography, radar, convection band, heavy rain cells

Acknowledgments. This work was funded by the Korea Meteorological Administration Research and Development Program under Grant CATER 2006-2304

Long-term behaviors of Bomb : Number and intensity

Mayu OKAZAKI, Shusaku SUGIMOTO and Kimio HANAWA
Tohoku University, Miyagi, Japan
okazaki@pol.geophys.tohoku.ac.jp

Abstract

Long-term variations of "Bomb" which is explosively developing extratropical cyclone are investigated by using sea level pressure (SLP) data from the NCEP/NCAR reanalysis during the period of 1948-2007. The Bombs are detected by following procedures. Step (1): the low is defined as SLP minimum with a large horizontal gradient, i.e., which is greater than 1 hPa / 5 degree, during winter (October to April). Step (2): life time of the low exceeds 24 hours. Step (3): a generation region of the low is within the region of 100E-150E, 20N-60N. Step (4): a deepening rate of the low exceeds 1 Bergeron. In the present study, we focus on behavior of big bomb, the central pressure of which is less than 990 hPa. The number gradually increases: 14 in 1950-1954 and 30 in 2000-2004. Most of big bombs tend to develop less than 970 hPa and some big bombs reach less than 960 hPa. The number of extreme bombs increases in recent years: 2 in 1950-1954 and 8 in 2000-2004.

Keywords: bomb, cyclone, around Japan, mid and high latitude, NCEP/NCAR

APPLICATION OF MID-IR CHANNEL TO RETRIEVAL OF AEROSOL OPTICAL DEPTH FROM GEOSTATIONARY SATELLITE

Mijin KIM, Jhoon KIM, Jong Min YOON
IEAA BK21 Program, Global Environmental Laboratory, Department of Atmospheric Sciences, Yonsei University, Seoul, Korea
mysky0110@yonsei.ac.kr

Abstract

These aerosols floating in atmosphere play a significant role in climate change. Aerosol has both direct and indirect effects in Earth climate system, but the quantitative estimates of their effect are still uncertain (IPCC 2007). From these reasons, it is very important to study aerosol properties and distribution. The Aerosol Optical Depth (AOD) retrieval algorithm utilizing GEO satellite can provide the global monitoring of aerosol in higher temporal resolution, but that has a lager retrieval error in AOD then other multiple-single-channel algorithms due to a limited number of channels and errors in estimating surface reflectance and aerosol properties.

As the signal received at the satellite consists of contributions from surface, atmosphere and aerosols in cloud free condition, it is the crucial to estimate surface reflectance to obtain AOD. Previous AOD algorithms for GEO satellites (e.g. Knapp *et al.*, 2002, Masuda *et al.*, 2002, Wang *et al.*, 2003) find surface reflectance from clear sky composite over previous 20 to 30 days visible channel data on the assumption that there is at least one clear day and surface reflectance variation is not significant for the periods. Air masses in East Asia, however, include both natural and anthropogenic aerosols due to persistent dust storms with growing air pollutants [e.g. Chu *et al.*, 2005]. Therefore estimated surface reflectance includes background optical depth (BOD) effect, and retrieved AODs have a large error.

The MID-IR channel is sensitive to visible surface reflectance, but it is not to AOD. These characteristics of the MID-IR channel can contribute to the AOD retrieval algorithm in estimating surface reflectance more accurate. In this study, AOD at 0.55 μm over East Asia is retrieved from two channels of visible (0.67 μm) and MID-IR (3.7 μm) on board a Geostationary (GEO) satellite, MTSAT-1R. First of all, surface reflectance of MID-IR channel is calculated. To apply MID-IR surface reflectance into retrieval of AODs at 0.55μm, it has to be converted to visible surface reflectance. For that reason, the correlation between surface reflectance from previous algorithm and the new result is estimated with consideration of NDVI, and then MID-IR surface reflectance is converted to visible surface reflectance by using those correlations.

The results of this study suggest the possibility of using MID-IR channel in AOD algorithms. Better surface reflectance can be obtained regardless of aerosol presence, which leads to more accurate AODs. However, in using the MID-IR channel, one should note that the large parts of signals for the MID-IR channel depend on the surface temperature. Mid-IR signal, moreover, is sensitive to dust unlike other aerosol types.

Keywords: aerosol optical depth, surface reflectance, GEO, mid-ir channel

Tentative Properties of Aerosols Derieved from GOSAT TANSO-CAI Data and Plans for Validation

Nobuyuki KIKUCHI[(1)], Akiko HIGURASHI[(1)], Tatsuya YOKOTA[(1)], Satoru FUKUDA[(2)], Teruyuki NAKAJIMA[(2)]
(1) National Institute for Environmental Studies, Tsukuba, Japan
(2) Center for Climate System Research, The University of Tokyo, Kashiwa, Japan
kikuchi.nobuyuki@nies.go.jp

Abstract

GOSAT (IBUKI), launched on 23 January 2009, observes the concentrations of carbon dioxide and methane using TANSO-FTS. GOSAT has another image sensor TANSO-CAI for observing the optical properties of aerosols and clouds. The aerosol and cloud properties are used for correcting the effect of aerosols and clouds on the spectra obtained by TANSO-FTS. We describe about the aerosol properties derived from TANSO-CAI.

TANSO-CAI has 4 band (0.38μm, 0.674μm, 0.870μm, 1.60μm) and can derive the optical thickness of 3 aerosol types, accumulation mode, salt and dust. Accumulation mode aerosol includes 2 aerosol types, sulfate and soot, divided by the volume ratio. Comparing the TANSO-CAI radiance with the lookup table of the results of radiation transfer calculations, aerosol properties are determined. Maximum A Posteriori method (MAP method) is used to obtain the optimum solution of aerosol properties. Minimum reflectance is used for the surface properties as aerosol effects are ignored. Band1 (0.38μm) is a useful channel for determining aerosol properties above land, because reflectance of land surface at 0.38μm wavelength is very small. Using 0.38μm band, slightly signal of aerosol can be detected above dark land.

The optical thickness, single scattering albedo and phase function of aerosols are needed for correcting the effects of aerosols on TANSO-FTS. TANSO-FTS has 3 SWIR band (0.76μm, 1.64μm, 2.0μm). The aerosol properties derived by TANSO-CAI should be converted to the aerosol properties at the wavelength of TANSO-FTS band. For the conversion, it is assumed that the size distribution each aerosol type is fixed in each shape, and the Mie scattering theory is used for calculating the optical properties of each aerosol type with the complex refractive indices of the element of each aerosol types.

Validation of aerosol properties is planed using SKYNET and AERONET data. In addition, we install skyradiometers at Moshiri in Japan and Bremen in German, where are the validation sites of TANSO-FTS. Skyradiometer data are analyzed with skyrad pack, and screened out cloud contaminations. Skyrad pack derives the optical thickness, single scattering albedo and size distribution of aerosols from diffused solar radiance measurements. At 1.6um wavelength, diffused solar radiance measurements detect few signals, so we developed an algorithm to derive the aerosol optical thickness from direct solar radiance measurements. The idea of this algorithm is that contamination of water vapor absorption at 1.6μm wavelength is reduced with 0.94μm water vapor band measurements.

Keywords: GOSAT, TANSO-CAI, aerosol, SKYNET, skyradiometer,

Development of aerosol classification and retrieval algorithm using 1α+1β+1δ data of ATLID/EarthCARE

T. Nishizawa[1], N. Sugimoto[1], I. Matsui[1], A. Shimizu[1], B. Tatarov[1], and H. Okamoto[2]

1. National Institute for Environmental Studies, Tsukuba, Japan,

2. Tohoku university, Sendai, Japan

nisizawa@nies.go.jp

We started developing an algorithm that classifies three aerosol components that are water-soluble, dust, and soot particles and estimates their vertical profiles in extinction coefficient, using all the three-channel data of ATLID installed on EarthCARE satellite (JAXA/ESA) which will be launched in 2013. The ATLID three-channel data are the extinction coefficient (α), backscattering coefficient (β), and total depolarization ratio (δ) at the wavelength of 355nm (1α+1β+1δ data). In the algorithm, the mode radii, standard deviations, and refractive indexes for each aerosol type are prescribed based on previous studies; the shapes for water-soluble and soot particles are assumed to be spherical. Spheroid models are introduced into the algorithm to capture the nonsphericity of dust. The algorithm for ATLID is developed combining two types of aerosol classification and retrieval algorithms that we have developed until now. One of the algorithms retrieves the vertical profiles of extinction coefficient for water-soluble, dust, and soot particles using 1α (532nm) + 2β (532 and 1064nm) lidar data. In the algorithm, the mode radii, standard deviations, and refractive indexes for each aerosol type are assumed; the shapes for each aerosol component are assumed to be spherical. The other algorithm retrieves the vertical profiles of extinction coefficient for water-soluble, dust, and sea-salt particles using 2β (532 and 1064nm) + 1δ (532nm) lidar data. Similar assumptions are used in the algorithm, but the shape for dust particles is assumed to be spheroid, improving the performance of the algorithm. In the presentation, we will show the ATLID algorithm and the sensitivity study of the algorithm using the simulated lidar signals as well as the results of the applications of the 1α + 2β and 2β + 1δ algorithms to the observed data.

Keywords: Aerosol, Algorithm, Lidar, ATLID, EarthCARE

CO-BC Relations from Satellite Remote Sensing

Jungbin Mok, Jhoon Kim, Jaehwa Lee

IEAA BK21 Program, Department of Atmospheric Science, Yonsei University, Seoul, Korea

.

Recent development in satellite remote sensing, with its global coverage now enables us to investigate correlation between aerosols and pollutant gases. MOPITT (Measurement of Pollution in the Troposphere) and MODIS (Moderate Resolution Imaging Spectroradiometer) onboard the Terra satellite has observed CO (carbon monoxide) density and AOD (Aerosol Optical Depth) since 1999. Increases of CO, a very important gas in tropospheric chemistry, in atmosphere can reduce the self-purification ability of atmosphere, thus modifies atmospheric chemical, physical, and climatological properties. Also, CO has similar source with BC (black carbon) and is good tracer due to long life time in the atmosphere. BC aerosol has been regarded as a potential factor causing global warming (*IPCC*, 2007). Sources of both CO and BC are related to incomplete combustion, but sinks are different.

MODIS-OMI algorithm (*Kim et al.*, 2007) is used to classify aerosol types into four types – BC, soil dust, sulfate, and seasalt (*Jeong and Li*, 2005; *Kim et al.*, 2007) using OMI's AI to determine radiative absorption of aerosol and MODIS's AE (Angstrom Exponent) to determine size of aerosol. The MODIS-OMI algorithm and MOPITT allow us to investigate the correlation between BC and CO. The correlation between BC and CO becomes better than that between MODIS fine mode AOD and CO in most regions. By comparing these results with MODIS fire counts, enhanced correlations are found for CO with BC in the region of biomass burning and wild fires. Good correlation between CO and BC suggests possibilities that CO can be used as surrogates of BC and validate the classified BC aerosol from remote sensing. In Southern Africa, however, the correlation between BC and CO becomes worse than that between fine mode AOD and CO. Wind fields, sources of aerosols, and distance from the source regions are suggested to explain the difference in the correlation.

Global Satellite Mapping of Precipitation using Moving Vector and Kalman Filter (GSMaP_MVK)

Tomoo Ushio, Kazumasa Aonashi, Takuji Kubota, Shoichi Shige, Misako Kachi, Riko Oki, Ken'ichi Okamoto, Takeshi Morimoto and Zen-Ichiro Kawasaki
Osaka University, Osaka, Japan
ushio@comm.eng.osaka-u.ac.jp

Abstract

Estimation of the global distribution of precipitation with high accuracy and resolution has long been one of the major scientific goals. The making of precipitation maps on a global basis is important for modeling of the water cycle, maintaining the ecosystem environment, agricultural production, improvements of weather forecast precision, flood warning, and so on.GSMaP (Global Satellite Mapping of Precipitation) is a project aiming (1) to produce high-precision and high-resolution global precipitation maps using satellite-borne microwave radiometer data, (2) to develop reliable microwave radiometer algorithms, and (3) to establish precipitation map techniques using multi-satellite data for the coming GPM era. The GPM project is a follow-on mission of the TRMM (Tropical Rainfall Measuring Mission) under international cooperation including the United States, Japan, and other countries, which will extend TRMM observation to higher latitudes with 3-hour sampling at any given point on the earth.

The GSMaP_MVK system, short for Global Satellite Mapping of Precipitation using Moving Vector and Kalman fiilter, uses a Kalman filter model to estimate precipitation rate at each 0.1 degree with 1-hour resolution on a global basis. The input data sets are precipitation rates retrieved from the microwave radiometers and infrared images to compute the moving vector fields. Based on the moving vector fields calculated from successive IR images, precipitation fields are propagated and refined on the Kalman filter model, which uses the relationship between infrared brightness temperature and surface precipitation rate. This Kalman filter–based method shows better performance than the moving vector–only method, and the GSMaP_MVK system shows a comparable score compared with other high-resolution precipitation systems.

Keywords: precipitation, satellite, infrared radiometer, microwave radiometer

PROPOSING THE SIMPLIFICATION OF THE MULTI-LAYER URBAN CANOPY MODEL

Ryosaku IKEDA* and Hiroyuki KUSAKA**
* Graduate School of Life and Environmental Sciences, University of Tsukuba, Ibaraki, Japan
** Center for Computational Sciences, University of Tsukuba, Tsukuba, Ibaraki, Japan
s0820923@u.tsukuba.ac.jp

Abstract

We propose the simplification of the multi-layer urban canopy model. Four types of multi-layer urban canopy models; the Level 4, Level 3, Level 2 and Level 1 models are developed to reduce the computational load of the heat budget calculations at the wall surface. Then, each canopy model is compared with observations in Tokyo. The results show that the simulated temperatures from the four models are close to the observed ones, and the temperature differences among the four models are very small. However, additional model inter-comparison study based on idealized simulations indicate that the difference between the Level 2 and 1 models and the Level 4 model becomes larger when the sky view factor (SVF) is smaller than 0.19 in summer and 0.40 in winter. On the other hand, the difference between the Level 3 model and the Level 4 model is very small under any sky view factor in both seasons. Therefore, the Level 3 model can be used instead of the Level 4 model in any conditions, while the Level 2 and 1 models are proposed to be used under conditions with a large SVF. From the simplification, the amount of computational memory is reduced by 0.43 times for the Level 3 model compared to the Level 4 model, and the CPU time is cut down by a factor of 3 in the Level 3 model when the vertical canopy layer is seven.

Keywords: Multi-layer urban canopy model, Simplification

SENSITIVITY OF WRF MODEL TO INPUT-DATASETS AND SURFACE PARAMETERS FOR HEAT ISLAND

Yuko AKIMOTO, Hiroyuki KUSAKA
University of Tsukuba, Tsukuba city, Japan
s0820919@ipe.tsukuba.ac.jp

Abstract

The urban heat island has been recognized for many years and many researchers have performed urban climate studies in order to mitigate the phenomenon.

Most of earlier studies were performed utilizing the approaches with the statistical analysis and observation in the urban climate field. However, recently, numerical simulation has also been one of the main methods in this field. For instance, the Weather Research and Forecasting Model (WRF), which is designed as next generation model after the MM5, has been recognized world-wide.

The WRF requires the inputs of atmospheric data, land surface data and sea surface data to create the initial and boundary conditions. Several statistical data, such as land use and terrain data are also needed. Additionally, when the model is run, it needs some parameter table files that contain surface parameter values for each land use type. If the users don't have their own datasets or parameter tables, they will have to use the default input datasets and table-files. In the default, the land use data is created by the United States Geological Survey (USGS), thus the surface parameter values are estimated based on the land cover in U.S. Therefore, it is necessary to retune these parameters and gear them towards the subsequent research area. If the performance of the WRF is sensitive to these input data or surface parameters, the forecast accuracy of the model will be improved by resetting the parameters or altering the input data. Several researches had individually estimated the sensitivity of the WRF to some of parameters and input-datasets in order to confirm the speculation. However, the sensitivity has not been sufficiently conducted yet.

In this study, we quantitatively estimate the sensitivity of the WRF to the input-datasets and surface parameters for surface temperature. Furthermore, we examine what the most sensitive factor is. In the presentation, we will show the results of these sensitivity experiments.

Keywords: WRF, sensitivity experiments, surface parameters, land use data

Performance of the WRF model as a high resolution urban climate model

Hiroyuki Kusaka, Fei Chen, Mukul Tewari, Jimy Dudhia, Yukako Miya, and Yuko Akimoto

Abstract

The Weather Research and Forecasting (WRF) model has been developed as the next generation model after the MM5, which has been widely used globally. The number of urban climatologists who use WRF for urban climate study has been lately increasing. Recently, the performance of the WRF has been confirmed in several case studies with regards to the urban heat islands. However, the results for the climate simulations have not been validated. In this study, we report the performance of the WRF as a regional climate model with high spatial resolution for urban climate study. Numerical integrations of the model are conducted for 7 consecutive years from July 27st to September 1st. Thereafter, the monthly averaged surface air temperature and accumulated precipitation for the 7 years are validated against the observations. Additionally, an inter-comparison study of the land surface model is performed.

Building Wind Characteristics at Skyscraper Area

Kyoo-seock Lee[1], Wencheng Jin[1],

[1] *Department of Landscape Architecture, Sungkyunkwan University, Suwon, 440-746 Korea*
leeks@skku.edu
Tel) 82-31-290-7845

I. Introduction

Tall buildings have been built in Seoul since 1990s. It induces many urban microclimatological and air hygienic impact to nearby area like reduced solar radiation, pollutant concentration, sunlight block and gusty winds. Of the above-mentioned environmental impacts by tall buildings, gusty winds called building wind occur by descending turbulences due to the upper air blocking by tall buildings. When the wind descends, it makes three-dimensional turbulence around the buildings and makes eddy effects and prevents the air pollutants from being dispersed to surrounding area. However, there are few studies in measuring building wind. Thus, this study aims to observe the building wind and figure out the wind characteristics of skyscraper area...

II. Materials and Methods

The study site is Dogok Subway Station Area at Gahngnam-gu in Seoul, Korea. From the 1980s, the population of study site has grown rapidly mainly due to the urbanization and the development began for housing construction. Especially, there are nine skyscrapers whose heights are more than 164 meters within one block at the study site. In this block, the height of the tallest building is 264 meters. The Tall building are used for business and commercial use in foreign countries such as Germany and Japan, but these skyscrapers are used for residential purpose in South Korea.

The wind data has been observed for more than one year which includes wind speed and wind direction. For measuring wind data, 2-d wind monitor (propeller-type), 3-d ultrasonic wind monitor (RM-Young 500) and Campbell CR1000 and CR4000 data logger were used. The wind has been observed at A station and B station. The wind speed data were classified according to Beaufort scale. After analysis, it was derived that there are strong building winds at the study site and the origin of building wind was investigated using synoptic meteorological data and urban building geometry.

WIND PATH EFFECT OF RIVER IN URBAN HEAT ISLAND

Hirofumi SUGAWARA[1], Ken-ichi NARITA[2] and Min Sik KIM[2]

[1]National Defense Academy, Yokosuka, Japan, hiros@nda.ac.jp
[2]Nippon Institute of Technology, Miyashiro, Japan

Abstract

The urban heat island phenomenon is one of the serious problems in atmospheric environemt. In summer, rivers in city can mitigate the problem by two tpyes of cooling effect. One is due to the cooler water body than the atmosphere. Another is the wind path which leads cooler sea breeze. City planners need quantitative evaluation of these effects in the heat island mitigation, and therfore we meteorologist should inspect the mechanizm of cooling. In this study, we discuss the wind path effect based on the observed data.

Observation was made in Tokyo in 2007. We choose small (~20 m width) river which runs from north to south. The river mouth was 5 km south from the measurement site. The terrain was almost flat and low buildings (~10 m high) spread over around the mesurement site. We took trubulence measurement by sonic anemometer and infrared hygrometer at 4 m above the water surface. Short and longwave radiation flux were also measured above the water. Air temperature distribution was measured in 400x400 m surrounding city area.

Inland penetration of sea breeze was found at 8:00 on 19 Aug. 2007 at the measurement site. At the river, sea breeze front reaches faster (10~20 min.) than at the surrounding city area. The upward sensible heat flux increases above the river after the sea breeze passed (Fig.1). The quadrant analysis clarified that the increased heat flux was caused by downward motion of the cooler air. This upward heat flux at 4 m high was larger than the heat flux at water surface which is evaluated from the bulk method. Therefore, air in the river was cooled more from the upper air (sea breeze) than the water surface. The turbulence analysis showed that the cooler river air was transferred to the warmer surrounding city area.

Keywords: urban climate, river, ventilation

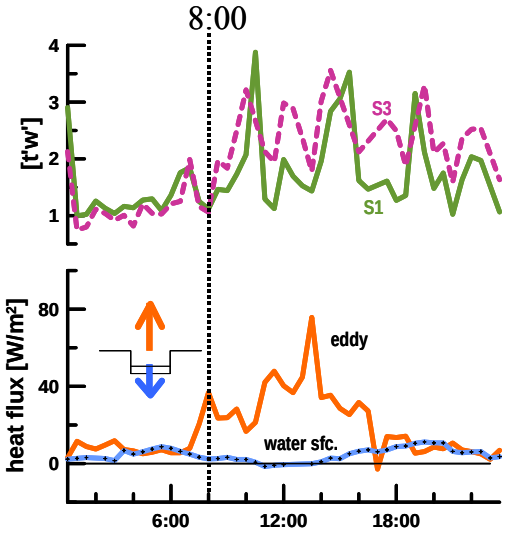

Figure 1. Time series of the heat flux at 4m high above water (orange), at the water surface (blue), the first quadrant component of heat flux (t'>0, w'>0, green), and the third one (t'<0, w'<0, pink).

Effect of Urban Land Cover and Pollution in a Heat Wave Event in Nanjing, China

Jie Song, Professor, Department of Geography, Northern Illinois University, DeKalb, IL 60115, USA, Email: jsong@niu.edu,

Zhihong Jiang, Professor and Director, Key Laboratory of Meteorological Disaster of Ministry of Education, Nanjing University of Information and Science Technology, Nanjing, 210044, China, Email: zhjiang@nuist.edu.cn

Hong YunMa, Ph.D student, Key Laboratory of Meteorological Disaster of Ministry of Education, Nanjing University of Information and Science Technology, Nanjing, 210044, China, Email: mhypony@126.com(Corresponding author)

Abstract

Effective albedo is lower above urban land cover than rural areas due to multiple reflection and absorption of canyon surfaces. In the meantime, higher concentration of fine particles in the summer has led to the reduction in the incoming shortwave radiation. In this paper, we examined the opposing effect of urban land cover and air pollution to a heat wave event by using Weather Research and Forecast (WRF) model coupled with land surface model (Noah) and a simple one-layer urban canopy model (UCM). Our study focused on an extreme heat wave that hit the southern Jiangsu Province with daily maximum air temperature consistently above 37 degree Celsius in Nanjing during July 24 to August 2, 2007, when Subtropical high pressure dominated the Yangtze River Delta. Modeling has included the shadowing effect of urban canyon and anthropogenic heating in the UCM, as well as the scattering effect of increased aerosol in the WRF radiation scheme. It is found that increased aerosol concentration in the boundary layer can lower surface air temperature by 1-2 degrees due to the reduced shortwave radiation; however, the combined effect of urban canyon and anthropogenic heating has overwhelmed the aerosol cooling effect. Modeled results have been evaluated with field observations and remote sensing data.

Key words: urban, aerosol, shortwave radiation, heat wave, numerical model

A simulation of localized heavy rainfalls in Fukuoka City

Yukiko Hisada, Shinpei Todaka and Nobuhiro Matsunaga
Department of Earth System Science and Technology,
Kyushu University, Fukuoka 816-8580, Japan
Email todaka@esst.kyushu-u.ac.jp

Abstract

It is reported that these days, the occurrence frequency of localized heavy rainfalls called "Guerrilla thunder storm" is increasing in Tokyo, Osaka and other Japanese megacities. Localized heavy rainfalls lead the flood of urban rivers and inflow of a large amount of water and sediment to the city area and give severe disasters and damages to the infrastructures of cities. The occurrence frequency of the localized heavy rainfalls increases also in Fukuoka City year by year. It is very difficult to predict when and where such a heavy rainfall happens, and therefore, it makes taking previously measures more difficult. At the first step, it is very important to reveal the mechanism of the generation of the localized heavy rainfalls in each megacity.

We tried to simulate the localized heavy rainfall which occurred in Fukuoka city on 8 August, 2008 using the Weather Research and Forecasting model (WRFV3.0). The simulation result agrees well with the localized heavy rainfall.

Keywords: localized heavy rainfall, WRF, urban climate

NUMERICAL STUDY ON TRANSIENT FLOW ASSOCIATED WITH DOWNSLOPE WIND IN THE LEE OF ZAO MOUNTAIN

Masahiro SAWADA[1], Weiming SHA[1], Takeshi YAMAZAKI[1], Toshiki IWASAKI[1], Hironori IWAI[2], Shoken ISHII[2], Kohei MIZUTANI[2], Toshikazu ITABE[2], Izumi YAMADA[3], Dai MATSUSHIMA[4].
[1]Department of Geophysics, Graduate School of Science, Tohoku University, Sendai, JAPAN
[2]National Institute of Information and Communications Technology, Tokyo, JAPAN
[3]Electronic Navigation Research Institute, Sendai, JAPAN
[4]Chiba Institute of Technology, Chiba, JAPAN
sawada@wind.geophys.tohoku.ac.jp

Abstract

Zao-oroshi is a strong northwesterly downslope wind around northeast Japan in the lee of Zao Mountain under the winter monsoon season. Zao-oroshi often yields small-scale disturbances and wind shear, so that the understanding and forecasting of these severe phenomena are important for aviation safety.

Doppler Lidar is useful to detect such local severe phenomena from several hundred meters to several kilometers, and provide the valuable data for validation of high-resolution simulation. Thus, Doppler Lidar observation was conducted at Sendai airport, which is located in the lee of Zao Mountain, from 13 to 17 February 2008. From the Lidar observation, the headwind (easterly wind) and streak are captured near the surface. The purpose of this study is to investigate what degree high-resolution numerical simulation can express the structure of transient flows observed by Lidar, such as the headwind, streak and variability of wind speed.

The simulations of Zao-oroshi are carried out using nonhydrostatic model with 500-m/100-m mesh through dynamical downscaling. In 500-m mesh simulation, the lee waves with a horizontal wavelength of about 20 km are clearly reproduced in the lee side of Zao Mountain. Under the lee waves, headwind structure is captured in the 100-m mesh simulation. The horizontal scale of headwind region is several hundred-meters. A comparison of simulated wind speed and Lidar observation is conducted.

Keywords: transient flow, downslope wind, Lidar

NUMERICAL EXPERIMENT ON DUST DEVILS AND THEIR LIFTING DUST PARTICLES IN A DIURNALLY-EVOLVING CONVECTIVE MIXED LAYER

Junshi ITO[1], Hiroshi NINO[1] and Mikio NAKANISHI[2]

[1]Ocean Research Institue, The University of Tokyo, Tokyo, Japan
[2]National Defense Academy, Kanagawa, Japan

Email junshi@ori.u-tokyo.ac.jp

Abstract

Dust devils are small-scale vertical vortices that often occur in deserts and bare land during early afternoon in the fine weather conditions, where convective mixed layers are formed due to strong heat fluxes from the ground. We perform numerical experiment to reproduce diurnally-evolving convective mixed layers by means of a large eddy simulation model from 700 LST (Local Standard Time). The boundary and initial conditions of the experiment are horizontally uniform, thus there is no vertical vorticity in the domain of the experiment at 700 LST. However, when convection is more energetic and the cellular convection prevail between 1200 LST and 1600 LST, vortices with significant large vertical vorticity and pressure depression near the ground, which should correspond to dust devils, are found at the vertexes of updraft bands of the cellular convection. Cellular convection is likely to form in a weak general wind condition, therefore a weak general wind is preferable for dust devil occurrence.

The simulated dust devils have two distinct morphologies: a one-celled and a two-celled structure. Vortices with a two-celled structure have larger pressure depression than those with a one-celled structure. Some of them have a one-celled structure initially, but later evolve into a two-celled structure.

Since extraordinary large tangential winds within dust devils can blow up dust particles under even a weak general wind condition, they may play an important role in the dust transports in synoptic scales. We examine the ability of dust devils to disperse dust particles from the ground into convective mixed layers with using a simple model for dust particles floatation and advection. Without a general wind, dust particles are floated by dust devils in the model. They are lifted to upper part of convective mixed layers by strong updrafts around dust devils, and then gradually descend and spread into whole the convective mixed layer.

Keywords: convective mixed layer, dust devil, vortex

ADJUSTMENT TECHNIQUE OF OBSERVED WIND BY ROUGHNESS PARAMETER AND LOGARITHMIC LAW: DIVERGENCE FIELD OVER THE KANTO PLAIN

Yoshihito SETO and Hideo TAKAHASHI
Department of Geography, Tokyo Metropolitan University, Hachioji, Japan
seto@mx2.ttcn.ne.jp

Abstract

The purpose of this study is to clarify vertical structure and diurnal variation of local wind systems including land-sea breeze over the Kanto region. For an index of the vertical motion of the atmosphere that direct observation is difficult, quantity of divergence is calculated from observed surface wind. But, it cannot be ignored the influence on the wind velocity by difference of altitude because anemometers height in each observation point is various. Therefore, the roughness parameter according to the wind direction of each observation point in 1997 was estimated by the land utilization around the observation point. Based on an empirical formula used by Kuwagata and Kondo (1990), an estimate formula newly made with a multiple regression analysis was used for an estimate of roughness parameter. With the adjustment formula of the wind velocity based on logarithmic law, the adjustment of the wind velocity was applied.

Typical sea breeze day was extracted, and the characteristic of wind and divergence field that averaged every time were examined. The correlation of the quantity of divergence in remarkable divergence area was calculated to understand the relations with this area and convergence area. AMeDAS data in 2004 was mainly used in this study. At 9:00, the divergence area was formed in Tokyo Bay (called Area-TB). And, there was sea breeze circulation between convergence area of the neighborhood of Tokyo. At 11:00, a valley wind developed in North Kanto, and valley wind circulation was seen between the convergence area of the mountainous district neighborhood of North Kanto and the divergence area of the prefectural border neighborhood of Gunma and Saitama (called Area-GS). At 15:00, with the development of the large-scale sea breeze, valley wind circulation in North Kanto becomes indistinct. With it, the Area-TB comes to have negative correlation with the Area-GS. When the development of the large-scale sea breeze was remarkable, it was shown that the Area-GS corresponding to the valley wind circulation was weakened. We will want to discuss validity of this adjustment technique and consider atmosphere stability for adjustment.

Keywords: local circulation, land-sea breeze, roughness parameter, logarithmic law

WIND TUNNEL EXPERIMENT FOR DIFFUSION OF VOLCANIC GAS ERUPTED FROM MIYAKE ISLAND

Akihiro HORI, Kazuo KURIHARA* and Kosuke HASHIMOTO
*Meteorological Research Institute, Tsukuba, Japan
Meteorological & Environmental Sensing Technology INC., Ami, Japan
*kkurihar@mri-jma.go.jp

Abstract

This study is to develop an experimental method to simulate the diffusion of volcanic gas by using a wind tunnel. By using observed data such as the heght of volcanic gas and the amount of gas emission, we estimated gas concentration on the ground. The results are consistent with observed gas concentration data.

We studied the case of Miyake Island, because the Japan Meteorological Agency and other research institues keep the observed data such as the top height of the volcanic gas H (m), the amount of SO_2 emission from the volcano Q (ton/day), the ground level SO_2 concentration C (ppm), and so on since its eruption in June 2000,

We focused on the ground level SO_2 concentration observed at Miyake Airport, which is located at about 3 km ESE from the volcano. We listed the observed data that satisfied the following conditions simultaneously: 1) Q is available (data were gathered by a helicopter); 2) the wind speed U (m/s) is greater than 10 m/s (in order to assume the neutrally stratified flow); 3) the wind direction is nearly WNW (so that the airport is located at the downwind of the volcano); and 4) SO_2 is detected at the airport. Finally we selected the data with the gas height H ranged from 200m to 800m.

The experiments were conducted in a wind tunnel of the Meteorological Research Institute with the model of Miyake Island which is 1/10,000 in scale and has a gas outlet corresponding to the crater with 200 m diameter in real scale. Under wind velocity of 10 m/s, we studied three cases, H = 200, 600 and 800 m. The gas concentration was measured with Beckman Model 400 hydrocarbon analysers.

To compare our experimental results with the observed data, we converted the concentrations in the wind tunnel into real scale, by using the observed values of Q and U.

The results fulfilled our aim to simulate the diffusion of volcanic gas in the wind tunnel with the parameter of observed gas height H.

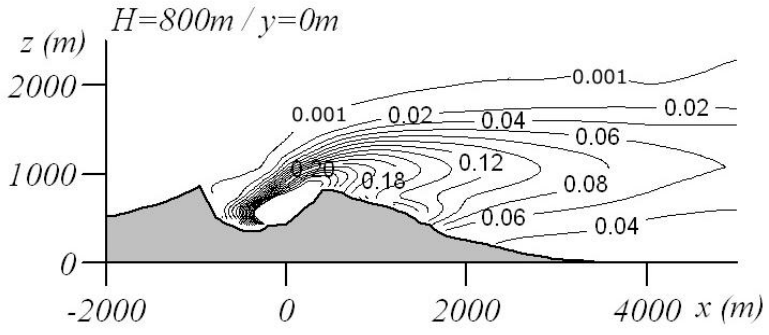

Fig. Contour of the gas concentration normalized by erupted concentration C_0. The top height of volcanic gas, H = 800 m.

Keywords: Wind Tunnel Experiment, Volcanic Gas, Diffusion, Miyake Island

CHANGES IN THE RELATIONSHIP BETWEEN THE ANNUAL CYCLE AMPLITUDE AND ENSO IN A CGCM SIMULATION

Jung CHOI and Soon-Il AN
Department of Atmospheric Sciences / Global Environmental Laboratory,
Yonsei University, Seoul, South Korea
jungchoi@yonsei.ac.kr, sian@yonsei.ac.kr

Abstract

The relationship between the annual cycle amplitude of sea surface temperature (SST) in the eastern tropical Pacific and the ENSO variability has been examined by coupled general circulation models (CGCMs)s as part of the IPCC-AR4-CMIP3 model evaluation. Each model has own characteristics of the simulated mean state, ENSO, the annual cycle and their relationship.

The results suggest that the correlation between annual cycle amplitude and ENSO amplitude could not be a regular sign. For instance, in some decades, the ENSO variability and the annual cycle amplitude are positively correlated, however, they are negatively correlated in the other decades.

It seems that the tropical Pacific annual mean state has a impact on their relationship. Generally, the combined effects of changes of the mean state, ENSO, and annual cycle could make to define the relationship between the annual cycle amplitude and ENSO variability themselves.

Keywords: ENSO, Pacific, Annual cycle

A COMPARISON OF CHINA AMDAR REPORTS AND SOUNDING DATA

Jue-Jing HAN, Yuan WANG
NanJing University, NanJing, China
qinqinghan@smail.nju.edu.cn

Abstract

A study of meteorological reports from Aircraft Meteorological Data Relay (AMDAR) System including entire sample on ascent、descent、cruise, has been performed to estimate observation errors for wind and temperature. Observations were collected over China for a period of 23-month. After quality control designed by China meteorological message center, 60% data are removed, error of temperature and wind reduces around 2℃(or m s^{-1}) respectively.

Results of comparison between AMDAR reports and sounding data show rms error of temperature is 1.93℃, 36° for wind direction and 3.5～3.8 m s^{-1} for wind speed (resultant wind and wind components). Correlation coefficient of AMDAR reports and sounding data is over 0.65, especially that of temperature is hight to 0.99, wind (resultant wind) correlation coefficient is around 0.9, and 0.65 for wind direction. The study provides an overview of combination of sounding and AMDAR observations beneathe 8 kilometers in the boundary layer, although the statistics indicate rms errors are somewhat large, they are acceptable.

Key words: AMDAR reports, sounding data, rms error

IMPACT OF DIFFERENT DIFFUSION SCHEMES ON SIMULATED RAINFALL : LAND-OCEAN CONTRAST

Sun-Hee SHIN[1], Kyung-Ja HA[1], Masahide KIMOTO[2] and Akio KITOH[3]
[1]Division of Earth Environmental System, Pusan National University, Busan, Korea
[2]Center for Climate System Research, University of Tokyo, Japan
[3]Climate Research Department, Meteorological Research Institute, Tsukuba, Japan

* Corresponding Author: shin@mri-jma.go.jp

Abstract

The impact of vertical diffusion schemes on simulated precipitation has been investigated using the two diffusion schemes, the Mellor and Yamada level 2 (MY) and the Holslag and Boville (HB) schemes in the CCSR NIES model. The results indicate the HB scheme reproduced strong vertical mixing over land, especially in summer hemisphere, which has apparent diurnal variation due to strong vertical mixing in the convective boundary layer. The MY scheme displayed relatively weak vertical mixing over land, but strong mixing over the ocean. MY scheme tends to strongly reproduce the local mixing by wind shear compared to the HB scheme.

The variations in the thermodynamic feature were due to the difference in the PBL scheme results in the warmer and drier air over land and relatively colder and wetter air over the ocean. Such an apparent contrast over land and ocean leads to a horizontal gradient in temperature and changes the large scale circulation. The change in sea level pressure over the western equatorial Pacific, induced by the HB scheme, results in changes in the zonal and meridional pressure gradients between the equator and subtropical region, which is the main driving force of the low-level divergence. A weakening of low-level easterly winds due to changes in the zonal and meridional pressure gradients has a great influence on the rising motion in the western Pacific, together with the low-level moisture content advected towards the off-equatorial area.

Keywords: vertical diffusion scheme, vertical mixing over land and ocean, precipitation

PRECIPITATION CHARACTERISTICS OF APHRO_PR, HIGH-RESOLUTION DAILY PRECIPITATION DATA

Kenji KAMIGUCHI[1)], Osamu ARAKAWA[1)], Haruko KAWAMOTO[2)],
Akiyo YATAGAI[2)] and Masato NODZU[2)]
1) Meteorological Research Institute, Tsukuba, Japan
2) Research Institute for Humanity and Nature, Kyoto, Japan
kkamigu@mri-jma.go.jp

Abstract

We have been producing a long-term high-resolution daily precipitation data in Asia based on the huge number of rain-gauge observations under the project named "Asian Precipitation Highly-Resolved Observational Data Integration Towards Evaluation of the Water Resources" (APHRODITE). This data is intended to be used such as for water budget analysis, validation of high-resolution climate model and trend analysis of precipitation extremes.

The interpolation algorithm is based on the combination of the spherical version of Shepard's distance-weighting method (Shepard, 1968; Willmott et al., 1985) and Mountain Mapper method (Schaake et al., 2004). Interpolation is performed on horizontal 0.05 degree grid box, then the interpolated data is converted to 0.5 degree grid for public release (The data can be downloaded at the following site: http://www.chikyu.ac.jp/precip/index.html).

With spatially dense observations, sophisticated interpolation technique and careful quality control procedure, our dataset APHRO_PR is considered to be more reliable than the other observed precipitation data. Compared with GPCP-1DD, APHRO_PR captures better in orographic precipitation over high elevation and steep terrain area such as the Himalaya and the West Ghats of India.

In this presentation, in addition to the statistical characters of APHRO_PR, some of the challenges to improve interpolation techniques are also discussed.

Keywords: precipitation, observation, interpolation

INTRODUCTION OF EAST ASIAN DROUGHT MONITORING SYSTEM

Su-Bin OH, Do-Woo KIM, Ji-Sun LEE, Ki-Seon CHOI and Hi-Ryong BYUN
Pukyong National University, Busan, South Korea
hrbyun@pknu.ac.kr

Abstract

This study introduces the East Asian drought monitoring system that has been operated since 2008. Website is http://atmos.pknu.ac.kr/~intra2. This system serves drought variations such as intensity, duration, etc. It displays not only spatial but also temporal distribution of drought with monthly time step.

The Effective Drought Index (EDI; Byun and Wilhite, 1999), an intensive measure that considers the precipitation accumulation with the weighting function of time passage, is the main idea of the system. The other hydrological variable such as Available Water Resources Index (AWRI: Byun and Lee, 2002) is provided also. For these calculations, we used monthly precipitation data of 298 stations that located in South Korea, North Korea, China and Japan. Start years of data in stations are various from 1777 to 1973 in South Korea, 1973 to 1981 in North Korea, 1874 to 1952 in China and 1877 to 1901 in Japan.

The main advantages of this system are as follow. 1) It helps us to detect where and when the drought occurred, and how the drought situation is going over East Asia. 2) Because using the long-term period data, it is useful to detect the change of precipitation and drought climate. 3) It could be utilized in selection of drought case and fundamental data of after studies. 4) The drought diagnosis and evaluation are obtained from every month update, so it will be contribution to management and mitigation of drought in East Asia.

Keywords: Drought monitoring, East Asian drought, monitoring system, Effective Drought Index, Available Water Resources Index

NUMERICAL SIMULATION OF BLOCKING USING NICAM INSTALLED AT CCS, UNIVERISTY OF TSUKUBA

Kensuke Kato,Yuko Shimo and Hiroshi L. Tanaka

Center for Computational Science, University of Tsukuba,
Tsukuba Japan (Last Author)
tanaka@ccs.tsukuba.ac.jp

Abstract

A new type of ultra-high resolution atmospheric general circulation model is developed by the Center for Climate System Research, University of Tokyo and Frontier Research Center for Global Change/Japan Agency for Marine-Earth Science and Technology. The new model is designed to perform cloud-resolving simulations by directly calculating deep convection and meso-scale circulation, which plays a key role not only in the tropical circulations but also in the general circulation of the atmosphere. The model is called the Nonhydrostatic Icosahedral Atmospheric Model: NICAM. NICAM is installed in the high-performance computing systems PACS-CS and T2K-Tsukuba at the University of Tsukuba, Japan. The PACS-CS is a PC Cluster system of 10.35 T flops in the Linpack Benchmark, which consists of 2560 nodes (cores), connected by 20480 Gigabit Ethernet cables, and the T2K-Tsukuba is another PC Cluster system of 95 T flops by Appro Xtreme-X3 Supercomputer consisting of 10368 cores.

A series of numerical experiments are conducted using NICAM with various horizontal resolutions from 224 km (Glevel=5) to 7 km (Glevel=10). An atmospheric blocking is simulated with an initial condition of 27 November 2007; interpolated from the Grid Point Value (GPV) analysis data provided by the Japan Meteorological Agency (JMA) with Glevels from 5 to 9. It is found that the blocking is predicted from the initial condition one week before, but the intensity of the blocking appears to be weak for all resolutions. The results suggest that the horizontal resolution is not essential for simulating a blocking. It is shown that the accuracy of the initial condition and model physics are the more important that the model resolution.

Keywords: Blocking, NICAM, PACS-CS, T2K-Tsukuba

Dynamics and Statistics of Arctic Cyclones Compared with Tropical and Extra-tropical Cyclones

Shinji TAKAHASHI and H. L. TANAKA

Graduate School of Life and Environmental Sciences, University of Tsukuba,
Tsukuba Japan (First Author)
s0510356@ipe.tsukuba.ac.jp

Abstract

The dynamics and statistical analysis of Arctic cyclones in the summer period (JJA) of 2005-2008 are examined using the JCDAS data. The frequency of the cyclone tracks, the vertical structure of the vortex tube, air temperature, wind and the characteristic features of the life cycle of the cyclones are investigated. These factors are compared with the extratropical cyclones that are excited by baroclinic instability and a tropical cyclone (Hurricane KATRINA in 2005) which are excited by the conditional instability of the second kind (CISK). The Arctic cyclone displayed several interesting characteristics; their life cycles are long (maximum: 27.75 days, five Arctic Cyclones average: 20.85 days, all cyclones average: 2.3 days) and the direction of movement of the cyclones are random. Furthermore, the cyclones exhibit a barotropic structure and are observed just below the polar vortices at the 500 hPa height field. The vertical structure of the vertical p-velocity also indicates the distribution of the updraft at the cyclone center and the downdraft above the 200 hPa height. The distribution and the vertical structure of air temperature at 200 hPa height showes the presence of a warm core. Thus, the Arctic cyclones have several interesting characteristics and are assumed to be created due to the warm core in the stratosphere; the warm core are formed as a result of the downdraft with adiabatic compressive heating from the upper levels of the stratosphere.

Key Words : Arctic Cyclone, Tropical Cyclone, Polar Vortex, Warm Core.

Interaction between the Baroclinically Unstable Wave and the Subtropical and Polar-frontal Jets

Fuyuki Fujiwara and Hiroshi L. Tanaka

Graduate School of Life and Environmental Sciences, University of Tsukuba,
Tsukuba Japan (First Author)
s0820946@u.tsukuba.ac.jp

Abstract

In the upper troposphere, the subtropical jet and the polar-frontal jet exist in both of the Nothern ans Southern Hemisphere. The strength and location of the polar-frontal jet is variable, where as that of the subtropical jet is relatively steady. The action of these westerly jets is related to the baroclinically unstable wave. By Tanaka and Tokinaga(2002), it confirmed that two different kinds of baroclinic instability exist; the Polar mode excited by the baroclinicity of the polar-frontal jet and the Charney mode exited by the baroclinicity of the polar frontal jet. These baroclinic instabilities has different feedback process that make the polar-frontal jet weaker or stronger.

In this study, baroclinic instability of nothern hemisphere is investigated, using a method of expansion in 3D normal mode function introduced by Tanaka and Kung(1989). Here, the 3D normal mode function consist of vertical structure functions as the vertical normal modes and Hough harmonics as the horizontal normal modes. The basic states used for the linear stability analysis are observed zonal mean wind for strong and weak polar vortex and a virtual one which is added the anomaly by the strength of the AO index to the climatic average.

As a result of the eigenvalue problem for such basic states, we confirmed that the polar mode become the most unstable mode exceeding the Charney mode in each wave number when the polar vortex is strong enough. And we also confirmed that the structure of dipole Charney mode becomes the polar mode as the strength of polar-frontal jet is increase.

Keywords: Baroclinic instability, Polar frontal jet, Charney mode

Predictability of the Arctic Oscillation Index Using a Barotropic General Circulation Model

Shingo Kato and Hiroshi L. Tanaka

Center for Computational Science, University of Tsukuba,
Tsukuba Japan (Last Author)
tanaka@ccs.tsukuba.ac.jp

Abstract

The Arctic Oscillation (AO) is one of the dominant atmospheric variabilities characterized as opposing atmospheric pressure patterns in northern middle and high latitudes. The oscillation exhibits a ”positive phase” with relatively low pressure over the polar region and high pressure at midlatitudes.

In this study, we investigated the predictability of the Arctic Oscillation Index (AOI), which is related to the zonal mean polar jet anomaly, and an index of the winter weather in the Northern Hemisphere, using a barotropic general circulation model. This model developed by Tanaka (1998) predicts the vertical mean component (i.e., barotropic component) of the atmosphere with an external forcing of the barotropic-baroclinic interactions. In order to correct the bias of the model, the ensemble forecast using some error averages before the initial time was performed.

As a result, it is found that the prediction skill of AOI varies considerably from one year to another. Compared to the prediction skill of AOI in AO positive winters with that in AO negative winters, however, the correlation coefficient between the forecast and the observation is more than 0.7 even for one month prediction in AO positive winters. On the other hand, the predictability of AOI in AO negative winters is about 2 weeks at most, but the ensemble forecast considering the bias correction showed better results than the control run. Consequently, it is concluded that AOI could be predicted exceeding two weeks by predicting the barotropic component of the atmosphere.

In order to improve the prediction skill, we need to consider another method to correct the bias of the model, and to study the mechanism of the AO in more detail.

Keywords: Arctic Oscillation, Arctic Oscillation Index, Barotropic Component, Predictability, Ensemble Forecast

DATA ANALYSIS OF ARCTIC OSCILLATION SIMULATED BY GLOBAL WARMING PREDICTION MODELS

Masahiro Ohashi and Hiroshi L. Tanaka

Life and Environmental Sciences, University of Tsukuba,
Tsukuba Japan (First Author)
s0820928@ipe.tsukuba.ac.jp

Abstract

The Arctic Oscillation (AO) is a dominant atmospheric phenomenon characterized as opposing atmospheric pressure patterns between the middle and high latitudes. As a long-term variability of surface temperature associated with the Arctic Oscillation Index (AOI) shows high correlation with the recent global warming, it attracts more attention that the AO is an important research problem in the study of global warming.

In this study, we analyze the AO simulated by 10 Atmosphere-Ocean General Circulation Models for the Intergovernmental Panel on Climate Change Fourth Assessment Report (IPCC-AR4). Control scenarios used in this study are the '20th Century Climate in Coupled Model' in 1901-2000 and the 'Special Report on Emission Scenarios-A1B' in 2001-2099.

As a result, a primary mode of the empirical orthogonal functions in winter unexceptionally represents the AO pattern in all models. Four models that have some ensemble members simulate the observed variability of global mean surface temperature well. We then analyze the AO separated in internal variability and response to the external forcing in the decadal time scale using the four models. The internal variability appears commonly as the AO pattern, however, the response pattern of the external forcing varies widely depending on models and scenarios. The multi-model mean shows AO-like structure. In addition, the time series of the AOI represents a monotonic positive trend superimposed on substantially large internal variability after the late 20th century with the increase of greenhouse gases. Yet, the time series of the AOI for 20th century for each model is quite different, and no model can reproduce the observed time series of the AOI. It is concluded that the decadal variability of the AO can be explained mostly by the internal variability of the atmosphere.

Keywords: Arctic Oscillation, Arctic Oscillation Index, Global Warming

THE DIFFERENCES IN ENERGY SPECTRUM OF NICAM BY DIFFERENT HORIZONTAL RESOLUTIONS

Koji Terasaki, H. L. Tanaka
Graduate School of Life and Environmental Sciences,
University of Tsukuba, Tsukuba, Japan
koji@ccs.tsukuba.ac.jp

Abstract

A new type of ultra-high resolution atmospheric general circulation model is developed by the Center for Climate System Research, University of Tokyo and Frontier Research Center for Global Change/Japan Agency for Marine-Earth Science and Technology. The model is called the Nonhydrostatic Icosahedral Atmospheric Model: NICAM. NICAM is installed in the high-performance computing systems PACS-CS and T2K-Tsukuba at the University of Tsukuba, Japan. It is very important to investigate the characteristics of a new model from various points of view. In this study, the characteristic of the energy spectrum in the zonal wavenumber domain of NICAM is examined. A series of numerical experiments are conducted using NICAM with various horizontal resolutions from 224 km (Glevel-5) to 3.5 km (Glevel-11). Glevel-11 experiment was run with ES (Earth Simulator).

The energy spectra of most of horizontal resolutions obey -3 power law in synoptic and sub-synoptic scales (wavenumbers k= 5 to 30). However, the energy slope for glevel-5 becomes much steeper around zonal wavenumber k=10. Nastrom and Gage (1985) explained that the energy spectrum near the tropopause at wavelengths below about 400 km appears to follow the -5/3 power.This scale corresponds to about k=70 near 45 degree N. In this study, it is found that the energy spectra for k > 30 for glevel-8 to 11 follow the -5/3 power. It may be suggested that higher horizontal resolutions are required in order to represent the -5/3 power spectrum in meso scales.

Keywords: NICAM, energy spectrum, zonal wavenumber

NUMERICAL SIMULATION OF TROPICAL CYCLONES USING NICAM INSTALLED AT CCS, UNIVERSITY OF TSUKUBA

Yuko Shimo, Takuro Aizawa and Hiroshi L. Tanaka

Center for Computational Science, University of Tsukuba,
Tsukuba Japan (Last Author)
tanaka@ccs.tsukuba.ac.jp

Abstract

A new type of ultra-high resolution atmospheric general circulation model is developed by the Center for Climate System Research, University of Tokyo and Frontier Research Center for Global Change/Japan Agency for Marine-Earth Science and Technology. The new model is designed to perform cloud-resolving simulations by directly calculating deep convection and meso-scale circulation, which plays a key role not only in the tropical circulations but also in the general circulation of the atmosphere. The model is called the Nonhydrostatic Icosahedral Atmospheric Model: NICAM. NICAM is installed in the high-performance computing systems PACS-CS and T2K-Tsukuba at the University of Tsukuba, Japan. The PACS-CS is a PC Cluster system of 10.35 T flops in the Linpack Benchmark, which consists of 2560 nodes (cores), connected by 20480 Gigabit Ethernet cables, and the T2K-Tsukuba is another PC Cluster system of 95 T flops by Appro Xtreme-X3 Supercomputer consisting of 10368 cores.

A series of numerical experiments are conducted using NICAM (with various horizontal resolutions from 224 km (Glevel=5) to 7 km (Glevel=10). A pronounced tropical cyclone is simulated over the Gulf Stream with the numerical simulation with Glevel=8, starting from an initial condition of 21 June 2008 in the model (which is absent in the real atmosphere), and reaches the mature stage on the 5 July 2008. Since the tropical cyclone is generated in the NICAM atmosphere from the genesis stage, the details of its life cycle are analyzed. The fine structures of vorticity, vertical motion, and specific humidity are analyzed for this event.

Keywords: Tropical cyclone, NICAM, PACS-CS, T2K-Tsukuba

THE STANDARD DIVISION OF THE HEATSTROKE PREVENTION INDICATOR

FUKAZAWA Hiraku, FUKUOKA Yoshitaka

Rissho University, Kumagaya, Japan
E-mail:098w00001@ris.ac.jp

Abstract

Today, there are some indicators of heatstroke prevention. The indicator that is utilized most is "An indicator for the heatstroke prevention during exercises" of the Japan Sports Association. The Wet-bulb Globe Temperature (WBGT) is defined as a criterion the indicators. However, we do not understand it quantitatively how we are easy to suffer from heatstroke when rank rises by the standard division. Then, this study quantified it each standard-division and compared it.

In this study, we calculated original index “Dangerous index”. (D= {(Population / Unit Population) P/A} / (B / A) = (P’B)/A^2. Where D is used as “Dangerous Index”, P as the number of people at first aid transportation, P’ as correction of P, A as the observation days, B as days of occurred on first aid transportation in observation days.)

In the result (Table 1), it is easy to suffer from about 20 times heat stroke when we get nervous in a "severe caution" rank from a "caution" rank, and 2 times when a “danger” rank from a “severe caution” rank. In other words, if it become more than 35 ℃ from under 28-31 ℃, we are easy to suffer from about 40 times heatstroke. However, we want to consider it in future at the other metropolis and districts although we analyzed only Saitama in this study.

Keywords: heatstroke, prevention, WBGT, Dangerous Index, Saitama-prefecture

Table 1 Dangerous Index in Saitama Prefecture.

	Saitama	Kumagaya	Tokorozawa	Koshigaya	Kuki	Chichibu	Iruma	Ave.
Danger	0.83	0.23	0.25	0.51	0.83	0.23	0.12	0.43
Severe Caution	0.32	0.11	0.10	0.12	0.37	0.14	0.18	0.19
Caution	0.06	0.01	0.00	0.01	0.02	0.00	0.00	0.01
Careful	0.00	0.00	0.00	0.00	0.00	0.00	0.00	0.00
Safety	0.00	0.00	0.00	0.00	0.00	0.00	0.00	0.00